PRIFYSGOL ABERYSTWYTH UNIVERSITY

SUPRAGLACIAL SYSTEMS BIOLOGY OF DYNAMIC ARCTIC MICROBIAL ECOSYSTEMS

A thesis submitted for the degree of

Philosophiae Doctor

(Doctor of Philosophy)

by

Jarishma Keriuscia Gokul

(MSc, BTech (Hons), BSc)

Interdisciplinary Centre for Environmental Microbiology

Institute for Biological, Environmental and Rural Sciences

Aberystwyth University

May 2017

DECLARATION

Word count of thesis: ……**57 348**……

DECLARATION

This work has not previously been accepted in substance for any degree and is not being concurrently submitted in candidature for any degree.

Candidate name ……**Jarishma Keriuscia Gokul**……

Signature ……

Date ……**30 May 2017**……

STATEMENT 1

This thesis is the result of my own investigations, except where otherwise stated. Where correction services have been used, the extent and nature of the correction is clearly marked in a footnote(s).

Other sources are acknowledged by footnotes giving explicit references. A bibliography is appended.

Signature ……

Date ……**30 May 2017**……

STATEMENT 2

I hereby give consent for my thesis, if accepted, to be available for photocopying and for inter-library loan, and for the title and summary to be made available to outside organisations.

Signature ……

Date ……**30 May 2017**……

SUMMARY

Arctic glacier surfaces are a biologically active region of the cryosphere, supporting several cosmopolitan microbial taxa. Bacterial communities across the different ice surfaces are spatially variable and significantly influenced by biogeography and biogeochemistry. In summer, the supraglacial surface reveals extensive cryoconite hole coverage that is correlated to surface albedo, melt rate, mass balance and biological activity. However, the relative importance of temporal changes on bacterial community composition and activity in these supraglacial niches have yet to be determined. To enhance this knowledge, community dynamics of bacteria in cryoconite, snow and meltwater streams were investigated synthetically and on Foxfonna ice cap, Foxfonna valley glacier and the Greenland Ice Sheet. By means of microscopy, metabolomics and high throughput sequencing of 16S rRNA genes and cDNA from 16S rRNA, the summer bacterial community was evaluated to determine the relative importance of taxa on supraglacial surfaces. This aided in unravelling the complex interactions that are prevalent in a simple microbial niche exposed to unique environmental conditions, nutritional deficits and geological constraints. Overall, the bacteria on Foxfonna and Greenland supraglacial surfaces display distinct seasonal transient behaviour. Taxa appear selective to their physical environment and biogeochemical state in the cryosphere, characterized by integral associations with the photoautotrophic *Cyanobacteria*, *Phormidesmis priestleyi*, that mediates formation of a robust microhabitat conglomerated with humics, extracellular polymeric substances and minerals that are essential to the diverse and productive cryoconite community. The rare biosphere provides a source for heterotrophic bacterial recruitment in cryoconite, snow and stream habitats, the latter of which exhibit high abundances of proteobacterial subclasses only minimally dissimilar from cryoconite during the boreal summer. Network analysis predicts that these taxa may be responsible for the observed seasonal shifts of activity in favourable conditions, while generating the essential nutrient reserves required during winter dormancy periods.

ACKNOWLEDGEMENTS

"Appreciation is a wonderful thing.
It makes what is excellent in others belong to us as well."

— Voltaire

I would like to extend my sincere gratitude to my excellent supervisory team, Arwyn Edwards, Luis Mur and Tristram Irvine-Fynn, for their continued multifaceted assistance, support and guidance during four years of immensely enjoyable molecular and physical science as a member of the Cryosphere Microbiology Lab.

Thank you to the South African National Research Fund (NRF), for awarding me a prestigious Study Abroad Scholarship, without which this work would not be possible.

My thanks to Karen Cameron and Andy Hodson for assisting Arwyn and Tris with sample collection at field sites on the Greenland Ice Sheet and Foxfonna respectively. Additional thanks go to Gareth Griffith, Hilary Worgan, Dylan Gwynn-Jones, Alan Cookson, Luis Mur and Arwyn Edwards, for the use of their lab facilities, Kathleen Tailliart and Manfred Beckman for mass spectrometric processing, Joe Cook and Emma Wharfe for geochemistry processing, Eli Saetnan for support with co-occurrence networks, Matt Hegarty for performing Illumina sequencing, Nia Blackwell, Susan Girdwood, Toby Wilkinson and Andrew Detheridge for assistance with Ion Torrent sequencing and their priceless combined technical support.

My appreciation goes to an ever-supportive cryosphere team: Sara Rassner for her invaluable research advice, PhD fellows Nia, Richard, Ottavia, André, Aaliyah, as well as research students Sean, Jeremy and Tom for maintaining an exuberant lab atmosphere during the largest scale of metabolomic preparation known to IBERS.

I am grateful to Jenny, Dave, Brian, Tony and Jen, for welcoming me into their fold, especially Marta, Rose and Hannah for their continued support.

Thank you to Abercoustic (formerly Aberystwyth Glee Club), particularly Georgia and Megan, and The University Singers, for helping me find my voice and the much-anticipated musical interludes.

Special thanks to Kiri Kolt for her support and friendship through the ups and downs during these last few years and Graham Brand for teaching me to trust myself above all else.

Finally, I would like to express my lifelong gratitude to my parents and sister for their never-ending support in the face of prosperity and adversity while guiding me to the next stepping stone in life, one that my 10-year-old self dreamt of: exploring and understanding how the universe and the organisms within it work together.

Ubuntu.

— J.K.G.

TABLE OF CONTENTS

LIST OF FIGURES

CHAPTER 6

CHAPTER 7

LIST OF TABLES

CHAPTER 7

LIST OF ABBREVIATIONS

°	degrees
µL	microlitre
µm	micrometer
µM	microMolar
g	Relative Centrifugal Force
km²	Square kilometers
kPa	kiloPascal
L	Litres
M	Molar (Mole per Litre)
m	metres
m/z	mass to charge ratio
mg	milligrams
mL	millilitres
mM	milliMolar
mm	millimetres
ng	nanograms
nm	nanometers
nM	nanoMolar
pM	picoMolar
rpm	revolutions per minute
s	second
a.s.l.	Above Sea Level
ACA	Apparent Cryoconite Area
AWS	Automatic Weather Station
C	Celsius
D8	Flow directed into lowest adjacent pixel only
DEM	Digital Elevation Model
Dinf	Flow partitioned between adjacent lower pixels
E	East/Eastings
FAA	Flow Accumulation Area
GPS	Global Positioning System
IR	Incident Radiation
LWR	Long wave radiation
N	North/Northings
PDD	Positive Degree Days
PDH	Positive Degree Hours
PosHrs	Hours with temperature above °C
SWR	Short wave radiation
UV	Ultraviolet
Z	elevation

ANOVA	Analysis of Variance
CAP	Canonical Analysis of Principal co-ordinates
dbRDA	distance-based Redundancy Analysis
distLM	distance-based Linear Modelling
PCA	Principal Components Analysis
PCO	Principal Co-Ordinates Analysis
PERMANOVA	Permutational Analysis of Variance
PLS-DA	Partial Least Squares Discriminant Analysis
PLSR	Partial Least Squares Regression
SD	Standard Deviation
ρ	Spearman Rho correlation
BC	Betweenness Centrality
BLAST	Basic Local Alignment Search Tool
cDNA	complimentary Deoxyribonucleic Acid
CER	Closest Environmental Relative
CLSM	Confocal Laser Scanning Microscopy
CNR	Closest Named Relative
DNA	Deoxyribonucleic Acid
FDR	False Discovery Rate
FI-ESI-MS	Flow Infusion Electrospray Ionisation Mass Spectrometry
KEGG	Kyoto Encycopedia of Genes and Genomes
NCBI	National Centre for Biotechnology Information
OTU	Operational Taxonomic Unit
PCR	Polymerase Chain Reaction
QIIME	Quantitative Insights into Microbial Ecology
RA	Relative Abundance
bp	base pairs
Ca^{2+}	Calcium ion
Chl *a*	Chlorophyll *a*
Cl^{-}	Chloride ion
dNTP	deoxynucleotide triphosphate
EPS	Extracellular Polymeric Substances
Fe_2^{+}	Ferrous ion (Iron)
Mg^{2+}	Magnesium ion
N	Nitrogen
NH_3	Ammonia
NO_2-	Nitrite ion
NO_3^{-}	Nitrate ion
rRNA	ribosomal Ribonucleic Acid
S_2	Disulphide
SO_4^{2-}	Sulphate ion
TCA	Tricarboxylic Acid

CHAPTER 1 - INTRODUCTION

The cryosphere constitutes approximately 10% of the Earth's surface (Buzzini *et al.*, 2012) and consists of glaciers, icy seas and lakes, ice caps and continental ice sheets, and frozen ground (Benn and Evans, 2010). Together they form an essential component of the Earth's biosphere, linking feedback mechanisms influencing surface energy, moisture fluctuations, clouds, precipitation, hydrology and atmospheric and oceanic circulation. Glacial ecosystems range from subglacial lakes isolated for millennia to ephemeral microbial-mineral aggregates at the ice surface. Snow and ice covered areas have been investigated to understand their contribution to climate change and the effect of anthropogenic factors on the well-preserved polar regions of the Earth (I.P.C.C., 2013). Arctic and Antarctic environmental systems are increasingly exhibiting drastic changes in their characteristics in a short period of time, due to the trend in global warming reported around land and ice surfaces, the troposphere (>12 km in altitude) and stratosphere (12 - 45 km in altitude), and oceans of these regions (Smith, 2011; I.P.C.C., 2013). The most recent of these are calving events on Peterman Ice Sheet (Haggin, 2012; Mooney, 2017), Larson C ice shelf (Rice, 2017) and record lows in Arctic sea ice generation (Le Page, 2017).

The physical, biogeochemical and microbiological characteristics of glaciers play an integral role in the survival of the European Alpine (Sharp *et al.*, 1999), High Arctic (Skidmore *et al.*, 2000) and Norwegian Arctic (Hodson *et al.*, 2008) glacier ecosystems. Glacial ecosystems are subdivided into 3 zones (Figure 1. 1) that were

designated after microbes were recovered from within each of these zones (Price, 2000; Christner *et al.*, 2003b; Stoeck *et al.*, 2007): the subglacial region located at the ice and bedrock interface, the englacial region defined as the area within the glacial ice and the supraglacial region, which is the air-exposed surface of the glacier. Each habitat is subject to extreme local (environmental) pressures (temperature, wind, ultraviolet and visible radiation), with glacial surfaces additionally influenced by snow accumulation and ablation, elevation and altitude, impacting biological fecundity and survivorship. The ecology of glacier environments is strongly influenced by marine and ice margin habitats as a result of proximity, in the form of aeolian transport of dust particulates and microbial propagules (Griffin *et al.*, 2001; Harding *et al.*, 2011).

Cold habitats form a unique and novel locale for significant microbial diversity, functional potential and activity (Cowan and Ah Tow, 2004; Hodson *et al.*, 2008). Mountain glaciers, ice sheets and shelves, bedrock, sea ice, icebergs and snow of the Arctic and Antarctic, show abundant psychrophilic and psychrotolerant communities inhabiting niche ecosystems, with both biotic and abiotic factors influencing their establishment and proliferation in the different habitats (Price, 2000; Skidmore *et al.*, 2000; Castello and Rogers, 2004; Hell *et al.*, 2013; Mitchell *et al.*, 2013). Recent advancements in the understanding of cryospheric environments have encouraged the investigation of the role of microbes in glacial processes. Despite the increased focus on research of these regions in the last decade, there is still considerable

knowledge and diversity to be uncovered about microbiota in cold ecosystems and how they function (Cowan and Ah Tow, 2004; Hodson *et al.*, 2008).

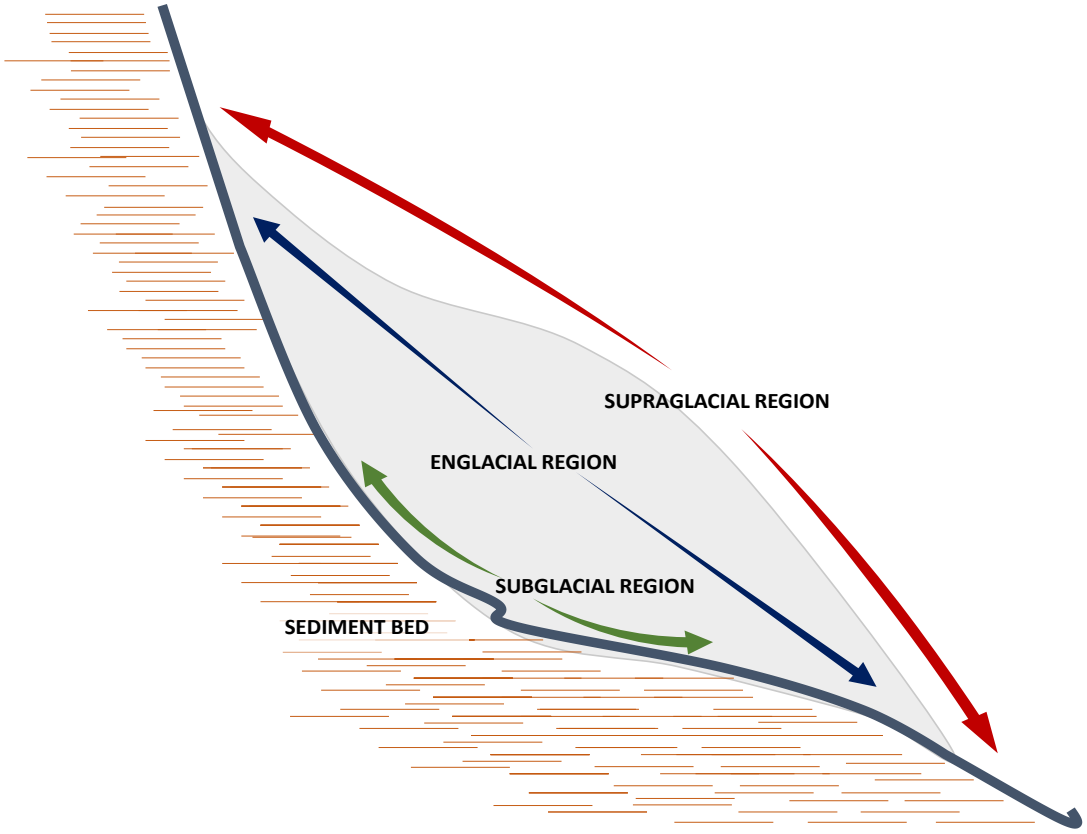

Figure 1. 1 A general depiction of subglacial, englacial and supraglacial zones. The subglacial zone lies close to the bedrock, the englacial zone is within the ice, which has ephemeral lakes and active water flowing through, and the supraglacial zone is on the surface and is one of the most photosynthetic regions of glaciers.

1.1. THE SUPRAGLACIAL ECOSYSTEM OF GLACIERS AND ICE SHEETS

The supraglacial zone is the uppermost layer on glaciers, that is characterised by annual and seasonal fluctuations in glacial mass balance and temporal and spatial variations that influence the rate of glacial melt, thereby glacier recession. Polar glaciers receive relatively lower snow accumulation and experience correspondingly low ablation when compared to temperate glaciers, resulting in a slower response to localised weather and climatic conditions (Benn and Evans, 2010). This creates a

unique set of parameters for microbial life inhabiting the glacial photic zone (Edwards *et al.*, 2014a), that has the perfect combination of the elements essential for life (heat, light and liquid water), making it an extremely photosynthetically active ecosystem for a zero degrees Celsius environment (Hodson *et al.*, 2008).

1.1.1. The effect of aeolian distribution on ice surfaces

Aerobiological and biogeographical investigations have highlighted the roles of weather, stochastic environmental processes and anthropogenesis in the physical distribution, diversity and survival of microbes that utilise the troposphere and stratosphere as a habitat and conduit (Womack *et al.*, 2010; Smith, 2011). It is proposed that natural (volcanic eruptions, thunderstorms and monsoons) and anthropogenic effects (air traffic and industrialization) influence the microbial diversity and transport of stratospheric air to the poles via Brewer Dobson circulation, depositing microbes and dust particulates to cold regions (Griffin *et al.*, 2001). Reports on climate and precipitation patterns have shown that live or dead airborne microbes contributing to cloud and ice condensation nuclei (Burrows *et al.*, 2009) have a greater chance at falling onto the ice, as a result of gravitational stimulation or precipitation. This is in contrast to microbes in the stratosphere that are likely to travel greater distances, as has been documented in cases of animal (Griffin *et al.*, 2001), human (Chen *et al.*, 2010) and plant (Haga *et al.*, 2013) infectious diseases. Strong local aerial transport of microbiota has been recorded over the High Arctic and Antarctic snow region, however, a proportion of non-local biota (bacterial and eukaryote) have also been observed and previously detected in small sub unit rRNA

gene region analysis, indicating global aeolian transport as a contributing factor (Hughes and Lawley, 2003; Pearce *et al.*, 2009; Cowan *et al.*, 2011; Harding *et al.*, 2011). This may provide an explanation for the appearance of albedo-affecting dust particles on polar ice and snow from global locations and in relation to their effect on melt in the larger climate change question.

1.1.2. Microbial ecology and diversity of ice sheets and glaciers

Microbial communities that inhabit supraglacial microniches are derived from aeolian transport (Cowan and Ah Tow, 2004), microbial and nutrient inoculants from the englacial zone (Sharp *et al.*, 1999; Hodson *et al.*, 2008) and marine and ice-marginal region aerosols, aiding in the formation of hotspots of microbial activity on the weathering crust (Harding *et al.*, 2011; Edwards *et al.*, 2013c). This thesis focuses on the High Arctic (Figure 1. 2A) and Greenlandic (Figure 1. 2B) ice caps, ice sheets and glaciers that have an ecologically important role in the polar biosphere as a result of the polar amplification effect and their communities being highly sensitive to environmental changes. As such they serve an important ecological purpose from a research standpoint, as ecosystem health can be projected from microbial responses to widespread environmental stressors.

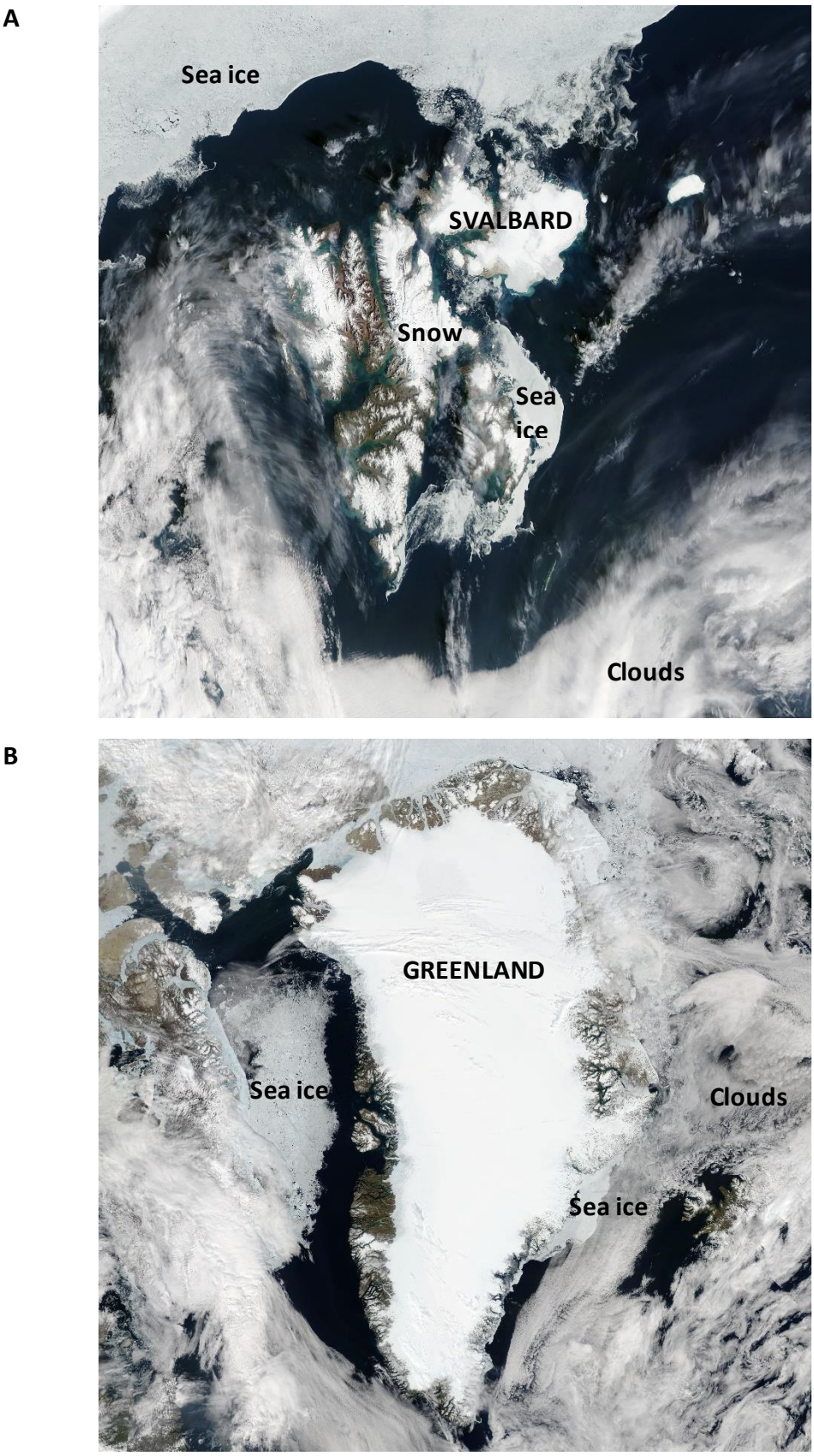

Figure 1. 2 Moderate Resolution Imaging Spectroradiometer (MODIS) images of (A) the Svalbard archipelago as it appeared on 9 August 2015 and (B) Greenland as it appeared on 29 June 2015. Photo credit: NASA Earth Observatory.

The supraglacial habitat is a reservoir of microbial life (Vincent, 2000; Priscu and Christner, 2004) and is characterised by a cosmopolitan consortium residing in snow packs, supraglacial streams and cryoconite holes formed from dust particulates (Table 1. 1). The diversity observed in this ecosystem is contributed by heterotrophic and phototrophic bacteria, microalgae, phytoflagellates, fungi, viruses, rotifers, tardigrades and diatoms (Hodson *et al.*, 2008; Edwards *et al.*, 2014b; Lutz *et al.*, 2015a; Rassner *et al.*, 2016), that have been cultivated and abundantly observed by rRNA sequence analyses, in snowpacks, supraglacial streams and cryoconite on the glacial surface (Stibal *et al.*, 2006; Harding *et al.*, 2011; Cameron *et al.*, 2012; Hell *et al.*, 2013; Edwards *et al.*, 2014b).

Table 1. 1 Microbial taxa commonly observed in cryosphere environments.

Microorganism	**Habitat**	**References**
Acidobacteria	Air, snow, sediment	Harding *et al.* (2011), Cameron *et al.* (2012), Edwards *et al.* (2014b), Cameron *et al.* (2016)
Actinomycetes	Air, snow, sediment	Harding *et al.* (2011), Cameron *et al.* (2012), Edwards *et al.* (2014b)
Bacteroidetes	Air, snow, sediment	Harding *et al.* (2011)
Cyanobacteria	Air, snow, sediment	Stibal *et al.* (2006), Harding *et al.* (2011), Cameron *et al.* (2016)
Firmicutes	Air	Harding *et al.* (2011)
Alphaproteobacteria	Air, sediment	Harding *et al.* (2011), Zarsky *et al.* (2013), Edwards *et al.* (2014b)
Betaproteobacteria	Air, snow, sediment	Hell *et al.* (2013), Zarsky *et al.* (2013), Edwards *et al.* (2014b)
Gammaproteobacteria	Air, sediment	Harding *et al.* (2011), Zarsky *et al.* (2013), Edwards *et al.* (2014b)
Pennate diatom	Air, sediment	Harding *et al.* (2011), Stibal *et al.* (2006)
Cytophagales	Sea, sediment	Harding *et al.* (2011), Edwards *et al.* (2013b)
Roseobacter	Sea, sediment	Harding *et al.* (2011), Mortazavi *et al.* (2015)

Table 1. 1 Microbial taxa commonly observed in cryosphere environments (continued).

Microorganism	Habitat	References
Aquaspirilim arcticum	Snow, ice, sediment	Harding *et al.* (2011)
Chroococcales	Snow, ice	Harding *et al.* (2011)
Janthinobacterium	Snow, sediment	Mortazavi *et al.* (2015), Christner *et al.* (2003a)
Nostocales	Snow, sediment	Stibal *et al.* (2006), Cameron *et al.* (2012), Cameron *et al.* (2016)
Ochromonas	Snow, ice	Harding *et al.* (2011),
Oscillatoriales	Snow, sediment	Langford *et al.* (2010), Uetake *et al.* (2010), Cameron *et al.* (2012)
Polaromonas sp.	Snow, sediment	Mortazavi *et al.* (2015), Hell *et al.* (2013), Cameron *et al.* (2012)
Pseudomonas syringae	Snow, ice	Harding *et al.* (2011)
Rhodoferax	Snow, ice	Harding *et al.* (2011)
Cryptophyta	Snow, ice	Harding *et al.* (2011)
Bacillariophyta	Snow, ice, sediment	Stibal *et al.* (2006),
Chrysophycea	Snow, ice	Harding *et al.* (2011)
Chloromonas	Snow, sediment	Takeuchi and Kohshima (2004), Uetake *et al.* (2010), Lutz *et al.* (2016)
Chlamydomonas	Snow, sediment	Stibal *et al.* (2006), Lutz *et al.* (2016)
Microglena sp.	snow	Lutz *et al.* (2016)
Raphidonema sempervirens	Snow	Lutz *et al.* (2016)
Ancylonema nordenskiöldii	Snow	Takeuchi *et al.* (2003), Lutz *et al.* (2016)

Ice habitats are permeable systems that interlink habitats due to their hydrological drainage systems, comprising distinct effects, i.e. the ability of surface meltwater to penetrate the porous ice, the potential impact of glacial runoff into downstream ice and marine ecosystems and the establishment of ephemeral hydrological connections from supraglacial to subglacial habitats (Irvine-Fynn *et al.*, 2011). Water flow through the weathering crust promotes microbial transport down glacier (Irvine-Fynn *et al.*, 2012) and has the potential to regulate the structure and function of

cryoconite bacterial communities (Edwards *et al.*, 2011) through translocation of soluble materials and microbes. As habitats rich in microbial diversity, they are foci of supraglacial biochemical transformation, as well as delivery, storage and elution of dissolved organic and inorganic solutes, which are integral to sustaining the microbial ecology within hydrologically linked supraglacial habitats (Cook *et al.*, 2015a).

1.1.2.1. Snow-derived habitats

Up to 35% of the terrestrial area on Earth is covered in snow, either permanently, in the case of polar and high altitude regions, or temporarily, in the lower altitude cryosphere (Hell *et al.*, 2013). Ionic (Cl^-, NO_3^-, Mg^{2+}, Ca^{2+}, SO_4^{2-}) changes in snow, due to precipitation events and meltwater runoff, lead to pH and nutrient discrepancies that demonstrate seasonal and annual variation in Alpine (Waldner and Burch, 1996) and ice sheet nutrient budgets. Early in the melt season, solutes in surface waters are readily leached into the drainage system, creating a vertical water profile that has increasing concentrations with depth, when excluding horizontal advection through liquid vein networks (Knight, 1999). The importance of glacial meltwater phosphorous (P) concentrations has been readily observed, due to the effects on rock weathering and suspended sediments in catchment P dynamics, as well as the integral role of nitrate anion (NO_3^-) as a tracer of snowmelt and in the promotion of microbial activity (Hodson *et al.*, 2005).

Snow provides a habitat for microbial activity derived from precipitation and deposition, thereby driving integral feedbacks within the cryospheric ecosystem

(Miteva, 2008; Bachy *et al.*, 2011). However, this process additionally induces wash-out of cells and dilution or concentration of the original chemical composition, affecting structural changes in the seasonal bacterial communities. Ice and snowpack communities of the Arctic, Alpine and Antarctic are a dynamic reservoir for nutrients and create a unique ecosystem for microbial inhabitants (Miteva, 2008). Liquid veins between snow particles and liquid film on deposited mineral grain surfaces facilitate microbial transport, metabolism and survival in snow and ice (Miteva, 2008). The microbial consortium present is characterised by a complex and dynamic community of bacteria, algae, protozoa and rotifers that support carbon cycling through autotrophic fixation of carbon and ammonia oxidisation (Anesio and Laybourn-Parry, 2011), diatoms (*Bacillariophyceae*), fungi (primarily *Ascomycota*) and wind-dispersed spores and pollen grains from land plants (Felip *et al.*, 1995; Fountain *et al.*, 2009; Harding *et al.*, 2011; Hell *et al.*, 2013), the latter of which are largely inactive (Harding *et al.*, 2011). Photosynthetic psychrotolerant algae, evidenced by prolific snow algal blooms in summer periods (Lutz *et al.*, 2015b), may be the principle contributors to primary production and biogeochemical cycling (Miteva, 2008; Stibal *et al.*, 2012), as a result of their rapid initial onset upon melting. Additionally, the endemic bacterial community that is common to all cryospheric habitats may be integral in maintaining the geochemical parameters, as they are more sensitive to the availability of allochthonous carbon and local geology and physical location (Lutz *et al.*, 2016).

Meltwater runoff is one of the least studied hydraulic process on ice sheets, despite them contributing to more than half the loss of the total mass of the Greenland Ice

Sheet during the summer (Smith *et al.*, 2015). Meandering ephemeral streams have an essential role in meltwater transport between habitats in the supraglacial zone and the englacial and subglacial zones, and are subjected to pronounced daily temperature fluctuations (Wilhelm *et al.*, 2013) and seasonal changes in weathering crust permeability, which control storage and transmission of nutrients and microbes within the weathering crust (Cook *et al.*, 2016b). This contributes to the diversity of glacier-fed streams (Wilhelm *et al.*, 2013) by seeding the neighbouring environments with intact microbial cells (Irvine-Fynn *et al.*, 2012), as well as providing nutrients and dissolved organic carbon across the ice sheet. In glacial stream environments, primary producers, in the form of algal and cyanobacterial biomass, are the major sustainers of the heterotrophic community members, supported by low dissolved organic carbon biomass and concentrations (Battin *et al.*, 2001), as a result of hydrological disturbances (Hock, 2005). Members of the class *Betaproteobacteria* have been identified as high abundance glacial stream communities, consistent with other oligotrophic freshwater ecosystems, despite taxonomic identification being limited to the family level (Battin *et al.*, 2001; Wilhelm *et al.*, 2014).

1.1.2.2. Sediment-rich habitats

Sediment deposition and organic matter on the glacial surface reduces the ice surface albedo, inducing supraglacial melting in warmer summer periods that results in the formation of cryoconite holes (Figure 1. 3A), quasi-circular cylindrical depressions in the ice (Takeuchi, 2002; Anesio *et al.*, 2009; Hodson *et al.*, 2010b; Cook *et al.*, 2015b) at high latitude and high Alpine regions (MacDonell and Fitzsimons, 2008; Miteva,

2008). These holes freeze over during winter and sometimes form entombed microhabitats isolated from the atmospheric system upon internal melting during colder summer months (Figure 1. 3B). These darkened regions of ice have a unique physiology and ecology (Langford *et al.*, 2010) that interact with the hydrology of the porous ice surface (Edwards *et al.*, 2011; Cook *et al.*, 2015a; Cook *et al.*, 2016b). Investigations into the composition of cryoconite at the level of aggregates and individual granules, has profoundly flourished in a brief period (Takeuchi *et al.*, 2001b; Hodson *et al.*, 2010b; Langford *et al.*, 2010). Distinct geographical differences exist in cryoconite size, with Chinese glaciers having granule diameters from 1.3 - 98 µm compared to Svalbard glaciers, with diameters of 0.02 - 2000 µm. Furthermore, insights on cryoconite structure and diversity allowed the realisation of their integral role as a significant ecological and climatic microbial ecosystem in the supraglacial habitat (Cameron *et al.*, 2012; Edwards *et al.*, 2013b; Edwards *et al.*, 2013c; Cook *et al.*, 2015b).

A

B

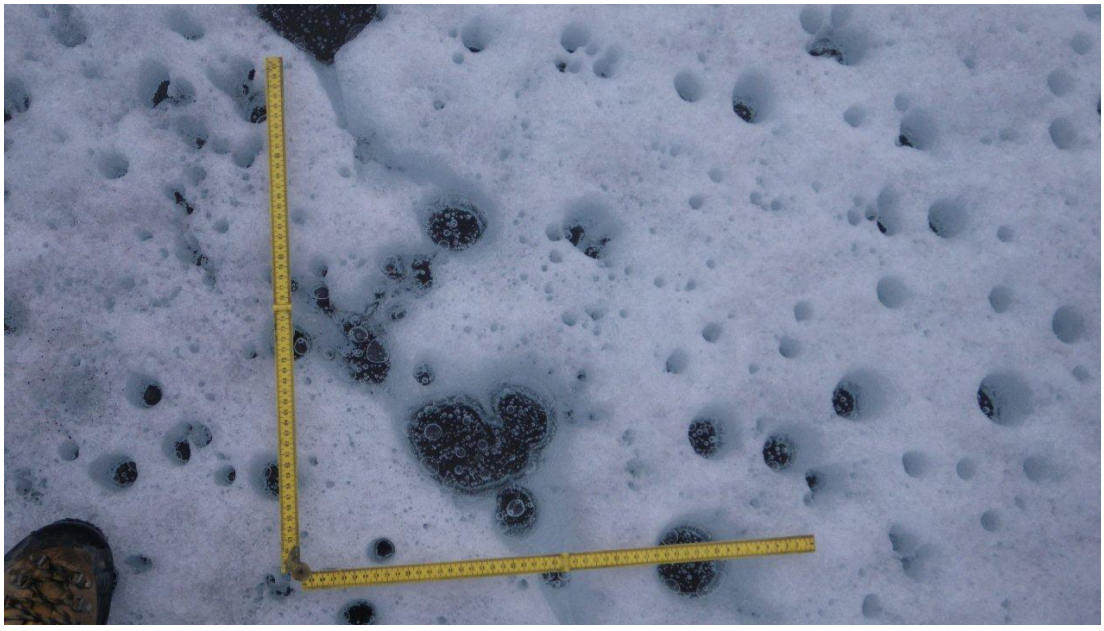

Figure 1. 3 Cryoconite holes as witnessed on the surface of Greenland glaciers. The cylindrical depressions exist with (A) a layer of melt water over cryoconite sediment in summer and with (B) thin ice lids in winter. Photo credit: Dr. Arwyn Edwards. Icy Bear for scale.

Accumulation and adhesion of surface dust particles, humic material and microbiota accelerates glacier melting, independent of global warming or cooling trends. Humic acids maintain the presence of liquid water on glacier surfaces and chemical conditions on individual granules (Takeuchi *et al.*, 2001b; Takeuchi, 2002), while the extracellular polymeric substances (EPS) exuding microbiota adhere to the particles (Langford *et al.*, 2010) and utilise solar incident radiation to photosynthesise (Cook *et al.*, 2010). This increases intrinsic temperatures, melting the ice and forming cryoconite holes containing microcosms of liquid water, aeolian particulates and mineral aggregates, fungal (Edwards *et al.*, 2013a), algal (Mueller *et al.*, 2001) and bacterial assemblages (Cameron *et al.*, 2012; Bellas *et al.*, 2013; Edwards *et al.*, 2013b; Margesin *et al.*, 2013; Edwards *et al.*, 2014b; Gokul *et al.*, 2016).

Many investigations have revealed that colonization of mineral debris by *Cyanobacteria* promotes the formation of cryoconite aggregates (Takeuchi *et al.*, 2001b; Langford *et al.*, 2010; Takeuchi *et al.*, 2010), which further accelerates surface melting (Irvine-Fynn *et al.*, 2011; Irvine-Fynn *et al.*, 2014) and supraglacial carbon cycling, during the melting season (Cook *et al.*, 2010; Yallop *et al.*, 2012). Accumulated dust particles form a single layer of wet, granular material (Cook *et al.*, 2016a), creating a eutrophic habitat that supports a complex, yet truncated, food web (Hodson *et al.*, 2008; Miteva, 2008; Anesio and Laybourn-Parry, 2011). Analysis of the microbial diversity and chemical components reveal a niche rich in eukaryotic algae, (diatoms and snow microalgae) and *Cyanobacteria* (Stibal *et al.*, 2006) that act as photosynthesizers, and numerous other species of psychrotolerant and psychrophilic

heterotrophic bacteria. Photosynthetic *Cyanobacteria* are recognized as chief contributors to primary production in cryoconite holes, providing a foundation for heterotrophy by *Alpha*- and *Betaproteobacteria*, *Bacteroidetes, Actinobacteria* and *Firmicutes* (Hodson *et al.*, 2008; Edwards *et al.*, 2013b; Møller *et al.*, 2013). Virus-like particles (VLP) also colonize cryoconite holes (Rassner *et al.*, 2016) and play a significant role in nutrient and carbon recycling. Granular aggregates have a distinctly higher VLP:bacteria ratio (8) compared to water (0.24), validating the presence of living and active microorganisms, as their activity is directly proportional to their ability to infect living microbes (Hallbeck, 2009).

1.1.3. Specialisation of microbiota to supraglacial environments

Most early research on cold adapted organisms centers on understanding the diverse mechanism of psychrophilic response to cold and other stressors (Deming, 2002). These psychrotolerant (more common) and psychrophilic (less common) microbes have evolved features to encourage their survival on glaciers and ice sheets that experience uniquely high incident radiation and low temperatures (Denef *et al.*, 2016) (Table 1. 2). This includes seasonal dormancy in endemic bacteria like *Polaromonas* (Shade *et al.*, 2012), pigment production by algae and C*yanobacteria* (Remias *et al.*, 2005; Jungblut *et al.*, 2010), production and reuse of extracellular polymeric substances by cyanobacterial communities (Stuart *et al.*, 2015; Chrismas *et al.*, 2016), ultraviolet protective sheaths (Morgan-Kiss *et al.*, 2006), expression of enzymes and cryoprotectants preventing freeze-thaw induced cell lysis (Morgan-Kiss *et al.*, 2006; Edwards *et al.*, 2013b) and higher concentrations of polyunsaturated

membranous fatty acids and intracellular lipids (Edwards *et al.*, 2013b; Zalar and Gunde-Cimerman, 2014).

Table 1. 2 Microbial mechanisms of response to stressors.

Mechanism	Action	Reference
Extracellular polymeric substances	Buffering and cryoprotection against ice damage and salinity. Adherent nature permits biochemical transfer between adjacent cells.	McLean (1918), Ewert and Deming (2013), Chrismas *et al.* (2015)
Cold shock proteins	Protein folding and DNA transcription, regulation, recombination translation. Cold active enzymes favour high flexibility amino acids for improved access to catalytic sites.	Beales (2004), Ewert and Deming (2013)
Cell membrane stress-sensing regulatory systems	Two components regulatory systems. Morphological (cell shape) modifications. Increased membrane rigidity.	Ayala *et al.* (2012), Ewert and Deming (2013), Edwards *et al.* (2013c)
UV radiation response	Carotenoid production for quenching. Antioxidant compounds. Mycosporin-like amino acid synthesis.	Beales (2004), Morgan-Kiss *et al.* (2006), Ewert and Deming (2013)

A key component to understanding nutrient cycling and ecosystem development in supraglacial ecosystems involves understanding the relationship between microbial community structure and function (Hodson *et al.*, 2008). Nutrients in cryoconite are supplied via snow, rain, marine and terrestrial aerosols in addition to microbial metabolism and necromass, leading to seasonal granule growth and aggregation, mostly in summer months and are entombed during winter or cold periods, but still remain biologically active (Takeuchi *et al.*, 2010). Microbes in supraglacial aquatic habitats are usually limited by access to biomass limiting macronutrients such as

phosphorous (P), nitrogen (N), silica (Si) and iron (Fe), due to high bioreactivity, high turnover rates or inaccessibility due to chemical state. These elements are essential for biological utilisation and energetic metabolism processes. Shot-gun sequencing of cryoconite metagenomic DNA identified contiguous regions that associate microbes with N, sulphur (S), Fe and P cycling processes that correspond with ammonia recycling, organic and inorganic sulfur metabolism, aromatic metabolism and anaerobic degradation, phosphate metabolism, Fe^{2+} and Fe^{3+} acquisition (Edwards *et al.*, 2013b). Carbon and nitrogen cycling and photoautotrophism in cryoconite holes and ice surface habitats are likely to be accounted for by highly active *Cyanobacteria* from the genera *Phormidium* and *Leptolyngbya* (Chrismas *et al.*, 2016) and microalgal genera *Chlamydomonas*, *Chloromonas* and *Microglena* (Møller *et al.*, 2013; Lutz *et al.*, 2015b). Chemoautotrophic or heterotrophic bacterial and viral processes are assumed to play a role in overall biogeochemical cycling in glaciers (Hodson *et al.*, 2008) in order to maintain cellular processes in supraglacial communities.

1.2. BIOGEOGRAPHIC, BIOTIC AND ABIOTIC EFFECTS ON SUPRAGLACIAL HABITATS

The adoption of macrobiotic ecological analytical processes in microbial ecology has recently revolutionised the understanding of microbes and their functional roles (Nekola and White, 1999; Martiny *et al.*, 2006). In the last decade, several studies have highlighted the effects of taxa-area interactions (Shade *et al.*, 2013), distance decay effects (Bell, 2010), temporal scaling of microbial diversity (Swenson *et al.*,

2013) and spatial distributions (Stibal *et al.*, 2015b). These studies have shown that microbial diversity often varies through geographic time and space, based on environmental factors such as latitude, elevation, degree of isolation and habitat (Fierer *et al.*, 2005). Recent rapid changes in glacial ecosystems validate the newfound focus on biogeographical patterns and potential mechanisms that generate these patterns (Martiny *et al.*, 2006; van der Gast, 2015). Extreme environments such as ice caps, glacial outlets and ice sheets can be considered ideal habitats for novel microbial biogeography studies, as they are relatively low in microbial diversity and microbiota can be distributed by passive mechanisms in the environment (Darcy *et al.*, 2011; Franzetti *et al.*, 2013). This is in addition to their vastly different topography that has the potential of influencing microbial community structure. The interactions of glacial systems with climate, water and landscape assume considerable scientific and societal concern, which pre-dates findings that glaciers, ice caps and ice sheets comprise microbial ecosystems (Hodson *et al.*, 2008). It is now well recognised that the activity of biologically diverse microbial ecosystems associated with glacial habitats interact with both the dynamics of glacial systems and influence biogeochemical cycles (Edwards *et al.*, 2014b; Hood *et al.*, 2015; Rime *et al.*, 2016). Furthermore, there is valid support for both global cosmopolitism and local endemicity of geographical distribution across genotypes of individual species (Franzetti *et al.*, 2013). This knowledge allows improved prediction of the role of underlying spatial patterns on the larger scale role of microorganisms.

1.3. IMPACT OF CLIMATE CHANGE ON POLAR SYSTEMS

Glaciers and ice sheets experience brief periods of annual melt, with a vast majority of European glaciers experiencing increasing rates of recession since the 1980s, according to the Glaciers CLIM 007 (E.E.A., 2016). Dramatic repercussions have been witnessed in the last decade, affecting record breaking melt rates on the Greenland Ice Sheet between 2007 and 2016 (N.S.I.D.C. *et al.*, 2016), heightening the presence of dark areas of liquid water, thereby promoting biogeochemical cycling on the surface, particularly for microbial communities associated with sediment, covering substantial portions of the ice and snow (Anesio and Laybourn-Parry, 2011). Anthropogenic contributions to environmental emissions in the form of carbon, methane, chlorofluorocarbons and nitrous oxides (greenhouse gases) have exhibited remarkable increases since 1750 (I.P.C.C., 2013; I.P.C.C., 2014). This is primarily due to the increased use of fossil fuels and changes in land use in the industrial era and between 1980 and 2011. Glacier retreat is estimated to reduce the current volume of glaciers by 22 - 84% under moderate and 38 - 89% high greenhouse effects. A large proportion of these glaciers show drastic decreases in net mass balance since 1985 (E.E.A., 2016). Past trends indicate an increase in thickness of some ice caps at high elevations in north-eastern Svalbard, however overall estimates show a declining mass balance (Nesje *et al.*, 2008; Engelhardt *et al.*, 2013; Hanssen-Bauer *et al.*, 2015). This effect is primarily attributed to increased summer temperatures, however additional influence is afforded by changes in winter precipitation, reduced albedo and debris coverage (Bevan *et al.*, 2007; Lang and Erpicum, 2015). Localised environmental factors and anthropogenesis may not be the sole drivers of climate change and CO_2 content in the atmosphere, as the strongest influences in cryosphere

niche community dynamics are generated by carbon and nitrogen production from microbial activity in High Arctic glaciers (Hell *et al.*, 2013).

1.4. SUPRAGLACIAL SYSTEMS BIOLOGY

Examining the metaorganism, in this case the microbial community, at the level of DNA, RNA, proteins and metabolites, along with *in situ* environmental characteristics, can unravel the interaction between different parts of the glacial ecosystem ultimately responsible for its emergent properties. High throughput technologies have revolutionised the 'omics approach to microbial community characterisation, as a consequence of metagenomic, metatranscriptomic, metaproteomic, metabolomic and stable isotope probe (SIP)-omics to investigate community structure, function activity and interactions (Abram, 2015). Individually, these techniques each have inherent flaws that can be overcome by data integration, establishing a highly coherent interpretation of microbial community structure, diversity and activity in environmental ecosystems.

Snow and freshwater (Hell *et al.*, 2013; Møller *et al.*, 2013), glacier ice (Miteva, 2008), outlet glaciers (Mikucki and Priscu, 2007; Řeháková *et al.*, 2009) and sediments on the surface and below glaciers (Stibal *et al.*, 2012) have been characterised using a variety of microbiological, metagenomic and metabolomic techniques. A substantial amount of research in the last decade has been aimed at understanding the biological and environmental controls of snow and cryoconite microbial communities. Considerable effort has gone into describing these communities in Svalbard (Edwards

et al., 2011; Edwards *et al.*, 2013c; Grzesiak *et al.*, 2015), Austrian Alpine regions (Edwards *et al.*, 2014b; Wilhelm *et al.*, 2014), Alaska (Takeuchi *et al.*, 2003), China (Takeuchi *et al.*, 2010) and Antarctica (Anesio and Laybourn-Parry, 2011; Cameron *et al.*, 2012) using traditional microbiological methods, clone library sequencing and high throughput metagenome sequencing. As such, further insight into the emergence and dispersal of cryoconite communities (Edwards *et al.*, 2013a; Edwards *et al.*, 2013c) and the communities in their direct surroundings (Hell *et al.*, 2013) has been brought to light, as well as a thorough analysis of the communities physical, chemical and thermodynamic characteristics and the geological characterization of individual cryoconite granules (Takeuchi *et al.*, 2001b; Hodson *et al.*, 2010b; Edwards *et al.*, 2013c).

Recent research has provided insight into the active supraglacial community of Greenlandic cryoconite and ice through 16S cDNA sequence analysis (Stibal *et al.*, 2015b; Cameron *et al.*, 2016). Investigations into the cryoconite metabolome reveal the high relative influence of solar radiation on the community, predominantly for primary production and extracellular polymer production (Cook *et al.*, 2016a). Svalbard glaciers have also provided a source of metabolomic insights, particularly for microalgal communities and their roles as primary producers that additionally promote the albedo-mediated melt (Lutz *et al.*, 2015b). However, little evidence exists for the merging of these different data on a temporal and spatial scale, providing an incomplete depiction of the supraglacial environment in these locations that are sensitive to climatic and ecological changes on the surface. A systems

approach to supraglacial microbial ecology would permit the elucidation of the associations between microbes in the glacial photic-zone, capturing the interconnected nature of the physical and biological processes that predominate it.

1.5. THESIS AIMS AND OBJECTIVES

1.5.1. Central hypotheses

Cryoconite holes are well recognised "ice-cold hot-spots" of microbial diversity and activity on Arctic and mountain glaciers (Edwards *et al.*, 2013a). The mobility of cryoconite debris in cryoconite holes open to the atmosphere and hydraulic porosity of the ice surface mean these are dynamic and inter-dependent habitats, seeded and nourished by nutrient and microbial deposition in snowpacks and ephemeral streams. Consequently, cryoconite ecosystems and the associated weathering crust habitats on an individual glacier comprise a metacommunity assembled by predominantly deterministic mechanisms. The recounted literature has revealed the remarkable chemistry, community structure and diversity of cryoconite holes, however limited information exists defining the exact mechanisms responsible for their establishment and longevity. As the dominant microbes of cryoconite habitats, bacteria are integral to heterotrophic and photoautotrophic metabolism prevalent in the cryoconite food web. Ergo, they can provide crucial insights on cryoconite biosphere fluctuations at the genetic and metabolic level. To this end, the following three key hypotheses were proposed:

a. Cryoconite formation is a result of biotic interactions from initial allochthonous input on the glacier surface, whereby filamentous and

extracellular polymeric substance producing microbiota adhere microbially colonised particulates to sustain a metabolically active niche,

b. The glacial surface bacterial community is sensitive to climatic changes, whereby escalating temperatures, solar incident radiation and linked habitats impact species selection,
c. Supraglacial bacterial assemblages are governed by interspecies competition, whereby taxon-taxon interactions in any specific habitat fluctuate over a transitory period.

1.5.2. Research aims and objectives

The structure and function of readily abundant bacterial communities in the glacial photic zone can be predicted via the application of multiple, complementary and interdisciplinary 'omic approaches. In this body of work, these techniques were applied to gain an improved understanding of the complex interactions of the cosmopolitan organisms that survive under unique chemical, environmental and geological restraints across the Svalbard and Greenland glacial landscapes, from the scale of localised individual cryoconite holes to an entire ice sheet. To fulfil this aim, three main objectives were constructed:

a. To unravel the mechanism of cryoconite conglomeration by active seed communities,
b. To characterise the bacterial community of High Arctic glacier cryoconite and surfaces and their relationship with differing topography and seasonal microclimate,

c. To investigate the influence of temporal and spatial dynamics on cryoconite and surface bacterial community structure and function.

1.5.3. Thesis structure and experimental design

This thesis comprises 5 distinct elements that detail the investigations of cryoconite under optimal conditions in a synthetic microcosm (Chapter 3), the effect of distance, time and space decay on the biodiversity of cryoconite communities on an Arctic ice cap (Chapters 4 and 5), an Arctic valley glacier (Chapter 6), and the Greenland Ice Sheet (Chapter 7), addressing objective a (Chapter 3), objective b (Chapters 4, 6 and 7) and objective c (Chapters 3, 4, 5 and 6). Research focuses on the bacterial contingent as they numerically dominate the phylogenetic diversity in the Arctic cryosphere. Eukaryotic microbiota are mentioned where they indicate key involvement in primary productivity. Experiments were designed to highlight microbial contributions to cryoconite aggregation by microscopy and metabolite fingerprinting, and further unravel details of the taxa present and active in natural scenarios, by means of 16S rRNA gene and 16S cDNA high throughput sequencing methods and sample specific metabolite profiles.

CHAPTER 2 - GENERAL METHODS

Consistent application of technical, chemical and molecular procedure is essential to perform highly reliable cross environment comparisons. In this piece of work, general methods have been applied in each experimental chapter to evaluate bacterial diversity and function. These techniques are described in the following pages, with any minor modifications and specific techniques discussed in detail within respective chapters.

2.1. LOCATION OF FIELD SITES

Svalbard is a Norwegian Archipelago consisting of smaller islands located 74° to 81° north latitude, and 10° to 35° east longitude, with Spitsbergen being the largest island. The landforms were created from repeated freeze thaw events during the ice age resulting in the plateaus being carved into fjords, valleys and mountains. West of this lies Greenland, that houses the world's second largest ice sheet, at 71.7069° north latitude and 42.6043° west latitude. The terrain is mostly flat, apart from a region with a narrow, mountainous rocky coastline. The climate in both regions can be described as Arctic to Sub-Arctic, with majority of their terrestrial surfaces covered by ice and snow and influence from the marine environment at the peninsula. In Svalbard, Foxfonna glacier near Longyearbyen, was sampled at the ice cap for Chapters 4 and 5, and along a transect of the unnamed north facing valley glacier (hereafter Foxfonna valley glacier) for Chapter 6. In Greenland, sampling took place at the Kangerlussuaq S6 weather station in southwest Greenland for Chapter 7.

2.2. SAMPLE COLLECTION AND PROCESSING

Sampling of all glaciers occurred during the summer ablation season. Samples were collected by Dr. Arwyn Edwards (Foxfonna ice cap and Greenland Ice Sheet), Prof. Andy Hodson and the Hodson lab (Foxfonna ice cap), Dr. Tristram Irvine-Fynn (Foxfonna ice cap and valley glacier) and Dr. Karen Cameron (Greenland Ice Sheet). The location of each sampling site was recorded by GPS to approximately 10 m accuracy. Environmental conditions that were recorded at each site are detailed in individual chapters. All laboratory processes were performed under sterile conditions in a bleach-decontaminated horizontal laminar flow safety cabinet, Model 50548/1 with a 99.999% HEPA filter (MDH Ltd, Hants, UK), using DNA and RNA free plastic ware and reagents.

2.2.1. Cryoconite sample collection

Cryoconite debris from summer cryoconite was aspirated into sterile 2 mL microcentrifuge tubes using sterile syringes (Figure 2. 1A), preserved in LifeGuard™ Soil Preservation Solution (MO BIO Laboratories Inc., Carlsbad, CA, USA) and frozen at -20°C before being transferred to -80°C frozen storage and thereafter transported in insulated chilled containers to the UK for long term storage at -80°C.

A

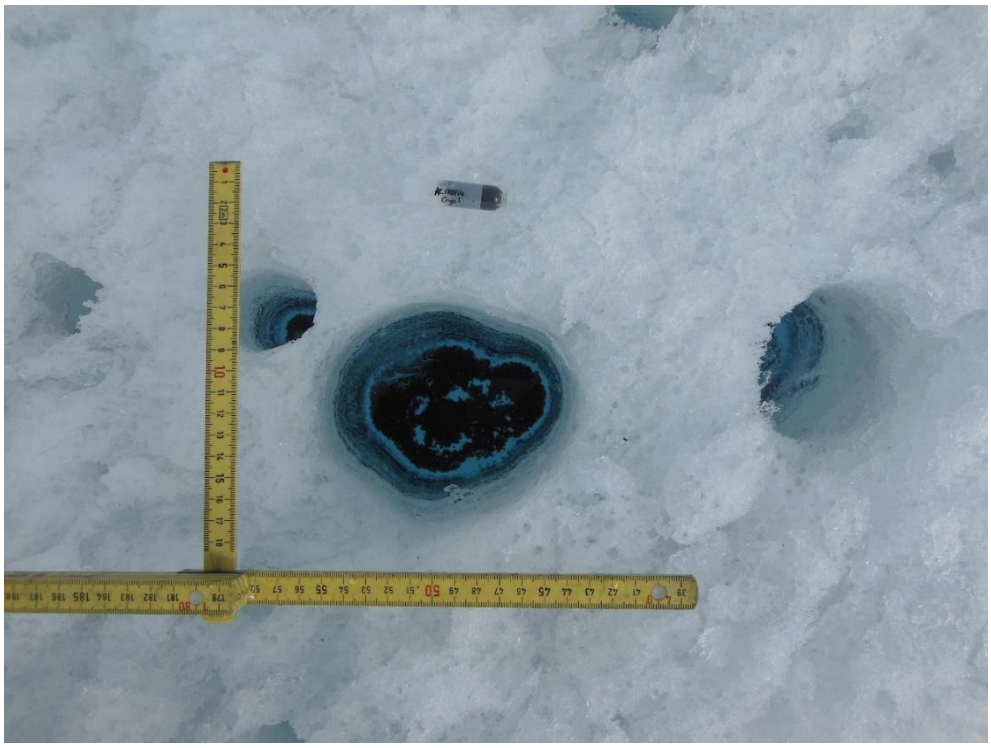

B

Figure 2. 1 Sample acquisition on the Greenland Ice Sheet in July 2014 depicting (A) sediment collection from a cryoconite hole and (B) snow collection from around weather station S6. Photo credit: Dr. Karen Cameron.

2.2.2. Glacial water sample collection

Snow from the ice sheet surface was aseptically collected by scooping samples into sterile Whirl-Pak® bags (Nasco) (Figure 2. 1B) before aseptic melting in sterile beakers, while stream water was collected by aspiration with sterile syringes as with cryoconite. Samples were filtered into Sterivex GP 0.22 µm polyethersulfone filters (Millipore, MA, USA), preserved in LifeGuard™ Soil Preservation Solution (MO BIO Laboratories Inc., Carlsbad, CA, USA) and the ports sealed with the outlet and inlet caps. Stabilized samples were stored on ice in an aluminium container for up to two weeks before transferring to -20°C and transporting to the UK for storage at -80°C.

2.3. METABOLOMICS

Large scale studies of the metabolites extracted from environmental samples allows insight into the interactions occurring within the metabolome (Viant, 2007; Tang, 2011; Lankadurai *et al.*, 2013; Soule *et al.*, 2015). In cryoconite this can be used to ascertain integral microbial pathways and biotic and/or abiotic influences essential for life in an extreme habitat through metabolic profiling and bioinformatic discovery.

2.3.1. Metabolite extraction

In sterile 1.5 mL microcentrifuge tubes (Starlab UK Ltd, Milton Keynes, UK), 3 acetone-cleaned glass beads (Sigma-Aldrich Company Ltd, Poole, UK) were added to cryoconite samples that were freeze dried in a Leybold Hereus Lyovac GT2 vacuum pump at 1 kPa, with a -30°C refrigerated condensation trap (Oerlikon Leybold

Vacuum UK, Chessington, UK) and stored frozen at -80°C until homogenising at 30 Hz for 2 minutes in a Retsch® MM200 ball mill (Retsch GmbH and Company, Haan, Germany). To this, 1 mL of 3°C chloroform:methanol:water (1:2.5:1, HPLC-grade, Fisher Scientific Ltd, Loughborough, UK) was added and the sample agitated thoroughly at 3°C on a Vortex-Genie® 2 Vortex with the MO BIO vortex attachment (MO BIO Laboratories Inc., Carlsbad, CA, USA). Samples were then subjected to centrifugation at 5 000 ×*g* for 3 minutes (3°C) and the supernatant dispensed into clean 1.5 mL microcentrifuge tubes (Cook *et al.*, 2016a) before extract preparation for mass spectrometry.

2.3.2. Mass spectrometry and data processing

Extracts were prepared for mass spectrometry by resuspending 50 µL of the solvent in 200 µL of 70% methanol:water (4°C) in a 2 mL borosilicate glass vial (HiChrom Limited) with Target MicroSert™ flat base inserts (National Scientific Company, Rockwood, TN, USA) and sealed with polytetrafluoroethylene (PTFE) seal aluminium crimp caps (Thermo Scientific™, Waltham, MA, USA). Vials were agitated for 5 seconds with a vortex and stored at -20°C until analysis by Flow Injection Electrospray Ionisation Mass Spectrometry (FI-ESI-MS) using a linear ion trap quadruple (LTQ) mass spectrometer (ThermoFinnigan, San Jose, CA) at the IBERS High Resolution Metabolomics Laboratory (Edward Llwyd Building, Penglais, Aberystwyth University). Data was acquired over the 100 - 1 400 exact ionisation mass (m/z) range and imported into MATLAB (The MathWorks Inc., Natwick, MA, USA), binned to unit mass and then normalised to percentage total ion count (Beckmann *et al.*, 2008). The

resulting data was routinely handled in Microsoft Excel 2013 and imported into PyChem, version 3.0.5g Beta (Jarvis *et al.*, 2006) to generate metabolite loading profiles for multivariate analyses of the obtained metabolites (Edwards *et al.*, 2014b). Metabolites of interest were tentatively identified using the Kyoto Encyclopaedia of Genes and Genomes (KEGG) database and significant predicted metabolites were extracted from the original dataset for multivariate statistical analysis in PRIMER 6/PERMANOVA+ (Clarke and Warwick, 2001), Metaboanalyst 3.0 for univariate statistical analysis, hierarchical clustering analysis (Xia *et al.*, 2015) and PyChem for chemometric and partial least squares (PLS) regression modelling (Jarvis *et al.*, 2006). Models were cross validated using full cross validation whereby data were randomly split into a training set, a cross-validation set and an independent test set. Best fit was assigned by proximity and heterogeneity of samples along the linear fit.

2.4. NUCLEIC ACID EXTRACTION PROCESSES AND TREATMENT

The extraction techniques employed enabled the isolation of high quality DNA and RNA using a chemical-physical lysis approach (Chapter 4) and MO BIO extraction kits (Chapter 6 and 7). While DNA yields have been recorded as high, using classical DNA extraction methods, the change to kit-based extraction was necessary for reduced residual ethanol in samples that could potentially hamper high performance sequencing, as well as being more time efficient considering the quantity of extractions performed in Chapters 6 and 7. All centrifugation steps were performed at 13 000 ×*g*, unless otherwise stated.

2.4.1. Nucleic acid extraction from Foxfonna ice cap cryoconite

DNA from cryoconite granules was extracted using the hexadecyltrimethylammonium bromide-phenol-chloroform bead-beating extraction and polyethylene glycol precipitation (Griffiths *et al.*, 2000) method, as per Hill *et al.* (2016). In 2 mL centrifuge tubes, 0.5 mL of CTAB (10% hexadecyltrimethylammonium bromide, 0.7 M NaCl, 240 mM potassium phosphate, pH 8.0) buffer was added to 100 mg of each sample before the addition of four 3 mm sterile glass beads (Sigma-Aldrich Company Ltd, Poole, UK) and 0.5 mL of phenol-chloroform-isoamyl alcohol (25:24:1) (NBS Biologicals Ltd, Cambridgeshire, UK). Samples were vortexed and subjected to bead beating for 30 seconds at maximum speed in a Mini Beadbeater-8 (BioSpec Products, Bartlesville, OK, USA) before centrifugation for 10 minutes. Five hundred millilitres of chloroform-isoamyl alcohol was added to the aqueous phase which was then vortexed and centrifuged as before. The supernatant was treated with 1 mL polyethylene glycol (PEG-6000) (Fisher Scientific Ltd, Loughborough, UK), then allowed to precipitate at ambient temperature for 2 hours and centrifuged at 12 000 ×*g* for 20 minutes at 4°C. Precipitated DNA was washed twice with 1 mL 70% ethanol (Fisher Scientific Ltd, Loughborough, UK), centrifuged for 20 minutes and the resultant pellet air-dried in a Savant Speed Vac® SPD121 Concentrator with Refrigerated Condensation Trap (Thermo Scientific™, Waltham, MA, USA) before resuspension in 50 µL of 1× *tris*(hydroxymethyl)aminomethane (Tris) - ethylenediaminetetraacetic acid (EDTA) (TE: 1 mM Tris, pH 8, 1 mM EDTA) buffer. All samples were quantified on a NanoDrop® ND-1000 Spectrophotometer (NanoDrop® Products, Wilmington, DE, USA) and then stored at -20°C for downstream processing.

2.4.2. Nucleic acid extraction from Foxfonna valley glacier and Greenland Ice Sheet samples

2.4.2.1. Cryoconite nucleic acids

Cryoconite DNA and RNA were co-extracted using the PowerBiofilm™ RNA Isolation kit (MO BIO Laboratories Inc.). Briefly, 100 mg of cryoconite was added to the PowerBiofilm™ Bead Tube and resuspended in a 350 µL mixture of Solution BFR1/β-mercaptoethanol (βME, 345 µL:5 µL) and 100 µL of Solution BFR2, homogenised and incubated at 65°C for 5 minutes. The tubes were secured to a MO BIO vortex adapter (MO BIO Laboratories Inc.) and agitated at maximum speed for 20 minutes before centrifugation for 1 minute at room temperature. The supernatant was transferred to a collection tube, incubated in 100 µL Solution BFR3 at 4°C for 5 minutes and thereafter subjected to centrifugation as before. A 450 µL aliquot each of Solutions BFR4 and BFR5 was added to the supernatant in a clean collection tube, homogenised and centrifuged on a spin filter column for 1 minute. The column was washed with 650 µL of Solution BFR6 and subjected to centrifugation as before to remove all traces of the buffer, before addition of 400 µL of Solution BFR8 and centrifugation as previously described. The filter was thereafter sequentially washed and centrifuged with 650 µL each of Solution BFR6 and BFR5, before a 2 minute centrifugation to remove all residual wash and the filter transferred into a clean sterile 2 mL collection tube for elution of nucleic acids in 100 µL of Solution BFR9. The elutant was thereafter stored at 4°C for downstream processing or -80°C until ready for use.

2.4.2.2. Glacial water nucleic acids

DNA and RNA were co-extracted from snowmelt and stream water using the PowerWater® Sterivex™ DNA Isolation kit (MO BIO Laboratories Inc., Carlsbad, CA, USA). The manufacturer's protocol was modified to permit co-extraction of DNA and RNA on the recommendation of MO BIO Laboratories Inc. (DeForce, 2014). All extractions were performed by addition of 900 µL ST1B with added ST1A:βME (880 µL:20 µL) to the Sterivex™ filter unit via the inlet port. The filter unit was secured to a MO BIO vortex adapter and agitated at minimum speed for 5 minutes, the filters inverted and again agitated for 5 minutes. Nine hundred microliters of Solution ST2 was added and the filter incubated at 70°C for 10 minutes, before cooling at room temperature for 2 minutes and the 5 minute vortex agitation process repeated. One millilitre of air was pushed into the Sterivex™ filter using a 3 mL syringe attached to the inlet port, while inverted, allowing backpressure to withdraw the lysate into the syringe. The lysate was then added to a 5 mL PowerWater® Sterivex™ glass Bead Tube and subjected to agitation on the MO BIO vortex adapter, as performed previously, before centrifugation at 4 000 ×*g* for 1 minute at room temperature. The supernatant was then transferred to a clean collection tube and treated with 300 µL of Solution ST3, homogenised, incubated at 4°C for 5 minutes and then subjected to a 1 minute centrifugation step. The resultant supernatant was transferred to a clean 5 mL collection tube, to which 1.5 mL of Solution ST4 and 1.5 mL 100% ethanol was added and homogenised and the collective supernatant filtered through a 20 mL syringe:binding column unit attached to a PowerVac Manifold (MO BIO Laboratories Inc, Carlsbad, CA, USA) with Luer-Lok™ stopcock attachments. The syringe was removed and 800 µL of Solution ST5 added directly to the binding column and the

vacuum applied before repeating this process with Solution ST6 and again ST5. The column was dried between washes by drawing air through the filter for 1 minute between each solution. The binding column was then placed in a collection tube for further drying by centrifugation for 2 minutes. The dried filter was transferred to a clean collection tube and 100 µL sterile RNAse free water applied for elution by centrifugation for 1 minute. The elutant was maintained at 4°C for immediate downstream processing or stored at -80°C.

2.4.2.3. DNase treatments and cDNA synthesis

All RNA samples were subjected to treatment with DNase to remove all traces of DNA. This was performed using the MO BIO RTS DNase kit (MO BIO Laboratories Inc., Carlsbad, CA, USA) on 25 µL of the extracted nucleic acids (sections 2.4.2.1 and 2.4.2.2), according to the manufacturer's instructions. The procedure involved addition of 2:5 µL RTS DNase:RTS DNase buffer per reaction, followed by incubation at 37°C for 40 minutes. To this, 5 µL of RTS Removal Resin was added and incubated for 10 minutes at room temperature, with frequent agitation on a vortex. This mixture was then subjected to centrifugation at 13 000 ×*g* and the supernatant, free from DNA, used for reverse transcription.

Aliquots of each RNA sample were used as template in first strand cDNA synthesis via reverse transcription with SuperScript™ III Reverse Transcriptase (Invitrogen™, Carlsbad, CA). Briefly, 2 µL universal 16S rRNA gene region primer 1389R (5' - ACG GGC GGT GTG TAC AAG - 3'), 20 µL RNA extract and 4 µL deoxynucleotide

triphosphates (dNTP mix, Promega, Madison, WI, USA) was added to a nuclease free microcentrifuge tube, to a final volume of 20 µL. This mixture was incubated at 65°C for 5 minutes, then cooled to 4°C for 1 minute on a Bio-Rad iCycler™ thermal cycler (Bio-Rad Laboratories Inc., Hercules, CA, USA). To this, 8 µL of 5× First Strand buffer and 2 µL 0.1 M DTT was added, homogenised and heated up to 40°C before addition of 2 µL SuperScript™ III RT. This was then incubated at 35°C for 2 minutes, 50°C for 60 minutes, and the enzyme finally deactivated at 70°C for 15 minutes. The product was then used as template in downstream PCR amplifications.

2.5. 16S rRNA GENE REGION AMPLIFICATION

The 16S rRNA gene region was targeted for polymerase chain reaction (PCR) amplification using universal bacterial primers and optimised cycling conditions. PCRs were performed in a Bio-Rad iCycler™ thermal cycler (Bio-Rad Laboratories Inc., Hercules, CA, USA).

2.5.1. 16S rRNA gene region library generation

PCR reactions were comprised of 1× GoTaq® G2 Flexi Buffer, 2.5 µM GoTaq® G2 Flexi DNA polymerase (Promega, Madison, WI, USA), 200 µM of dNTP mix, 2.5 mM $MgCl_2$, 250 nM each of forward oligonucleotide primer 27F (5' - AGA GTT TGA TCM TGG CTC AG - 3') and reverse oligonucleotide primer 1389R (5' - ACG GGC GGT GTG TAC AAG - 3') and 1 - 5 ng template DNA, adjusted to a final volume of 25 µL with molecular grade water (Fisher Scientific Ltd, Loughborough, UK). Primers were synthesised by

Eurofins Genomics (Eurofins Genomics, Ebersberg, Germany) or Invitrogen Ltd. (Invitrogen™, Thermo Fisher Scientific, Carlsbad, CA, USA) and used at a working concentration of 50 µM with DNA/RNase free water (MO BIO Laboratories Inc.). Cycling conditions were 94°C for 3 minutes (initial denaturation), 32 cycles of: 94°C for 30 seconds (denaturation), 51°C for 45 seconds (primer annealing), 72°C for 30 seconds (extension) and 72°C for 1.25 minutes (final extension). Negative controls with no template DNA were included in each PCR batch and were treated exactly as the samples. Amplicons were quantified on a NanoDrop® ND-1000 Spectrophotometer (NanoDrop® Products, Wilmington, DE, USA) and stored at -20°C when not in use.

2.5.2. Amplicon confirmation by electrophoresis

Amplification of PCR products was confirmed by agarose gel electrophoresis in 1.5% (w/v) 0.5× Tris-Borate-EDTA (TBE) buffer (89 mM Tris-HCl, 89 mM Boric Acid, 1 mM EDTA, pH 8) at approximately 7 volts.cm^{-1} for ± 30 minutes. The gel matrix consisted of agarose (Melford Laboratories Ltd, Ipswich, UK) suspended in 0.5× TBE with 0.5× SafeView nucleic acid stain (NBS Biologicals Ltd, Cambridgeshire, UK) as the visualising agent; DNA was electrophoresed with 1× loading dye (Bioline, London, UK) alongside 5 µL HyperLadder™ I (Bioline, London, UK). Gels were visualised in ultraviolet (UV) using the Bio-Rad Molecular Imager® Gel Doc™ XR+ Imaging System (Bio-Rad Laboratories Inc., Hercules, CA, USA) and images processed in Bio-Rad Quantity One (version 4.6.8) software. Primary PCRs were used as template for nested PCRs in downstream high throughput sequencing PCRs.

2.6. HIGH THROUGHPUT NEXT GENERATION SEQUENCING LIBRARY PREPARATION AND SEQUENCE PROCESSING

Bench top sequencing platforms have revolutionised the field of microbial ecology, converting an expensive, largescale application into a streamlined, cost effective, time and labour efficient process, fulfilling the needs of smaller laboratories. Libraries are constructed by the addition of platform specific barcoded DNA adapters to the template DNA molecules, enabling binding of the library fragment to either a microbead surface in the Ion Torrent PGM system or a glass flow cell in the Illumina platform, and consequent amplification by emulsion PCR or bridge PCR respectively (Figure 2. 2). Sequencing is performed by sequential flooding on non-labelled native nucleotides, integrating products of proton release in Ion Torrent instruments, while in Illumina sequencing, the four differently labelled nucleotides are flushed over the flow cell in parallel, incorporating the specific fluorescent labels attached to the nucleotide. Comparisons of bacterial profiling using 16S rRNA gene regions on the Ion Torrent Personal Genome Machine™ and Illumina MiSeq® platforms show taxonomic identification was reliable for both platforms (Salipante *et al.*, 2014), with low error rates in the range of 0.4 - 1% (Knief, 2014).

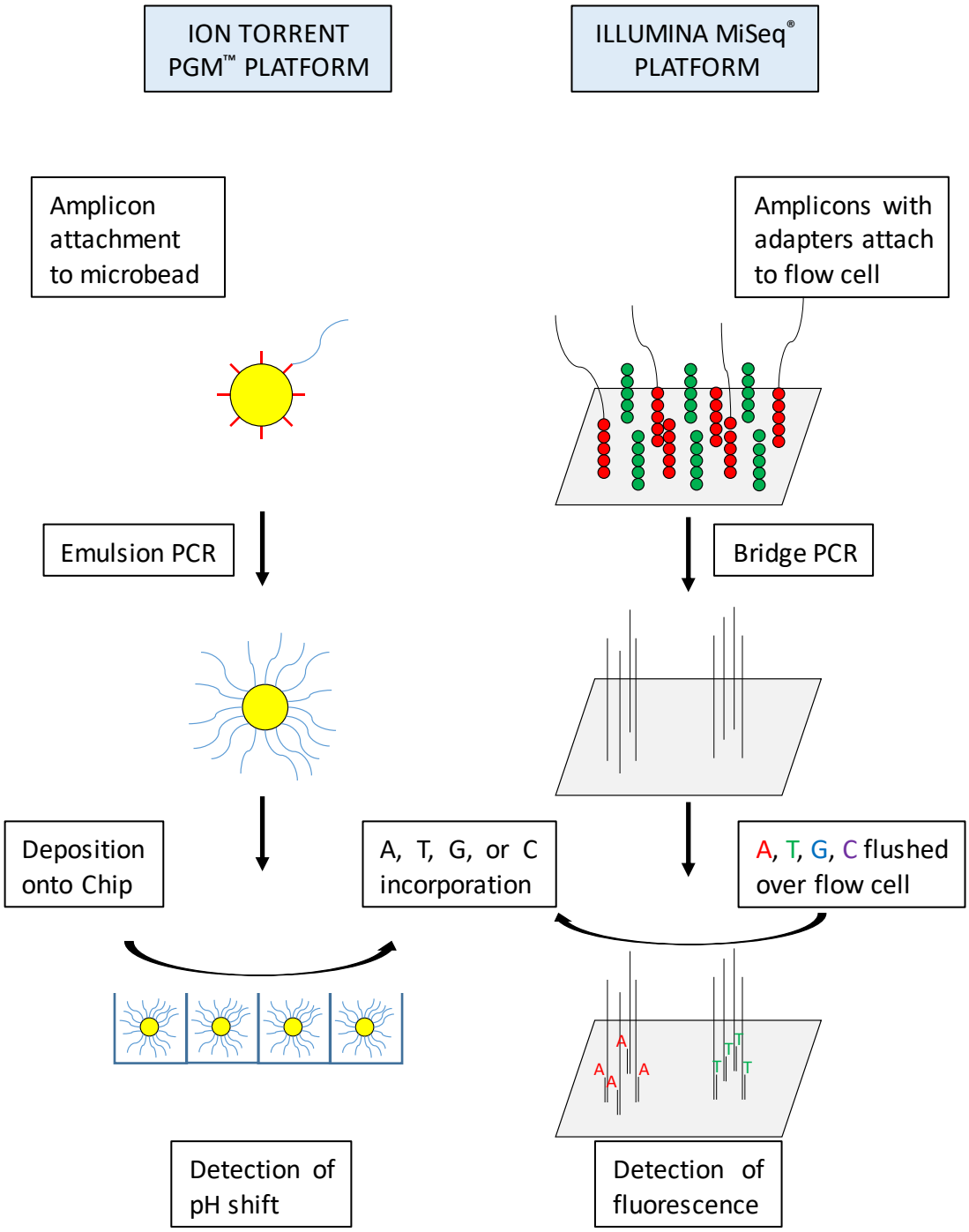

Figure 2. 2 Schematic representation of the library preparation and sequencing process in the Ion Torrent PGM™ and Illumina MiSeq® platforms.

2.6.1. Ion Torrent 16S rRNA gene region library generation

Primers targeting the 400 bp V1 - V2 region of the 16S rRNA gene generated amplicons by nested multiplexed PCR with a unique forward barcode sequence and adapter and reverse primer (Table 2. 1). Each PCR contained 2.5 - 10 ng template DNA, 1× GoTaq® G2 Flexi Buffer, 2.5 µM GoTaq® G2 Flexi DNA polymerase (Promega, Madison, WI, USA), 200 µM of dNTP mix, 2.5 mM $MgCl_2$ in a master mix with 0.1 pM barcoded forward primer 27F, 0.1 pM reverse primer 357R, per reaction. Cycling conditions were 95°C for 2 minutes (initial denaturation), 22 cycles of: 95°C for 30 seconds (denaturation), 60°C for 30 seconds (primer annealing), 72°C for 45 seconds (extension) and 72°C for 7 minutes (final extension). Products were confirmed by gel electrophoresis (detailed in section 2.5.2), treated with Agencourt® AMPureXP® Beads (Beckman-Coulter Genomics) for removal of short fragment DNA and then quantified on a NanoDrop® ND-1000 Spectrophotometer. Samples were normalised to equimolar concentration and pooled for sequencing on the Ion Personal Genome Machine (Ion Torrent PGM™, Life Technologies, Carlsbad, CA, USA).

Table 2. 1 Barcodes used for Ion Torrent PGM™ Sequencing of the hypervariable V1 - V2 region of 16S rRNA gene region on Foxfonna ice cap (Chapter 4).

27F Primer ID	Ion Barcode Sequence 5'-3' (10)	27F Primer ID	Ion Barcode Sequence 5'-3' (10)
NGS_V1-V2_1	CTA AGG TAA C	NGS_V1-V2_20	CAG ATC CAT C
NGS_V1-V2_2	TAA GGA GAA C	NGS_V1-V2_21	TCG CAA TTA C
NGS_V1-V2_3	AAG AGG ATT C	NGS_V1-V2_22	TTC GAG ACG C
NGS_V1-V2_4	TAC CAA GAT C	NGS_V1-V2_23	TGC CAC GAA C
NGS_V1-V2_5	CAG AAG GAA C	NGS_V1-V2_24	AAC CTC ATT C
NGS_V1-V2_6	CTG CAA GTT C	NGS_V1-V2_25	GAT CTG CGA T
NGS_V1-V2_7	TTC GTG ATT C	NGS_V1-V2_26	CAG CTC ATC A
NGS_V1-V2_8	TTC CGA TAA C	NGS_V1-V2_27	CAA ACA ACA G
NGS_V1-V2_9	TGA GCG GAA C	NGS_V1-V2_28	GCA ACA CCA T
NGS_V1-V2_10	CTG ACC GAA C	NGS_V1-V2_29	GCG ATA TAT C
NGS_V1-V2_11	TCC TCG AAT C	NGS_V1-V2_30	CGA GCA ATC C
NGS_V1-V2_12	TAG GTG GTT C	NGS_V1-V2_31	AGT CGT GCA C
NGS_V1-V2_13	TCT AAC GGA C	NGS_V1-V2_32	GTA TCT GCG C
NGS_V1-V2_14	TTG GAG TGT C	NGS_V1-V2_33	CGA GGG CCC G
NGS_V1-V2_15	TCT AGA GGT C	NGS_V1-V2_34	CAA ATT CGG C
NGS_V1-V2_16	TCT GGA TGA C	NGS_V1-V2_35	AGA TTG ACC A
NGS_V1-V2_17	TCT ATT CGT C	NGS_V1-V2_36	AGT TAC GAG C
NGS_V1-V2_18	AGG CAA TTG C	NGS_V1-V2_37	GCA TAT GCA C
NGS_V1-V2_19	TTA GTC GGA C	NGS_V1-V2_38	CAA CTC CCG T
27F Forward Primer A-key (30) NGS_V1-V2		CCA TCT CAT CCC TGC GTG TCT CCG ACT CAG	
357R Reverse Primer P1-key (23) PGM_V1-V2_Rev		CCT CTC TAT GGG CAG TCG GTG AT	
Template specific sequence-3' (19)		AGA GTT TGA TCM TGG CTC AG	

2.6.2. Ion Torrent 16S rRNA amplicon processing and sequencing

Removal of non-specific DNA was performed using the E-Gel® SizeSelect™ clean-up (Invitrogen™, Carlsbad, CA, USA) process, according to the manufacturer's instructions. Samples were aspirated from collection wells, and the library quantified on the Agilent 2100 Bioanalyser and Agilent High Sensitivity DNA chip (Agilent Technologies, Santa Clara, CA, USA). Libraries diluted to 26 pM were prepared with the Ion PGM™ Sequencing 400 Kit (Life Technologies, Carlsbad, CA, USA), which involved emulsion PCR for individual DNA templates to attach to Ion Sphere Particles (ISPs) on the Ion OneTouch 2 platform, enrichment on the OneTouch ES to remove

negative template ISPs and the final library loaded onto an Ion 316v2 chip for sequencing, all in accordance with the EmPCR Ion PGM™ Template OT2 400 and the Enrichment Ion PGM™ template OT2 400 manuals (2014b). Chip initialisation, loading and sequencing was performed according to manufacturer's instructions in the Sequencing Ion PGM™ Sequencing 400 manual (2014a). Libraries were sequenced at 1 200 flows and the sequencing flows processed into base-calls in the Torrent Suite™ Software (version 4.6). Sequence data was demultiplexed, the barcodes removed in MOTHUR v1.31.2 (Schloss *et al.*, 2009; Detheridge *et al.*, 2016), and the final output converted to fastq format and imported into QIIME 1.9.0 (Caporaso *et al.*, 2010).

2.6.3. Illumina MiSeq® 16S rRNA region library generation

Amplicon libraries were generated from the V3 - V4 hypervariable region of bacterial 16S rRNA gene region amplicons using primers constructed by Klindworth *et al.* (2013). Illumina sequencing overhang adapters were attached to the amplicons by nested PCR. Each 12.5 µL PCR contained 1 - 5 ng template DNA, 200 nM of 16S forward primer S-D-Bact-0341-b-S-17 (5' - TCG TCG GCA GCG TCA GAT GTG TAT AAG AGA CAG CCT ACG GGN GGC WGC AG - 3'), 200 nM reverse primer S-D-Bact-0785-a-A-21 (5' - GTC TCG TGG GCT CGG AGA TGT GTA TAA GAG ACA GGA CTA CHV GGG TAT CTA ATC C - 3') and 11.42 µL Platinum® PCR SuperMix High Fidelity (Invitrogen, Carlsbad, CA, USA). Cycling conditions were 94°C for 5 minutes (initial denaturation), 25 cycles of: 94°C for 30 seconds (denaturation), 55°C for 2 minutes (primer annealing), 72°C for 1 minute (extension) and 72°C for 5 minutes (final extension). This was followed by short fragment removal using the Montage™ PCR plate filtration

system (Millipore) according to manufacturer's instructions. Index PCR was performed using the Nextera XT Index Kit (Illumina) on a TruSeq® Index Plate Fixture (Illumina Inc., San Diego, CA, USA) to obtain unique combinations of the N7 and S5 primer barcodes (Table 2. 2). Each PCR contained 2.5 µL of Index Primer 1, 2.5 µL of Index Primer 2, 18 µL Platinum® PCR SuperMix High Fidelity and 2 µL (10 ng) DNA to a final volume of 25 µL. PCR cycling conditions were 95°C for 3 minutes (initial denaturation), 8 cycles of: 95°C (denaturation), 55°C (primer annealing) and 72°C (extension) for 30 seconds each, and 72°C for 5 minutes (final extension). The 300 bp product was confirmed by gel electrophoresis and amplicons were purified from short fragments using the Montage™ PCR plate filtration system.

Table 2. 2 Dual Index primers used in the Nextera XT Index Kit on the Foxfonna valley glacier (Chapter 6) and Greenland Ice Sheet (Chapter 7).

Index 1 i7 ID	**Adapter Sequence 5'-3'**
N701	TCG CCT TA
N702	CTA GTA CG
N703	TTC TGC CT
N704	GCT CAG GA
N705	AGG AGT CC
N706	CAT GCC TA
N707	GTA GAG AG
N708	CCT CTC TG
N709	AGC GTA GC
N710	CAG CCT CG
N711	TGC CTC TT
N712	TCC TCT AC
Index 2 i5 ID	**Adapter Sequence 5'-3'**
S502	CTC TCT AT
S503	TAT CCT CT
S504	AGA GTA GA
S505	GTA AGG AG
S506	ACT GCA TA
S507	AAG GAG TA
S508	CTA AGC CT
S517	GCG TAA GA
Index 1 Read 5'-3'	CAA GCA GAA GAC GGC ATA CGA GAT [i7] GTC TCG TGG GCT CGG
Index 2 Read 5'-3'	AAT GAT ACG GCG ACC ACC GAG ATC TAC AC [i5] TCG TCG GCA GCG TC

2.6.4. Illumina MiSeq® 16S rRNA and 16S cDNA amplicon processing and sequencing

Products generated in the Index PCR process were quantified on the Epoch™ Microplate Spectrophotometer (BioTek) and pooled to an equimolar concentration. The pooled library was electrophoresed and extracted from a 1.5% agarose gel as described in section 2.5. DNA with a fragment length of 400 bp was excised with sterile scalpel blades and purified with the QIAquick® Gel Extraction Kit (Qiagen, Hilden, Germany), according to the manufacturer's instructions. Final library

quantification was performed using the Qubit® Fluorometer and Qubit® dsDNA HS Assay Kit (Life Technologies, Carlsbad, CA, USA). Libraries were sequenced at the IBERS Translational Sequencing Facility (IBERS Phenomics Centre, Gogerddan, Aberystwyth, Ceredigion SY23 3EE) on the Illumina MiSeq® platform (Illumina Inc., San Diego, CA, USA), using the MiSeq® Reagent Kit, version 3 (Illumina Inc., San Diego, CA, USA). Initial processing of Illumina MiSeq® sequence data was performed in BaseSpace® (Illumina Inc., San Diego, CA, USA). Data were demultiplexed and the indices removed. Reads were trimmed to remove readthrough into the adaptor sequence at the 3' end (Hegarty, 2015). Sequence files were generated in the fastq format and imported into QIIME 1.9.0 for merging of paired end reads.

2.7. BIOINFORMATIC AND STATISTICAL ANALYSIS

2.7.1. Sequence filtering and processing

Individual sample fastq files were combined to a single fasta file with unique sample identities to probe the dataset for chimeric sequences using either USEARCH6.1 (Edgar *et al.*, 2011) or ChimeraSlayer (Haas *et al.*, 2010). Chimeric sequences were then removed and a UCLUST clustering algorithm (Edgar, 2010) applied to select operational taxonomic units (OTUs), while representative OTUs were selected at 97% identity for taxonomy assignment using the RDP method (Wang *et al.*, 2007) and the Greengenes 13_8 database, version August 2013 (DeSantis *et al.*, 2006). This permitted the generation of OTU tables that were filtered to a 0.01% OTU presence threshold, then rarefied to the lowest number of reads and the alpha diversity indices calculated. Raw data output from QIIME 1.9.0 and mass spectrometry output was

routinely handled in Microsoft Office 2013, using MS Excel for producing charts and tables for further data analysis. The closest named environmental and cultured relatives comprising 99% abundance were identified using the BLAST sequence analysis tool (McEntyre and Ostell, 2012). For consistency, each OTU, when mentioned, is referred to by the most detailed taxonomic assignment made and the reference number of the OTU assigned during OTU selection.

2.7.2. Univariate statistical analysis

Analysis of variance (ANOVA) tests of diversity statistics, relationships between OTUs and environmental variables were performed in Minitab 17 (Minitab® Inc.), for analysis of high throughput sequences and Metaboanalyst 3.0, for metabolomic statistical analysis and determining major variables of interest.

2.7.3. Multivariate statistical analysis

Biological and environmental data was imported into PRIMER 6/PERMANOVA+ for multiple multivariate analyses. All data were uniformly transformed to the fourth root before analysis. Bray-Curtis resemblance matrices were calculated from OTU abundance matrices which were then used to observe spatial differences and similarities using ordination graphs, principal co-ordinates analysis (PCO) and canonical analysis of principal co-ordinates (CAP). Permutational analysis of variance (PERMANOVA) was tested on OTU abundance, with 999 unrestricted permutations to observe the significance of pertinent variables as will be outlined in each

experimental chapter. Normalised environmental variables and metabolite concentrations were converted to Euclidian distance matrices for analysis by the Mantel-based Spearman rank correlation function, RELATE and distance-based redundancy analysis (dbRDA) for correlation to biological data.

2.8. CO-OCCURRENCE NETWORK ANALYSIS

Co-occurrence networks allow graphical interpretation of the interactions between biological communities and environmental characteristics using the probability of co-occurrence or differences in community composition. Using 16S amplicon data, bacterial co-occurrence in environmental ecosystems can be established, in addition to inferences of ecological roles of less understood microbial taxa from OTU abundance data.

Statistical computing for network generation was performed in R (The R Foundation), where a vector representing OTU abundance was generated for individual OTUs in each sample as indicated by the formula:

$$x_i = [x_{i1}, x_{i2}, \dots, x_{i37}] \ (i = 1, \dots, 755)$$

To reduce sequencing effort bias, x_i values less than 5 was set to zero (Zhang *et al.*, 2013) and OTU vectors containing <8 non-zero elements were removed to reduce false high correlations (Berry and Widder, 2014). Pairwise Spearman correlations between all vectors were calculated and the associated *P* value corrected for multiple comparisons with a Benjamini-Hochburg adjustment. Using the iGraph package in R

(Csardi and Nepusz, 2006), a community network was created based on significant correlations ($\rho > 0.7$ and adjusted $P < 0.05$), incorporating all vectors. Community detection was based on "walktrap", a random walk algorithm in iGraph (Pons and Latapy, 2006). Network parameters were compared with the Erdös-Renyi random model of a network of equal size. For both observed and random model communities, network parameters were calculated using the iGraph package. The community network structure was used to identify OTUs central to community structuring and/or function i.e. "bottlenecks" within the community, and are defined as nodes with highest betweenness centrality, a count of the number times the bottleneck appears on the shortest paths between all other pairs of nodes (Peura *et al.*, 2015).

CHAPTER 3 – MORPHOLOGICAL AND METABOLIC CHARACTERISATION OF CRYOCONITE GRANULE DEVELOPMENT

3.1. INTRODUCTION

Cryoconite ecosystems are recognized as major foci of microbial biodiversity and activity on bare glacial ice (Edwards *et al.*, 2011; Cameron *et al.*, 2012; Cook *et al.*, 2015b), which influence ice surface albedo (Bøggild, 1997; Takeuchi, 2002) at the glacier surface. The composition and structure of cryoconite bacterial communities on both Arctic and Alpine glaciers, are closely related to the rates of microbial activities and the composition of cryoconite organic matter (Edwards *et al.*, 2011; Edwards *et al.*, 2013b; Edwards *et al.*, 2014b). Cryoconite biota include viruses, bacteria, fungi, other micro eukaryotes and meiofauna (Sawstrom *et al.*, 2002), which actively contribute to carbon and nitrogen cycling (Hodson *et al.*, 2007; Segawa *et al.*, 2014).

The granules themselves are characterised as biotic aggregates that entangle aeolian debris as a result of the action from filamentous *Cyanobacteria* (e.g. *Phormidium*, *Phormidesmis* or *Leptolyngbya* sp.) (Hodson *et al.*, 2010b; Langford *et al.*, 2010). This promotes the development of cryoconite-forming microbial communities that are distinctive from other supraglacial habitats (Edwards *et al.*, 2013c; Musilova *et al.*, 2015). Cross section analysis by Takeuchi *et al.* (2001a) revealed that the density of the layers reflect the annual growth rate of the granules in each melt season. As such granule size and cohesion are directly dependable on the ability of the cyanobacterial

layers to bind smaller fragments, the reduced heterotrophic consumption of carbohydrates and reduction in photosynthesis, respectively (Langford *et al.*, 2010). However, insight into the process of debris accumulation during initiation of cryoconite holes and the role of the microbial consortium on the granule formation process is not fully understood. Enhancing the understanding of the molecular changes driving the formation of cryoconite granules is thus integral for deciphering the environmental impact of cryoconite.

Despite the increased attention on the effect of cryoconite microbes on ice surfaces, insufficient evidence has been garnered for specific biotic mechanisms driving temporal evolution of pioneering cryoconite holes, including physical characteristics of the sediment influenced by the microbial ecology and metabolism. Metabolomics has been extensively employed in plant, human and model organism systems for disease diagnosis and drug discovery (Tang, 2011), with recent interest developing in terrestrial (Baran *et al.*, 2015), marine (Viant, 2007) and glacial environments (Lutz *et al.*, 2015b; Cook *et al.*, 2016a) to understand the substrate specialisation and stress response in microbes at a metabolic level.

The 'cryoconite casserole' experiment designed by Musilova *et al.* (2016) investigated the interannual effect of microbially mediated organic carbon accumulation. Therein, it was noted that the greatest albedo reduction was observed at the end of one simulated summer season. This led to the assumption that key metabolic events during a single summer are integral to the trophic lifestyle of a pioneer cryoconite

hole. Therefore, the aim of this chapter was to observe the process of establishment of a newly seeded cryoconite community by replicating the environmental constraints under controlled laboratory conditions and analysing the cryoconite microcosm created through a combined microscopic and metabolic approach. It can be hypothesised that

a. There is an increase in visually detectable biomass, extracellular polymeric substances and chlorophyll *a*, attributed to debris accumulation, pioneer microbes and filamentous *Cyanobacteria*,
b. The pioneer cryoconite metabolome is profoundly different from the established metabolome, as a consequence of enhanced early microbial growth.

3.2. EXPERIMENTAL DESIGN

This experiment was designed to mimic the formation and development of bacterial assemblages in natural cryoconite over a typical sampling season in the Arctic, i.e. 40 days (6 weeks) of incubation in simulated Svalbard summer conditions. This was achieved by creation of a synthetic cryoconite hole (Musilova *et al.*, 2016) in ice-submerged Petri dishes containing inactive and active cryoconite sediment submerged in artificial meltwater (AMW) designed from ice chemistry recounted in Sawstrom *et al.* (2002), Stibal *et al.* (2010) and Hell *et al.* (2013). This was maintained in a walk-in refrigerator at a temperature of 3°C and simulated natural light (82 × 2000 lux) (Figure 3. 1).

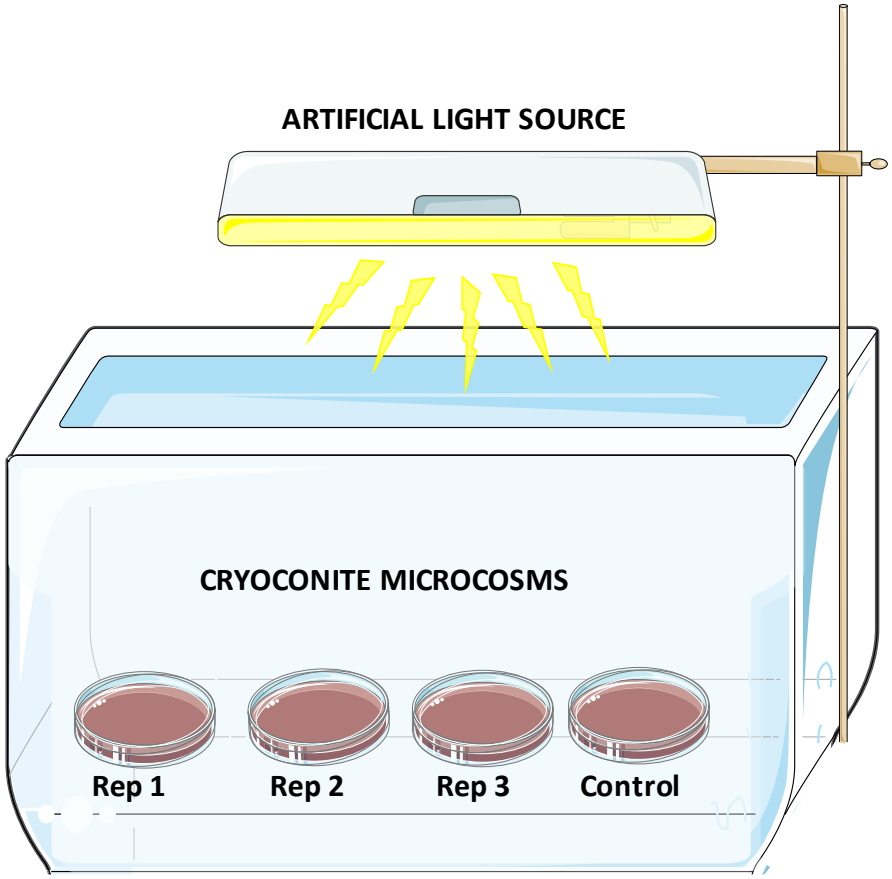

Figure 3. 1 Representation of the laboratory setup for the cryoconite evolution and development experiment. Newly seeded microcosm replicates, 1 to 3, and a control microcosm of established cryoconite were incubated at 3°C, under simulated natural light.

3.2.1. Microcosm treatment and sampling protocol

Cryoconite was sourced during July - August 2015 from Midtre Lovenbreen, a polythermal valley glacier in western Svalbard that has experienced mostly negative mass balance, resulting in deglaciation in response to warming mean annual temperatures. Bulk cryoconite was heat treated at 500°C in a furnace for 24 hours to remove all traces of organic and living matter, then cooled to room temperature. This was added to a Petri dish of natural cryoconite (containing actively growing microbes) in the ratio 8 g:2 g. The cryoconite was then covered with 1× AMW (1 000× AMW stock solution: 10 mL each of NaCl (0.7 mg.L^{-1}), NH_4NO_3 (0.015 mg.L^{-1}), KH_2PO_4 (0.06

mg.L^{-1}), $MgSO_4$ (1 mg.L^{-1}), $CaCl_2$ (0.5 mg.L^{-1}), Na_2NO_3 (0.2 mg.L^{-1}), sodium acetate (0.1 mg.L^{-1}), glucose (0.1 mg.L^{-1}), sucrose (0.1 mg.L^{-1}) and galactose (0.1 mg.L^{-1}) in 500 mL sterilized ultra high quality Milli-Q® water, pH 5.5 - 6.2 and filter sterilised). Microcosms were incubated on ice as previously described. Cryoconite was collected bi-weekly from 28 January 2016 from 3 replicate newly seeded microcosms (S) and 1 control established microcosm (C) containing only furnaced cryoconite (Figure 3. 2). A 1 mL volume was decanted to microcentrifuge tubes and stored at -20 °C and 100 µL aliquot of each sample was stored separately for microscopic analysis.

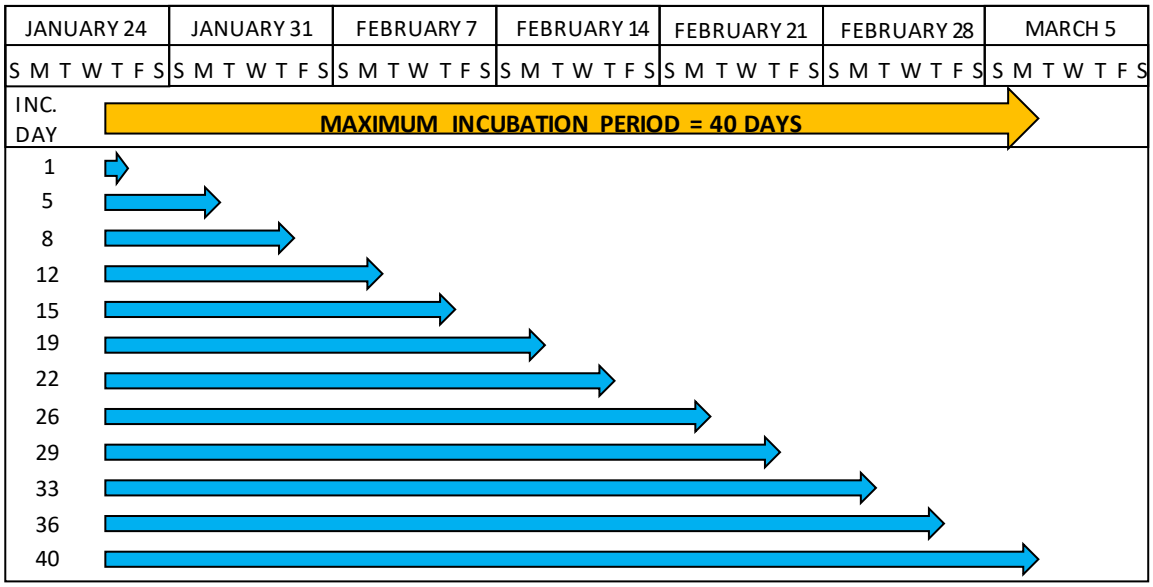

Figure 3. 2 Gantt chart of sampling schedule for cryoconite microcosms. Incubation started on 28 January 2016 and concluded on 07 March 2016; samples were collected bi-weekly.

3.2.2. Fluorescence microscopy of cryoconite granules

Excitation of fluorescent molecules at specific wavelengths results in emission spectra that can inform on the content of microbial cultures and populations. To observe microbial growth, fluorescence microscopy was performed using specifically

targeted stains. SYBR®Gold Nucleic Acid Gel stain has an excitation wavelength of 300 nm (UV), 495 nm (visible light) and an emission wavelength of 537 nm, thus its use in the visualisation of nucleic acids at an excitation range of 450 - 495 nm. EPS can be observed as light blue/white under UV, when stained with calcofluor white. Chlorophyll *a* can be detected by observing light emission of wavelength 620 - 750 nm (red) upon excitation with light of wavelength 495 - 570 nm (green). These basic stains were used to observe microcosm samples for changes in microbial activity.

Granules were suspended in 20 µL sterile artificial meltwater, incubated in 2× SYBR®Gold Nucleic Acid Gel Stain (Molecular Probes, Invitrogen Inc.) for 50 minutes and thereafter introduced to 0.01× calcofluor white for 5 minutes (Gerphagnon *et al.*, 2013) for visualisation by confocal laser scanning microscopy (CLSM) under blue, green and UV spectra, using the Leica DM 6000 B Automated Research Microscope (Leica Microsystems, Milton Keynes, UK) with the fluorescence function. Images were captured using Laser Microdissection Software (Leica Microsystems, Milton Keynes, UK). Physical descriptions of granules were assessed using the Powers sedimentary particle roundness and angularity scale (Figure 3. 3).

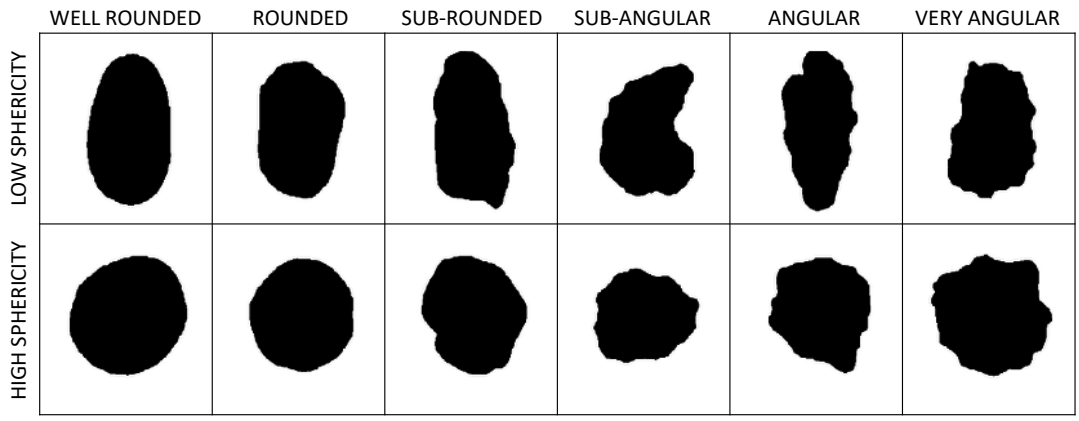

Figure 3. 3 The sedimentary particle roundness and angularity scale used to characterise physical shape of individual cryoconite granules from microscopy images. Modified from MacLeod (2002).

3.2.3. Digital image processing

Images were processed using the public domain image processing software, ImageJ IJ 4.46r (National Institute of Mental Health, Bethesda, Maryland, USA). Each pixel in an image constituted a single data point with a brightness proportional to its magnitude relative to the whole dataset. Pixels were calibrated to the scale measurement on each image for manual measurement of the principal axes (length (L) x width (W)) of the cryoconite grain using the 'LINE' tool (Takeuchi *et al.*, 2001a; Irvine-Fynn *et al.*, 2010). Semi-automated measurement of granules was performed on threshold adjusted binary images to calculate Feret Diameter (longest distance between any two points), using the 'ANALYSE PARTICLES' tool (Irvine-Fynn *et al.*, 2010).

3.2.4. Metabolome profiling by mass spectrometry

Whole metabolite extraction was performed on 48 samples of established and newly seeded microcosms for metabolic profiling by mass spectrometry. Sediment was freeze dried to obtain 0.1 g dry weight cryoconite from which metabolites were extracted using the 1:2.5:1 chloroform:methanol:water method detailed in Chapter 2, section 2.3.1. Extracts were prepared by suspending the solvent in 70% methanol before broad range whole metabolome mass spectrometry by flow-injection electrospray ionization (FI-ESI) as described in Chapter 2, section 2.3.2, alongside 144 technical replicates. The resultant metabolite concentration output was processed for univariate chemometric analysis, hierarchical clustering and partial least squares (PLS) regression modelling.

3.3. RESULTS

3.3.1. Microscopic analysis of synthetic cryoconite granules

Microscopic evaluation of individual cryoconite granules showed varied morphology, ranging from angular to round and high to low sphericity, with negligible difference between established and newly seeded microcosms (APPENDIX I, Table I. 1). The mean Feret Diameter for the 48 granules observed in this study was 445.190 ± 164.074 (SD) µm in established microcosms and 463.688 ± 168.01 (SD) µm in replicate test microcosms. This corresponded well with manually measured mean granule size of the established granules (417.28 ± 161.371 (SD) µm × 276.902 ± 70.088 (SD) µm) and replicate test microcosms (432.847 ± 149.99 (SD) µm × 278.54 ± 98.117 (SD) µm).

Newly seeded cryoconite was characterised by isolated single granules of sediment (Figure 3. 4A). Evidence of microbial biomass was observed in Figure 3. 4B from the abundance of green fluorescence excited under ultraviolet light and was substantial when compared to the established cryoconite granule (inset). Extracellular polysaccharide fluorescence was less abundant in established microcosms compared to replicate test microcosms, where very small zones of fluorescence were visible under blue light excitation. The large bright spot (Figure 3. 4C) that existed separate from the granule under visible light appeared to be crystalline mineral in nature. Chlorophyll *a* was indicated by red fluorescence under green light excitation in Figure 3. 4D and exhibited prominent expression on the surface of the granule.

Mid-incubation samples were a mix of granular and filamentous cryoconites (Figure 3. 5A) with moderate nucleic acid (Figure 3. 5B) and EPS fluorescence (Figure 3. 5C), as well as evidence of chlorophyll *a*-rich filamentous regions beginning formation (Figure 3. 5D). Both EPS and chlorophyll *a* presence corresponded to areas of high nucleic acid presence.

Upon confocal microscopy of the later incubations of the experiment, cryoconite consisted predominantly of microbial filament aggregates, mineral particulates (Figure 3. 6A) and EPS. SYBR®Gold fluorescence was abundant, consistent with the presence of nucleic acids (Figure 3. 6B). Granules exhibited extensive filament-like extrusions under ultraviolet light, indicating EPS production (Figure 3. 6C) and green light, indicating chlorophyll *a* production (Figure 3. 6D). Established microcosms

retained their quasi-circular appearance and displayed lower nucleic acid fluorescence, but higher EPS and chlorophyll *a* fluorescence than observed in newly seeded microcosms.

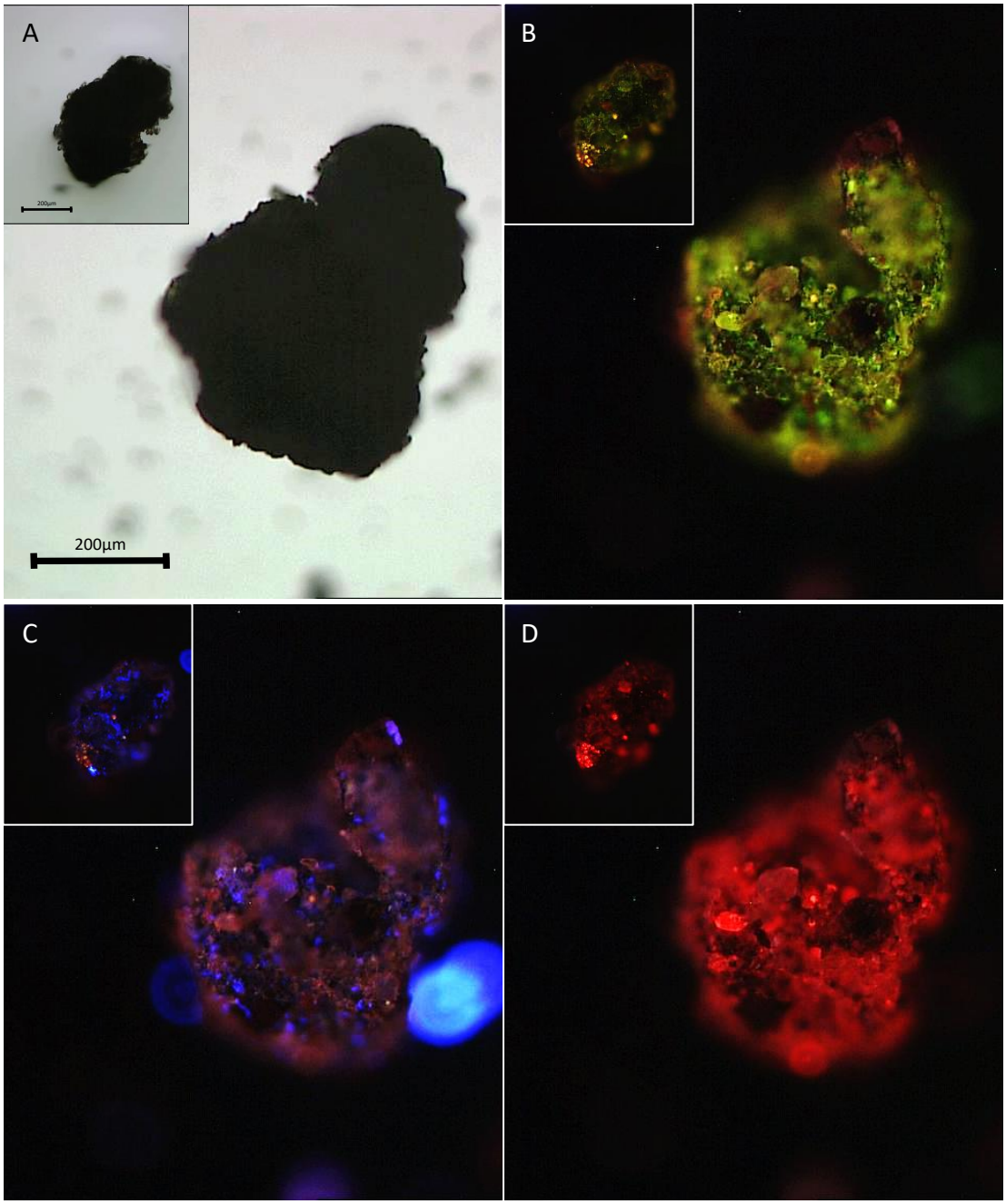

Figure 3. 4 Fluorescence microscopy of a cryoconite granule from day 0 showing (A) the intact granule under visible light, (B) nucleic acid fluorescence with clear microbial growth, (C) EPS and (D) chlorophyll *a* presence. Inset: day 0 control microcosm.

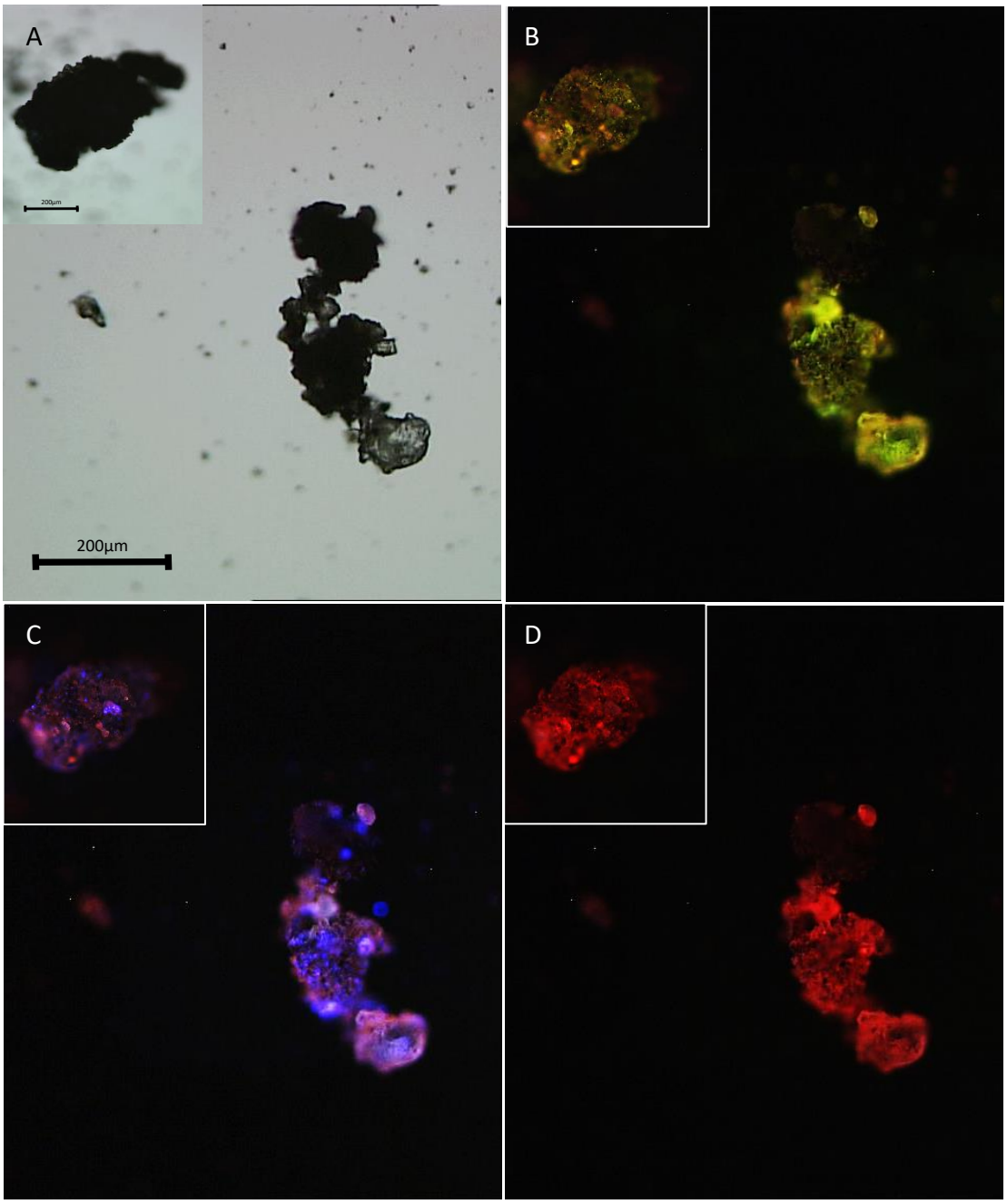

Figure 3. 5 A cryoconite granule from incubation day 12 demonstrating (A) the irregular shape of the cryoconite under visible light, (B) nucleic acid fluorescence showing an abundance of microbial biomass, (C) EPS in regions of blue-white fluorescence and (D) chlorophyll *a* fluorescence with small red cyano-filaments starting to become visible. Inset: day 12 control microcosm.

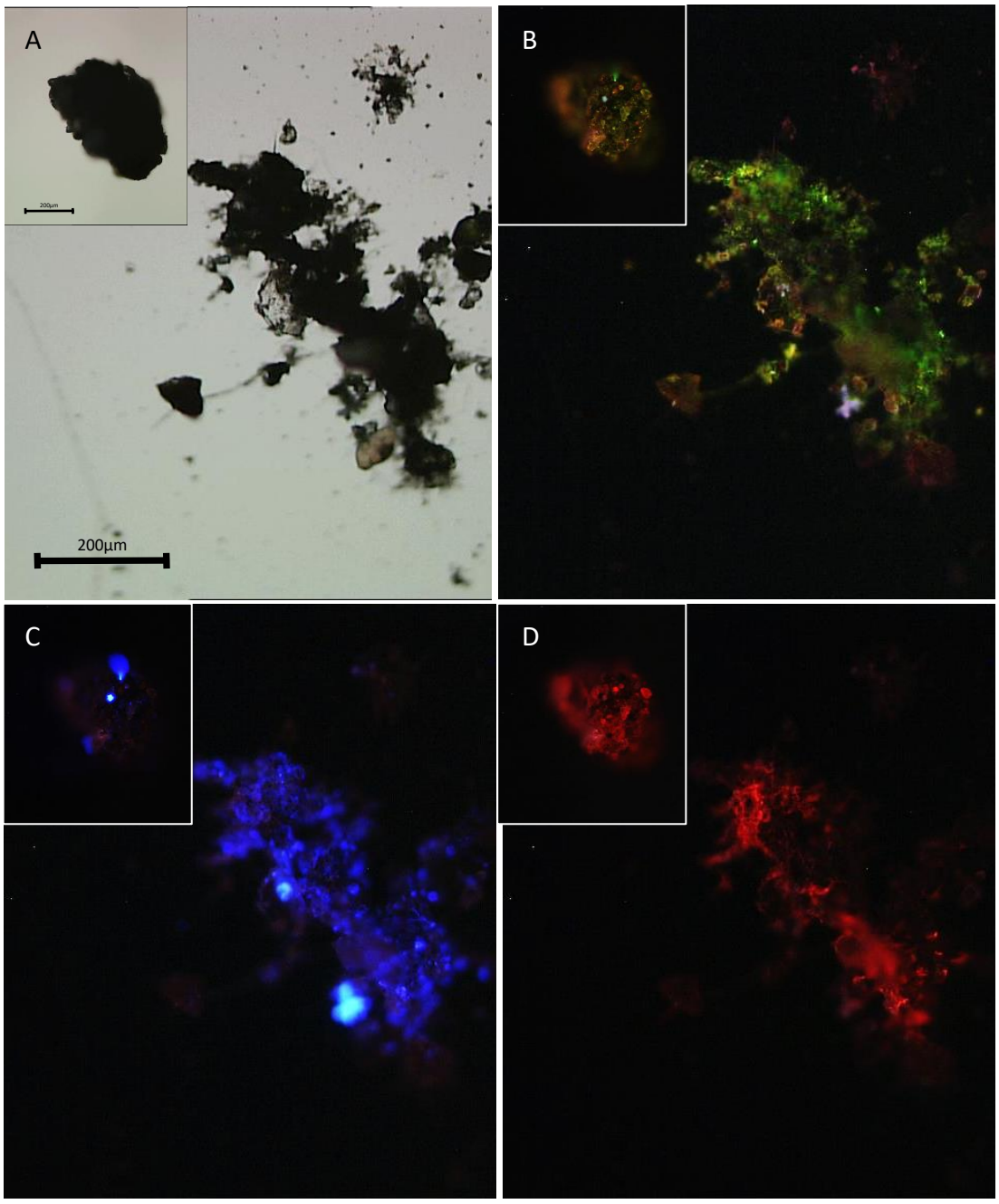

Figure 3. 6 Cryoconite granule from day 33 showing (A) the granule under visible light, (B) nucleic acid fluorescence, (C) EPS fluorescence and (D) chlorophyll *a* fluorescence. Note the abundance of visible red cyanobacterial filaments on the entire granule in all images. Inset: Day 33 control microcosm.

3.3.2. Metabolite profile of synthetic microcosm communities

Metabolites extracted from 192 microcosm technical replicates generated 3 134 peaks in the exact mass range 62.98493 - 683.09247. These exhibited discrete clustering when viewed by principal co-ordinates analysis (PCA). Closer investigation of established microcosms using PCA, discriminant function analysis (DFA), hierarchical cluster analysis (HCA) and partial least squares regression (PLSR) revealed remarkable temporal influence on the metabolome (Figure 3. 7A and B), with clear separation of metabolites expressed early in the incubation period from those expressed later (Figure 3. 7C). As such, the incubation day model ideally fits PLS regression, inferring its role as the main predictor of the metabolome (Figure 3. 7D). Permutational multivariate analysis of variance (PERMANOVA) of fourth root transformed Bray-Curtis metabolite matrices confirms the significant impact of the duration of incubation on the metabolome (pseudo-F = 1.7755, $P = 0.001$).

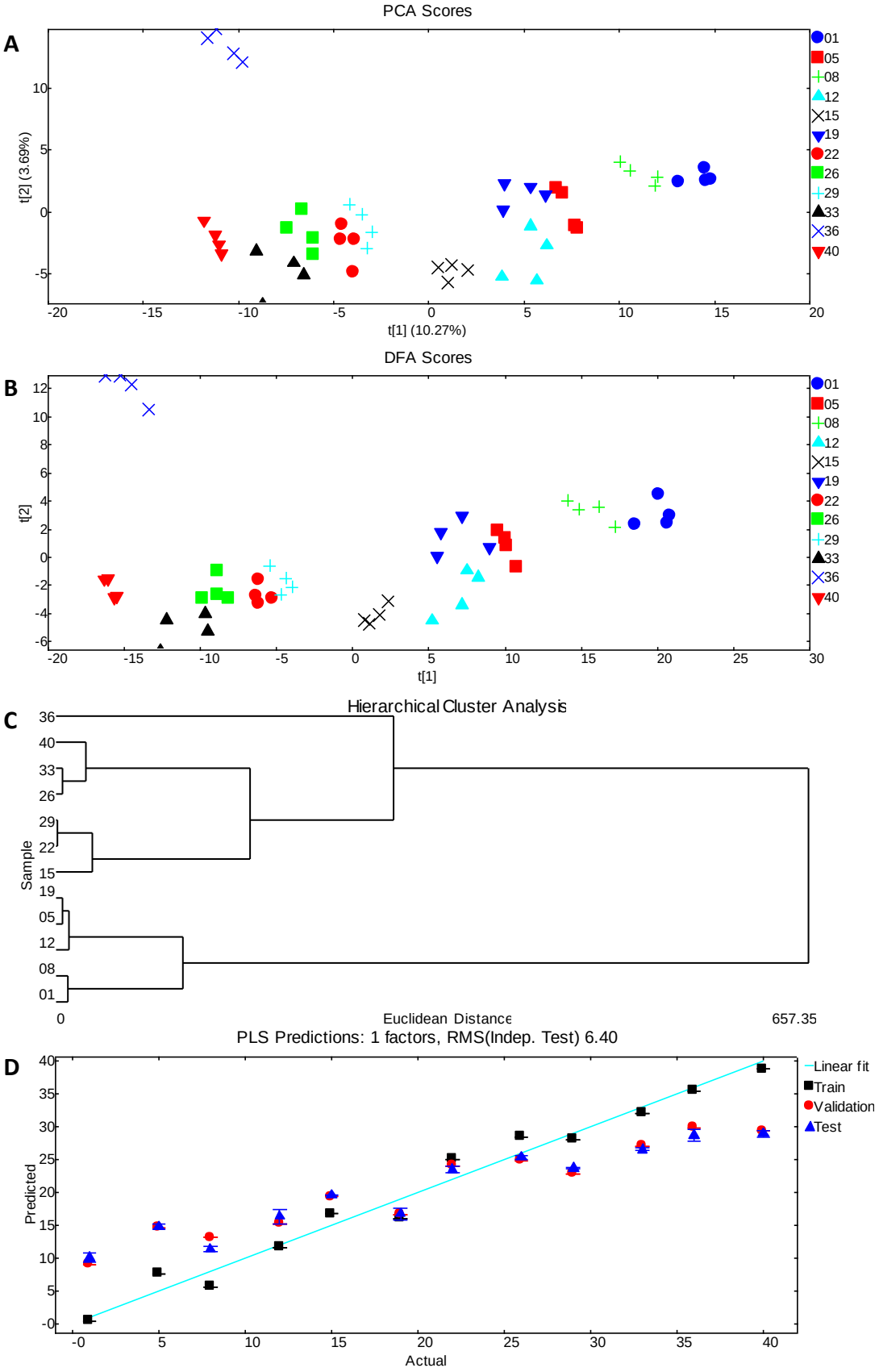

Figure 3. 7 Chemometric analysis of the synthetic established cryoconite microcosm presenting (A) the principal co-ordinates analysis, (B) discriminant function analysis, (C) hierarchical cluster analysis and (D) partial least squares regression, highlighting the influence of temporal variation under optimal summer conditions.

In contrast, the newly seeded cryoconite metabolome exhibited marked clustering from incubation day 1 to 12, after which the metabolite profile appeared to converge. It is interesting to note the high variance on incubation days 5, 15, 19, 22 and 40 (Figure 3. 8A and B). There was distinct separation of early, middle and late incubation metabolites (Figure 3. 8C), further highlighting the significant effect of incubation time on newly seeded communities and is supported by PERMANOVA (pseudo-F = 2.6247, $P = 0.001$). PLS regression demonstrated that incubation time acts as the main predictor of metabolome structure before day 26, after which an alternative driver is responsible for the observed metabolomic profile (Figure 3. 8D).

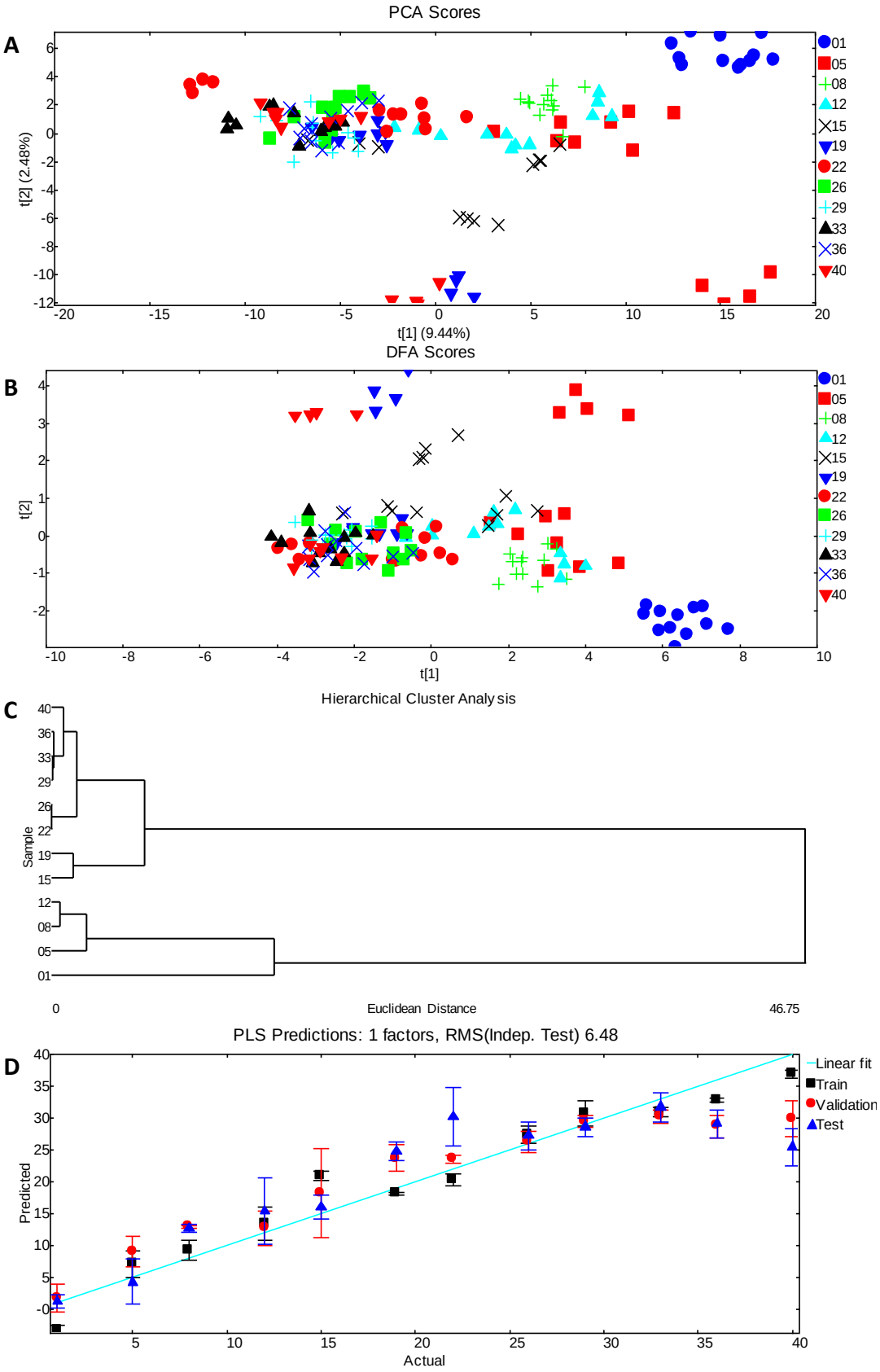

Figure 3. 8 Chemometric analysis of newly seeded synthetic cryoconite microcosms analysed by (A) PCA, (B) DFA, (C) HCA and (D) PLS regression modelling exhibited distinct temporal metabolite clustering, separating early and late metabolite expression.

3.3.2.1. Tentative metabolite and pathway identification

Statistical analysis of metabolites using Metaboanalyst 3.0 was used to visualise the microcosm cryoconite metabolome. Post hoc analysis of variation (ANOVA) was performed to identify the major metabolites contributing to the variation in the metabolome. This enabled the identification of 518 variables in established cryoconite that were significant to the microcosm metabolome at $P < 0.01$ and a false discovery rate (FDR) of less than 0.05. As the exact mass of metabolites exhibited minute changes at the four decimal digit scale and the scope of the metabolite databases being limited, it was more efficient to identify the top-scoring metabolites that constituted the major variables of interest. These were tentatively identified using exact mass ion standards from the KEGG database (APPENDIX I, Table I. 2).

Hierarchical cluster analysis (HCA) revealed that established cryoconite metabolites formed 3 distinct clusters (Figure 3. 9) characterised by intermediates and by-products of the tricarboxylic acid (TCA) cycle, metabolites associated with polyamine metabolism, nucleic acid biosynthesis and precursors of the coenzymes nicotinamide adenine dinucleotide (NAD^+) and nicotinamide adenine dinucleotide phosphate ($NADP^+$). Cluster 1 exhibited high initial expression that diminished over time, while the converse was evident in cluster 2, that was further distinguished by elevated concentrations of xanthoxic acid, cinchonine and adenosine during late incubation. Cluster 3, composed of formic acid, sinapyl-alcohol and dehydroshikimate, demonstrated fluctuating concentrations that peaked during early or late incubation.

Random forest classification determined that S-lactaldehyde was the metabolite responsible for majority of the variation in established cryoconite.

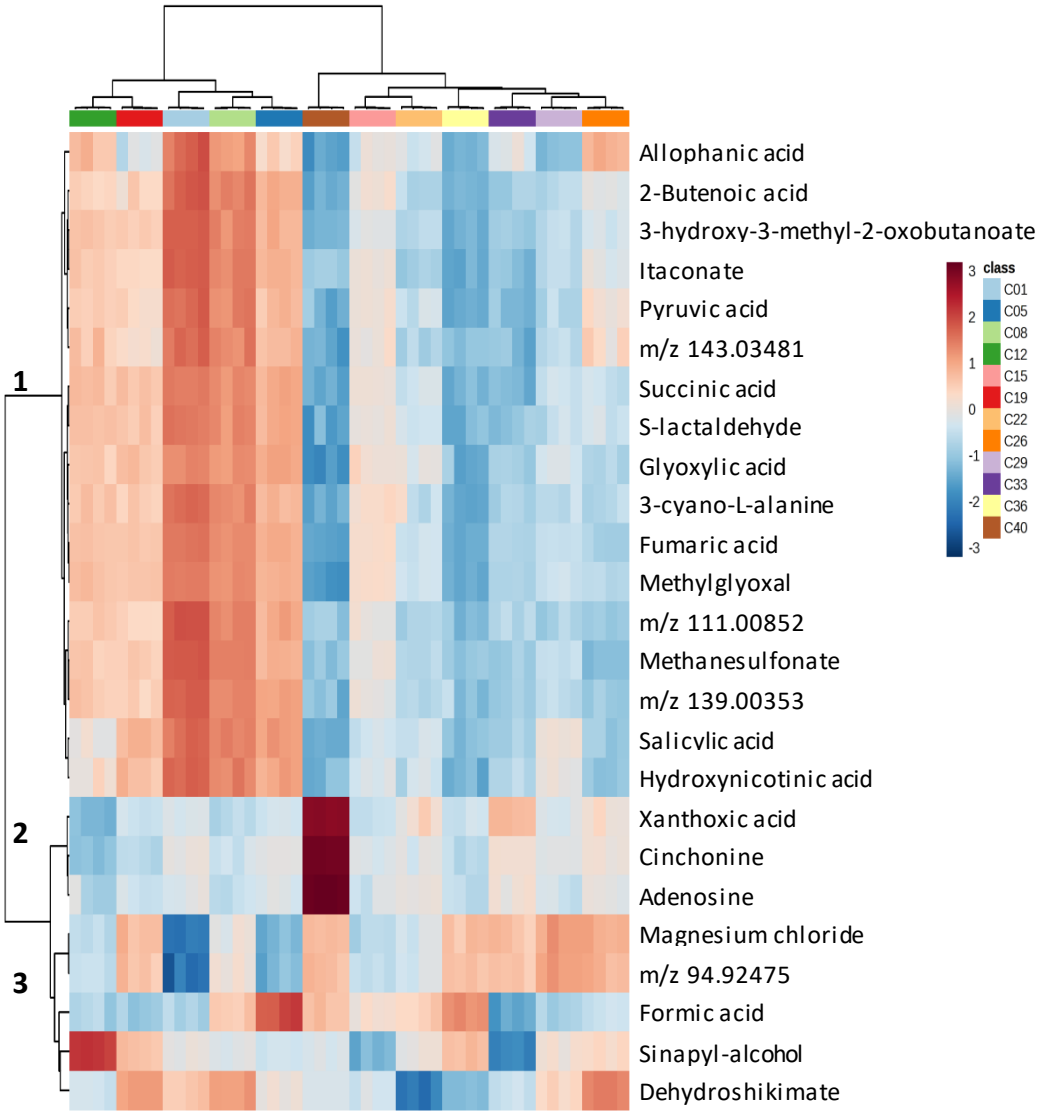

Figure 3. 9 Hierarchical cluster analysis of the 25 top-scoring ANOVA metabolites from established cryoconite microcosms incubated for 40 days. The metabolite fingerprint is characterised by high expression of nucleic acid, amino acid and tricarboxylic acid metabolites.

ANOVA of the newly seeded synthetic microcosm metabolome revealed 875 significant metabolites (P <0.01, FDR <0.05), of which the top-scoring 50 were assigned tentative identities (APPENDIX I, Table I. 3) before representation in HCA (Figure 3. 10). Newly seeded cryoconite microcosms exhibited three distinct metabolite clusters.

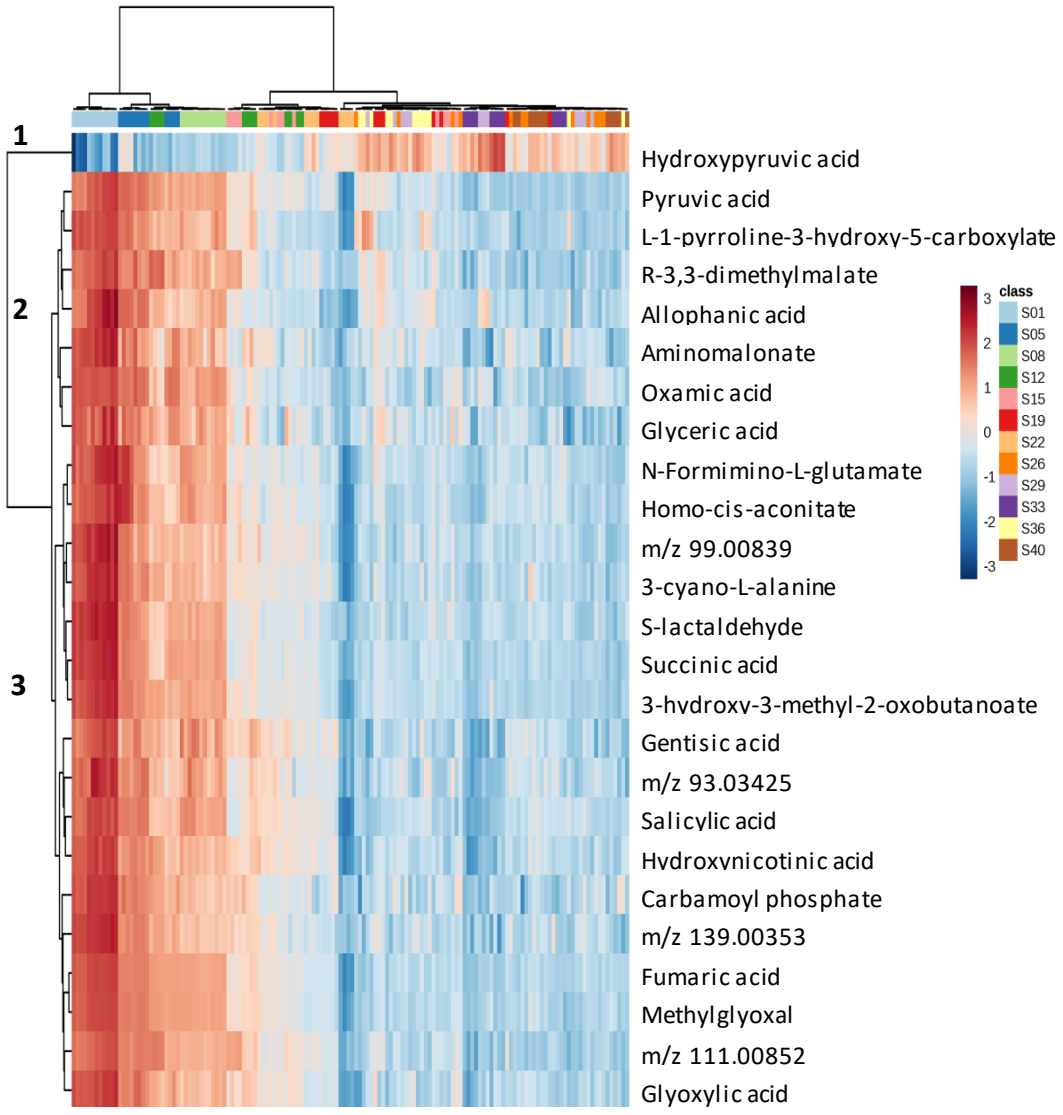

Figure 3. 10 Hierarchical cluster analysis of the 25 top-scoring ANOVA metabolites in newly seeded synthetic cryoconite microcosms. The metabolite profile shows high expression of major variables of interest during the early period that decline over the duration of the incubation.

Clusters 2 and 3 demonstrated elevated concentrations of metabolites during the early incubation period. This steadily declined until late incubation, with the exception of hydroxypyruvic acid that increased in concentration over the 40 day incubation period. Eleven of these metabolites were consistent with the established cryoconite metabolome, again highlighting the integral nature of the TCA cycle, polyamine metabolism and nucleic acid biosynthesis. In the newly seeded cryoconite metabolome, salicylic acid was identified as the main variable contributing to majority of the variation.

To establish the metabolites responsible for temporal variation in newly seeded synthetic cryoconite microcosms, random forest classification was performed at each sampling point. Tentative identification of these metabolites revealed the integral contribution of amino acid metabolism during early cryoconite development, with the appearance of more complex metabolites towards the end of the incubation period when metabolite variability was low (Table 3. 1).

Table 3. 1 Random forest selection of major variables of interest from newly seeded cryoconite metabolites during incubation.

Incubation day	Exact mass	Tentative ID	Metabolomic Pathway
1	139.03988	Methylimidazoleacetic acid	amino acid metabolism
5	102.95649	Hydroxypyruvic acid	amino acid metabolism
8	172.83059	-	-
12	409.18954	1-palmitoylglycerol 3-phosphate	glycerophospholipid
15	118.94184	3-mercaptopyruvic acid	amino acid metabolism
19	110.97545	Hydroxymethylphosphonate	antibiotic biosynthesis
22	309.20926	Icosenoic acid	fatty acid
26	311.1679	Yakuchinone A	acetate-malonate pathway
29	153.05563	Imidazole pyruvate	amino acid metabolism
33	162.89396	Molybdate	prokaryotic ABC transporter
36	294.18446	N6,N6-Dimethyl-adenosine	minor RNA modification
40	399.16815	S-acetylphosphopantetheine	citrate lyase activation

3.3.2.2. Tricarboxylic acid, amino acid and nucleic acid pathways

The tricarboxylic acid (TCA) cycle is the biochemical hub of living cells, providing the essential primary and secondary precursors for aerobic respiration. The highest contributing pathway in newly seeded microcosms was established as the TCA cycle, expressing 94.2% of the observed metabolome variance in the first two PCs (Figure 3. 11A). Congruent with previous analysis of the whole metabolome, minimal clustering was evident from the point of inoculation, as well as sparse arrangement of metabolites later in the incubation period. Further analysis by hierarchical clustering also supported previous evidence for high TCA metabolite activity and expression during early incubation that decreases over time (Figure 3. 11B).

Little contrast was prevalent in the TCA metabolites from established microcosms that exhibited discrete clustering of all metabolites, explaining 96.7% of the variation

in the metabolome in PCs 1 and 2 (APPENDIX I, Figure I. 1A). The HCA analysis revealed consistent low concentrations for the duration of the incubation, apart from day 40 (APPENDIX I, Figure I. 1B), which was in stark contrast to newly seeded microcosm metabolism.

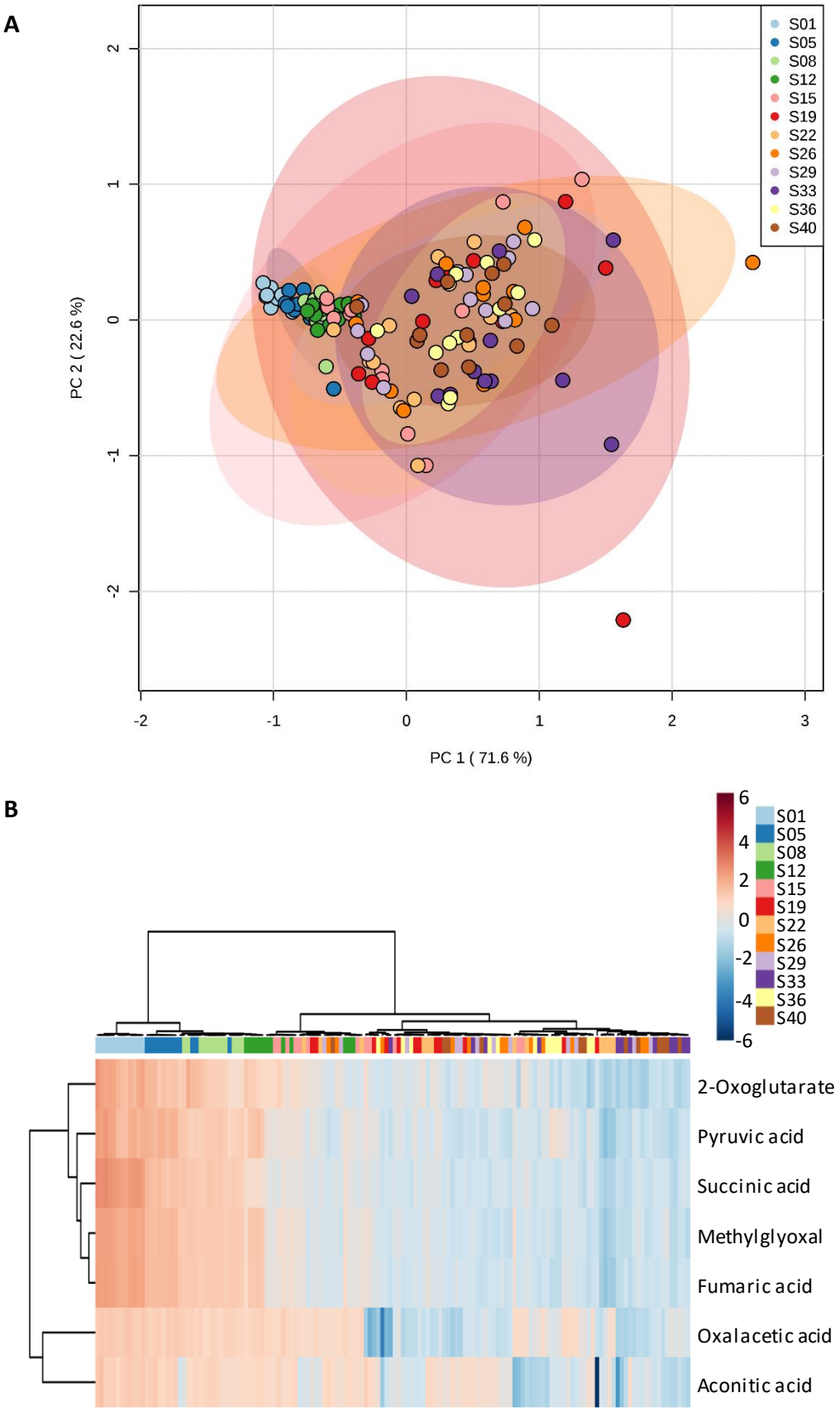

Figure 3. 11 Newly seeded cryoconite microcosms revealed profound contribution from the TCA cycle, based on (A) principal component ordination and high expression of the metabolites in (B) hierarchical cluster analysis.

A similar effect was observed in a large proportion of significantly contributing polyamine metabolites identified by post hoc ANOVA. Polyamines are an essential class of metabolites ubiquitous to all kingdoms and play roles in gene transcription, translation, expression and stress resistance. A cumulative 45.1% of the observed variation in the newly seeded microcosms was attributed to PCs 1 and 2 when observed by PCA (Figure 3. 12A), with evident clustering by incubation day. The HCA exhibited an interesting difference, however, as moderate concentrations of 5'-Methylthioadenosine, glutamine, N-acetyl-L-glutamate and cinchonine were observed for the duration of the incubation period (Figure 3. 12B). In established microcosms, PCA showed association of metabolites from week 1 - 3 and week 5 - 6 explaining 46.5% of the variation in PCA of the metabolic profile (APPENDIX I, Figure I. 1C), while HCA exhibited a similar profile as newly seeded microcosms, albeit with minor changes in the significant variables (APPENDIX I, Figure I. 1D).

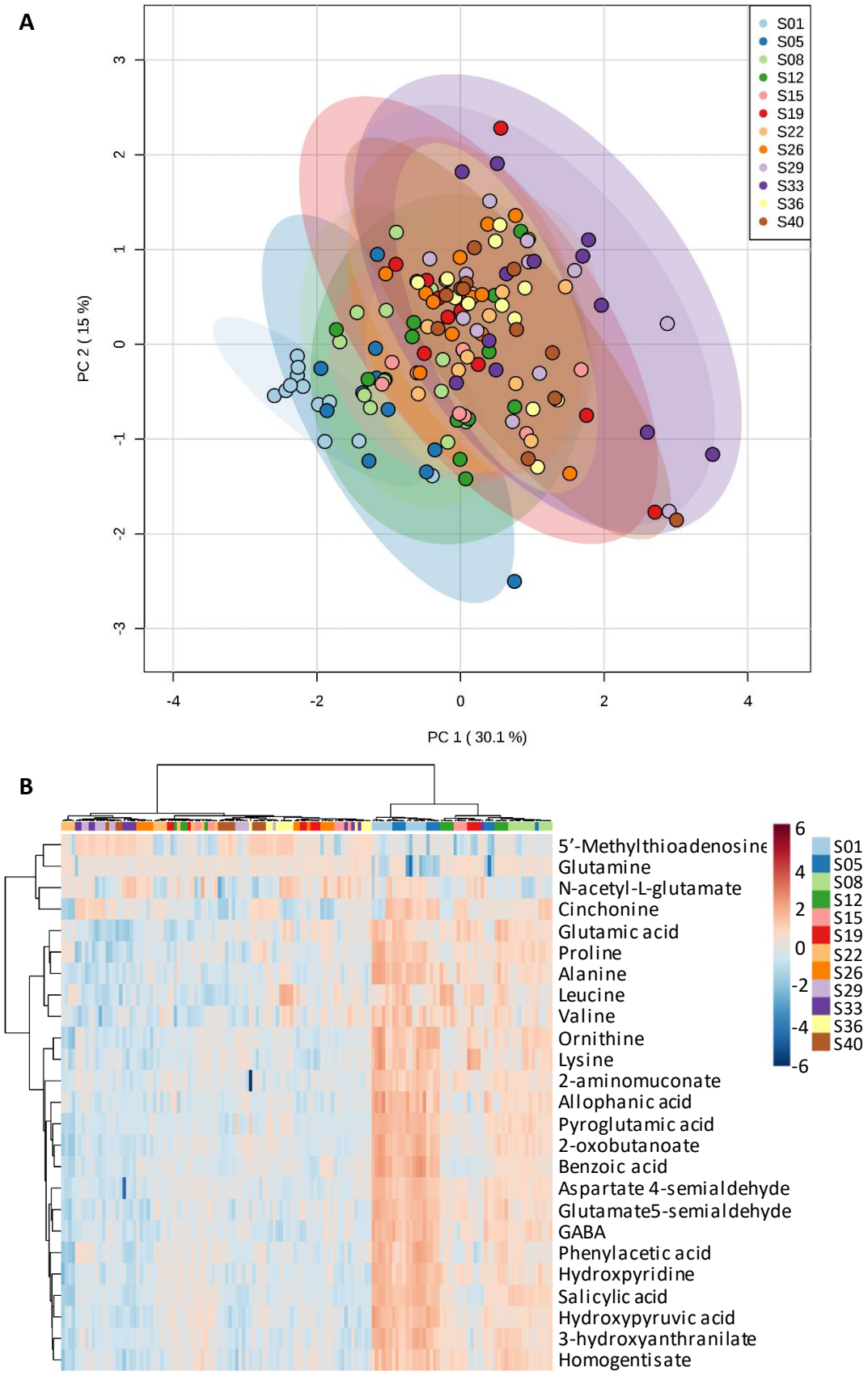

Figure 3. 12 Metabolites involved in amino acid metabolism were integral to newly seeded cryoconite as displayed in (A) principal component analysis. (B) Hierarchical cluster analysis was characterised by a cluster of metabolites exhibiting a temporal increase in metabolite concentration.

As the key molecules for the continuity of macro and microorganisms, nucleic acids are the biopolymeric building blocks of DNA and RNA. Forming the third prominent pathway, nucleic acid metabolism and biosynthesis also revealed high contribution from PCs 1 and 2 (36.3%) and distinct, albeit overlapping, confidence intervals in the PCA ordination (Figure 3. 13A). HCA analysis, however, showed one cluster of metabolites exhibiting high temporal variation similar to both TCA and amino acid metabolism intermediates, along with two clusters that were characterised by lower fluctuating concentrations throughout the incubation (Figure 3. 13B). Nucleic acid metabolism contributed more to the variation of established microcosms (46.8% in the first 2 PCs) with discrete clustering by incubation day, particularly at day 40 and day 19 (APPENDIX I, Figure I. 1E), which coincided with the temporal changes in metabolite concentration from high to moderate to low (APPENDIX I, Figure I. 1F).

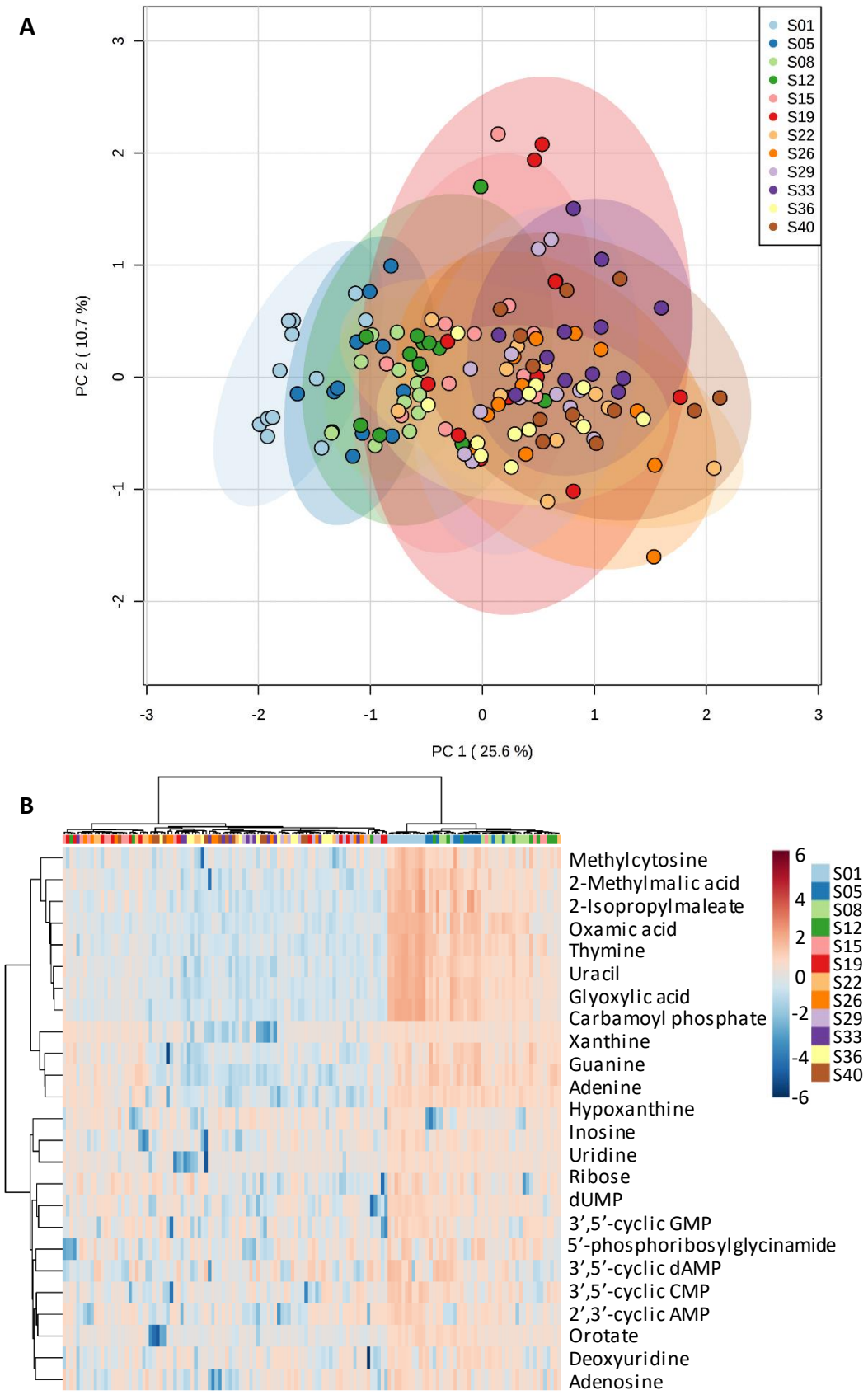

Figure 3. 13 Nucleic acid metabolism of newly seeded cryoconite showed temporal clustering in (A) principal component analysis, while (B) moderate concentrations of metabolites were exhibited for the entire incubation period in hierarchical cluster analysis.

3.4. DISCUSSION

Cryoconite holes are well characterised as environments rich in both organic and inorganic particulate matter. Biogeochemical interactions on the ice and granule surface play a key role in entraining and retaining aeolian debris, enhancing the rate of melt on glaciers worldwide (Hodson *et al.*, 2010b). As such, it is essential to understand their mechanism of formation and the involvement of the diverse microbial communities known to be abundant in this microhabitat. However, there are few studies that detail the formation of these cryoconite granules (Takeuchi *et al.*, 2001a; Langford *et al.*, 2010). This study was aimed at elucidating the physical mechanics of sediment conglomeration and to establish metabolic markers of early cryoconite establishment in a controlled setting.

Fundamental metabolic processes are consistent across all kingdoms and produce low molecular weight compounds that can be categorised as primary or secondary metabolites in the Embden Meyerhof-Parnas Pathway (EMP), Entner-Doudoroff Pathway (EDP) and Pentose Phosphate Pathway (PPP). Primary metabolic processes are essential for optimal growth, development and reproduction, due to their generating cell components in the form of lipids, vitamins, polysaccharides and intermediates for amino acid and nucleotide synthesis. Secondary metabolites (antibiotics, ergot alkaloids, naphthalenes, nucleosides, peptides, phenazines, quinolines, terpenoids and complex growth factors) are required for an organism to maintain viability for a finite period, when confronted with suboptimal abiotic conditions (Scott, 1985). The energy required to power metabolic pathways is mostly

generated through heterotrophic metabolism processes: the tricarboxylic acid (TCA) cycle, the glyoxylate cycle, electron transport and oxidative phosphorylation, anaerobic respiration and fermentation, autotrophic processes using inorganic NH_3, NO_2^-, S_2, and Fe^{2+} generated from degradative cellular processes, photolithotrophic and photoorganotrophic reactions (Prescott *et al.*, 2002).

It is important to consider that, compared to more mature 'omics approaches, where sequence analysis is readily available via web-interfaces, bioinformatic programming and electronic databases, metabolomics is still a computationally evolving field, in addition to its emphasis on biochemistry and analytical chemistry techniques. The need to relate metabolite data to biology and metabolism through cheminformatics and bioinformatics requires the use of searchable databases and software tools for analysis and property, pathway or process modelling or prediction. Recent online tools, such as Metaboanalyst (Xia *et al.*, 2015), facilitate this process, however, the information contained in traditional metabolomic databases, such as KEGG (Kanehisa *et al.*, 2006) and MetaCyc (Krieger *et al.*, 2004), is often insufficient for environmental metabolomics as these resources are fashioned on human and model organism metabolites. As this study presents the most detailed metabolome-based investigation of cryoconite and environmental samples to date, previously established data and resources limited the identification of tentative metabolites and pathways and processes.

3.4.1. Microbial community establishment on the granule surface

Confocal laser scanning microscopy (CLSM) of newly established cryoconite granules demonstrated the changes in nucleic acid, extracellular polymeric substances and chlorophyll expression for the duration of a single simulated summer. Individual cryoconite granules reveal a rich microbial consortium that evolves over time from the action of filamentous *Cyanobacteria*. Their growth aggregates the surrounding debris and minerals to form cryoconite (Takeuchi *et al.*, 2001b) and additionally coincides with the early cryoconite metabolome, highlighting metabolites integral to microbial growth and cellular proliferation. Comparison with control microcosms demonstrate that this process is absent in established cryoconite, as they have a previously established rich phototrophic and heterotrophic microbial matrix that maintains the well-recognised stable quasi circular shape.

Particulate associated biomass contributes greatly to the microbial community harboured in this habitat, consistent with primary colonisation in subglacial habitats (Mitchell *et al.*, 2013). The high initial microbial biomass observed in inoculum granules (Figure 3. 4) was key to these synthetic habitats exhibiting an increase in microbial biomass over time, with the appearance of cyanobacterial filaments mediating the agglomeration process. This is consistent with Langford *et al.* (2010), who successfully identified heterotrophic and autotrophic communities in cryoconite granules by confocal and scanning electron microscopy of DAPI (4',6-diamidino-2-phenylindole) stained samples. The potential of overestimating the cellular nucleic acid signal was a concern, as microbial EPS consists of lipids (Neu, 1996; Takeda *et al.*,

1998), polysaccharides (Costerton *et al.*, 1981), proteins and nucleic acids (Frolund *et al.*, 1996; Nielsen *et al.*, 1997). However, in these samples, areas expressing high EPS concentrations were not congruent with nucleic acid expression. Therefore, all observed DNA fluorescence was potentially of cellular origin from microbes attached to the sediment. It must be taken into consideration, however, that this observation could imply an inability of SYBR®Gold to penetrate the EPS, as specific dyes, such as SYTO 63 (Chen *et al.*, 2007) and DAPI (Langford *et al.*, 2010), have been recorded to permeate dense biofilms and bioaggregates better than others in aid of the identification of cellular nucleic material. Nonetheless, SYBR® stains are preferential markers of nuclear DNA in fluorescence and confocal laser microscopy (Suzuki *et al.*, 1997). In fact, SYBR®Gold is characterised by increased and persistent fluorescence signals (Shibata *et al.*, 2006) and is recognised as a superior stain when compared to its counterpart, SYBR®Green, for the staining of nuclear DNA.

Photosynthetic autofluorescence in all established samples were minimal, compared to newly seeded cryoconite, that demonstrated a vast quantity of chlorophyll pigment (Figure 3. 4D, Figure 3. 5D, Figure 3. 6D) that is associated with filamentous and unicellular *Cyanobacteria*, consistent with previous observations of Svalbard cryoconite by Langford *et al.* (2010). Similar high autotrophic biomass was reported by Bradley *et al.* (2016) in mesocosm experiments examining the evolution of proglacial soil microbial communities. Filaments observed in the cryoconite microcosms are consistent in measurement with *Phormidium* sp., *Lyngbya* sp., and *Oscillatoria* sp. (diameter 4 - 11 µm), while spherical clusters could potentially be

assigned to phototrophic bacteria or heterocyst forming *Cyanobacteria* from the order *Nostocales,* that are additionally capable of nitrogen fixation (Rippka *et al.*, 1979; Langford *et al.*, 2010; Bradley *et al.*, 2016). Photosynthesising filaments and high EPS expression appear slightly co-ordinated, implying the filamentous *Cyanobacteria* exude mucilaginous polymeric substances that adhere individual sediment, mineral and microbial particulates, consistent with the physical (Langford *et al.*, 2010) and genetic evidence (Chrismas *et al.*, 2016) of *Phormidesmis* species. The absence of photosynthetic metabolites among the major contributors to the newly seeded community metabolic profile is therefore incongruous to the physical appearance of these granules. This could imply a predominantly heterotrophic lifestyle in the pioneering cryoconite bacterial community, while *Cyanobacteria* play a chief role in granule stabilisation to raise the nutrient status, as demonstrated in the nutrient poor glacial forefield of Midtre Lovenbreen (Hodkinson *et al.*, 2003).

3.4.2. Newly seeded cryoconite metabolome indicates a prominent heterotrophic microbial community

Heterogenous distribution of nuclear DNA was observed in both newly seeded and established microcosms for the entire duration of the incubation. However, newly seeded communities were clearly richer in microbial aggregates, as evidenced by bright signals from fluorescence microscopy of SYBR®Gold stained nucleic acids. Ion Torrent 16S rRNA gene sequence data from mesocosm experiments and numerical modelling of proglacial soils in Midtre Lovenbreen, confirm that this observation is not limited to ice surface habitats (Bradley *et al.*, 2016). That study goes on to

demonstrate that pioneering communities in proglacial soils contribute to a net efflux of CO_2 due to low growth efficiency. The cryoconite microcosm habitat, however, demonstrates high initial metabolic activity across integral biochemical pathways essential for sustaining the newly seeded microbial community, indicative of a heterotrophic state.

Functional genes are adapted to exploit allochthonous nutrients, as emphasised in a metagenomic study of Alpine cryoconite by Edwards *et al.* (2013b). Microbial interaction with mineral surfaces and the metabolism of key species are critical for sustaining microbial life in nutrient poor habitats, as demonstrated in subglacial habitats where mineralogical controls, in addition to iron and sulphur remnants of the incubated minerals and glacial meltwater, structure the community (Mitchell *et al.*, 2013; Hodson *et al.*, 2015). Similar controls could be prevalent in the minerals and sediment constituting the newly seeded cryoconite community, where the redox environment and delivery of nutrients and organic matter by surface melt and aeolian distribution characterises their microbial ecology.

It is interesting to note that more energy (inferred from the presence of coenzyme NAD^+ and $NADP^+$ precursors) (APPENDIX I, Table I. 2 and Table I. 3) was being expended on the maintenance of these heterotrophs than for proliferation of new cells, as nucleic acid metabolism and biosynthesis was statistically ranked third in the newly seeded cryoconite metabolome, when considering the PCA scores (Figure 3. 13A). However, the observed 10% difference between the expression of this pathway

in pioneer and established microcosms can be deemed negligible, as temporal analysis displays remarkable similarities in the concentration of nucleic acid related metabolites during early, mid and late simulated summer.

The cryoconite microbial community is additionally exposed to a dramatic change in the surrounding chemistry, upon inoculation into a new habitat, be it natural or synthetic. As such, their metabolism is required to modify to contend with the adequate supply of readily available nutrients (Brooks *et al.*, 2011). However, simulated and natural cryoconite holes are confirmed depauperate or oligotrophic systems (Cook *et al.*, 2015b), thus a strong stress response from the summer cryoconite metabolome is absent, as the seed community would have acclimatised to the recurrent yet transient environmental changes. It is therefore expected that both established and newly seeded synthetic microcosms highlight the tricarboxylic acid cycle, indicative of high levels of aerobic respiration in the cryoconite microcosms by production of usable chemical energy in the form of ATP. However, the expression between these two microcosms differ as expected, given their differences in sediment, and consequently microbial, composition.

Established communities exhibit homogeneous expression of TCA metabolites (APPENDIX I, Figure I. 1B), implying that these communities have consistent low levels of activity during the summer period. A contrast is clear in the TCA cycle of newly seeded cryoconite holes that exhibit a strong temporal variation in initial cellular activity with a down regulation of these components over time. This is directly

indicative of the regulation of cellular respiration over time (Prescott *et al.*, 2002). The conversion of glucose to pyruvate is one of the integral committed steps in regulating the TCA cycle. In the pioneer cryoconite metabolome, there is strong expression of pyruvate, succinate and fumarate that are additionally variables of major statistical variation. Their high concentration suggests that the microbial community rapidly breaks down the available carbon-based fuels provided by the artificial meltwater before nutrient deprivation, in order to sustain or replenish the ATP required for cellular functioning. Metabolomic responses to carbon and nitrogen starvation observed in *Escherichia coli* and *Saccharomyces cerevisiae* are consistent with this observation (Brauer *et al.*, 2006). The process is regulated later in the incubation, as is documented by the lower, but uniform, concentrations of aconitate, an early TCA intermediate, and final TCA metabolite, oxaloacetate, that feeds back into the cycle at the first committed step. This creates a metabolism loop within the newly seeded cryoconite community that is sustained over time, resulting in the observed steady concentrations of TCA cycle intermediates (APPENDIX I, Figure I. 1B) exhibited by the heterotrophic microbes of the established community (Hodson *et al.*, 2005; Anesio *et al.*, 2009; Irvine-Fynn *et al.*, 2012).

It is important to note that CLSM of established communities (Figure 3. 4 - Figure 3. 6, inset) demonstrated the strongest autofluorescence signals from unicellular and filamentous photosynthesising microbes, particularly as there is metabolic evidence of carotenoid precursors and intermediates xanthoxic acid, phosphoric acid, abscisic acid and geranyl geranyl pyrophosphate (GGPP) (APPENDIX I, Table I. 2). Similar

autofluorescence has been observed in Langford *et al.* (2010), demonstrating highest prevalence of filamentous photoautotrophs in Midtre Lovenbreen cryoconite, where the seed community utilised as inoculum in this investigation was sourced, supporting research that minerology contributes to the structural heterogeneity of the newly forming cryoconite granule (Takeuchi *et al.*, 2001b; Stibal *et al.*, 2008; Hodson *et al.*, 2010b). As such, newly seeded cryoconite can be characterised as heterotrophic microhabitats, displaying prominent carbon metabolism with an absence of related photosynthetic metabolites, despite the abundance of photosynthesising filamentous *Cyanobacteria*. This provides molecular support for previous work on the role of cyanobacterial filaments in sediment aggregation, that are integral to the formation of individual cryoconite granules (Langford *et al.*, 2010; Takeuchi *et al.*, 2010).

Established cryoconite habitats, in contrast, exhibit both phototrophic and heterotrophic metabolism, further highlighting the disparities between pioneering and established cryoconite habitats. The established synthetic microcosm assemblage is consistent with the initial work on cryoconite holes by Takeuchi *et al.* (2000), that demonstrated the protracted unstable lifecycle of cryoconite in natural systems. These cryoconite granules persist for 3 - 7 years before deteriorating and restarting the sediment agglomeration process. Additionally, the annual melt season growth related processes, indicated by concentric growth rings (Takeuchi *et al.*, 2001b), consequently changes the granule structure and microbial community in

successive active seasons (Musilova *et al.*, 2016), albeit minimally, which ultimately modifies the glacier surface.

3.5. SUMMARY

Investigating the development of cryoconite from sediment to granule highlights the dichotomous trophic nature of cryoconite ecosystems. This is mediated by the abundant pioneering microbial community that is established during the first summer period following inoculation of the ice surface, consistent with previous studies on newly seeded communities on ice surfaces (Musilova *et al.*, 2016). Cyanobacterial filaments and polymeric exudates from recognised cryoconite microbiota are essential to granule formation (Langford *et al.*, 2010), while the remaining microbial community is responsible for the highly heterotrophic lifestyle that sustains the cryoconite microbiome, during pioneering stages of metabolism and granule formation. This is inferred from high levels of pyruvate metabolism and the presence of numerous TCA cycle intermediates, that most likely continue to sustain the community in the following melt seasons, potentially through a nutrient loop mechanism. Once established, the microbial community employs the abundant phototrophic bacteria and *Cyanobacteria* for carbon metabolism, as demonstrated by the expression of carotenoid metabolites and related intermediates in established communities during the same period. Furthermore, the expression of polyamines and nucleic acids essential for growth and metabolism of living biomass in cryoconite, demonstrate that both pioneer and established habitats experience their highest

growth rates early in the melt season, stabilising them for potential changes in external factors that can affect the microbiology of the system.

CHAPTER 4 – BACTERIAL BIOGEOGRAPHY OF HIGH ARCTIC ICE CAP CRYOCONITE IN FOXFONNA, SVALBARD

This chapter has been adapted from the original 2016 publication by the author - APPENDIX VI:

Gokul, J. K., Hodson, A. J., Saetnan, E. R., Irvine-Fynn, T. D. L., Westall, P. J., Detheridge, A. P., Takeuchi, N., Bussell, J. S., Mur, L. A. and Edwards, A. 2016. Taxon interactions control the distributions of cryoconite bacteria colonizing a High Arctic ice cap. *Molecular Ecology*, 25, 3752–3767.

Study conceived by A.J.H., J.K.G. and A.E. Fieldwork conducted by A.E., T.I.F., J.S.B., N.T. and A.J.H. Laboratory work conducted by A.E., J.K.G., P.J.W. and A.P.D. Data analysis conducted by J.K.G., E.R.S., T.I.F., L.A.J.M. and A.E. Manuscript written by J.K.G., E.R.S., T.I.F. and A.E.

4.1. INTRODUCTION

Ice caps are defined as terrestrial ice masses that are unconstrained by the topography of their underlying terrain and are shaped by their surface mass balance. They are distinct from ice sheets, having a surface area of less than 50 000 km^2 (Benn and Evans, 2010). Ice cap glaciers provide an attractive model system for exploring the biogeography of microbial community development. While studies of species turnover across elongated environmental gradients, for example at the ice sheet scale, could provide further insights, these would be across a broader, potentially continental biogeographical scale, since ice sheets span latitudinal and climatological gradients. As a consequence of ice cap surface topography, the associated microbial communities are likely to be situated within strong local environmental gradients in the same locality. Consequently, the influence of seasonal melting upon community history or the response of cryoconite bacterial communities to environmental drivers

prevailing within stable, low gradient ice masses is unknown. This is likely to be the consequence of truncated environmental gradients associated with a low-complexity landscape responding to melt associated drivers over a short dynamic range as the melting season proceeds rapidly.

While previous studies show evidence of discrepancies between inter-regional and inter-glacier cryoconite bacterial communities (Edwards *et al.*, 2011; Cameron *et al.*, 2012), the drivers and extent of spatial variation at the scale of individual glaciers are unclear. High-resolution sampling of cryoconite on a single Svalbard valley glacier recently found only moderate evidence for changes in the properties of cryoconite granules across the ice surface (Langford *et al.*, 2014). Likewise, Edwards *et al.* (2011) reported that inter-glacier differences outweighed very weak distance decay relationships in bacterial community structure on three Svalbard valley glaciers. Furthermore, the temporal dynamics of cryoconite bacterial communities are less clear, with contrasting inferences made from intra-seasonal sampling of cryoconite ecosystems at the margin of Greenland's Ice Sheet in two recent studies (Musilova *et al.*, 2015; Stibal *et al.*, 2015b).

While the role of filamentous *Cyanobacteria* is pivotal to the formation of stable cryoconite granules (Langford *et al.*, 2010) harbouring a diverse community of bacterial heterotrophs, their role as keystone species or ecosystem engineers is as yet unestablished (Edwards *et al.*, 2014b). Furthermore, their interactions with the considerably abundant heterotrophic communities (Hell *et al.*, 2013; Edwards *et al.*,

2014b), combined with the physical conditions presented, are imperative to understanding the community dynamics on an ice cap glacier.

In this chapter, cryoconite was collected from the area across an ice cap in the High Arctic Archipelago of Svalbard, which was constrained by a high resolution digital elevation model, permitting a detailed analysis of the bacterial biogeography in relation to the topography of the ice cap. By employing high throughput Illumina sequencing of the 16S rRNA gene region, the assembly of the cryoconite bacterial communities were evaluated to test the following hypotheses:

a. The relative influence of dispersal on an ice cap can be predicted by distance decay relationships,
b. The effect of environmental and biotic filters can be evaluated by examining correlations between physical parameters and taxon interactions of ice cap cryoconite microbiota respectively.

4.2. SAMPLING AND EXPERIMENTAL TECHNIQUES

4.2.1. Description of Foxfonna

A total of 38 samples were collected from elevations above 700 m a.s.l. of a dome shaped ice cap at 78˚ 08' N, 16˚ 07' E on the 23rd of August 2011, towards the end of an ablation season in an approximately average net mass balance year (-0.38 m water equivalent). The dome measured approximately 4 km^2 in central Svalbard (Rutter *et al.*, 2011) and is located alongside two small outlet glaciers: Rieperbreen to the west

and an unnamed outlet glacier to the north (Figure 4. 1A). A typical evaluation of melt indicates a short period over summer (approximately 45 days) during which there was an annual average net surface mass balance 0.25 ± 0.36 (SD) m water equivalent from 2007 - 2014 (Rutter *et al.*, 2011). The variability is caused by occasional positive balance years during 2008 and 2012. The development and exposure of cryoconite debris was promoted by the melting overlaying ice, as is common at high elevations during late summer in Svalbard (Wadham *et al.*, 2006). Sampling was undertaken at four sectors on the ice cap surface: G1, G2, G3 and G4 (Figure 4. 1B).

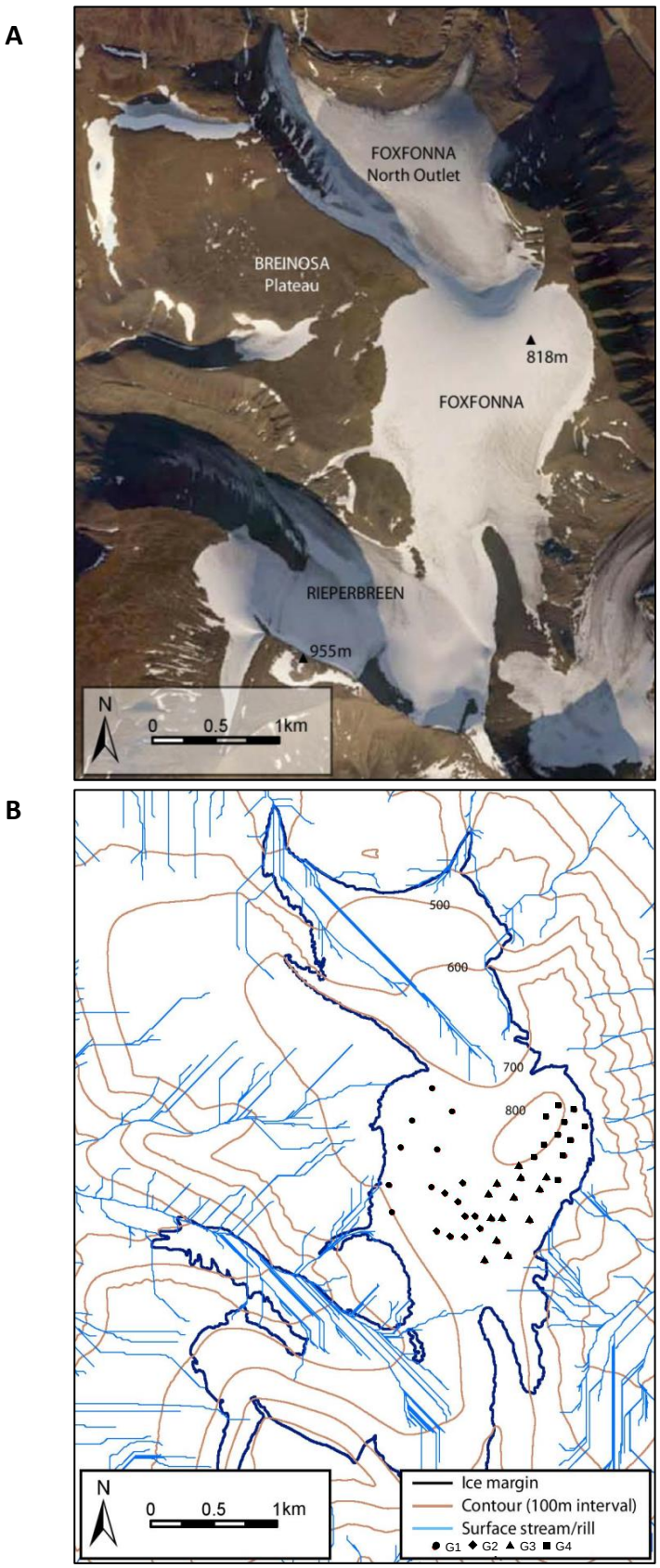

Figure 4. 1 Map of Foxfonna ice cap on Svalbard with (A) aerial overview and (B) extracted digital elevation model, indicating sample points distinguished by sector within the figure key. Image credit: Dr. Tristram Irvine-Fynn.

4.2.2. Surface conditions on Foxfonna ice cap

A digital elevation model (DEM) of the ice cap surface was compiled by Dr. T. D. L. Irvine-Fynn as described in Gokul *et al.* (2016). Using ArcGIS software (ESRI), slope, aspect, curvature and hydrological flow indices were calculated and further environmental effects (flow accumulation area (FAA) and meltwater discharge) were extrapolated from this (Irvine-Fynn *et al.*, 2011; Irvine-Fynn and Edwards, 2014). Additional surface conditions were calculated from the DEM and air temperature records from the weather station on the northern outlet glacier, including potential incident radiation receipt for all locations across the ice cap (Irvine-Fynn *et al.*, 2014). Measures of melt positive degree days (PDD) and positive degree hours (PDH) (Hock, 2005) were derived from the weather station records using a local air temperature lapse rate of -0.65 °C per 100 m elevation. This range of environmental parameters (APPENDIX II, Table II. 1) was extracted and normalized in PRIMER 6/PERMANOVA+ for multivariate statistical analyses.

4.2.3. Experimental procedures

Cryoconite samples were collected aseptically, stored and transported as per Chapter 2, section 2.2.1. Nucleic acids were extracted using the hexadecyltrimethylammonium bromide-phenol-chloroform bead-beating extraction and polyethylene glycol precipitation (Griffiths *et al.*, 2000) method (Chapter 2, section 2.4.1) before 16S rRNA gene region amplification (Chapter 2, section 2.5), Ion torrent library preparation (Chapter 2, section 2.6.1) and sequencing (Chapter 2, section 2.6.2) was conducted. Sequence data are available at EBI-SRA SRP067436:

PRJNA306097. Bioinformatic analysis was performed in QIIME 1.9.0 on the generated sequence data (Chapter 2, section 2.7) and a combined biotic and abiotic co-occurrence network created in R from vectors representative of the OTU and environmental variables (Chapter 2, section 2.8).

4.3. RESULTS

4.3.1. Phylogenetic community composition

Ion torrent sequencing yielded 4 609 547 reads from 37 cryoconite holes, across the four sectors. Samples were collectively rarefied to 8 419 reads and further filtered to represent 0.01% of the population, generating a total of 755 bacterial OTUs. These were assigned to 13 phyla using a 97% similarity cut-off. *Proteobacteria* was observed to dominate communities in all sectors (28.8% RA), followed by *Actinobacteria* (21.8% RA), *Cyanobacteria* (18.4% RA), *Bacteroidetes* (7.0% RA), *Chloroflexi* (5.5% RA), *Gemmatimonadetes* (4.85% RA) and *Acidobacteria* (1.77% RA). Within individual sectors (Figure 4. 2), *Proteobacteria* was the abundant phylum in sectors G1 - G4, with RAs of 31.5%, 24.5%, 28.9% and 29.2%, respectively. *Actinobacteria*, on the other hand, were the second most abundant in G1 (23.9% RA), G2 (22.9% RA) and G4 (24.7% RA). The phylum *Cyanobacteria* was second most represented in the sequence data from sector G3 (21.7% RA) and third in sectors G1 (20.0% RA), G2 (14.6% RA) and G4 (17.5% RA). Within the *Proteobacteria*, *Betaproteobacteria* dominated over other classes (16.2% RA), followed by *Alphaproteobacteria* (6.8% RA). No significant differences were observed in the Shannon diversity indices

(ANOVA, F = 0.4, *P* = 0.754) and evenness value (ANOVA, F = 0.27, *P* = 0.845) between the four sectors (APPENDIX II, Table II. 2).

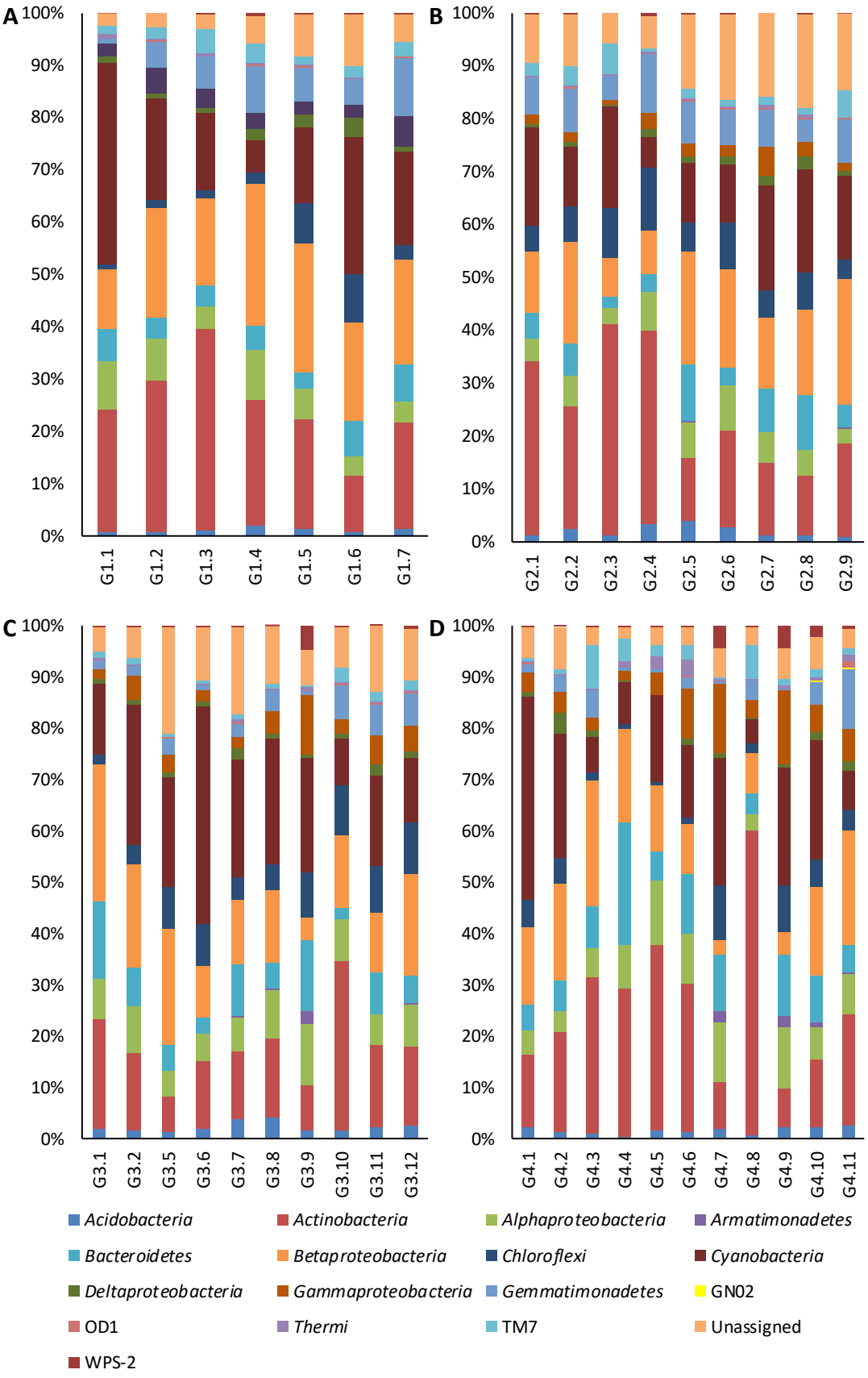

Figure 4. 2 Bacterial composition of cryoconite sampled from sectors (A) G1, (B) G2, (C) G3 and (D) G4 on Foxfonna ice cap using Greengenes assigned phyla from 16S rRNA gene semiconductor sequencing.

4.3.2. Environmental influence on bacterial community structure

Majority of the environmental factors gathered for all points displayed a significant sector separation effect (PERMANOVA, pseudo-F = 3.0622, *P* = 0.001 with 999 permutations) as established by canonical correspondence analysis (Figure 4. 3A). This is further supported by marginal tests of geographic position (Northings, Eastings, elevation, slope and aspect), melting season duration (summer positive degree days and hours, positive hours, number of hours with incident radiation) and biotic factors (chlorophyll *a* concentration and apparent cryoconite area) explaining 29.2% of the total variation when predicted in stepwise fashion using an adjusted R^2 distance-based linear modelling (distLM) (Figure 4. 3B, APPENDIX II, Table II. 3).

Of these, sequential tests revealed positive degree days in summer as the most influential, followed by slope, Northings, apparent cryoconite area and Eastings (APPENDIX II, Table II. 4). Wetness, FAA, incident radiation, positive degree hours and elevation did not contribute significantly to the final model (*P* >0.05). Additionally, each combination of sectors is significantly different (Pairwise PERMANOVA, t = 1.48 - 2.27, *P* = 0.001 - 0.007), suggesting a clear positional effect on ice cap surface community structure. Grouping the RA by phylum resulted in a significant difference (pseudo-F = 2.43 - 5.74, *P* = 0.001 - 0.007) being observed for all phyla except *Acidobacteria* and *Thermi*.

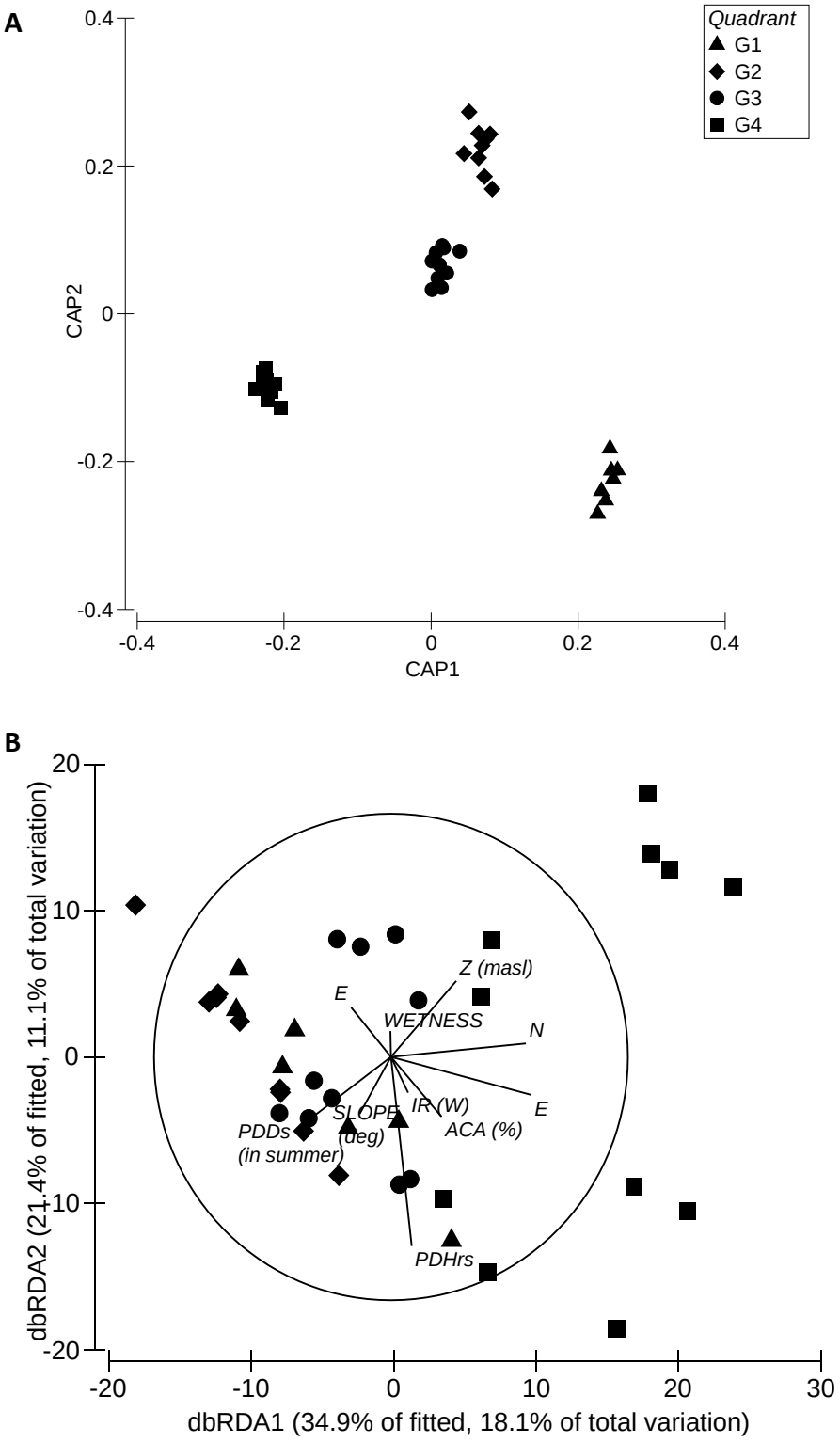

Figure 4. 3 Ordination-based analysis of Foxfonna ice cap cryoconite communities showing the (A) canonical analysis of principal co-ordinates with distinct sector separation and (B) the distance-based redundancy ordination generated from distance-based linear modelling of the environmental parameters.

4.3.3. Distance decay effect on bacterial cryoconite community structure

Potential pairwise distance decay relationships were tested for in Bray-Curtis similarity of fourth root transformed OTU relative abundance and geographic distance of holes at distances between 77 and 1 664 metres. The distance decay plot of the overall community (Figure 4. 4) displayed a weak relationship between geographic distance (m) and community dissimilarity. This is confirmed by RELATE analysis, which revealed a moderate spatial influence upon overall community structure ($\rho = 0.275$, $P = 0.001$). This effect is accounted for by significant Spearman correlations (Table 4. 1) for 5 out of 14 observed taxa.

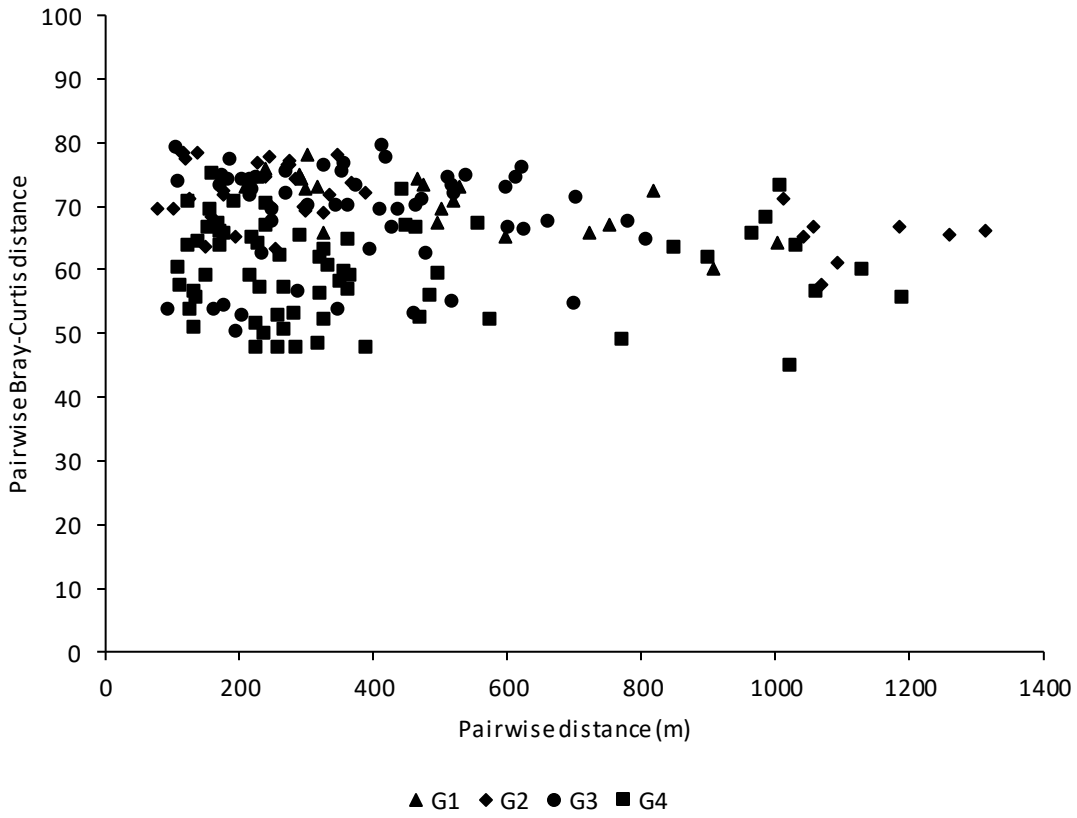

Figure 4. 4 Distance decay relationship between pairwise Bray-Curtis distance matrix of 16S rRNA gene sequences and pairwise physical distance.

Table 4. 1 Spearman correlation between matrices of physical and Bray-Curtis distance by phylum provided via RELATE analysis.

Phylum	**Rho**	***P* value**
Chloroflexi	0.36	0.001
Unassigned	0.397	0.001
Acidobacteria	0.256	0.012
Gemmatimonadetes	0.219	0.025
Proteobacteria	0.188	0.045
TM7	0.146	0.063
Cyanobacteria	0.154	0.065
Actinobacteria	0.123	0.114
Bacteroidetes	0.113	0.141
Thermi	0.094	0.174
OD1	0.086	0.203
WPS-2	0.079	0.233
Armatimonadetes	-0.019	0.549
GN02	-0.111	0.887

4.3.4. Cryoconite communities have a dominant generalist core

The distribution and dominance of specific bacterial taxa in cryoconite across the Foxfonna ice cap was explored using an occupancy plot of the mean relative abundance of OTUs (clustered at 97%) across all samples in comparison to the number of samples containing each OTU (Barberán *et al.*, 2012). The cryoconite bacterial community was strongly dominated by a small number of taxa (Figure 4. 5). Of the 755 OTUs present in the data set, only 16 OTUs were present at a mean RA greater than 1% per sample. The cross-sample cumulative RA of these 16 OTUs was strongly correlated with mean RA (Pearson r = 0.99, P <0.0001), indicating minimal variation in their RA in sites across the ice cap. Strikingly, all 16 OTUs with a mean RA of >1% per sample were present in at least 36 of the 37 cryoconite samples analysed and in all 37 samples for 13 of those OTUs. Consequently, these 16 OTUs were collectively considered a group of core taxa which was both ubiquitous and abundant

within the cryoconite bacterial community. BLAST-based closest environmental relatives (CER) and closest named relatives (CNR) of core taxa (Table 4. 2) revealed the core OTUs closely match uncultured sequences (CER % ID 97 - 99%) mainly from cryospheric (13 OTUs) and soil (3 OTUs) habitats worldwide and were more distantly related to taxa cultivated from soil (14 OTUs, CNR % ID 88 - 98%) and Antarctic *Cyanobacteria* (2 OTUs).

A long tail distribution of less abundant, variable occupancy, non-core taxa was also present (Figure 4. 5). Across both core and tail populations, mean RA was positively correlated with occupancy (Spearman R = 0.77, P <0.001). The tail population of the cryoconite bacterial community on Foxfonna comprised OTUs affiliated to at least 9 phyla, including the proteobacterial classes *Alpha-*, *Beta-*, *Delta-* and *Gammaproteobacteria*. The core OTUs included representatives of *Actinobacteria* (5 OTUs), *Cyanobacteria* (2 OTUs), *Proteobacteria* (1 *Alphaproteobacteria* OTU, 3 *Betaproteobacteria* OTUs and 1 *Gammaproteobacteria* OTU) and single OTUs from each of *Bacteroidetes*, *Chloroflexi*, *Gemmatimonadetes* and an unassigned OTU. Of these OTUs, an OTU assigned to the filamentous cyanobacterial genus *Leptolyngbya,* denovo-40205, appeared very prominent, being present in all 37 sites and at a mean RA (12.5%) four times greater than the next most dominant OTUs, an actinobacterial taxon affiliated to *Microbacteriaceae* and a *Betaproteobacteria* OTU, both present at 4.4 - 4.5% mean RA. All remaining core OTUs present revealed a mean RA range of 1.0 - 2.9% and included an OTU affiliated to the filamentous cyanobacterial genus *Phormidium* (1.14% mean RA, at 36 sites).

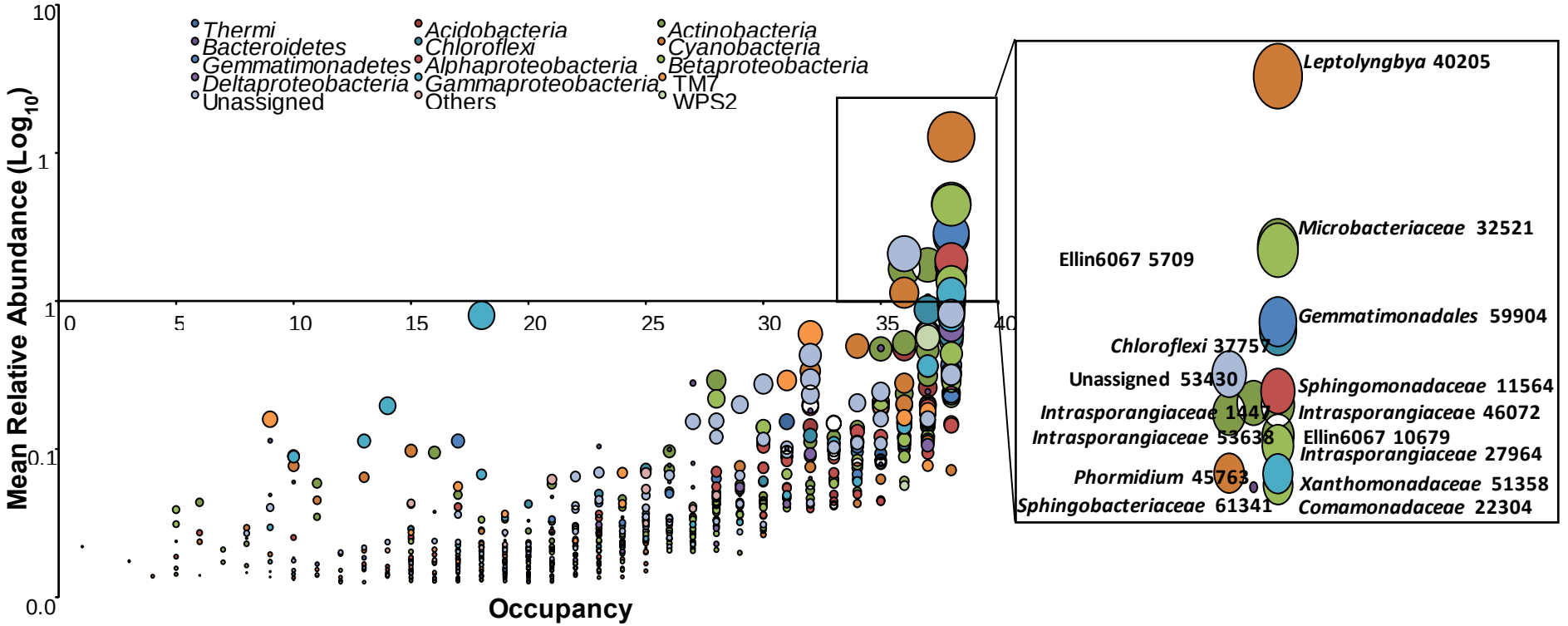

Figure 4. 5 The occupancy plot, i.e. the presence of an OTU at a site, of Foxfonna ice cap cryoconite bacterial communities reveals a core of dominant generalist bacterial taxa (annotated exploded view in inset). Bubble size is proportional to $\log_{10}$ of total relative abundance and are shaded by taxonomy.

Table 4. 2 BLAST identity of closest environmental relatives (CER) and closest named relatives (CNR) of core taxa on Foxfonna ice cap.

Greengenes ID	Closest Environmental Relative (CER)	CER Accession	CER %ID	CER Habitat	Closest Named Relative (CNR)	CNR Accession	CNR %ID	CNR Habitat
Sphingobacteriaceae-61341	Uncultured *actinobacterium* clone IC4008	HQ622724.1	99	Svalbard ice	*Pedobacter daechungensis*	NR_041507	89	Korean lake sediment
Microbacteriaceae-32521	*Frigoribacterium* sp. MP117	KC256951	99	Tibetan glacier	*Frigoribacterium* sp. MP117	KC256951	99	Tibetan glacier
Intrasporangiaceae-46072	Uncultured bacterium clone ANTLV2_G12	DQ521529	98	Lake Vida ice, Antarctica	*Oryzihumus* sp. aerobe-19	KP185144	93	Korean grassland
Chloroflexi-37757	Uncultured bacterium clone gls106	KC286738	98	Chinese glacier	*Azospirillum* sp. YM 195	GU396257.1	89	Sugarcane rhizome
Intrasporangiaceae-27964	Uncultured bacterium clone gs34	JF420640	97	German glacier sediment	*Humibacter albus*	AM494541	91	sewage sludge
Gemmatimonadales-59904	Uncultured bacterium clone NC54g8_19617	JQ377159	97	FACE soil	Ellin5220	AY234571	92	soil
Phormidium-45763	Uncultured cyanobacterium clone LJ14_522	KM112145	98	Antarctic microbial mat	*Phormidium autumnale* Ant-Ph68	DQ493874.1	98	Signy island, Antarctica
Leptolyngbya-40205	Uncultured bacterium clone IC4002	HQ622720	98	Svalbard ice	*Phormidesmis priestleyi* ANT.L66.	AY493581	95	Antarctica
Xanthomonadaceae-51358	Uncultured gammaproteobacterium clone TSC52	EU359963	98	Taiwanese soil	*Pseudoxanthomonas sacheonensis*	HF585486	94	US soil
Betaproteobacteria-10679	Uncultured bacterium isolate LH2-01	EU440469.1	98	Stromatolite, Canadian Arctic	*Telluria mixta*	LN794206	92	Germany
Intrasporangiaceae-53638	Uncultured bacterium clone LD_RB_26	EU644104	97	Siberian tundra	*Ornithinimicrobium tianjinense*	JQ948045	92	China
Betaproteobacteria-5709	Uncultured bacterium clone KuyT-ice-10	EU263777.1	97	Tibetan glacier	*Massilia* sp. 4106	JX566591.1	90	Chinese soil
Comamonadaceae-22304	Uncultured bacterium clone F35	FJ230911.1	98	Chinese river	*Curvibacter*	FN543107	98	Putative symbiont
Intrasporangiaceae-1447	Uncultured bacterium clone KuyT-IWPB-17	EU263719.1	99	Tibetan glacier	*Eubacterium* sp. 4c	AY216882	93	French peat
Sphingomonadaceae-11564	Uncultured bacterium clone GB7N87003GM6UD	HM728220	98	Antarctic soil	*Novosphingobium* sp. R1-11	KP182170	96	Korean soil
Unassigned-53430	Uncultured bacterium clone GB7N87003FR93L	HM732819.1	98	Antarctic soil	*Rhizobium* sp. AC86c1	AY776225.1	90	Ethiopian soil

4.3.5. Core OTUs have high impact influences on tail and total OTUs

The effect of core OTU composition and environmental parameters on tail and total OTU relative abundances was examined, revealing that core and tail OTU populations are significantly different in relative abundance across all four sectors of the Foxfonna ice cap (PERMANOVA, pseudo-F = 4.42, *P* = 0.001; pseudo-F = 3.021, *P* = 0.001, respectively). The Bray-Curtis distance matrices of core and tail OTU RA exhibit a much stronger correlation against each other (RELATE; ρ = 0.88, *P* = 0.001) than to geographic distance (RELATE, ρ = 0.29, *P* = 0.01; ρ = 0.27, *P* = 0.001). Therefore, the interactions between core and tail OTU populations with environmental parameters were examined to enable an understanding of the relative importance of core taxa and environmental conditions in shaping the cryoconite bacterial community. When applying distLM with a matrix of core OTU RAs as predictors of tail OTU RA patterns (Figure 4. 6), all 16 core OTUs were very significant contributors (*P* = 0.001 - 0.041) in marginal tests (APPENDIX II, Table II. 5), with 9 of 16 core OTUs highly significant in the derived model based on sequential tests (APPENDIX II, Table II. 6). The latter model (adjusted R^2 = 0.54; R^2 = 0.75) is influenced most by the OTU *Sphingobacteriaceae*-61341, followed by *Microbacteriaceae*-32521, *Intrasporangiaceae*-46072, with *Intrasporangiaceae*-27964, *Leptolyngbya*-40205, *Chloroflexi*-37757, *Phormidium*-45763, *Intrasporangiaceae*-53638 and *Intrasporangiaceae*-1447 in decreasing order of influence, yet remaining statistically significant (APPENDIX II, Table II. 6, *P* = 0.001 - 0.004).

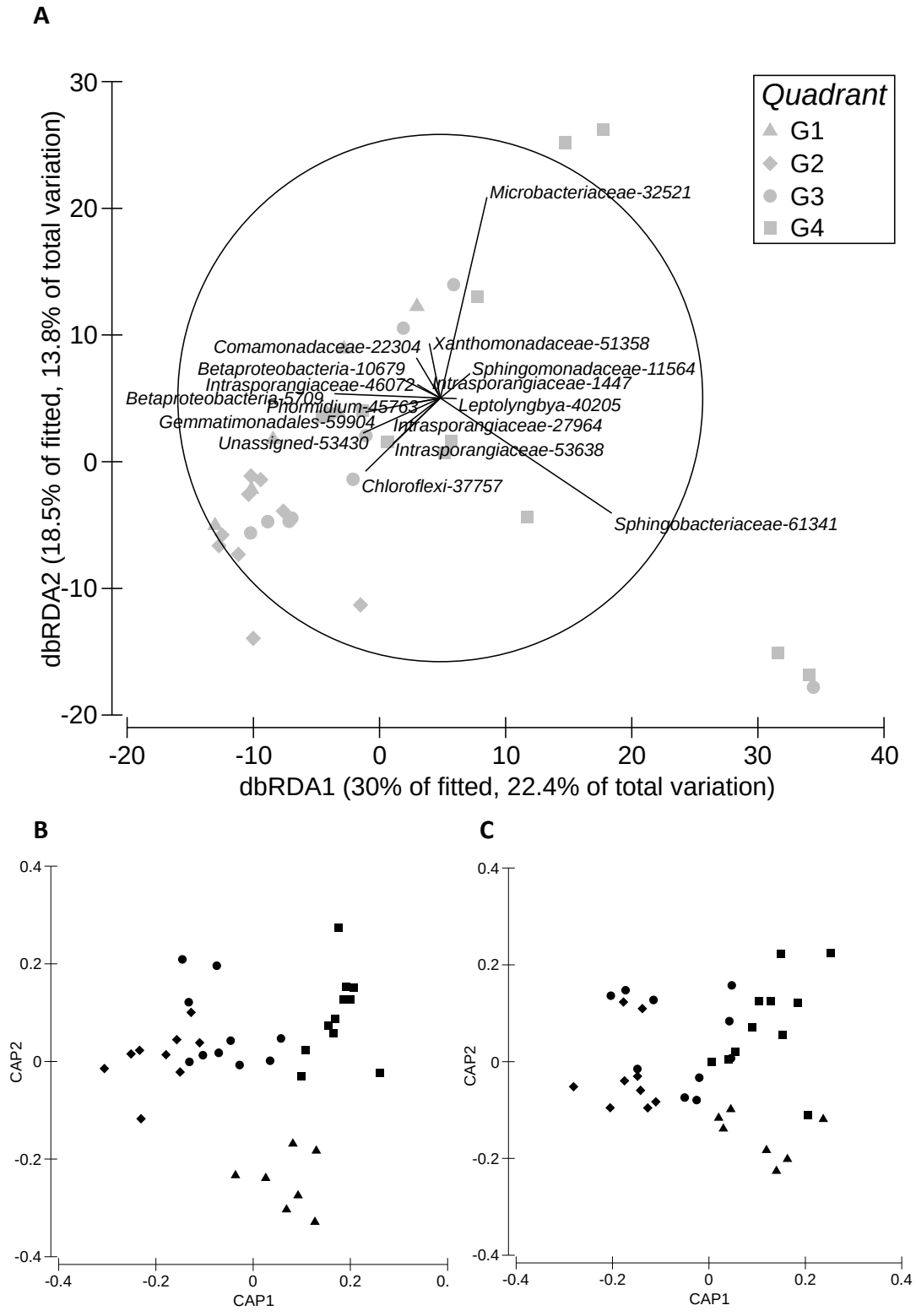

Figure 4. 6 Distance-based redundancy analysis (dbRDA) ordination plot of distance-based linear models of (A) core predictors of tail community structure and canonical analysis of principal co-ordinates (CAP) of (B) core and (C) tail community structures according to the sector.

Considering the apparent strength of core OTU influence in shaping the tail population, the relative influence of the core and environmental parameters upon the total and tail OTU populations was tested. All 16 OTUs and parameters relating to Cartesian position, chlorophyll content, apparent cryoconite area and melt season duration were significant predictors of total community structure (Figure 4. 7A) in marginal tests (APPENDIX II, Table II. 7), while parameters relating to energy receipt and melt (e.g. incident radiation or wetness) were not, except for hours of incident radiation. Sequential tests (APPENDIX II, Table II. 8) revealed the derived model (adjusted $R^2 = 0.60$, $R^2 = 0.84$) was heavily influenced by 8 core OTUs (cumulative $R^2 = 0.59$), principally *Sphingobacteriaceae*-61341 and *Microbacteriaceae*-32521, followed by OTUs assigned to *Intrasporangiaceae*, *Leptolyngbya*, *Chloroflexi* and *Phormidium* in decreasing order of influence. Subsequently, the least influential (but still statistically significant) predictors in the sequential tests were environmental parameters relating to geographic position (pseudo-F = 1.68 - 1.79, $P = 0.005 - 0.012$).

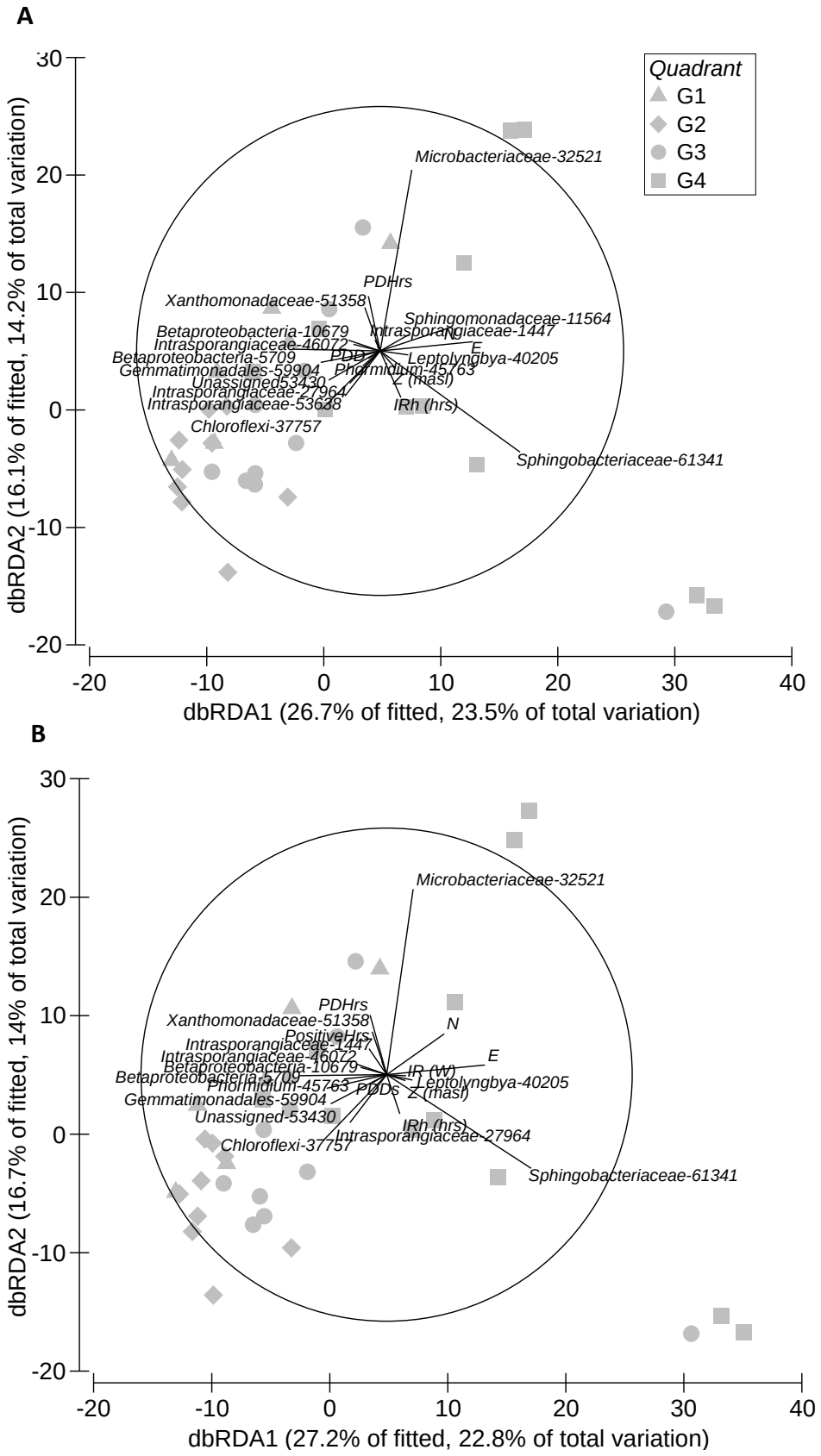

Figure 4. 7 Distance-based redundancy analysis (dbRDA) ordination plot of distance-based linear models for (A) core OTU and environmental parameters on total community and (B) core OTU and environmental parameters on tail community structure.

The strong trend for core OTU influence to predominate over the environmental parameters measured in shaping the bacterial community is clearly paralleled in distLM prediction of tail population OTUs (Sequential tests: APPENDIX II, Table II. 9, dbRDA plot: Figure 4. 7B, Marginal tests: APPENDIX II, Table II. 10), with *Sphingobacteriaceae*-61341 and *Microbacteriaceae*-32521 again the strongest predicting variables of tail OTU structure. A total of 8 core OTUs plus three environmental parameters (Cartesian position, hours of incident radiation) are significant predictors of tail OTU structures.

4.3.6. Co-occurrence network analysis of OTUs

A network of 145 nodes and 304 edges was created by analysing significant pairwise correlations between OTUs and environmental parameters. This network was highly modular (observed = 0.77, Erdös-Renyi model = 0.41), with a considerably longer average path length than expected from a random model of the same size (observed = 4.93, Erdös-Renyi model = 3.58). Environmental variables appeared unconnected to most OTUs in the network, apart from one small cluster of OTUs disconnected from the remaining network. This cluster correlated negatively with several environmental variables related to energy inputs, including positive degree day sum (PDD), hours with temperature above 0°C (PosHrs) and the positive degree day hours sum (PDH) (Figure 4. 8). The network contained several tightly clustered groups, disconnected or weakly connected with the remaining community.

Although some clustering of phylogenetic groups exists, most groups are comprised of OTUs from diverse taxa. Only one group is clearly determined by phylogeny, consisting of a small cluster of OTUs in the phylum *Cyanobacteria*. Bottleneck OTUs identified by the highest betweenness centrality score were dominated by OTUs of the phylum *Actinobacteria* (Table 4. 3). All bottleneck OTUs were connected to the largest cluster within the network through positive correlations, apart from *Leptolyngbya*-40205. This OTU links a tight cluster of *Cyanobacteria* OTUs through a negative correlation to OTUs in the largest network cluster. Six of the ten top-scoring bottleneck OTUs are present within the core population (mean RA >1%).

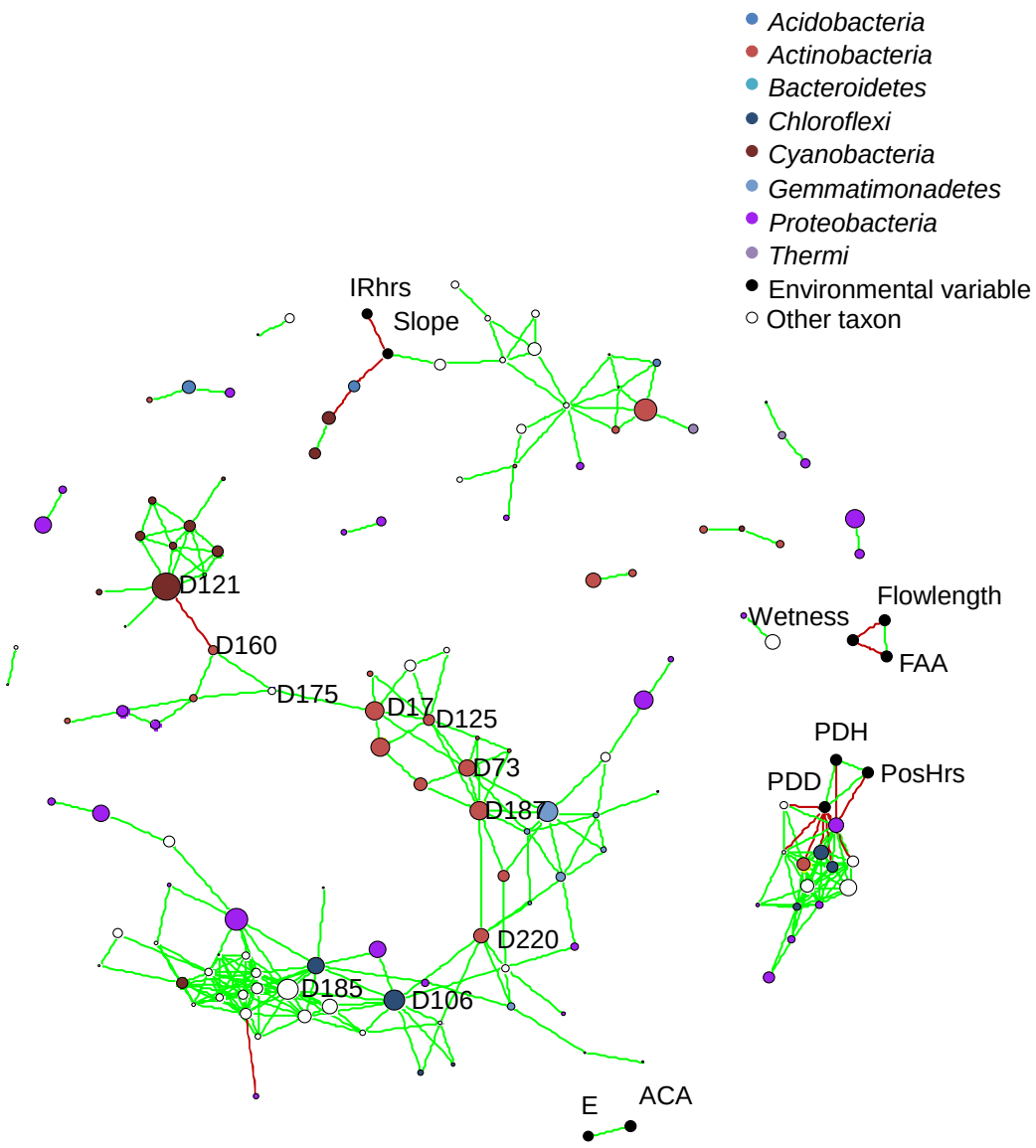

Figure 4. 8 Community network based on significant pairwise Spearman correlations between OTUs (green - positive correlation, red - negative correlation). Size of node is relative to average OTU abundance, while colour indicates OTU phylum. Environmental variables have been included as nodes in the network and are indicated in black.

Table 4. 3 Network bottlenecks identified as the OTUs with highest betweenness centrality (BC) metrics using Greengenes ID. Node ID matches those used in Figure 4. 8.

Node ID	OTU	Phylum	Class	Order	Family	Genus	BC	Mean RA >1
D220	Denovo-61555	*Actinobacteria*	*Acidimicrobiia*	*Acidimicrobiales*	C111	-	1318	
D106	Denovo-37757	*Chloroflexi*	C0119	-	-	-	1261	+
D187	Denovo-53638	*Actinobacteria*	*Actinobacteria*	*Actinomycetales*	*Intrasporangiaceae*	-	1102	+
D17	Denovo-1447	*Actinobacteria*	*Actinobacteria*	*Actinomycetales*	*Intrasporangiaceae*	-	973	+
D175	Denovo-51679	*Gemmatimonadetes*	*Gemmatimonadetes*	*Gemmatimonadales*	Ellin5301	-	915	
D160	Denovo-48894	*Actinobacteria*	*Acidimicrobiia*	*Acidimicrobiales*	EB1017	-	660	+
D121	Denovo-40205	*Cyanobacteria*	*Synechococcophycideae*	*Pseudanabaenales*	*Pseudanabaenaceae*	*Leptolyngbya*	619	+
D73	Denovo-27964	*Actinobacteria*	*Actinobacteria*	*Actinomycetales*	*Intrasporangiaceae*	-	617	+
D185	Denovo-53430	-	-	-	-	-	552	
D125	Denovo-41255	*Actinobacteria*	*Actinobacteria*	*Actinomycetales*	*Intrasporangiaceae*	-	536	

4.4. DISCUSSION

4.4.1. The bacterial community of Foxfonna ice cap

The geographic and environmental parameters prevalent on an ice cap is distinctly different from that of ice sheets and valley glaciers as a consequence of physical position, elevation, slope and topology. As such, it is important to observe their interaction with the bacterial community to extract their respective roles in shaping the community structure. This chapter presents the first study of bacterial biogeography on an ice cap. Here, the effect of geographic position significantly outweighs that of energy receipt and surface hydrology. However, the community structure is, by far, more sensitive to influence by the core population of heterotrophic bacteria and photosynthetic *Cyanobacteria*.

Semiconductor sequencing of bacterial 16S rRNA genes amplified from cryoconite distributed across Foxfonna ice cap revealed a highly diverse heterotrophic consortium of bacteria. Ice cap cryoconite is dominated by a core of generalist bacteria that are cosmopolitan in nature, which evidently promote taxon-taxon interactions between both the core and non-core communities. Cyanobacterial taxa appear to form a significant portion of the ice cap cryoconite community across sequence abundance, core taxa and in co-occurrence network analysis. The presence of filamentous *Cyanobacteria Leptolyngbya*-40205 is consistently highlighted in cryoconite across the dome and appears to be an influential player in both core and bottleneck communities. This taxon bears strong similarity (95% identity) to *Phormidesmis priestleyi*, a member of *Cyanobacteria* frequently identified from ice

and snow surfaces in previous studies of surrounding Svalbard glaciers (Edwards *et al.*, 2011) and the Greenland Ice Sheet (Cook *et al.*, 2016a; Uetake *et al.*, 2016). Its evolutionary proximity and substantial difference in BLAST identity confirms that this is a misrepresentation in the Greengenes database and all *Leptolyngbya* correlating with this ID in this compilation will henceforth be classified as *Phormidesmis* unless otherwise described.

Cyanobacteria have long been recognised as key microbes involved in granular aggregation and stability (Hodson *et al.*, 2010b; Langford *et al.*, 2010). The analyses presented in this chapter supports the notion that cryoconite bacterial communities develop as a consequence of autogenic ecosystem engineering (Edwards *et al.*, 2014b; Cook *et al.*, 2015b). As such, the ubiquitous nature and abundance of *Leptolyngbya*-40205 within the 16S sequence data are consistent with a role of an ecosystem engineer (Musilova *et al.*, 2015). This was further verified by microscopy in Chapter 3, where cyanobacterial filaments were essential to the initial conglomeration of granular aggregates from smaller debris particles, combined with their extrusion of extracellular polymeric substances during early cryoconite development (Langford *et al.*, 2014).

This does not preclude the role of the heterotrophic bacteria within the core and bottleneck OTU populations. Previous work has identified *Alpha-* and *Betaproteobacteria* as prominent cryoconite microbiota (Edwards *et al.*, 2014b; Stibal *et al.*, 2015b), and while these are well represented within the core population of

Foxfonna cryoconite, they are absent from the bottleneck OTUs. Instead there is a strong presence of *Actinobacteria* in ice cap cryoconite communities (Edwards *et al.*, 2011; Edwards *et al.*, 2014b), that are expressly prominent as top-scoring bottleneck OTUs that additionally constitute the core population. This is the first record of their role in the *structuring* of the cryoconite community. As the observed *Actinobacteria* OTUs display influence beyond that expected from their abundance (Power and Mills, 1995), they can be considered keystone taxa. It can therefore be inferred that while *Cyanobacteria* act as ecosystem engineers and *Proteobacteria* contribute to heterotrophic processes, specific *Actinobacteria* play a role in mediating key processes or biotic interactions which affect overall cryoconite community structure on the ice cap. Additionally, biotic factors may play an as yet unidentified role in the formation of cryoconite communities. Evaluating the relative roles of dispersal, environmental and biotic filters in shaping the cryoconite bacterial community is therefore necessary.

4.4.2. Bacterial community shaping by dispersal filtering

The distance decay effect states that the interaction between two locations declines as the distance between them increases (Nekola and White, 1999). Foxfonna ice cap is dome shaped and unconstrained by aspect in the surrounding topography as in valley glaciers, thus potential distance decay effects could be revealed. On an ice cap the bacterial community diversity and abundance can serve as an indicator of the interaction between cryoconite holes in close and far proximity of each other. Cosmopolitan taxa are predominant on glaciers (Darcy *et al.*, 2011; Franzetti *et al.*,

2013). Previous investigations into the shaping of cryoconite microbial communities on valley glaciers neighbouring Foxfonna has indicated a negligible distance decay influence (Edwards *et al.*, 2011). Foxfonna ice cap reveals a moderate but statistically significant distance decay effect consistent to both core and tail populations. These are particularly pronounced and significant for members of the phyla *Chloroflexi*, *Acidobacteria* and *Gemmatimonadetes*, where dispersal limitation or legacy traits may have conditioned these taxa at the phylum levels of taxonomic resolution (Chu *et al.*, 2010; DeBruyn *et al.*, 2011). It is worth noting that all but two core OTUs have closest environmental relatives exhibiting >97% identity of the 16S rRNA gene V1 - V3 region to cryospheric habitats (Table 4. 2). Coupling this with their ubiquity across the ice cap, likely due to redistribution across the ice surface, can suggest an important trait of these core taxa is their broad distribution across the cryosphere. This results in a locally abundant and ubiquitous core population derived from a global pool of propagules promoting potential colonization.

4.4.3. Influence of environmental filtering on bacterial community

Abiotic factors are highly influential in the shaping of microbial communities on glacier surfaces. It is interesting to note that factors affecting valley glacier communities, such as surface hydrology (wetness of the ice surface or extent of the FAA) (Edwards *et al.*, 2011; Stibal *et al.*, 2015b), fail to predict community structure in all distance-based models. This may be a direct result of the higher elevations and latitude with influence from the low mass balance observed during the selected sampling season, and contrasts with ice sheets as it is well recorded that strongly

ablated ice on the Greenland Ice Sheet that have long growing seasons confer high stability to resident cryoconite microfauna (Musilova *et al.*, 2015). On Foxfonna ice cap, the dome shape highlights the influence of geographic position and melt season duration as strong significant predictors of the prevalent diversity. This sharp contrast in melt duration effects between winter and summer periods is consistent with GIS work on the Barnes ice cap (Dupont *et al.*, 2012), but with a caveat that Foxfonna ice cap shows strong links between melt duration in the form of positive degree days (APPENDIX II, Table II. 4) and hours of incident radiation (APPENDIX II, Table II. 9). This leads to the notion that melt season duration is the essential predictor of ice cap bacterial communities, with minimal effect from the expected energetic and physical parameters that affect ice communities in less topographically constrained landscapes.

4.4.4. Influence of biotic filtering on ice cap cryoconite communities

Biotic filtering by taxon-taxon interactions (competition, cooperation and ecosystem engineering) has come to be recognised as an influential driver in environmental microbial community assembly (Goberna *et al.*, 2014). In glacial ecosystems, biotic filtering has been limited to the identification of algal primary colonizers on glacial surfaces (Lutz *et al.*, 2015a) or the role of filamentous *Cyanobacteria* as putative ecosystem engineers or keystone species (Edwards *et al.*, 2014b). On Foxfonna ice cap, it can be deduced that taxon interactions drive the assembly of cryoconite communities, based on the core bacterial taxa strongly predicting total and tail bacterial populations, specific core taxa proving better predictors than physical

parameters and the bottleneck effect afforded by taxa in a modular co-occurrence network.

Filamentous *Cyanobacteria* appear important to the cryoconite bacterial community, as observed in other work (Hodson *et al.*, 2010b; Langford *et al.*, 2010), particularly the OTU *Leptolyngbya*-40205 (Accession ID AY493581), but while their role as autogenic ecosystem engineers is presumed (West, 1990; Langford *et al.*, 2010; Edwards *et al.*, 2014b), they are not prominent keystone taxa. Instead, selected *Actinobacteria* OTUs are essential to the highly centralized bottleneck OTUs within the highly modular co-occurrence network (Figure 4. 8), representing keystone taxa whose influence exceeds their relative abundance within the community. Their positive correlation to other taxa argues against their role in competitive exclusion and instead allows speculation of their role in humification of dark organic matter associated with cryoconite (Takeuchi, 2002), based on their association with soil humus (Table 4. 2).

As an alternative method of phylogenetic clustering, the co-occurrence network derived here reveals a modular nature with taxonomically diverse modules. This is a common characteristic associated with taxon co-occurrence networks established for other polar habitats and is interpreted as a sign of metabolic plasticity (Vick-Majors *et al.*, 2014). The predominance of phylogenetically diverse modules may thus permit functional stability of the community in a fluctuating environment. Majority of these modules exhibit phylum-level diversity, except for an exclusively cyanobacterial

module which is negatively correlated with the largest module associated with all remaining bottleneck OTUs. The nature of the cyanobacterial module suggests that the autogenic ecosystem engineers exert limited influence upon community structure, unlike heterotrophic bottleneck OTUs. Therefore, filamentous *Cyanobacteria*, having engineered the cryoconite ecosystem by the aggregation and adhesion of aeolian organic matter and inorganic debris (Hodson *et al.*, 2010b; Langford *et al.*, 2010), are disconnected from the heterotrophic bacterial community of closely interacting taxa. As such, the assembly of the cryoconite bacterial community is highly biotically filtered and exhibits primary succession from phototrophic taxa associated with granule formation towards a highly interactive consortium of heterotrophic bacteria, which may act to humify the accumulated organic matter.

4.5. SUMMARY

The assembly of the bacterial community of microbial-mineral aggregates colonizing the High Arctic ice cap of Foxfonna is driven principally by biotic filtering. A dominant generalist core of taxa emerges, which includes filamentous cyanobacterial ecosystem engineers and a discrete group of keystone taxa within the *Actinobacteria*, likely humifying accumulated organic matter to darken the cryoconite. While there is evidence for a moderate distance decay effect in community similarity, it is notable that the core taxa possess close environmental relatives from the global cryosphere, linking microbial colonization processes interacting with glacier change at local scales with dispersal within the cosmopolitan cold biosphere.

CHAPTER 5 – BIOTIC AND ABIOTIC INFLUENCE ON THE METABOLOMIC PROFILE OF HIGH ARCTIC ICE CAP CRYOCONITE ON FOXFONNA, SVALBARD

5.1. INTRODUCTION

Investigations into the effects of biogeochemical reactions on the glacial environment, reveal the effect of biotic and abiotic parameters on the dissolved organic matter pool available to microbes for growth and metabolism (Hodson *et al.*, 2010b; Cook *et al.*, 2015b). The previous chapter revealed that biotic filtering is at the core of bacterial cryoconite community assembly, with cosmopolitan taxa from the phyla *Cyanobacteria* and *Actinobacteria* forming the stable core in an abundantly heterotrophic bacterial community. An indication of the interactions that persist between organisms in a specific environment can be elucidated by examination of low molecular mass metabolites by non-targeted metabolomics (Lankadurai *et al.*, 2013; Soule *et al.*, 2015).

While the process of identifying environmental metabolites is aided by online databases, there are intrinsic limitations to identification of small molecules, often identifying only a small fraction of metabolites in large datasets (Link *et al.*, 2015). When integrated with genomics, transcriptomics and proteomics, it has the potential to provide a description of the environmental state with a high degree of functional information pertaining to biotic and abiotic responses (Viant, 2007). Glacial habitats are characterised as simple ecosystems (Kohshima, 1987) that have fewer microbes compared to adjacent terrestrial and marine habitats (Hallbeck, 2009; Zhang *et al.*,

2013; Edwards and Cook, 2015). However, for an extreme habitat, they have substantial and distinct heterotrophic and phototrophic communities that are sustained by close integration between physical, geographical, biochemical and biological processes, as determined in the previous chapters. By observing the homeostatic controls and feedback mechanisms at the level of the metabolome, it may be possible to determine organism response to environmental stresses.

In glacial ecosystems, investigation of the metabolic structure and composition has been limited to the study of pure culture isolates of psychrophilic and psychrotolerant microbes (Ghobakhlou *et al.*, 2013; Tsuji, 2016), ice sheet metabolomes (Cook *et al.*, 2016a) and snow algae (Lutz *et al.*, 2015b), with only one previous study on the cryoconite metabolome of Arctic and Alpine ecosystems (Edwards *et al.*, 2014b). With the increased knowledge of the bacterial dynamics determined from Chapter 4, it is a logical step to subsequently identify the metabolically active processes in the cryoconite community. As the ice cap is a unique topographical feature of the glacial landscape, and the effect of temperature and incident radiation on the bacterial community was established to be significant, it is necessary to understand the intricate *molecular* interactions that persist in this environment and the magnitude of biotic and abiotic involvement.

The aim of this chapter was to therefore determine the bacterial and environmental drivers of metabolic function in cryoconite communities on a High Arctic ice cap. This was achieved by evaluation of the most significant metabolites and pathways,

relative to the environmental and biological interactions prevalent on Foxfonna ice cap. This tested the hypotheses that:

a. Differences in metabolic pathways are related to shifts in solar input on the ice cap due to topography,
b. Microbial influence on Foxfonna ice cap drives the observed metabolite profile in cryoconite.

5.2. METHODS

5.2.1. Experimental procedures

Cryoconite from 38 holes on Foxfonna ice cap (Chapter 4) was freeze dried and 0.1 g dry weight was measured into microcentrifuge tubes for metabolite extraction (Chapter 2, section 2.3.1). Samples were then prepared for non-targeted FI-ESI mass spectrometry and the data processed for chemometric analysis, hierarchical cluster analysis and PLS regression modelling (Chapter 2, section 2.3.2). Metabolomes were examined against environmental parameters described in Chapter 4, section 4.2.2 and APPENDIX II, Table II. 1 (Cartesian co-ordinates (E and N), dome geography (elevation, slope, aspect), solar and temperature input (PDD, PDH, IR (kW), IR (Hrs)), hydrology and cryoconite hole structure (FAA, curvature, wetness, flowlength) and chlorophyll *a* content), as well as with ice cap core and keystone bacterial taxa from Chapter 4, to investigate environmental and taxon influence on the metabolome. Additional modelling of the taxa-environment-metabolome relationship was established by distance-based redundancy analysis of Bray-Curtis transformed

metabolites against fourth root transformations of Euclidian distance of environmental variables and Bray-Curtis distance of core and keystone bacteria.

5.3. RESULTS

5.3.1. Overview of metabolites present in Foxfonna ice cap cryoconite

Mass spectrometry of the total metabolite extracts from all 38 cryoconite samples on the ice cap generated 1 398 discrete peaks in the metabolite profile. Initial PCA analysis of raw primary and secondary metabolites in PyChem (Jarvis *et al.*, 2006) showed that metabolites clustered based on the sectors G1, G2, G3 and G4 on the ice cap (Figure 5. 1A), where PCs 1 and 2 accounted for 34.16% of the variation in the community metabolites (Figure 5. 1B). Additionally, both hierarchical cluster analysis (HCA) of Euclidian distance and discriminant function analysis (DFA) confirmed that G1 and G2 grouped together, but were isolated from G3 and G4, creating an east-west separation of metabolites in these sectors (APPENDIX III, Figure III. 1).

A significant sector effect was observed from multivariate analysis using permutational multivariate analysis of variance (PERMANOVA, pseudo-F = 4.5046, P = 0.001), supporting the influence of physical geography on the metabolome. This sector effect is further supported by analysis of similarity (ANOSIM, R = 0.502, P = 0.001). However, a low level of correlation was observed between OTUs and metabolites in samples common to both datasets, according to the Spearman Rho analysis generated by Mantel-based tests (RELATE, ρ = 0.179, P = 0.04).

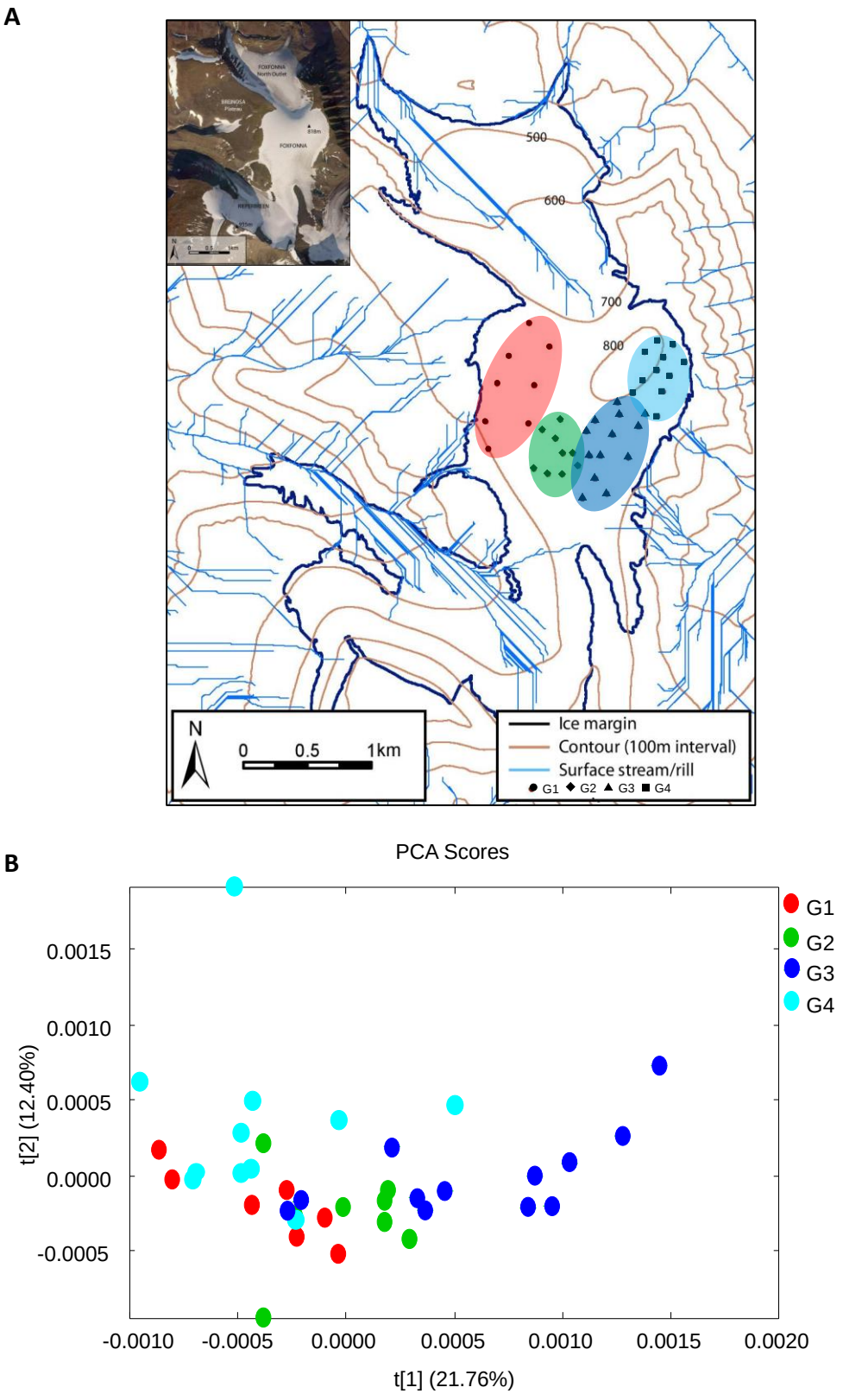

Figure 5. 1 Foxfonna ice cap contour map depicting (A) the original sampling sites in sectors G1, G2, G3 and G4 that correlate well with (B) principal component representation of the cryoconite metabolome, showing clear associations based on sector.

Metabolites of interest distinguishing between the four sectors of the ice cap were selected by random forest supervised classification. Post hoc analysis of variance of significant metabolites (ANOVA, P <0.05) (APPENDIX II, Table III. 1) showed that metabolites driving changes in the community also clustered by sector, consistent with the scores plots of the PLS discriminant analysis (Figure 5. 2A) (ANOVA, F range = 3.0163 - 78.421, P range = 1.32E-15 - 0.0428). Tentative identities were made for 70 metabolites on the KEGG database; metabolites of potential pathways of interest were extracted and further examined by hierarchical cluster analysis (Figure 5. 2B). These grouped into metabolic pathways essential for growth, development and reproduction in cryoconite hole communities. Metabolites driving community changes were representative of major metabolites involved in the TCA cycle, polyamine synthesis, lipid biosynthesis, nucleotide biosynthesis and carotenoid synthesis.

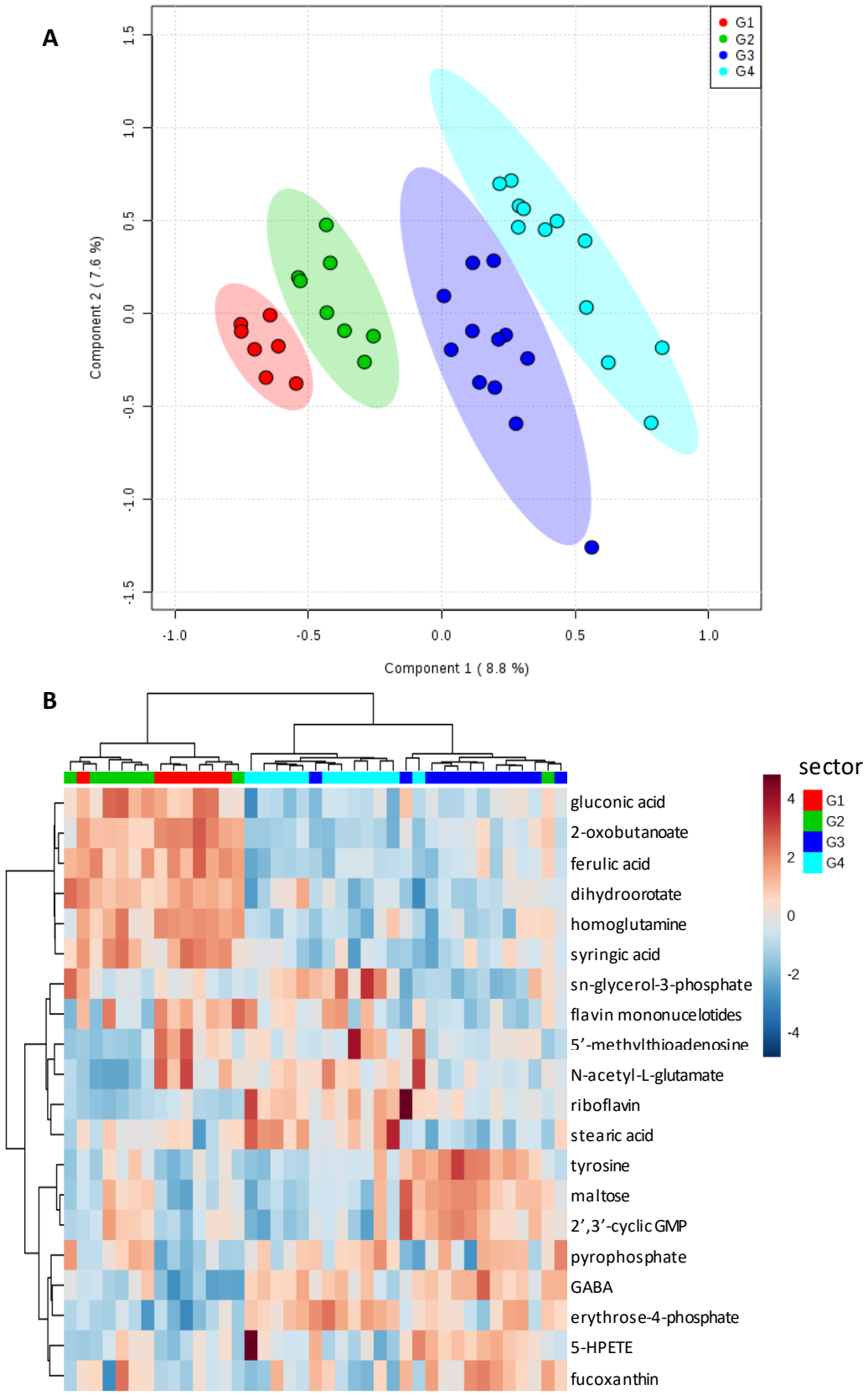

Figure 5. 2 Significant metabolites identified by ANOVA post hoc filtering suggest a strong sector-bias in both (A) PLS-DA scores with 95% confidence intervals and (B) hierarchical cluster of the metabolites, displaying the metabolite profile of important metabolites in the tricarboxylic acid cycle, nucleic acid, polyamine, lipid biosynthesis and photosynthesis pathways.

An examination of all metabolites using PLS linear regression modelling showed that environmental parameters and keystone and core bacterial taxa (Chapter 4) had an integral role in shaping the metabolome. While all metabolites did not fit the linear regression model for a sector-based bias, the taxon *Leptolyngbya*-40205, more accurately *Phormidesmis priestleyi* (Figure 5. 3A), strongly adhered to the expected proportional fit with additional, albeit minimal, influence from incident radiation (IR (kW), Figure 5. 3B) and hours of exposure to incident radiation (IR (hrs), Figure 5. 3C).

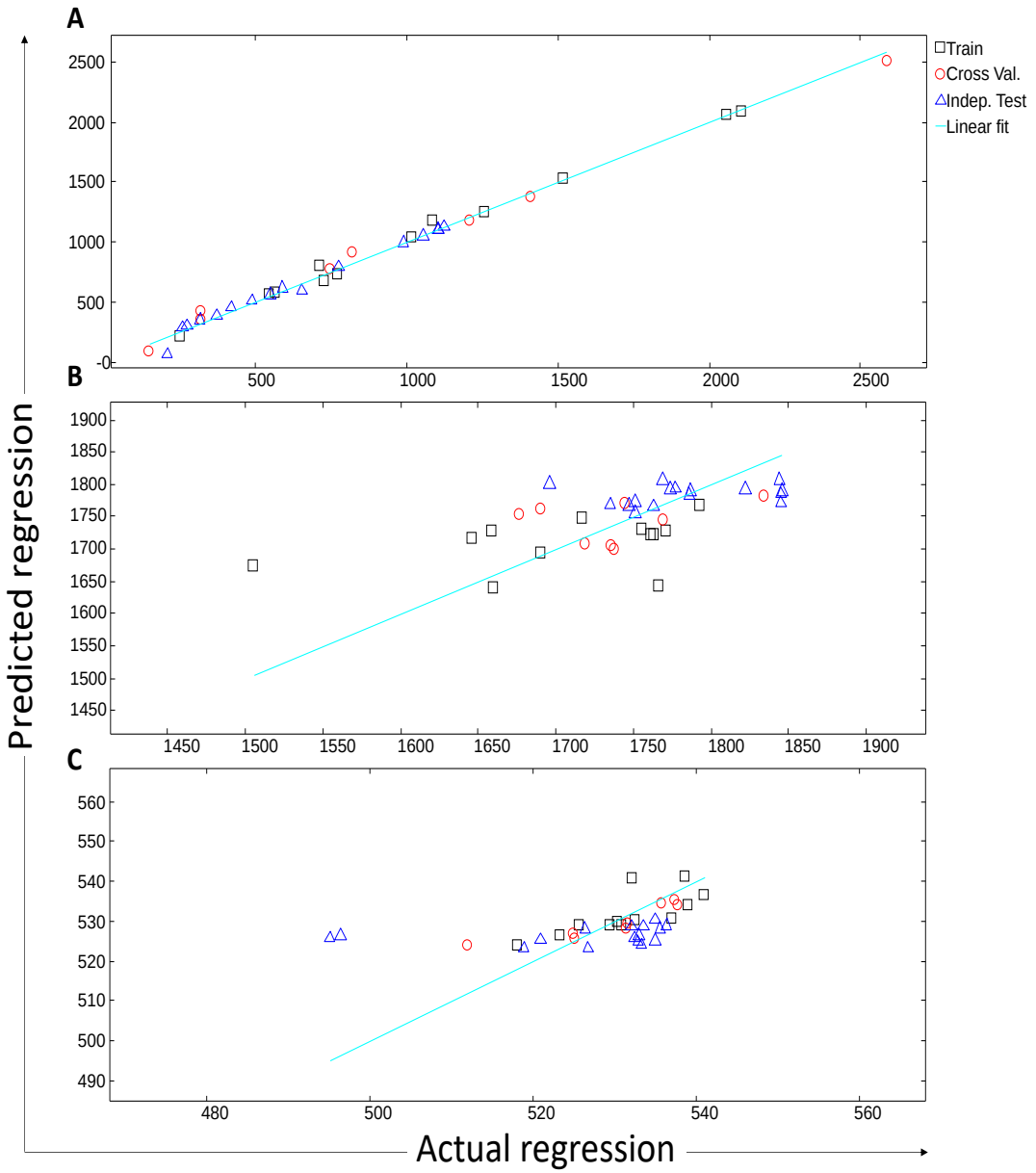

Figure 5. 3 Partial least squares regression of taxa and environmental variables predict that (A) core and key OTU, *Phormidesmis priestleyi*, best fits the regression model for Foxfonna ice cap cryoconite, while (B) incident radiation (kW) and (C) hours of exposure to light has a poor yet significant fit to the predicted model of the metabolome.

5.3.2. Intercorrelation of the ice cap cryoconite metabolome, environment and 16S rRNA gene sequences

Statistical significance of the combined effect of biotic and abiotic parameters necessitated analysis of the metabolites with predictor variables from core and keystone taxa (Chapter 4) and environmental variables modelled with distance-based redundancy at 999 permutations, eliminating non-related variables in a stepwise approach. The resultant ordination displayed clear and strong influence of the parameters separating the eastern sectors (G1 and G2) from the western sectors (G3 and G4) (Figure 5. 4). Predictor variables that best explained the total observed variation in redundancy ordination displayed positive and negative vector associations for taxa *Curvibacterium*-22304, *Frigoribacterium*-32521, *P. daechungensis*-61341, *P. priestleyi*-40205, *Novosphingobium*-11564, *Rhizobium*-53430, *Massilia*-5709 and *Eubacterium*-1447, in addition to the abiotic parameters N, E, aspect, ACA, PDD and chlorophyll *a*. The relative influence of biotic and abiotic factors as predictors of metabolite patterns were tested in the distance-based linear models, where marginal tests revealed 11 out of 18 environmental parameters (pseudo-F range = 2.3389 - 12.721, *P* range = 0.001 - 0.043) and 7 out of 20 OTUs (pseudo-F range = 2.9501 - 4.9933, *P* range = 0.001 - 0.035) were significant contributors (APPENDIX III, Table III. 2). Sequential tests using r-squared selection revealed that the derived model was heavily influenced by Cartesian position (E, pseudo-F = 12.721, *P* = 0.001; N, pseudo-F = 4.3482, *P* = 0.001), PDD (pseudo-F = 3.6469, *P* = 0.008) and chlorophyll *a* (pseudo-F = 2.2088, *P* = 0.033) (APPENDIX III, Table III. 3).

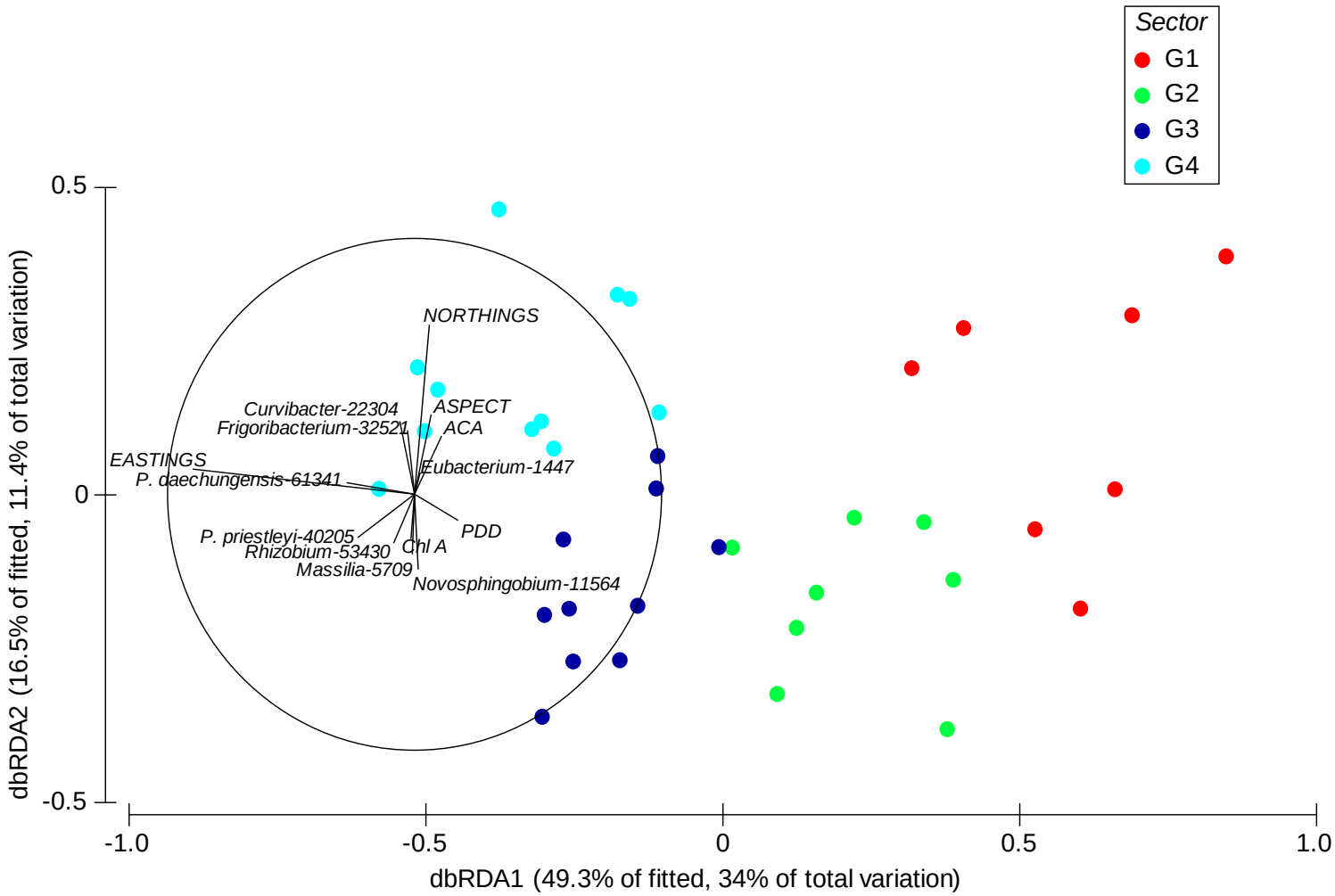

Figure 5. 4 Distance-based redundancy ordination plot of predictor variables from biotic and abiotic parameters best explaining the variation in the ice cap cryoconite metabolome, showing a distinct sector effect in predictor variables that correspond to metabolites.

5.3.3. Essential biological pathways are prominent in the ice cap cryoconite metabolome

5.3.3.1. Tricarboxylic acid pathway

TCA intermediates were identified as major sources of variation (71.7% in the first two PCs) with clear separation of metabolites in sectors G1 and G2 and some samples in sectors G3 by PLS-DA, (APPENDIX III, Figure III. 2). Distinct high activity was present in these three sectors compared to sector G4 and the remaining G3 metabolites, when viewed in hierarchical cluster analysis (Figure 5. 5A). The metabolites oxalacetate, oxoglutarate, 2-oxobutanoate and malate formed a discrete cluster with high activity in sectors G1 and G2. A second cluster was observed, consisting of succinate, oxaloacetate and fumarate, with the highest concentration of these metabolites in sectors G1 and G2. These metabolites exhibited low expression in sectors G3 and G4, which were additionally characterised by higher oxalosuccinate, citrate and aconitate expression. PLS regression of these TCA metabolites showed that elevation (Figure 5. 5B), PDH (Figure 5. 5C), IR (kW) (Figure 5. 5D), influenced the TCA pathway to a greater degree than bacterial core and keystone taxa.

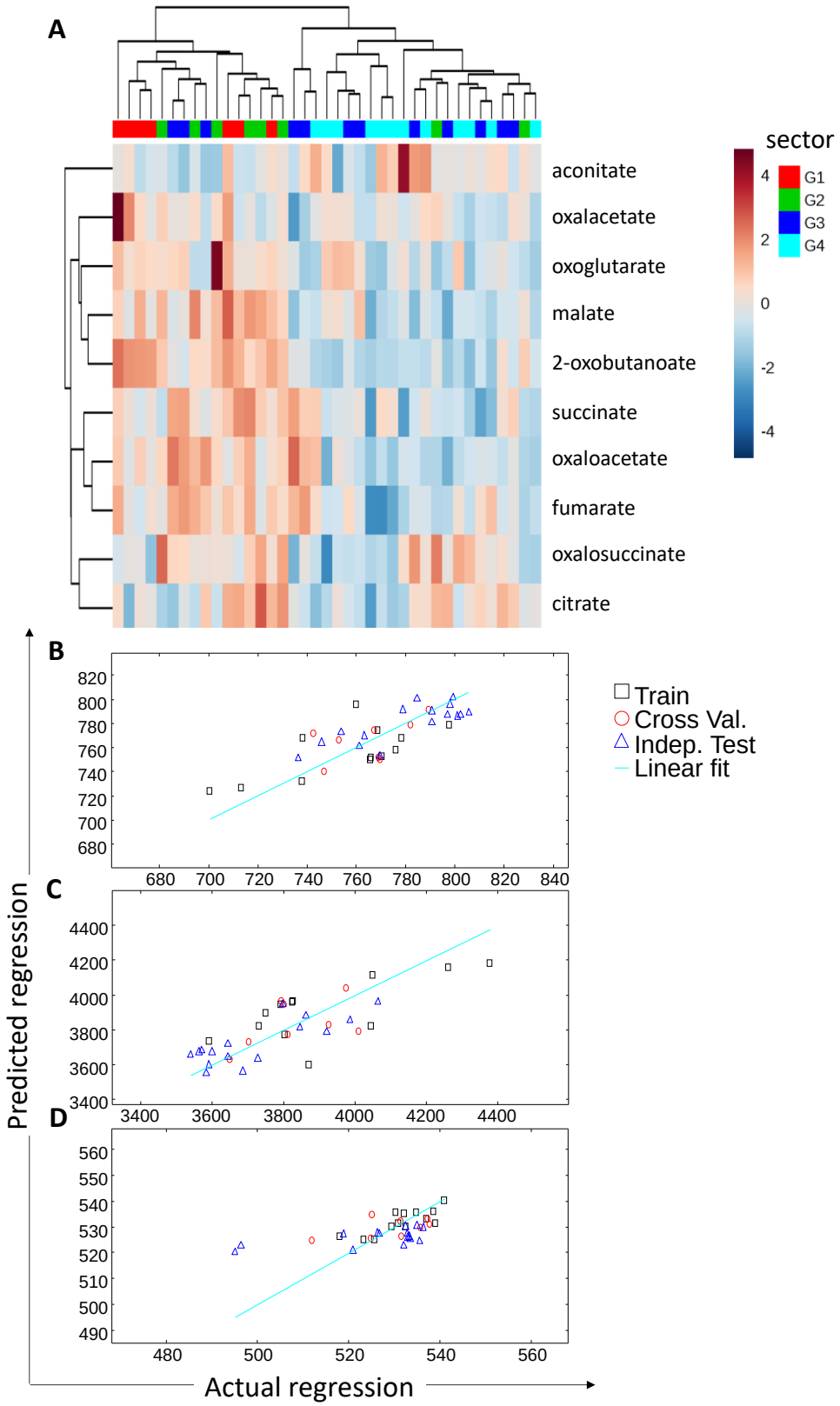

Figure 5. 5 The metabolite profile reveals (A) the high impact of the TCA cycle in Foxfonna ice cap cryoconite using hierarchical cluster analysis and further predicts the importance of (B) elevation, (C) PDH and (D) IR (kW) in shaping the TCA pathway.

5.3.3.2. Polyamine synthesis

Metabolites integral to polyamine synthesis explained 73.6% of total variation in the ice cap cryoconite metabolome, with an absence of separation of metabolites in PLS-DA components (APPENDIX III, Figure III. 3), but some evidence of discrete clustering for sectors G1 and G4. Sector G1 displayed a degree of disparity unobserved in sectors G2, G3 and G4 by HCA, particularly for the metabolites identified as gamma-aminobutyric acid (GABA), proline, pyrroline-5-carboxylic acid and ketoglutarate (Figure 5. 6A), which were present at extremely low concentrations in sector G1 compared to sectors G2, G3 and G4. Additionally, a high concentration of glutamate as well as higher concentrations of the similarly clustered glutamate semialdehyde and spermine was noted in sector G1. Metabolites ketoglutarate and citrulline were present at higher concentrations in G2 and G4, while ornithine, GABA and proline were distinctly higher in G3. When modelled against environmental parameters, these polyamine metabolites were predicted to have minimal influence from elevation (Figure 5. 6B), PDH (Figure 5. 6C) and IR (kW) (Figure 5. 6D).

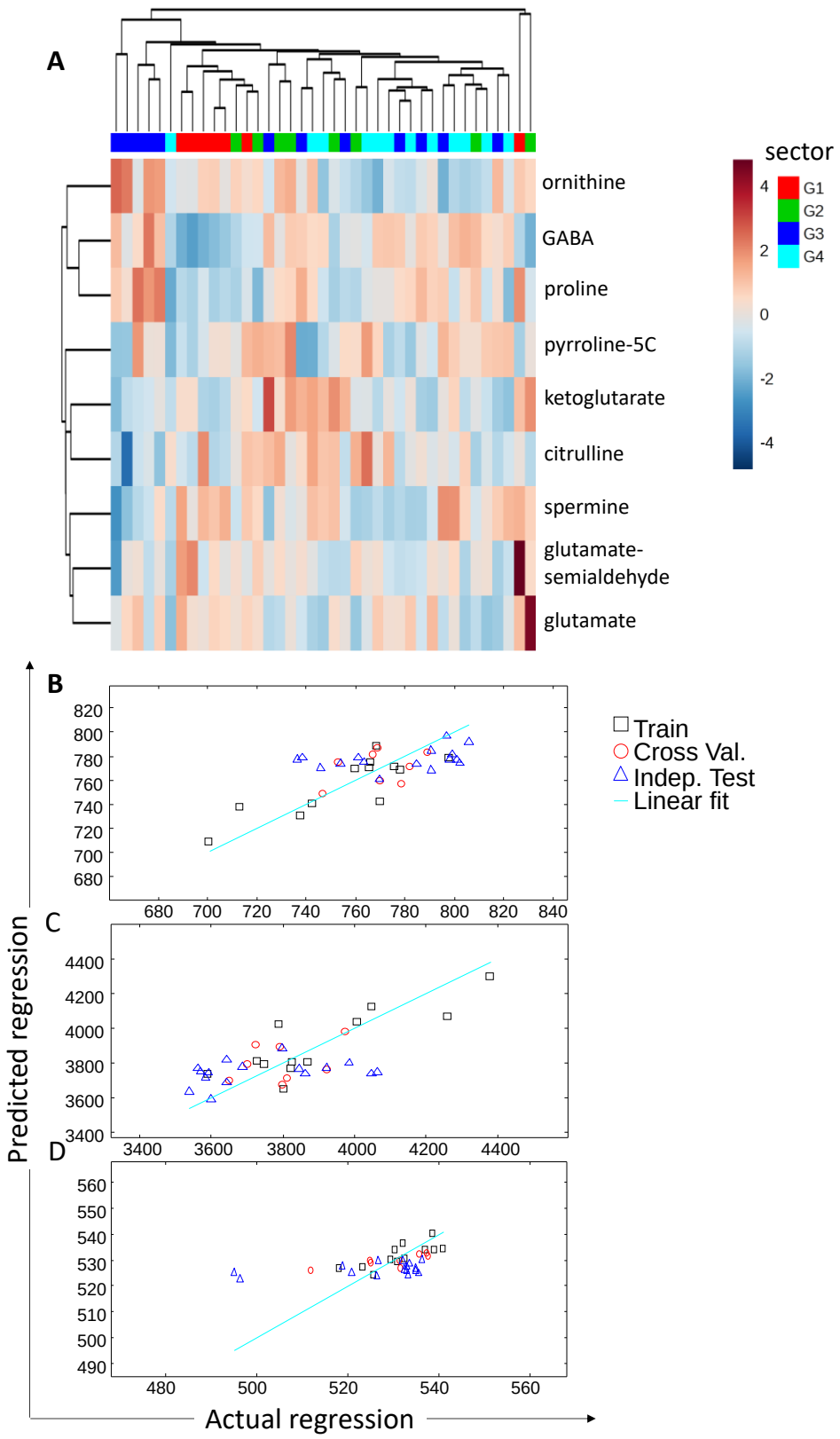

Figure 5. 6 Polyamine synthesis metabolites (A) differentiates sector G1 from sectors G2, G3 and G4 in HCA, with minimal prediction of the metabolite profile using environmental variables (B) elevation, (C) PDH and (D) IR.

5.3.3.3. Fatty acid biosynthesis

The primary role of fatty acids in all organisms is in maintaining the hydrophobicity of biological membranes, with additional roles in the provision of energy reserves, as protein targets and intracellular messengers. Metabolites associated with lipid breakdown products were identified as major sources of variation, explaining 56.6% of variation in PLS-DA, without obvious cluster separation in the 95% confidence interval components (APPENDIX III, Figure III. 4). In HCA, sectors G3 and G4 clustered separately, based on differences in their respective lipid metabolite profiles, while sectors G1 and G2 clustered together non-uniformly, as a result of the minimal similarity in the lipid profile. Sector G4 was distinctive with low overall fatty acid concentrations but high stearic acid and sn-glycerol-3-phosphate metabolites compared to the other 3 sectors (Figure 5. 7A). This is particularly striking for linolenic acid (Figure 5. 7B) and jasmonic acid (Figure 5. 7C) that revealed much lower expression in sector G4. Sector G3 displayed higher linoleic acid, hydroperoxyeicosatetraenoic acid (5-HPETE), palmitic acid, oleic acid, jasmonic acid, linolenic acid and arachidonic acid metabolite concentrations than sectors G1 and G2, where they were distinctly lower and more variable in lipid metabolite content across individual samples. The PLS regression model of lipid metabolites showed no distinct correlation to environmental or bacterial key and core taxa variables.

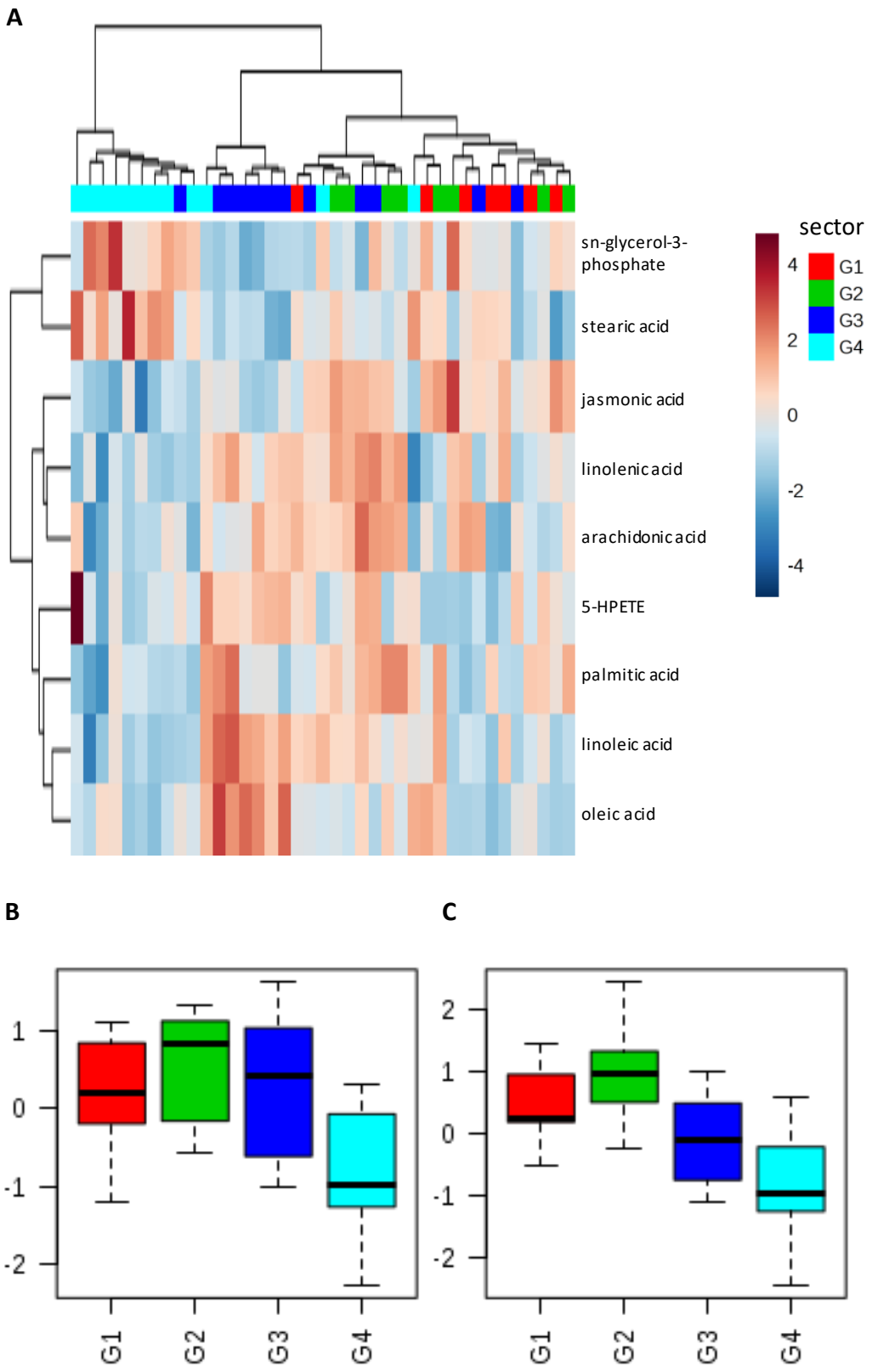

Figure 5. 7 Fatty acid metabolites of the Foxfonna ice cap cryoconite metabolome show (A) clustering by sector, with sector G4 distinguishing itself from G1, G2 and G3, particularly for the metabolites (B) linolenic acid and (C) jasmonic acid that had the highest impact on the lipid profile for G4.

5.3.3.4. Carotenoid biosynthesis

Carotenoids are a group of organic pigments produced by plants, algae and several bacterial and fungal species, and can be subdivided into xanthophylls (containing oxygen) and carotenes (purely hydrocarbon). High levels of varied expression were observed in the HCA with a sector-based separation pattern of most photosynthesis precursor molecules (Figure 5. 8A). However, in PLS-DA there was no clear separation of metabolites by sector (APPENDIX III, Figure III. 5), with components 1 and 2 accounting for only 25.6% of the observed variation. The xanthophylls, zeinoxanthin, xanthoxin and zeaxanthin, had higher expression in sector G1 in contrast to their distinctly lower concentrations in sectors G2, G3 and G4. Other photosynthetic compounds were inconsistent with any distinct pattern. PLS regression was better able to predict parameters influencing the photosynthetic pathways, highlighting the influence of IR (kW) (Figure 5. 8B) in the linear regression model for photosynthesis metabolites.

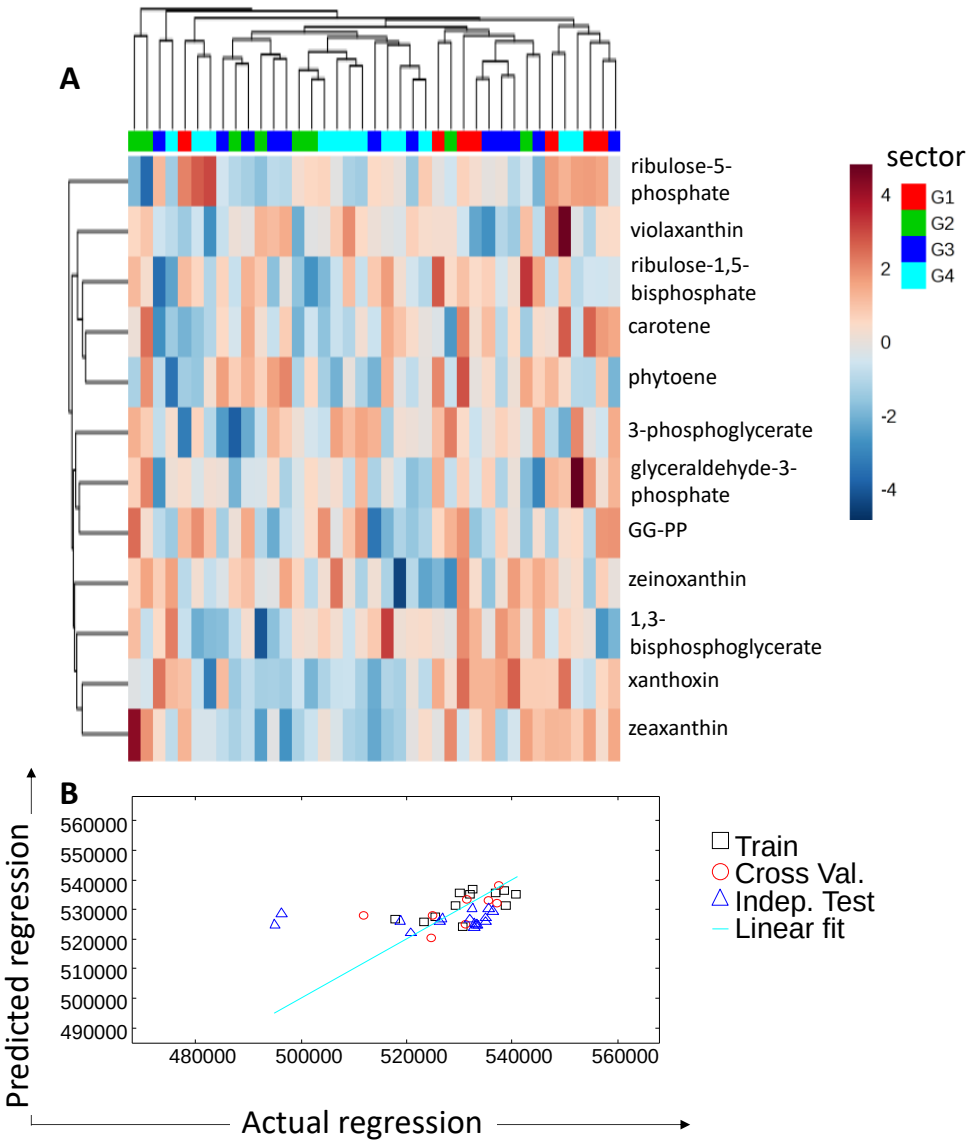

Figure 5. 8 Carotenoid biosynthesis highlighted photosynthetic compounds with high similarity across the ice cap showing (A) a lack of sector-based clustering in HCA. (B) PLS regression highlighted the influence of the environmental variable IR (kW) that best fitted the carotenoid metabolite profile of the ice cap cryoconite metabolome.

5.3.3.5. Nucleic acid synthesis

PLS-DA analysis showed separation of the sectors G1, G2, G3 and G4 (APPENDIX III, Figure III. 6), explaining 27.8% of the metabolite variation in components 1 and 2. HCA of tentatively identified nucleic acid metabolites revealed a distinct east-west clustering pattern for purine metabolites (Figure 5. 9A), however, little further information could be extrapolated from the HCA for insights into a sector-metabolome relationship. Sector G3 generally had low representation of adenine monophosphate (AMP), guanine monophosphate (GMP), the enzyme phosphoribosyl pyrophosphate (PRPP), thymidine and 3'5-cyclic deoxyAMP (dAMP), while adenosine and inosine had higher concentrations in samples from sector G4. Low concentrations of allantoin (Figure 5. 9B), uric acid (Figure 5. 9C), hypoxanthine, adenine, xanthine, inosine monophosphate (IMP) and adenosine diphosphate (ADP) were present in G3, while these same metabolites were present at higher concentrations in G1, G2 and G4.

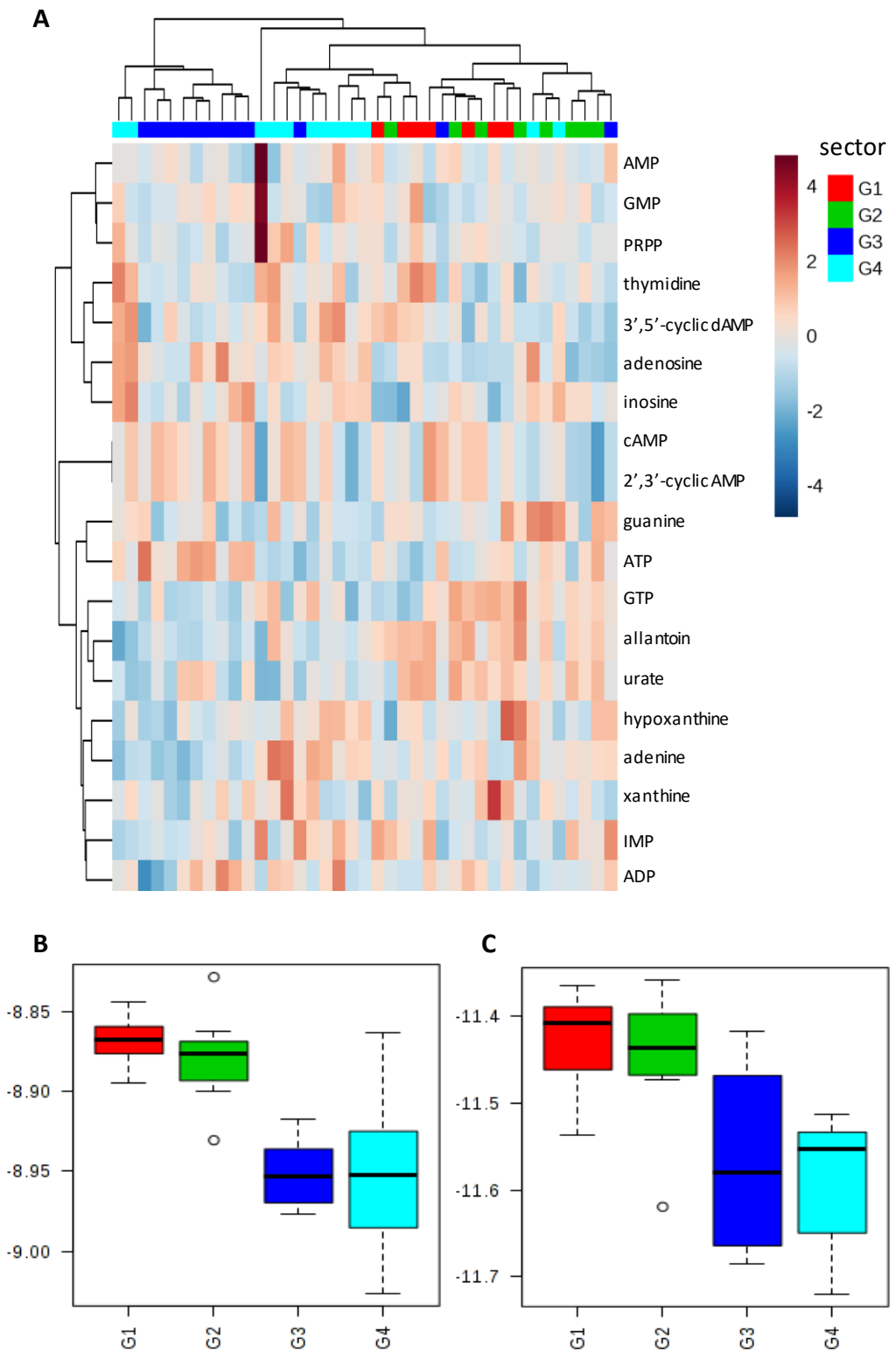

Figure 5. 9 The essential metabolites present in nucleic acid synthesis pathways show (A) an east-west sector effect in HCA, and identify (B) allantoin and (C) uric acid as key metabolites responsible for the separation of sectors G3 and G4 from G1 and G2.

5.4. DISCUSSION

Metabolomics-based characterisation of the interaction between organism and environment is a newly emerging 'omic approach that can provide great insight into the changes associated with climatic and biotic factors at the molecular level (Lankadurai *et al.*, 2013). In this chapter, it informs on the state of pathways and processes that are integral to microorganism function on an ice cap in the High Arctic.

5.4.1. The ice cap cryoconite metabolome

On Foxfonna ice cap the central metabolic pathway, the tricarboxylic acid cycle, was identified as highly significant on all sectors of the dome. The activity of the TCA cycle is affected by the availability of nutrients and stress inducing stimuli (Sadykov *et al.*, 2010). The TCA cycle links together carbohydrate, amino acid and fatty acid degradation in addition to providing precursors for various biosynthesis pathways that drive the generation of energy. The abundance of ketoglutarate, the crucial precursor feeding into the TCA cycle, and TCA intermediates, succinate and citrate, are suggestive of high ATP generation and thus aerobic microbial activity in east facing sectors G1 and G2 (Link *et al.*, 2015). The low TCA metabolite activity (apart from citrate, oxalosuccinate and aconitate) in west facing sectors may be attributed to preferential utilisation of the required α-ketoglutarate to generate glutamate for amino acid production and fatty acid synthesis. However, glutamate conversion is a reversible reaction, which could also account for sustained low levels of activity over the summer season.

It is evident that sector G1 metabolites are particularly sensitive to topographical orientation. High activity in the TCA cycle shows an active microbial population dominates this sector with good cellular proliferation inferred from purine and pyrimidine HCA activity patterns. When observed in combination with the high concentrations of photosynthesis metabolites, these factors could drive the greater N assimilation observed in the east most region of the ice cap.

Distance-based linear modelling can reveal possible intercorrelations between environmental and biological factors, which may appear less significant for microbes in simple regressions for individual pathways. In the dbRDA model, factors unrelated to Cartesian position, temperature and incident radiation were found to not be significant, as their impact on the metabolome may be minimal, despite significant influence of IR on 16S rRNA sequence data (Chapter 4). Alternatively, the correlation between individual biochemical pathway characteristics, bacterial abundance and physical dome parameters is weak when observed in isolation but are decidedly significant when assessed together in dbRDA. This implies either an attenuated effect of the investigated parameters due to the lack of interlinked biochemical pathways or an alternative microbial driver shaping these pathways.

5.4.2. Abiotic drivers on the Foxfonna ice cap metabolome predict the influence of incident radiation

Analysis of the environmental conditions experienced on Foxfonna ice cap shows that localised physical and geographic constraints play a significant role in driving bacterial

communities on the ice cap (Chapter 4). As such, these environmental variables were hypothesised to have an impact on key metabolic activities, particularly those relative to Cartesian location, temperature (Ghobakhlou *et al.*, 2013) and incident radiation (Cook *et al.*, 2016a). Numerous statistical tests predicted the effect of geographical location on the entire metabolome with a strong sector bias. Within individual pathways, an even more discrete sector effect was displayed in metabolites associated with the TCA cycle, nucleic acid biosynthesis and fatty acid biosynthesis, additionally exhibiting a distinctive east to west pattern of expression. Identification of environmental variables capable of predicting the observed structure of pathways was weak, however, a minimal degree of impact was afforded by energy derived from incident radiation (photosynthesis, TCA and polyamine metabolites), the total number of hours in a day with positive degree temperature and elevation (TCA and polyamine metabolites). This corresponds with other studies on the effect of solar radiation on cryoconite hole morphology, microbial activity and cellular modification by microbial stress-response on ice surfaces in the Arctic (Beales, 2004; Cook *et al.*, 2016a; Tsuji, 2016; Vonnahme *et al.*, 2016).

In support of the initial hypothesis, the influence of incident radiation on the overall metabolome had a significant, but diminished effect on the observed metabolic fingerprint of Arctic cryoconite. Irradiation across the entire ice cap is similar with only a slightly higher incidence on the south facing slope, which may contribute to the photosynthetic cryoconite community being most active in G1, despite detected *Cyanobacteria Phormidesmis priestleyi*, being predominant in 16S rRNA gene

amplicon sequencing libraries in all four sectors (Gokul *et al.*, 2016). Biological proliferation, and accordingly, activity, as indicated by nucleotide synthesis and TCA intermediates and products, respectively, are sensitive to incident radiation. Both processes appear homogeneous across the ice cap, apart from eastern sectors that exhibit raised biological activity. This is not surprising when observed in correlation with microbial abundance records in Chapter 4. Ketoglutarate, the crucial precursor metabolite that feeds into the TCA cycle, and TCA intermediates, succinate and citrate, is abundant in Foxfonna ice cap, suggestive of ATP generation in sectors G1 and G2 being sufficient to support high levels of microbial activity as a result of sufficient oxygen access via aerobic and anaerobic processes (Link *et al.*, 2015). This implies that there is sufficient energy generated from ATP and other bioenergetic precursor molecules in this system for other TCA intermediates to be redirected. In fact, the decrease in TCA metabolites in some sectors (with the exception of citrate, oxalosuccinate and aconitate) may be attributed to preferential utilisation of the required α-ketoglutarate to generate glutamate for amino acid production and nitrogen transport for regulatory biological processes in the community.

Several microclimate aspects evolve as a result of increase in elevation and climate changes along a gradient. Temperature, length of growing season and snow fall increases with elevation, while chemical and biological characteristics such as nitrogen mineralisation, decomposition and respiration decrease with elevation, causing an increase in C pools, as evidenced in soil studies (Daws and Rewcastle, 2015). N metabolites on the ice caps appear to have high rates of consumption of

amines, amides and amino acids, congruent with Alpine soils along an elevation gradient. Here, we observe a low nitrogen environment where nutrient cycling due to microbiological action heavily influences the rates of nitrogen assimilation.

5.4.3. Abundant phototrophic taxa intrinsically shape the Foxfonna ice cap metabolome

Primary production on supraglacial surfaces is driven by light (Anesio *et al.*, 2009; Franzetti *et al.*, 2016b). Majority of the organic carbon is attributed to autochthonous accumulation from cyanobacterial-mediated photosynthesis (Stuart *et al.*, 2015) or fixation from atmospheric carbon and metabolism of particulate carbon back into the atmosphere (Grzesiak *et al.*, 2015). These are pigment-dependant microbially-moderated processes, mediated by *Cyanobacteria* (Stibal and Tranter, 2007), psychrophilic algal blooms (Edwards *et al.*, 2016) and ascomycetous and basidiomycetous fungi (Singh *et al.*, 2014) observed on the ice surfaces. Respiration by heterotrophic microbes utilises the available carbon, generating a fluctuation in net ecosystem productivity brought about by seasonal changes, cloud cover and topology (Telling *et al.*, 2012).

The physical constraints of the cryoconite hole promotes functional integration and interaction between the diverse microbial consortium of the cryoconite hole, exerting significant impact on the cryoconite hole biogeochemical cycle. Foxfonna ice cap is dominated by a ubiquitous bacterial community identified by 16S rRNA sequencing of the V2 - V3 region, where the chiefly abundant and core member of

the consortium, *Phormidesmis*, is of cyanobacterial origin, alongside a prominent heterotrophic bacteria component of *Alphaproteobacteria*, *Betaproteobacteria* and *Actinobacteria* (Chapter 4). Observation of the surrounding snowpack has also identified the presence of red algal blooms on the ice cap during summer, colonising the area on the ice cap at elevations 600 - 700 m a.s.l. (Edwards *et al.*, 2016). These are typically *Chlamydomonas* and *Chloromonas* taxa (Lutz *et al.*, 2015b), that are both cosmopolitan and endemic to glacier ice surfaces in Svalbard.

Prediction of the high impact bacterial variables from key and core taxa showed that the influence of *Phormidesmis priestleyi* on the cryoconite metabolome far outweighs the influence all environmental variables, implying high activity and abundance of *P. priestleyi* in ice cap communities. The recently obtained *P. priestleyi* genome is characterised by cell wall and membrane biogenesis genes and EPS biosynthesis contiguous DNA segments (Chrismas *et al.*, 2016). The previous chapters have provided sufficient evidence of the integral role of filamentous *Cyanobacteria* in granule agglomeration by EPS production and chlorophyll pigment production (Chapter 3), encouraging formation of humics and their influence by solar effects and taxon-taxon interactions, driving the community (Chapter 4).

Summer cryoconite communities can alter their mainly autotrophic lifestyle to one more heterotrophic in nature when affected by diminished solar energy receipt, causing extracellular polysaccharide breakdown and photo adaptive stress responses in secondary metabolites (Cook *et al.*, 2016a). It is therefore not surprising that the

cryoconite metabolite profile of Foxfonna ice cap highlights significant influence by secondary carotenoids, that form a light harvesting complex for light in the range 450 - 570 nm in cell membranes (Ruiz-Sola and Rodríguez-Concepción, 2012). As accessory pigments, they redirect ATP to chlorophyll *a* production for primary production, in addition to xanthophylls facilitating the dissipation of excess excitation energy (Demmig-Adams *et al.*, 1996).

Microalgae play an added role on ice surfaces and in cryoconite holes, as the environment does not experience high levels of bioturbation (Gabet *et al.*, 2003), limiting fluctuations in the biogeochemical cycle of the cryoconite hole. While eukarya were not examined within the scope of the taxonomic study, the contribution of microalgal species to the cryoconite metabolome is previously well documented and supported in this study by a significant high abundance of ferulic acid ($F = 41.021$, $P = 1.49E\text{-}11$), an essential algal cell membrane component, and the high activity of the prominent algal stress hormones, in the form of unsaturated fatty acids (linoleic, linolenic, oleic and jasmonic acid), that trigger a respiratory burst in algal systems to control the growth of bacterial biofilms by limiting the action of degradative products (Kupper *et al.*, 2009). The presence of polar carotenoids frequently observed in snow red algal blooms (zeaxanthin, violaxanthin, fucoxanthin and zeinoxanthin) (Remias *et al.*, 2005; Guedes *et al.*, 2011) further supports the presumed role of microalgae on the ice cap, by offering increased glycerophospholipid membrane permeability and fluidity at low temperatures (Beales, 2004; Barria *et al.*, 2013; Sengupta and Chattopadhyay, 2013), in addition to

their role as light harvesters and in non-photochemical quenching of reactive oxygen and reactive nitrogen species (Zhu *et al.*, 2010).

Glacial habitats are well renowned as carbon, nitrogen and phosphorous poor systems, but are highly dependent on them for microbial growth (Hodson *et al.*, 2008). Essential biological macronutrients are maintained by breakdown of allochthonous organic matter by *in situ* biological processes. Each of the observed pathways in the metabolomic analysis of the Foxfonna ice cap substantiate high microbial activity and proliferation. As such, it is likely that the activity of autochthonous photoautotrophic microalgae and *Cyanobacteria* on the ice cap surface adds organic material that contains complex forms of nutrients that are essential for sustaining the heterotrophic community of ice cap cryoconite.

Mutualistic cyclic exchanges of metabolites between *Cyanobacteria* and the heterotrophic consortium of microbiota on ice caps influence nitrogen exchange, with specific interactions for improved nutrient acquisition by the detected *Cyanobacteria*. Nitrogen is a limiting factor in a multitude of biological processes in glacial microbial communities (synthesis of organic molecules, rates of primary production and respiration) (Stibal *et al.*, 2006), as a lack of allochthonous N results in reduced fixation. Svalbard cryoconite holes are, however, not nitrate limited and are recognised as net NH_3 producers, as cyanobacterial assemblages of *Pseudanabaena, Chroococcales* and *Nostoc* are responsible for aerobic nitrogen fixation directly from the atmosphere (Sawstrom *et al.*, 2002; Hodson *et al.*, 2005;

Acinas *et al.*, 2009; Cameron *et al.*, 2017). The presence of nitrification and denitrification genes have successfully been recorded in cryoconite (Cameron *et al.*, 2012; Zarsky *et al.*, 2013), providing evidence of N cycling within the cryoconite community for assimilation in nucleic acid and amino acid synthesis by the heterotrophic microbial community. This is further supported by metagenomic evidence of functional genes for N, S, Fe and P cycling in Alpine cryoconite for ammonia assimilation, nitrite and nitrate ammonification, sulphur oxidation and inorganic sulphur assimilation, iron transport, phosphate metabolism and cyanobacterial phosphate uptake (Edwards *et al.*, 2013b).

Majority of the significant metabolomic fingerprint can be attributed to high levels of microbial activity during summer months, however the main driver of the community is photoautotrophy-mediated by the *Cyanobacteria,* and potentially microalgae, witnessed as dominant on the ice cap during summer. Based on the high relative abundance of nucleic acid and polyamine metabolites, it can be inferred that the highly significant *Phormidesmis priestleyi*, along with the abundant microalgal taxa, are responsible for maintaining the summer heterotrophic community by carbon fixation for generation of dissolved organic matter, thereby mediating further humification and affecting surface albedo and IR effects. They are collectively responsible for majority of the NH_4 sequestration contributing to annual N_2 fluctuations on glacier surfaces and supplementing the cryoconite hole biogeochemical cycle.

5.5. SUMMARY

Determining a relationship between microbial communities, metabolism and downslope ecosystems requires understanding the link between the physical constraints and biogeochemistry across the landscape (Zak and Kling, 2006). The Foxfonna ice cap is composed of solar energy receipt dependant biosynthetic pathways, which can be linked to the established cryoconite communities. There is an indication of the preferential use of metabolites generated by energetically cheaper i.e. degradative pathways, to sustain cellular growth in this environment. Metabolites are often redirected for use in pathways such as amino acid synthesis, fatty acid synthesis and nucleotide synthesis to maintain biological functions under nutrient poor, low temperature and acidic pH conditions. Provision of the necessary organic matter required for the heterotrophic members of the community and autotrophic processes in this environment are governed by photosynthetic microalgae and *Cyanobacteria*, which form the core community of this environment and actively drive the cryoconite metabolome on glacial surfaces.

CHAPTER 6 – BACTERIAL COMMUNITY DYNAMICS OF HIGH ARCTIC VALLEY GLACIER CRYOCONITE IN FOXFONNA, SVALBARD

6.1. INTRODUCTION

Cryoconite holes greatly influence the melt rate on glaciers as a consequence of metabolic activity by a diverse range of microbes that occupy them (Cameron *et al.*, 2012; Edwards *et al.*, 2014b; Cook *et al.*, 2016a). This is in addition to the effect of surface albedo, snow melt and flow accumulation (Bøggild *et al.*, 2010; Irvine-Fynn *et al.*, 2011). Nutrient and metabolite analysis show that active microbial ecosystems prevail in cryoconite holes, generating sufficient nutrients from organic and inorganic sediments and surrounding melted glacier ice and photosynthesis. Recent research has established the prevalence of different *Cyanobacteria* of the genera *Leptolyngbya*, *Phormidium* and *Nostoc* (Stibal et al., 2006) and algae from the genera *Chlorophyceae*, *Chlamydomonas*, *Cylindocystis* and pennate diatoms (Stibal *et al.*, 2006; Lutz *et al.*, 2015b), which act as integral mediators of primary production (Remias *et al.*, 2005), respiration (Telling *et al.*, 2012) and carbon fixation on snow surfaces and in cryoconite (Anesio *et al.*, 2009). Active cyanobacterial taxa associated with cryoconite debris produce adhesive agents, extracellular polymeric substances (EPS), that enable the conglomeration of individual granules in cryoconite holes (Takeuchi, 2002; Hodson *et al.*, 2010b; Langford *et al.*, 2010).

Physical geography has a recognised profound effect on the microbial community at a localised scale, as a result of incident radiation and hydrology influencing their

activity at high elevation, as on Foxfonna ice cap. On valley glaciers, the increased slope and topology influences the flow accumulation area and, potentially, the seed microbial communities along the elevational gradient of Foxfonna. Cryoconite hole biogeochemistry and metabolic activity, inferred by spatial mapping and concentrations of organic biomass, extracellular polymeric substances, primary production (by measures of ^{14}C incorporation and chlorophyll concentration) and respiration (dissolved oxygen consumption), is variable across location. This is evidenced by previous investigations on the temporal and spatial diversity of cryoconite communities at three different Svalbard polythermal valley glaciers (Anesio *et al.*, 2009; Edwards *et al.*, 2011; Langford *et al.*, 2014).

Furthermore, analyses of multiple time points and localities are likely to yield further insights to the structure and function of glacial ecosystems (Edwards and Cook, 2015). Recent studies implying the temporal stability of bacterial communities in cryoconite ecosystems (Musilova *et al.*, 2015), coupled with the cosmopolitan distribution of core taxa documented in a variety of cryospheric habitats, imply the broader utility of insights from the Foxfonna ice cap. The importance of melt season duration as a physical parameter predicting the bacterial community structure is noted, and thus, examination of cryoconite ecosystems in discrete stages of melt season conditions is recommended, as this study sampled during the late melt season.

Space for time analysis of the cryoconite on ice surfaces enables an improved description of the microbe-environment interactions that influence the supraglacial ice surface. Similar studies in soil and permafrost have revealed the remarkable relationship between microbial communities and elevation (Schostag *et al.*, 2015; Zhang *et al.*, 2016), while in cryoconite, showed the distinct connection between lower gradients, cyanobacterial community structure and the role of allochthonous input from valley glacier sides and forefield (Langford *et al.*, 2014).

The previous chapter details the localised biogeography of the ice cap above Foxfonna outlet glacier. As the valley outlet is a linked neighbouring habitat, it becomes pertinent to investigate the down-valley effects on the cryoconite community, additionally forming a complementary topographical investigation of the Foxfonna glacial biosphere. As such, the primary aim of this chapter was to investigate the temporal effect on cryoconite bacterial communities along Foxfonna valley glacier and secondarily to determine how physical and climatic constraints, particularly those influenced by elevation, combined with intrinsic bacterial assemblage interactions on a valley glacier, affect the cryoconite metabolome. It is hypothesised that,

a. There is increased physical and chemical stability afforded by cryoconite granules over time, as a result of the combined action of carbohydrate agglomeration and primary production by photosynthesis,
b. Elevation-related effects will outweigh other spatial influences in bacterial richness, diversity and microbial metabolism,

c. Key metabolic compounds will be more sensitive to temporal differences, as a consequence of nutrient stability afforded by microbial activity.

6.2. METHODS

6.2.1. Site description

The Foxfonna valley glacier is situated in Svalbard at 78° 080' N, 16° 070' E (Figure 6. 1A). The glacier was formed by the outflow from Foxfonna ice cap dome and is geographically constrained by steep valley walls on the northern face of Foxfonna and the underlying bedrock topography. Similar to the dome, the bedrock is primarily made up of tertiary sandstone, siltstone and shale at the higher elevations, with older shales overlying sandstone beds at lower elevations (Hjelle, 1993; Dallmann *et al.*, 2001). Glacial surface characteristics were recorded and analysed, using the digital elevation model of the terrain to extract data for elevation (m a.s.l.), slope (°), aspect (°), curvature and flow accumulation area (FAA) (DEM analysis performed by Dr T. D. L. Irvine-Fynn). ArcGIS Solar Analyst was used to extract solar data, in the form of total incident radiation (IR) and IR between sample collection points from DOY 162, when average air temperatures at the Foxfonna weather station were above 0°C for consecutive days. The algorithm used a summer mean atmospheric transmissivity of 0.61 (Irvine-Fynn *et al.*, 2014) and 38% IR (Kupfer *et al.*, 2006), employing an 'overcast sky model' closely resembling the high proportion of cloud cover prevalent during the Svalbard summer.

Algal blooms were evident at lower elevations on the valley glacier from DOY 188 and at the transition between upper and lower sites from DOY 193. At day 198, distinct colonisation of red algae and microbial biofilms in slush were observed within the sampled transect and the top of the glacier.

6.2.2. Sampling procedure

Cryoconite was collected aseptically from 117 cryoconite holes on the valley glacier, as described in Chapter 2, section 2.2.1. Cryoconite holes were sampled for a duration of 5 weeks from 21 July 2011 to 17 August 2011, along a transect, FLC1-FLC8 (FLC1 = 406.26 m a.s.l., FLC2 = 250.24 m a.s.l., FLC3 = 474.63 m a.s.l., FLC4 = 429.8 m a.s.l., FLC5 = 525.6 m a.s.l., FLC7 = 580.7 m a.s.l., FLC8 = 601.5 m a.s.l.) (Figure 6. 1B), where increasing numbers correspond to increasing elevation along the transect. Additional samples were collected at low (FL2 = 495 m a.s.l.) and high (FL4 = 600 m a.s.l.) elevations of the glacier. Samples are described by collection date according to the day of year (DOY) and collection site.

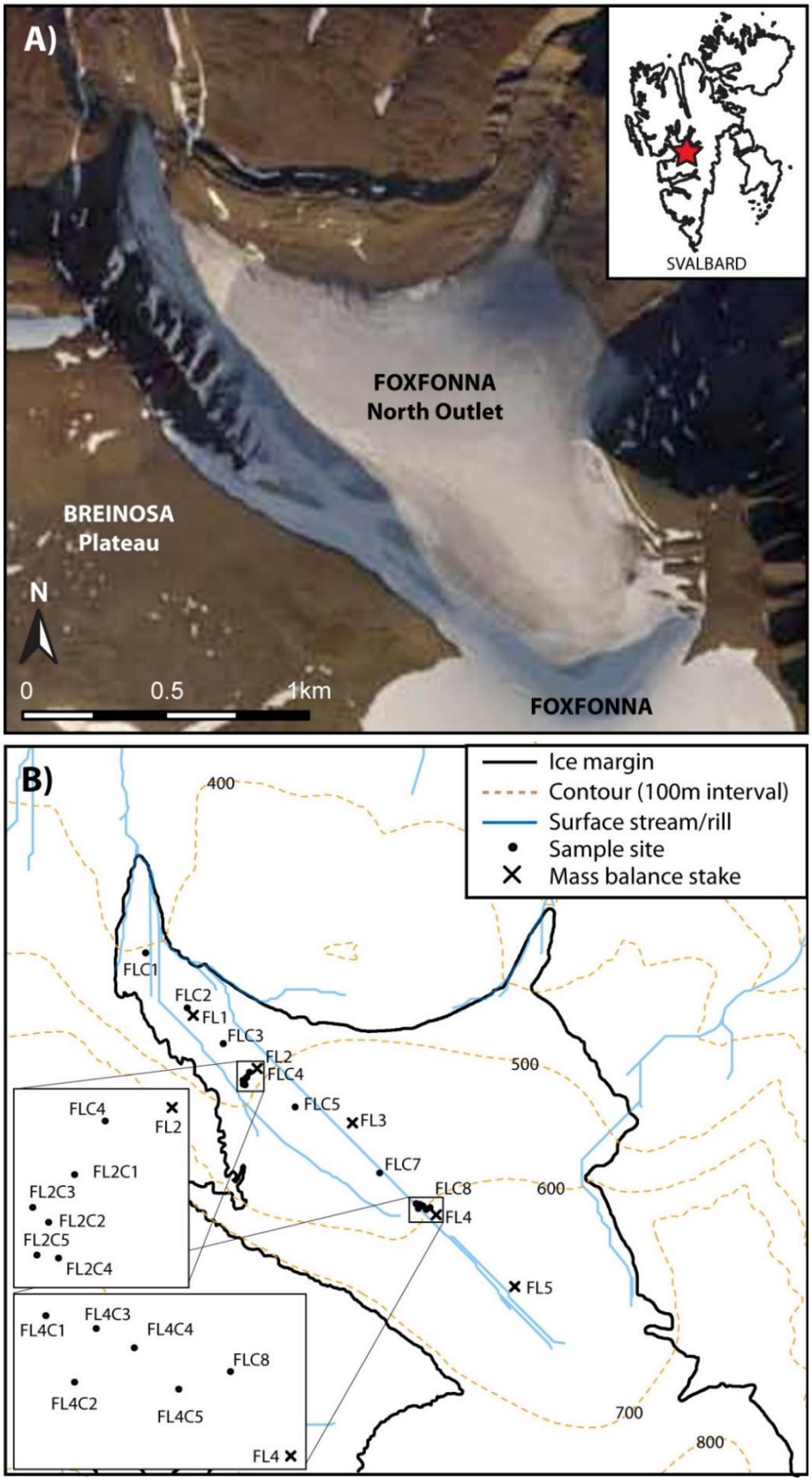

Figure 6. 1 Digital elevation model of Foxfonna valley glacier (A) in aerial view and (B) with topographical map displaying sample collection sites FLC, FL2 and FL4 and mass balance stakes along the gradient of the valley glacier. Image credit: Dr. Tristram Irvine-Fynn.

6.2.3. Experimental procedures

The application of multiple techniques for the detection and evaluation of community structure provides a useful method for disentangling the temporal and spatial community structure of microbial communities. The levels of chlorophyll *a* and extracellular polymeric substances (in the form of total carbohydrates) has been applied as an indicator of cyanobacterial and microalgal biomass in sediment biofilms and cryoconite (section 6.2.3.1 and section 6.2.3.2). As such, it provides an important link between the physical description of the valley glacier as a high algal biomass site, the 16S rRNA gene sequence diversity (section 6.2.3.3) and the metabolic activity (section 6.2.3.4) of cryoconite.

6.2.3.1. Spectrophotometric determination of chlorophyll in cryoconite

The presence of chlorophyll is used as an indicator of photosynthetic potential and thus microbial activity by *Cyanobacteria* and microalgae in sediments. Chlorophyll *a* extraction was performed as described in Warren (2008). A volume of 0.04 g of cryoconite and 0.1 g of 0.5 mm glass bead-beating beads (Sigma-Aldrich Company Ltd, Poole, UK) was immersed in 250 µL of methanol (Fisher Scientific Ltd, Loughborough, UK) in polypropylene cryovials. Vial contents were homogenised on a vortex mixer for 20 minutes before centrifugation at 13 000 ×*g* for 15 minutes. Two hundred microliters of the supernatant were transferred to a well of a 96-well microplate. Absorbance spectra between 300 nm and 750 nm were measured on a Multiskan™ GO Microplate Spectrophotometer, alongside blanks consisting of methanol to determine the baseline for absorbance measurements. A standard curve

for chlorophyll *a* (Sigma-Aldrich Company Ltd, Poole, UK) of known concentration was run in parallel for quantification.

6.2.3.2. Colorimetric carbohydrate analysis of cryoconite

High concentrations of carbohydrate-rich extracellular polymeric substances (EPS) are essential to sediment carbon cycling. The presence of EPS in Foxfonna cryoconite was therefore examined, using total carbon concentration as a proxy for EPS content. The dilute hot acid extraction protocol stipulated by Masuko *et al.* (2005) was used on 0.03 g of freeze dried samples of cryoconite in cryovials. Briefly, 100 µL of 0.5 M sulphuric acid (H_2SO_4) (Fisher Scientific Ltd, Loughborough, UK) was added to cryoconite and the contents homogenised on a vortex mixer for 5 minutes before being transferred to a water bath, where they were agitated at 200 rpm at 80°C for 2 hours. The vials were then centrifuged at 13 000 ×*g* for 10 minutes, after which 44 µL of the resulting supernatant was removed from each vial and transferred into a 96-well microplate. Thereafter, 130 µL of concentrated (18 M) H_2SO_4 and 26 µL of 5% phenol (aq.) (Sigma-Aldrich Company Ltd, Poole, UK) were added to each well in quick succession before incubation on quartz sand maintained at 90°C for 5 minutes, prior to cooling on ice for 5 minutes. Absorbance was measured at 490 nm on a Multiskan™ GO Microplate Spectrophotometer, with blanks of ultra-high quality (UHQ) water and a suspension of UHQ water with phenol and sulphuric acid, to determine the baseline for absorbance measurements. A standard curve of mannose (Sigma-Aldrich Company Ltd, Poole, UK) of known concentration was run in parallel for quantification.

6.2.3.3. Bacterial community profiling

Nucleic acids from 117 cryoconite samples were extracted using the PowerBiofilm™ RNA Isolation kit (MO BIO Laboratories Inc.) and is described in detail in Chapter 2, section 2.4.2.1, before amplicon amplification by PCR (Chapter 2, section 2.5), next generation Illumina library preparation (Chapter 2, section 2.6.3) and next generation Illumina sequencing (Chapter 2, section 2.6.4) using Illumina specific primers. Sequences were processed in QIIME (Chapter 2, section 2.7.1) to obtain an OTU matrix for taxonomic analysis, Minitab 17 and PRIMER 6/PERMANOVA+ (Chapter 2, section 2.7.2 - 2.7.3) for univariate and multivariate analysis and network analysis (R) (Chapter 2, section 2.8).

6.2.3.4. Metabolite fingerprint profiling

Aliquots of all collected samples were freeze dried for non-targeted metabolite profile mass spectrometry and the data processed as detailed in Chapter 2, section 2.3. Metabolites with significant contribution (P <0.01) to the environment were extracted for hierarchical analysis and tentative metabolite and pathway identification. Co-occurrence network analysis was performed (Chapter 2, section 2.8) to visualise the connections between ecologically important bacterial community members, metabolites and environmental parameters.

6.3. RESULTS

6.3.1. Chlorophyll *a* and extracellular polymeric substance content in valley glacier cryoconite

Chlorophyll *a* concentration of each sample was calculated from a standard curve (APPENDIX IV, Figure IV. 1). The chlorophyll *a* concentration was high on DOY 202 with a minimum average for all sites of 104.1595 ± 3 8.3544 (SD) $\mu g.g^{-1}$ cryoconite (Figure 6. 2A). This was followed by a sharp decline in average concentration at DOY 210 and a gradual increase in average concentration, for the duration of the sampling season. Unique peaks in activity were observed at the different elevations, with FLC1 displaying the highest concentrations at each time point (Figure 6. 2B). The differences in chlorophyll *a* content was therefore sensitive to temporal effects (ANOVA, F = 13.27, *P* = <0.0001) and elevation effects (ANOVA, F = 2.5, P = 0.0.0167).

Extracellular polymeric substance concentrations were calculated using the standard curve in APPENDIX IV, Figure IV. 2. The resulting data showed a disproportionately high average concentration of 194.555 ± 11.576 (SD) $\mu g.g^{-1}$ cryoconite at DOY 202. This was the minimum concentration obtained as final values exceeded those recognised by spectrophotometry. Thereafter, average concentrations were much lower, expressing significant temporal fluctuations (Figure 6. 2C) (ANOVA, F = 37.28, *P* = <0.0001). Further observation of the EPS concentrations at different elevations showed insignificant fluctuations in EPS concentration (ANOVA, F = 0.36, *P* = 0.9357), but demonstrated concentration peaks at FLC1 and FLC8 on DOY 210 and at FL2 on DOY 217 (Figure 6. 2D).

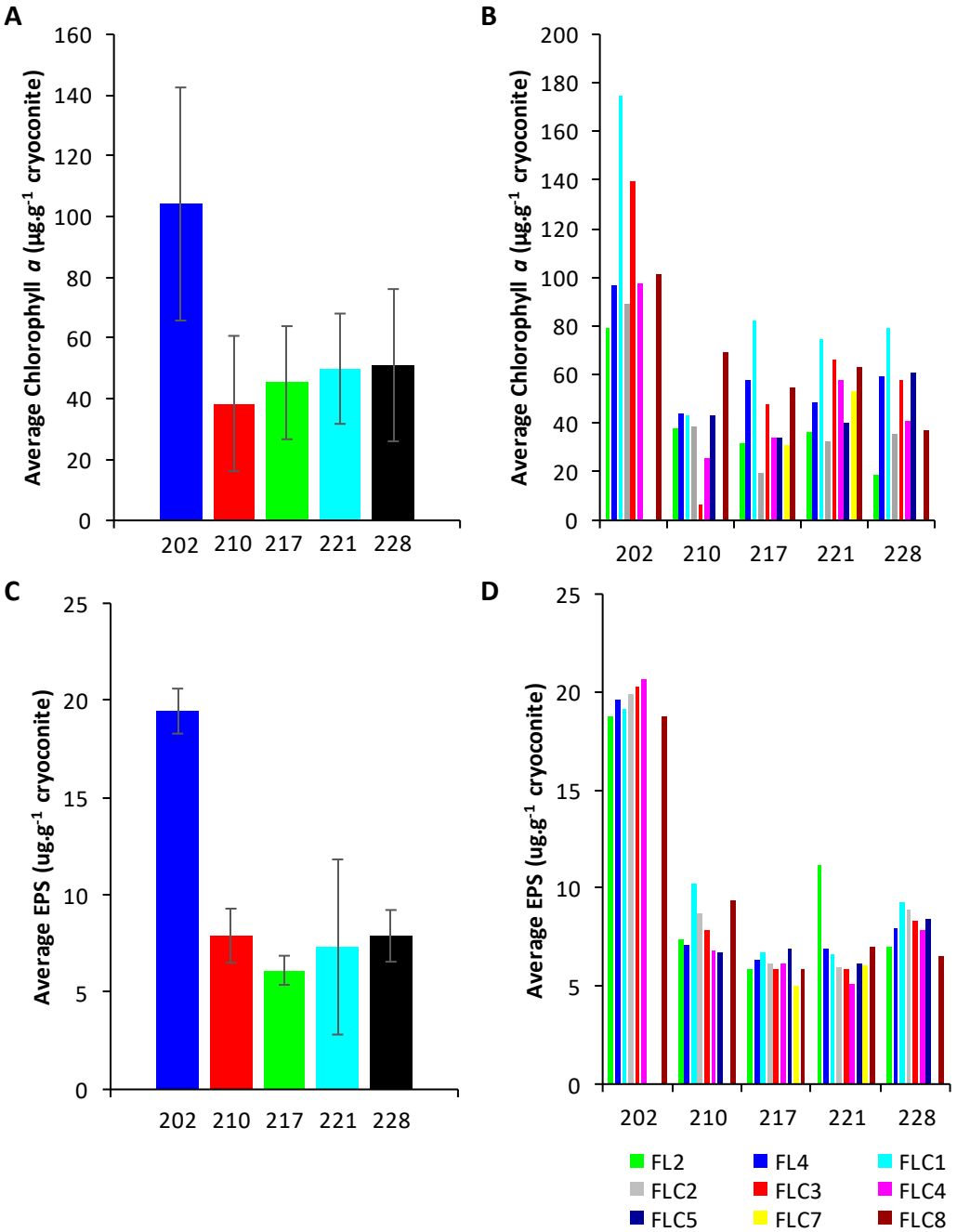

Figure 6. 2 Average concentrations of (A) temporal and (B) elevational chlorophyll *a* and (C) temporal and (D) elevational concentrations of EPS for Foxfonna valley glacier cryoconite. EPS concentrations for DOY 202 are minimum values at 10^{-1}; actual values exceed those displayed.

6.3.2. Description of the valley glacier bacterial communities

Of 117 cryoconite samples collected, a total of 109 provided sufficient DNA for downstream processing. High throughput sequencing generated a total of 761 613 reads for analysis on the QIIME 1.9.0 platform. Sequences were rarefied to 1000 reads, permitting the identification of 434 OTUs from 79 samples, 95.16% of which could be assigned beyond phyla taxonomic levels using the Greengenes 13_8 August 2013 database.

PCR amplified ultrapure water with no template controls were sequenced (Salter *et al.*, 2014) to eliminate the potential of reagent and laboratory contamination. Due to the low number of reads observed in negative controls being removed during rarefaction, the unfiltered matrix was examined separately, revealing 2 taxa (*Streptophyta* and *Phyllobacterium*) that were absent from PCR controls but present at more than 0.01% relative abundance in the combined samples, suggesting they were introduced at the DNA extraction stage. Additionally, top-scoring taxa with >3 reads were identified as *Microbacteriaceae*, *Streptophyta*, *Leptolyngbya* and *Sphingomonadaceae* (Table 6. 1).

Table 6. 1 Top-scoring potential contaminant taxa identified from negative control (NTC) sequences.

OTU	Greengenes ID	No of reads in NTC	BLAST ID	Accession ID	%ID
denovo-62678	f_*Microbacteriaceae*	29	*Salinibacterium amurskyense* IC A9	KU925169.1	99
denovo-57969	o_*Streptophyta*	18	*Roya obtusa*	KU646496.1	97
denovo-34111	g_*Leptolyngbya*	4	*Phormidesmis priestleyi* ANT.LG2.4	AY493580.1	99
denovo-20326	f_*Sphingomonadaceae*	3	*Polymorphobacter* sp. Ap23E	KX990242.1	99

The overall seasonal community of Foxfonna valley glacier was dominated by *Cyanobacteria* with a total phylum relative abundance (RA) of 39.65%, *Actinobacteria* with RA 25.87%, *Proteobacteria* with 16.43% RA, *Bacteroidetes* with 5.06% RA, *Firmicutes* with 4.18% RA, TM7 with 3.15% RA, *Acidobacteria* with 1.28% RA and unassigned phyla with 1.15% RA, providing 99% of bacterial diversity observed in cryoconite (Figure 6. 3). The remaining 1% was made up of the phyla WPS-2, *Planctomycetes*, *Chloroflexi*, *Armatimonadetes*, *Deltaproteobacteria*, *Verrucomicrobia*, *Thermi*, WS6, *Fibrobacteres* and *Gemmatimonadetes* (RA range 0.01% - 0.98%).

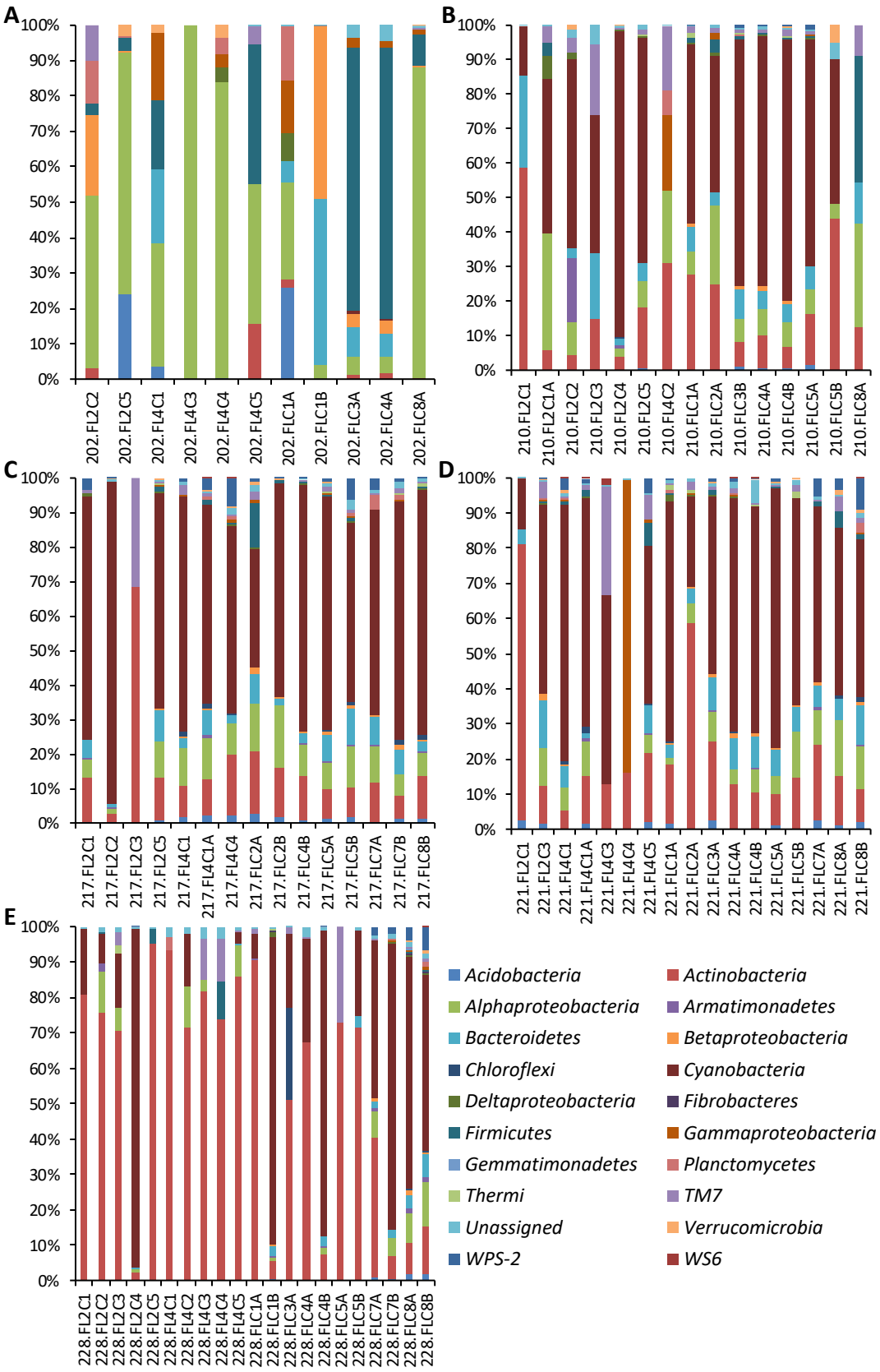

Figure 6. 3 Community composition of cryoconite holes along Foxfonna valley glacier display the changes in community members by phyla from (A) DOY 202 to (B) DOY 210, the consistent composition at (C) DOY 217 and (D) 221 and the end of season change at (E) DOY 228.

High relative abundance community members contributing to >1% RA over the duration of the sampling season highlighted 7 out of 434 OTUs: *Phormidesmis*-33968, *Microbacteriaceae*-62735, *Phyllobacterium*-19355, *Sphingomonadaceae*-20155, *Pseudanabaena*-17849, *Nostoc*-32859 and *Psychrobacter*-57929 (Table 6. 2). Top-scoring taxa had the highest count at DOY 202 (23) and decreased over time (DOY 210: 11, DOY 217: 11, DOY 221: 10, DOY 228: 3), however, DOY 210 to 221 had the highest phyla diversity contributed by OTUs from *Cyanobacteria*, *Actinobacteria* and *Proteobacteria* in top 3 ranking positions, with *Firmicutes* (DOY 210 and 221), *Bacteroidetes* (DOY 210 - 217), TM7 (DOY 210 - 221) and WPS-2 (DOY 217 - 221) forming the remaining high RA phyla.

Core community members were identified from high relative abundance OTUs using a minimum sample occupancy of >80%. *Phyllobacterium*-19355 was present in all samples at DOY 202 with the highest RA (23.23%). *Phormidesmis*-33968 was present in 14 out of 16 samples at DOY 210 (35.37% RA), 14 out of 15 samples at DOY 217 (42.1% RA) and 16 out of 17 samples at DOY 221 (35.58% RA); *Microbacteriaceae*-62735 was present in 14 out of 16 samples at DOY 210 (13.13% RA) and all samples collected on DOY 217, 221 and 228 (RA: 6.75%, 14.87, 50.04%). *Pseudanabaenaceae*-17849 was present in 12 out of 15 samples on DOY 217 (3.19% RA) and 15 out of 17 on DOY 221 (1.23% RA). *Sphingomonadaceae*-20155 was present in 13 out of 15 samples on DOY 217 (3.25% RA) and 15 out of 17 samples on DOY 221 (2.08% RA). *Nostoc*-32859 was also present in 13 out of 15 samples on DOY 217 (2.53% RA) and in 14 out of 17 samples on DOY 221 (2.49% RA).

Common core taxa were further characterised by BLAST-based CER and CNR, revealing close matches to uncultured taxa (99% ID match) from northern hemisphere ice and snow sites (4/7), deglaciated soil (1/7) and Antarctic water and cryoconite (2/7). Cultivated taxa demonstrated 98 - 99% ID match to Arctic and Antarctic marine and glacial taxa (4/7) and to individual taxa previously observed in root nodules (1), lake water (1) and in symbiosis with lichen species (1), revealing their cosmopolitan nature.

Table 6. 2 BLAST-based identity of common core OTUs detected on the Foxfonna Valley glacier with RA >1%, including the identity of the closest environmental (CER) and cultivated (CNR) taxa.

Greengenes ID	Closest Environmental Relative (CER)	CER Accession	CER %ID	CER Habitat	Closest Named Relative (CNR)	CNR Accession	CNR %ID	CNR Habitat
Leptolyngbya-33968	Uncultured *cyanobacterium* clone MIS88	FJ977129.1	99	Canadian microbial mat	*Phormidesmis priestleyi* ANT.LG2.4	AY493580.1	99	Antarctic benthic mat
Microbacteriaceae-62735	*Frigoribacterium* sp. L29	KF928885.1	99	Antarctic surface water	*Frigoribacterium* sp. L29	KF928885.1	99	Antarctic surface water
Phyllobacterium-19355	Uncultured bacterium clone PL3-9	EU527093.1	99	Tibetan glacier snow	*Phyllobacterium sophorae* strain CCBAU 03415	KJ685938.3	99	Root nodule
Sphingomonadaceae-20155	Uncultured *alphaproteobacterium* clone IC4022	HQ622730.1	99	Svalbard ice	*Sphingopyxis* sp. JJ2203	JX304649.1	98	Korean lake
Nostoc-32859	Uncultured bacterium clone IT2-45	KX247339.1	99	Deglaciated soil	*Nostoc* sp. 9.4.22	AY328896.1	99	Lichen symbiont
Pseudanabaena-17849	Uncultured *cyanobacterium* clone ADJ576	HQ230223.1	99	Canadian snow	*Pseudanabaena frigida O-302*	KT753326.1	100	Antarctic
Leptolyngbya-57985	Uncultured *cyanobacterium* clone CCH343	KT424930.1	99	Antarctic cryoconite	*Phormidesmis* sp. HOR_11_6	KU219729.1	100	Svalbard soil

Analysis of samples collected along the valley glacier by one way PERMANOVA showed that DOY and collection site are both significant predictors of the bacterial community on the glacier, however, DOY had a greater effect than collection site (DOY, pseudo-F = 4.3785, *P* = 0.001; collection site, pseudo-F = 1.6567, *P* = 0.003). Positional interpretation of OTUs in the Bray-Curtis matrix using canonical analysis of principal co-ordinates shows that the cryoconite community at DOY 202 is vastly different from the community at DOY 210, DOY 217, DOY 221 and DOY 228 (Figure 6. 4A). While some clustering of specific OTUs is clear at DOY 228, a greater number of OTUs cluster together with DOY 210 - 221 bacterial communities across a larger area. Clustering is evident at all elevations, with FLC1 existing as a separate cluster. Further clustering is discernible at other sites, with an overlap of OTUs in FLC1, 3, 4, 5 and FL2, as well as FLC5, 7, 8 and FL4 (Figure 6. 4B).

Analysis of the average similarity, within and between groups in pairwise fashion, shows that within each day, a significant effect is observed at site FL2, between 202 and 210 (t = 1.5389, *P* = 0.032), 210 and 228 (t = 1.4706, *P* = 0.049) and at site FL4, 202 and 217 (t = 2.0808, *P* = 0.034), 202 and 221 (t= 1.867, *P* = 0.009), 202 and 228 (t = 2.5053, *P* = 0.007), 217 and 228 (t = 3.0184, *P* = 0.016), 221 and 228 (t=2.0458, *P* = 0.008). No significant observations were made for samples FLC1, FLC2, FLC3, FLC4, FLC5, FLC7 and FLC8. Within each site, a significant effect is observed for DOY 228 between FLC and FL4 (t = 1.3628, *P* = 0.017), FL4 and FLC1 (t = 1.6988, *P* = 0.048), FL4 and FLC5 (t = 1.3578, *P* = 0.041) and FL4 and FLC7 (t = 2.4697, *P* = 0.047).

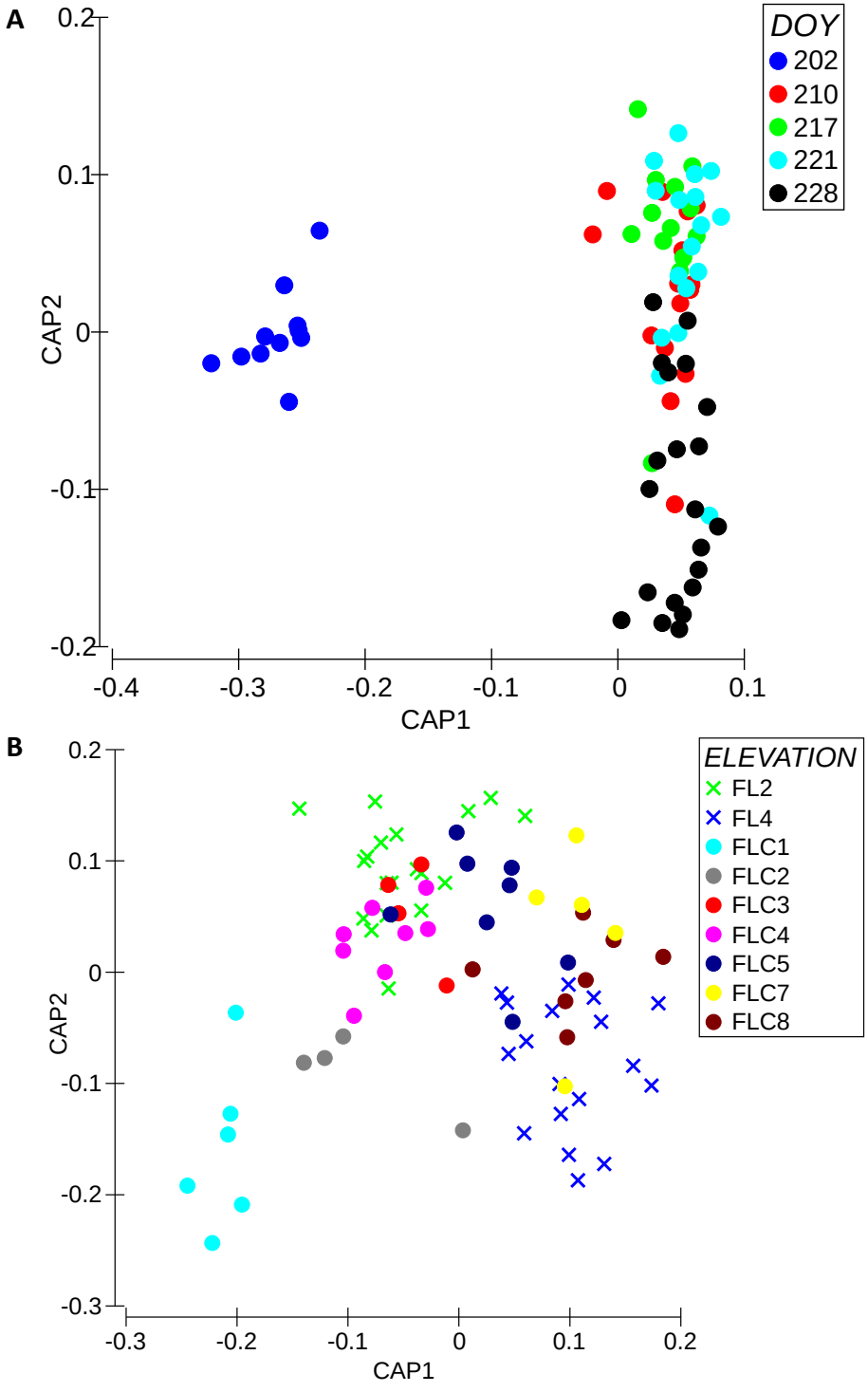

Figure 6. 4 Canonical ordination of Bray-Curtis distance indicating the effect of (A) day of year and (B) site elevation on the bacterial cryoconite community of the Foxfonna valley glacier.

6.3.2.1. Effect of environment on valley glacier cryoconite assemblages

Analysis of the data collected demonstrated the high significance of DOY (PERMANOVA, pseudo-F = 17.961, *P* = 0.001) and collection site (PERMANOVA, pseudo-F = 36.202, *P* = 0.001) on the environmental variables for the duration of the sampling period. Geographic parameters (Cartesian co-ordinates, elevation, slope, aspect and curvature) were significant for collection site in two way ANOVA (pseudo-F range = 21.07 - 104 874, *P* = <0.0001) but not DOY (pseudo-F range = 0.25 - 0.52, *P* range = 0.7229 - 0.9106). Weekly and total incident radiation (IR) were significant for both DOY (pseudo-F range = 6 479.96 - 68 910.21, *P* = <0.0001) and collection site (pseudo-F range = 8.12 - 8.22, *P* = <0.0001) and showed a pattern of alternating highs and lows for the 5 week sampling season, where weeks 1, 3 and 5 experienced high IR and weeks 2 and 4 low IR. FAA was highest for samples at FL4 and relatively high at FLC1 and FLC7, for the entire sampling season (pseudo-F range = 5.35 - 225.45, *P* range = <0.0001), however, no significant effect of water catchment was observed on the bacterial community and metabolomic profile over time (pseudo-F range = 0.44 - 0.49, *P* range = 0.7403 - 0.7817). Evaluation of the relationship between environmental variables and the bacterial diversity by biota and environment matching revealed the main predictors of diversity to be total IR received by the community (BEST, global test ρ = 0.504, *P* = 0.001). This is supported by the Spearman rank correlation in dbRDA using the adjusted R-squared model, identifying EPS concentration, total IR receipt, E and IR between sample collection as suitable predictors of the community (Figure 6. 5A) in stepwise sequential tests (APPENDIX IV, Table IV. 2), with the additional influence of chlorophyll *a* concentration, elevation, N and aspect in marginal tests (APPENDIX IV, Table IV. 3).

Furthermore, investigating the effect of both environmental and bacterial contributors revealed a greater cumulative significance than either group of variables alone. Marginal tests identified 6 out of 7 high RA taxa and 8 out of 12 environmental parameters (APPENDIX IV, Table IV. 4), while in sequential tests all 6 taxa and 4 environmental factors were identified as drivers of the community (APPENDIX IV, Table IV. 5). Redundancy ordination (Figure 6. 5B) identified the positive correlation of *Phyllobacterium*-19355, chlorophyll *a* and EPS to the community profile on DOY 202, *Microbacteriaceae*-62735 at DOY 228 and IR on the remaining bacterial population at all other observed sampling points.

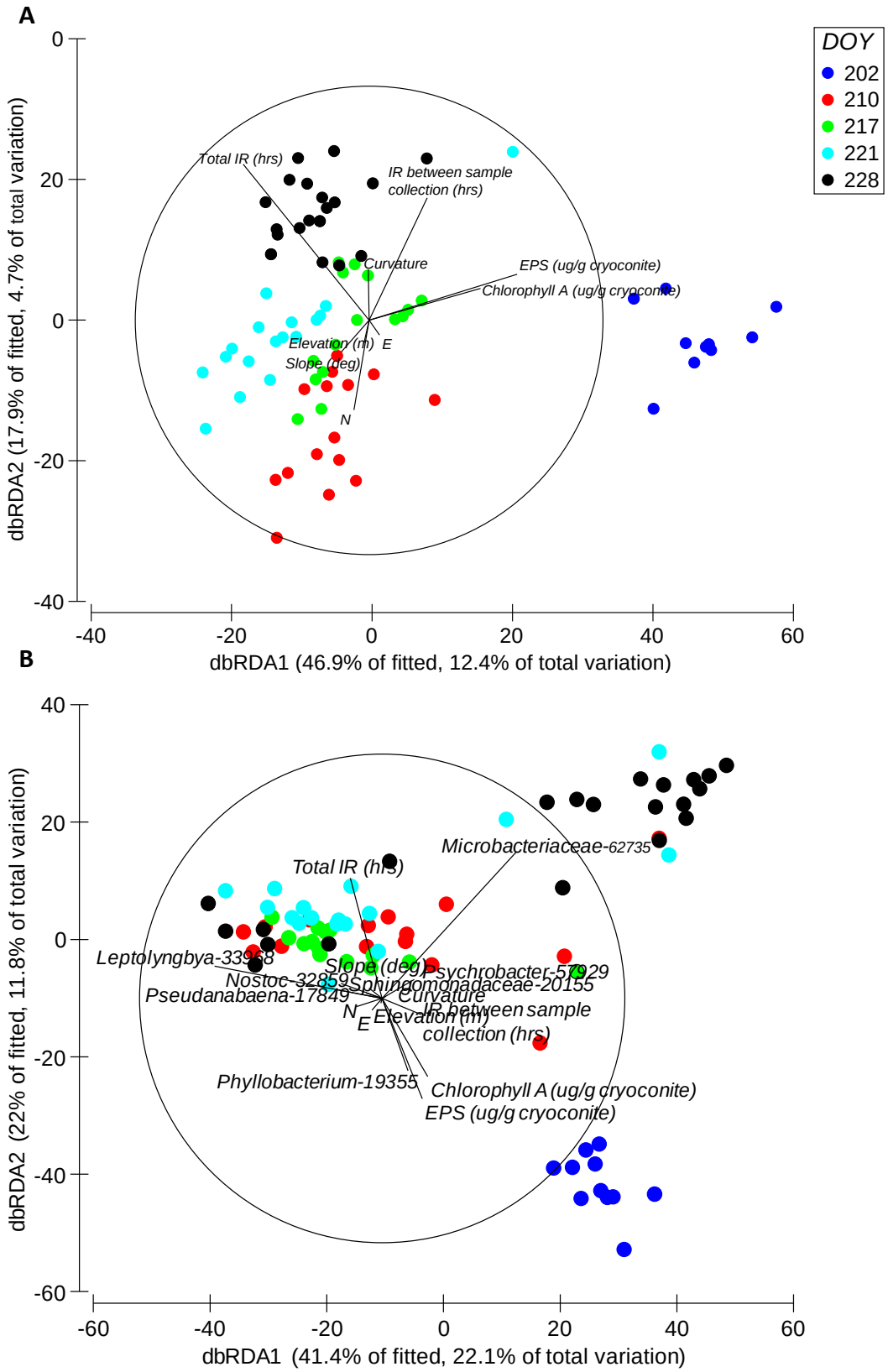

Figure 6. 5 Distance-based redundancy model of (A) environmental and (B) combined environmental and bacterial factors that predict the bacterial community composition on Foxfonna valley glacier.

Observing the environmental influence on a week-to-week basis revealed significant impact by environmental variables, solely for communities at DOY 210, 217 and 221. In marginal tests (Table 6. 3), E, elevation, N, chlorophyll *a* and IR between sample collection points could predict the bacterial community on these three sampling days (pseudo-F range = 1.709 - 2.063, *P* range = 0.008 - 0.048). Sequential tests (Table 6. 4) additionally highlight FAA as a predictor variable affecting the community on DOY 210 (pseudo-F range = 1.8224 - 2.063, *P* range = 0.007 - 0.038).

Table 6. 3 Marginal tests of the distance-based linear model of significant environmental and bacterial taxa predictors (*P* <0.05) of community structure from DOY 210 to DOY 221. SS = sum of squares, Pseudo F = test statistic.

DOY	Variable	SS(trace)	Pseudo-F	*P*	Proportion explained
210	E	5780.3	2.063	0.026	1.37E-01
	Elevation (Z, m)	5330.2	1.8792	0.031	1.26E-01
	N	5192.4	1.8238	0.032	0.12303
	Chlorophyll *a* ($\mu g.g^{-1}$ cryoconite)	4903.7	1.709	0.047	1.16E-01
217	Elevation (Z, m)	3777.4	1.9018	0.008	1.28E-01
	E	3645.6	1.8261	0.01	0.12317
	N	3619	1.811	0.017	1.22E-01
	IR between sample collection (hrs)	3706	1.8607	0.033	1.25E-01
221	E	3910.4	1.7979	0.047	0.10703
	N	3954	1.8204	0.048	1.08E-01
	Elevation (Z, m)	3941.4	1.8139	0.048	1.08E-01

Table 6. 4 Sequential tests of the distLM model of significant environmental and bacterial taxa predictors (*P* <0.05) of community structure from DOY 210 to DOY 221.

DOY	Variable	Adj R^2	SS(trace)	Pseudo-F	*P*	Proportion explained	Cumulative variance
210	E	7.06E-02	5780.3	2.063	0.016	1.37E-01	1.37E-01
	FAA D8 (m^2)	0.1712	4553.3	1.8224	0.038	1.08E-01	0.3488
217	Elevation (m)	6.05E-02	3777.4	1.9018	0.007	1.28E-01	1.28E-01

6.3.2.2. Temporal and spatial variations in cryoconite bacterial communities on Foxfonna valley glacier

Visual inspection of abundance data showed that the cryoconite community changed from *Alphaproteobacteria* dominated (DOY 202: 45.77% RA), to one strongly dominated by *Cyanobacteria* (DOY 210: 49.42% RA, DOY 217: 58.37% RA, DOY 221: 46.95% RA), which again changed to *Actinobacteria* dominated on DOY 228 (74.65% RA). There was low community diversity at DOY 202, a peak increase from DOY 217 to 221 and a decline at DOY 228, demonstrated by diversity indices (H', ANOVA F = 6.58, *P* = <0.0002), with significant but less impacting collection site influence (H', ANOVA, F = 3.59, *P* = 0.0333) (APPENDIX IV, Table IV. 6). No significant changes were observed in the evenness value for DOY (J', ANOVA, F = 0.78, *P* = 0.5402) and site (J', ANOVA, F = 1.56, *P* = 0.2186).

Each of the core OTUs were represented as high abundance OTUs (RA >1%), with fluctuating abundance during the 5 week sampling period. Majority of the diversity on DOY 202 is attributed to *Phyllobacterium*-19355 (23.23% RA), while other high abundance representing OTUs on this day belonged to the phyla *Proteobacteria* (12 OTUs), *Bacteroidetes* (2 OTUs), *Firmicutes* (5 OTUs), *Acidobacteria* (1 OTU) and *Planctomycetes* (2 OTUs). On DOY 210, dominance shifted to core OTU *Phormidesmis*-33968 (35.37% RA), with *Microbacteriaceae*-62735 (13.13% RA), *Sphingomonadaceae*-20155 (3.8% RA) and *Pseudanabaena*-17849 (1.99% RA) appearing among high abundance OTUs (*Cyanobacteria* (2 OTUs), *Actinobacteria* (1

OTU), *Proteobacteria* (4 OTUs), *Firmicutes* (1 OTU), *Bacteroidetes* (2 OTUs) and TM7 (1 OTU)) for this day.

On DOY 217, the high abundance OTUs present at DOY 210 still predominate among the high abundance OTUs in the phyla *Cyanobacteria* (3 OTUs), *Actinobacteria* (3 OTUs), *Proteobacteria* (1 OTU), TM7 (1 OTU), *Bacteroidetes* (2 OTUs) and WPS-2 (1 OTU), albeit at different relative abundances (*Phormidesmis*-33968: 42.1% RA, *Microbacteriaceae*-62735: 6.75% RA, *Pseudanabaena*-17849: 3.4% RA, *Sphingomonadaceae*-20155: 3.25% RA and *Nostoc*-32859: 2.53% RA). DOY 221 had the greatest representation of core OTUs, with *Phormidesmis*-33968 (35.58% RA), *Microbacteriaceae*-62735 (14.87% RA), *Psychrobacter*-57929 (4.88% RA), *Nostoc*-32859 (2.43% RA), *Sphingomonadaceae*-20155 (2.08% RA) and *Pseudanabaena*-17849 (1.23% RA), all present in the high abundance phyla consisting of *Cyanobacteria* (4 OTUs), *Actinobacteria* (1 OTU), *Proteobacteria* (2 OTUs), WPS-2 (1 OTU), TM7 (1 OTU) and *Firmicutes* (1 OTU). DOY 228 has the highest observed contribution by core OTUs *Microbacteriaceae*-62735 (50.04% RA) and *Phormidesmis*-33968 (19.53% RA), as well as *Phormidesmis*-57985 (1.04% RA) observed in the high abundance OTUs.

The similarity in bacterial community composition from DOY 202 to DOY 228 decreased with geographic distance, revealing a moderate, yet significant, distance decay effect (RELATE, $\rho = 0.104$, $P = 0.013$), when observing the Spearman rank correlation of Bray-Curtis similarity against pairwise distances at 999 permutations

(Figure 6. 6A). Spearman correlation analysis identified that DOY 210 and 217 possessed the only significant correlations with decreasing strength over time (Table 6. 5).

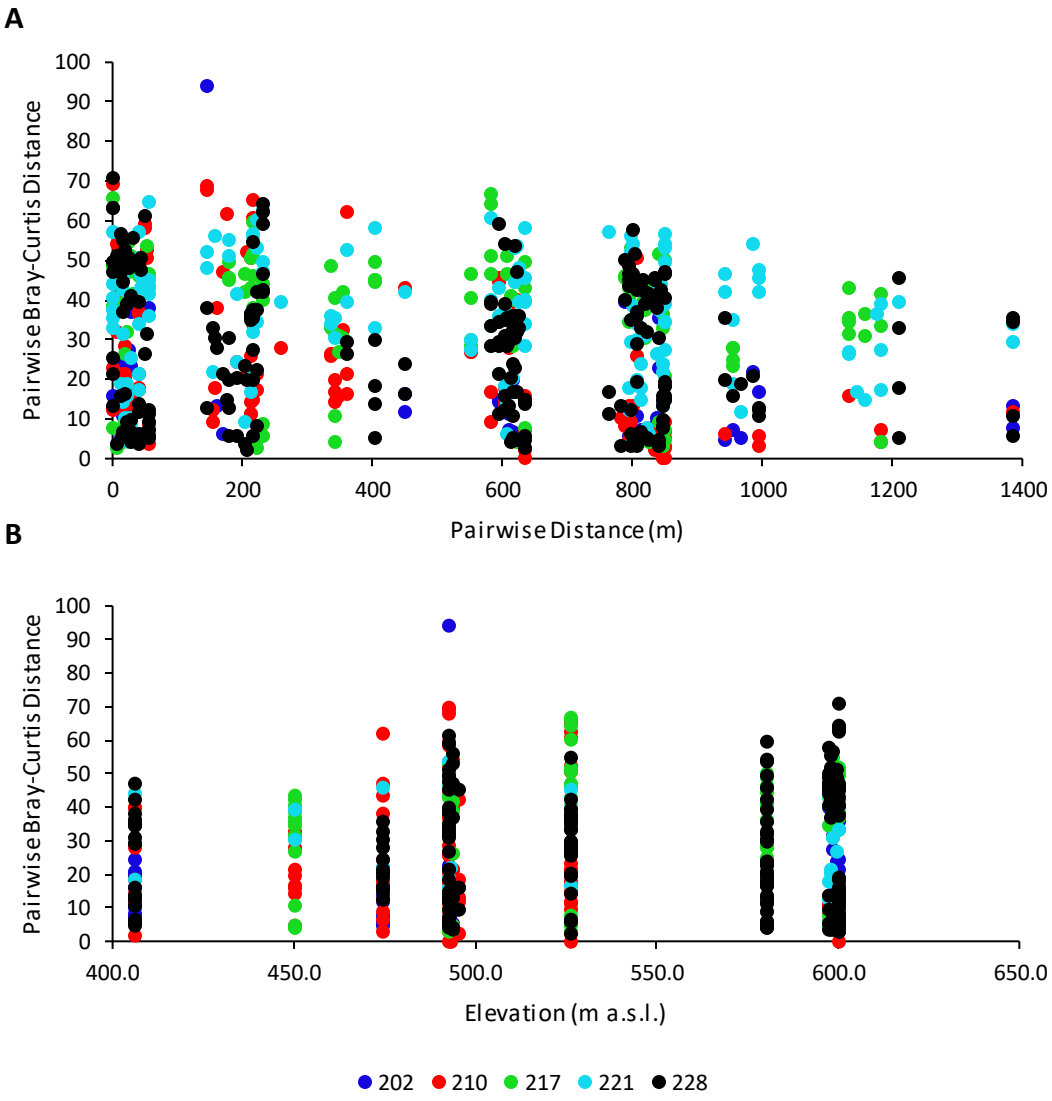

Figure 6. 6 Environmental decay models of Bray-Curtis distances with (A) pairwise geographic distance and (B) elevation between cryoconite holes at each sample collection day. There is a moderate seasonal distance decay effect and a negligible elevation decay effect for all days, apart from 210 that shows remarkable elevational decay.

Table 6. 5 Spearman correlations of pairwise geographic and Bray-Curtis distances for the bacterial community on each sampling day.

DOY	Rho	*P* value
202	0.137	0.119
210	0.429	0.03
217	0.226	0.037
221	0.098	0.147
228	0.124	0.069

Similar analysis using elevation revealed no distinct decay patterns along the elevation gradient, apart from DOY 210 that showed a remarkable decrease with an increasing gradient (Figure 6. 6B). Majority of this distance decay effect is contributed by 9 out of 17 phyla, when observed for the duration of the season (Table 6. 6). RELATE analysis highlighted the temporal effect of specific phyla that were significant to the distance decay model, demonstrating a particularly higher than average influence from *Betaproteobacteria* (DOY 202: ρ = 0.621, *P* = 0.024), *Gammaproteobacteria* (DOY 210: ρ = 0.816, *P* = 0.033), *Planctomycetes* (DOY 217: ρ = 0.459, *P* = 0.044) and WPS-2 (DOY 288: ρ = 0.699, *P* = 0.004).

Table 6. 6 Temporal distance decay of the 16S rRNA gene sequences reveals a significant decrease in community diversity as geographic distance increases, particularly for DOY 210, 217 and 228.

Phylum	**202 ρ**	***P***	**210 ρ**	***P***	**217 ρ**	***P***	**221 ρ**	***P***	**228 ρ**	***P***
Acidobacteria	-0.127	0.633	0.163	0.233	-0.004	0.47	-0.03	0.598	0.301	0.141
Actinobacteria	0.153	0.24	0.159	0.199	0.086	0.229	0.033	0.328	0.13	0.078
Alphaproteobacteria	0.111	0.165	0.278	0.107	0.007	0.419	0.186	0.053	-0.037	0.523
Armatimonadetes	-	-	0.3	0.204	0.042	0.313	-0.088	0.718	0.294	0.047
Bacteroidetes	-0.052	0.528	0.208	0.189	0.134	0.102	0.067	0.246	-0.13	0.667
Betaproteobacteria	0.621	0.024	0.621	0.024	0.129	0.165	0.119	0.124	-0.053	0.624
Chloroflexi	-	-	-0.674	1	-0.054	0.569	-0.048	0.549	0.866	0.329
Cyanobacteria	0.44	0.136	0.36	0.053	0.36	0.003	0.249	0.013	0.168	0.068
Deltaproteobacteria	-0.131	0.673	0.005	0.505	0.331	0.2	0.18	0.146	0.135	0.301
Firmicutes	0.034	0.361	0.146	0.275	-0.137	0.812	0.236	0.039	-0.161	0.657
Gammaproteobacteria	-0.19	0.499	0.816	0.033	0.158	0.138	-0.077	0.687	0	0.502
Planctomycetes	-0.174	0.673	0.794	0.171	0.459	0.044	-0.029	0.517	-0.334	0.74
Thermi	-	-	0.562	0.11	0.75	0.105	0.149	0.196	-	-
TM7	-	-	0.054	0.341	0.222	0.04	0.238	0.016	0.156	0.072
Unassigned	-0.067	0.646	0.063	0.348	0.231	0.024	0.053	0.254	0.171	0.029
Verrucomicrobia	-0.406	0.914	-0.198	0.777	0.322	0.041	-0.072	0.573	0	0.686
WPS-2	-	-	0.732	0.158	0.368	0.023	0.263	0.037	0.699	0.004

As the recorded environmental variables appear to minimally affect the valley glacier bacterial communities, it was worth investigating the effect of the changing core communities for the duration of the Arctic summer. An examination of the combined effect of OTUs and environmental parameters yielded an improved prediction of the total variation observed in the valley glacier community, particularly when investigated at individual sample collection points. Marginal analysis revealed significant influence of 8 high RA bacteria that were non-core (APPENDIX IV, Table IV. 7) with denovo-16065, denovo-47295 and denovo-29496 identified as significant predictors of community structure in sequential analysis for DOY 202 (APPENDIX IV, Table IV. 8). Furthermore, distance-based redundancy ordinations show affiliation of OTUs to samples at different elevations, specifically denovo-47295 at FLC3 and FLC4; all other taxa associations were non-elevation related (Figure 6. 7A). At DOY 210, core

taxa *Phormidesmis*-33968 and *Microbacteriaceae*-62735, exhibited the highest significance as predictor variables in both marginal and sequential tests, followed by E, N and elevation (Marginal tests: APPENDIX IV, Table IV. 9; Sequential tests: APPENDIX IV, Table IV. 10) with the addition of non-core taxon denovo-12431 in sequential tests. No discrete associations could be made in the dbRDA of the total community, apart from the community at FL3, FL4 and FL5 exhibiting sensitivity to curvature and *Pseudanabaena*-17849 (Figure 6. 7B).

By DOY 217, sequential analysis revealed significant influence by core and non-core taxa, particularly *Nostoc*-32859, *Pseudanabaena*-17849, denovo-33714, *Microbacteriaceae*-62735 and *Phormidesmis*-33968 (APPENDIX IV, Table IV. 11), in order of significance, while marginal tests additionally highlighted elevation, E, N and incident radiation between sample collection points (APPENDIX IV, Table IV. 12). This is supported by redundancy analysis (Figure 6. 7C), which further illustrates the effect of aspect, FAA and curvature on all but 1 sample from different elevations. The DOY 221 community revealed highest significant input by core taxa *Phormidesmis*-33968, *Microbacteriaceae*-62735, *Nostoc*-32859, *Pseudanabaena*-17849 and environmental variable N (Marginal tests: APPENDIX IV, Table IV. 13), with incident radiation between sample collection points and non-core taxa, denovo-38076, additionally significant in sequential analysis (APPENDIX IV, Table IV. 14). Redundancy analysis showed an affiliation of lower elevation sites (FLC1, FLC2, FLC3 and FLC4) to aspect and *Pseudanabaena*-17849 and higher elevations associated with FAA, IR, denovo-53742, denovo-33968, denovo-38076, denovo-32859, denovo-5379 and denovo-

20155 (Figure 6. 7D). At the end of the sampling season on DOY 228, *Microbacteriaceae*-62735 and *Phormidesmis*-33968 were the only significant predictors of community diversity by marginal tests (APPENDIX IV, Table IV. 15), while sequential analysis revealed just *Microbacteriaceae*-62735, E and N as significant predictors of community diversity (APPENDIX IV, Table IV. 16). Furthermore, *Microbacteriaceae*-62735 showed a strong positive association to majority of samples located at sites FL2, FL4, FLC3, FLC4 and FLC5, while slope, elevation, E and denovo-57985 appeared to have a positive relationship with sites FLC7 and FLC8 (Figure 6. 7E).

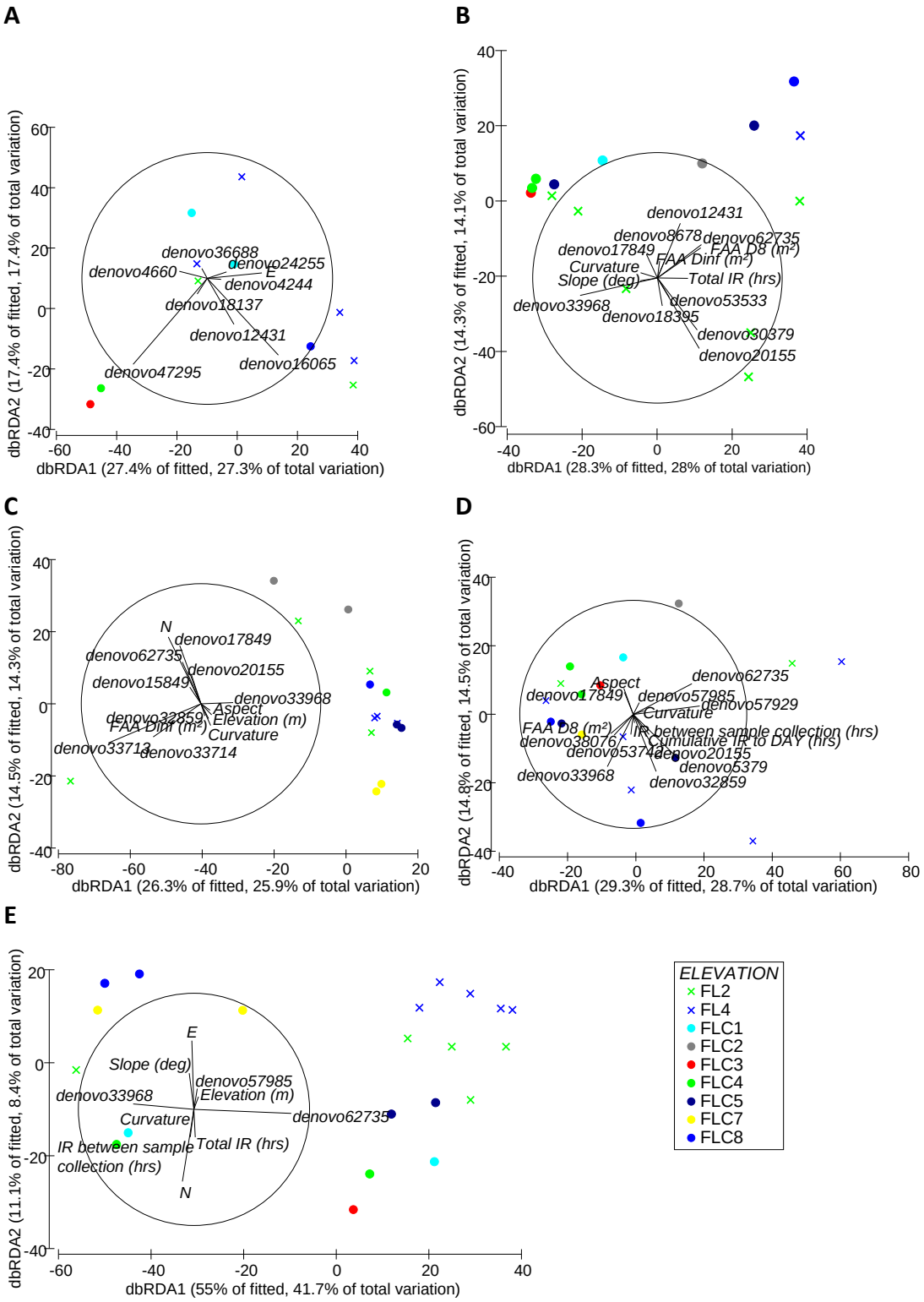

Figure 6. 7 Distance-based ordination of high relative abundance OTUs (>1%) and environmental parameters as predictors of the total community. Bacterial taxa have a greater influence on the community at (A) DOY 202, while both biotic and abiotic components influence the community at DOY (B) 210, (C) 217 and (D) 221. (E) DOY 228 community shows significant influence from high RA taxa and geographic parameters.

6.3.3. Metabolite overview and pathway identification of Foxfonna valley glacier cryoconite metabolome

The cryoconite from Foxfonna valley glacier generated a metabolic fingerprint of 2 623 metabolites. Ordination by PCA showed that all metabolites separate naturally, based on DOY and then by sample collection site (FLC/FL2/FL4), with 98.87% of the variation being explained in the first two PCs (Figure 6. 8). However, this was not significant when tested using permutational analysis of variance (PERMANOVA, DOY, pseudo-F = 1.0846, *P* = 0.272; site, pseudo-F = 0.87591, *P* = 0.594).

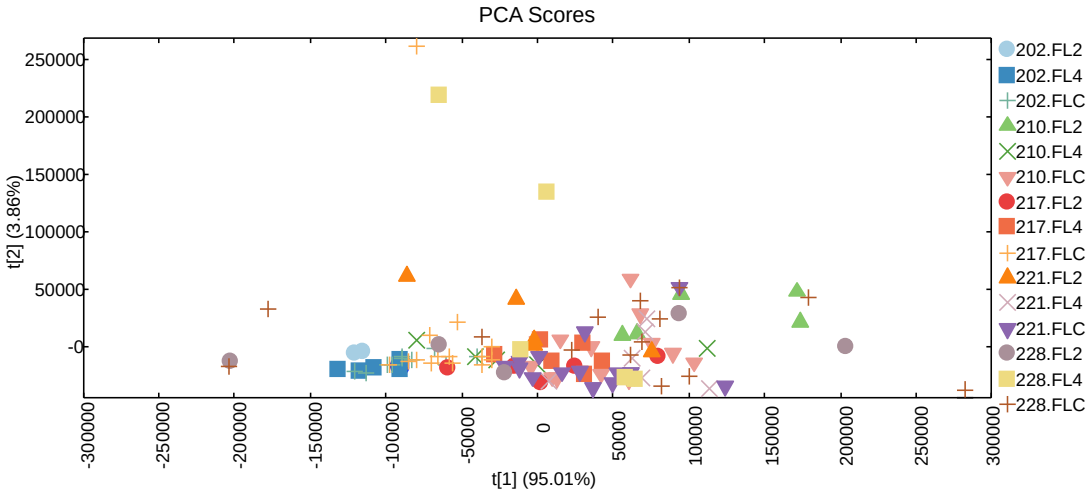

Figure 6. 8 PCA ordination of Foxfonna valley cryoconite metabolites classified using DOY and site. Majority of the variation observed is contributed by PC 1.

Prediction of metabolites revealed that a PLS linear regression model was unable to predict drivers of the metabolome, using environmental variables and core and keystone bacterial taxa as classifiers. This was supported by BEST analysis of environmental parameters (global test ρ = 0.101, *P* = 0.456) and RELATE analysis of both biotic and abiotic parameters (OTU: ρ = -0.161, *P* = 0.986; environmental

parameters: ρ = -0.113, *P* = 0.953). However, alternative prediction using distance-based linear modelling (stepwise elimination, adjusted R^2, 999 iterations) on the combined effect of bacterial and abiotic variables again revealed poor influence on the metabolome by environmental factors but *significant* influence by *Phormidesmis*-33968 in marginal tests (APPENDIX IV, Table IV. 17) and chlorophyll *a* concentration in sequential tests (APPENDIX IV, Table IV. 18). Redundancy ordination identified further influence on the metabolome by curvature, *Nostoc*-32859 and weekly incident radiation (Figure 6. 9).

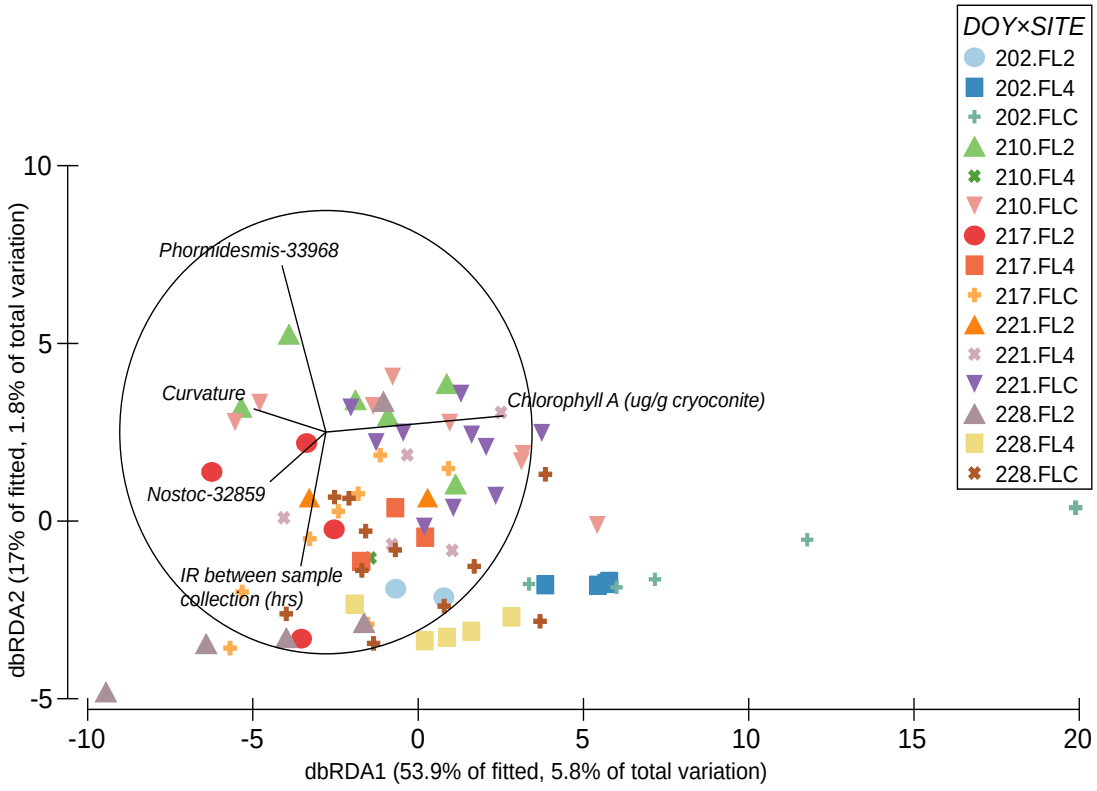

Figure 6. 9 dbRDA of metabolites with environmental, core taxa and key taxa with Spearman rank correlation >0.2 as predictors of metabolome structure.

PLS discriminant analysis revealed that variables influencing major changes were present at DOY 202 and DOY 217, where metabolites from sites FL2 and FL4 clustered separately from site FLC (Figure 6. 10). Random forest classification of these variables in HCA identified clustering of major variables of influence by DOY and site, with metabolites from DOY 202 (FLC, FL4 and FL2) clustering together and DOY 217 (FL2 and FL4) separating out from other days.

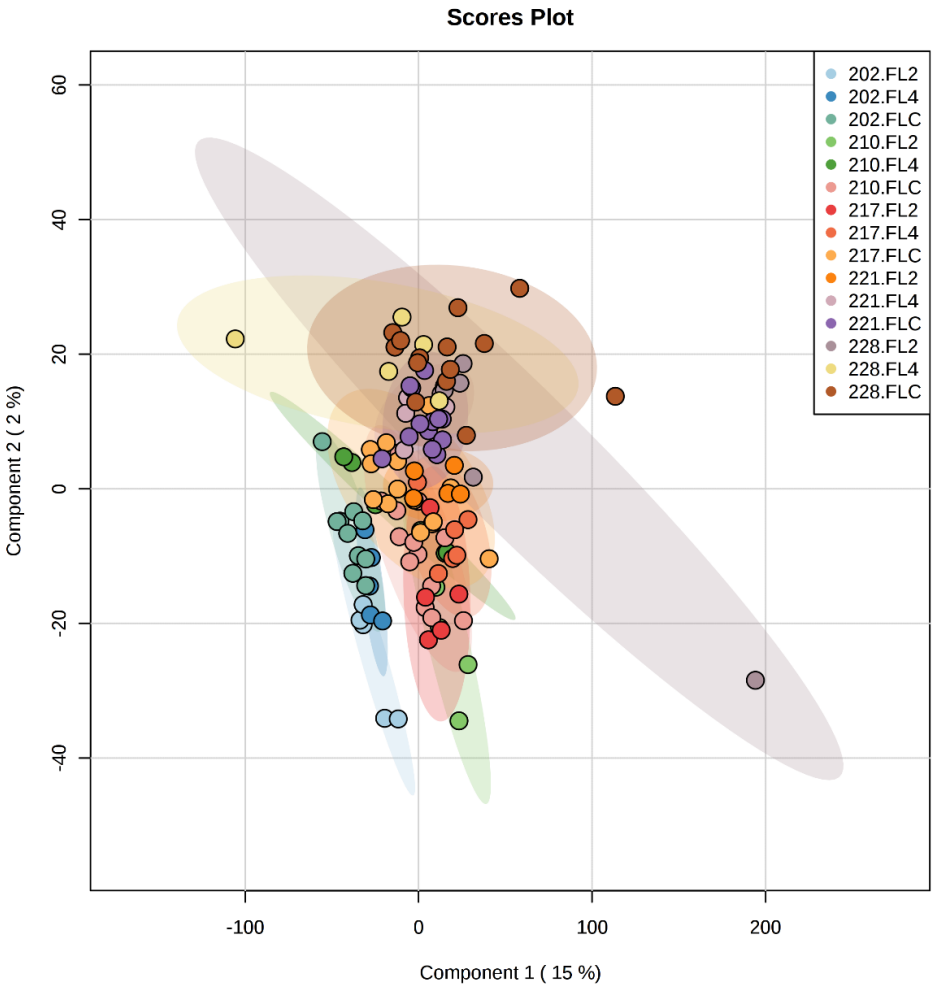

Figure 6. 10 PLS-DA of the metabolite profile from cryoconite holes across the Foxfonna valley glacier reveals a strong temporal effect, with additional separation of samples by site.

Post hoc ANOVA filtering (*P* <0.01, false discovery rate <0.01, exact mass <400 units) further reduced the number of analysable metabolites to 98, which were assigned tentative identities using the KEGG and DIME online databases (APPENDIX IV, Table IV. 19). HCA analysis revealed clustering of metabolites on DOY 202, with separation of sites FLC and FL4 from FL2 (Figure 6. 11). Additional clustering was evident for DOY 217, where FLC clustered separately from FL2 and FL4, DOY 221, where FLC and FL4 cluster together and DOY 228, clustering FLC and FL2. Major metabolites of interest aligned with pathways for amino acid biosynthesis, nucleic acid biosynthesis, nitrogen metabolism, fatty acid biosynthesis and the TCA cycle.

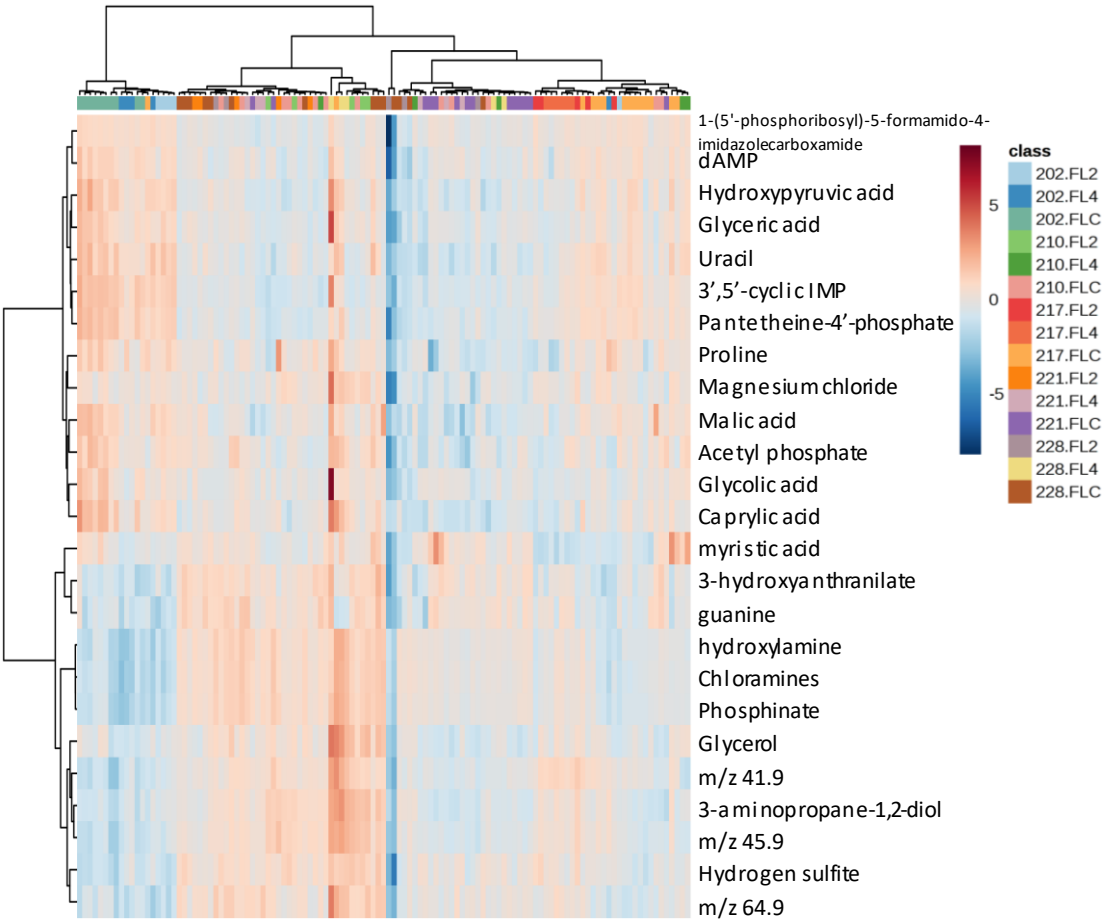

Figure 6. 11 HCA of major variables influencing the metabolome extracted using analysis of variance. DOY 202 shows separation of FLC, FL4 and FL2. Additional clustering is evident at DOY 217, DOY 221 and DOY 228, also showing separation by site.

6.3.3.1. Pathway analysis of valley glaciers

The high activity of majority of the significant metabolites infer high rates of microbial growth in abundantly active populations. There is evident clustering by both DOY and site, particularly at DOY 202, with distinct high concentrations of nucleic acid metabolites (Figure 6. 12A) and all extracted TCA cycle metabolites (Figure 6. 12B), intermediate concentrations of amino acid biosynthesis metabolites (Figure 6. 12C) and lipid synthesis metabolites (Figure 6. 12D), apart from the nitrogen metabolism metabolites that distinguish themselves with very low concentrations on this day (Figure 6. 12E). Additional distinct clustering and separation was observed on DOY 217, with high concentrations of metabolites at FLC for the TCA cycle and amino acid biosynthesis, intermediate concentrations at FLC and FL4 for nucleic acid synthesis and low concentrations at all DOY 217 sites for fatty acid and nitrogen metabolites. DOY 221 showed clustering with intermediate metabolite concentrations at FLC and FL4 for nucleic acid and nitrogen metabolites and low concentrations at FLC for amino acids. Metabolite patterns at DOY 228 revealed high concentrations of amino acid metabolites at FLC. One way permutational multivariate analysis of variance of metabolites in each pathway identified that DOY and collection site significantly influenced amino acid and fatty acid metabolites while nucleic acid, nitrogen cycling and TCA cycle metabolites were sensitive to DOY (Table 6. 7). All metabolites exhibited significant impact by the combined effect of these 2 main factors.

Table 6. 7 PERMANOVA results of each significant pathway identifying the contribution of factors day of year (DOY) and collection site.

Metabolic Pathway	**Source**	**df**	**SS**	**MS**	**Pseudo-F**	***P*(perm)**	**Unique perms**
Amino acid	DOY	4	787.96	196.99	9.4856	0.001	996
	Site	8	299.88	37.484	1.805	0.014	999
	DOY × Site	29	1148.6	39.606	1.9072	0.003	997
Fatty acid	DOY	4	465.62	116.4	6.3659	0.001	998
	Site	8	288.91	36.114	1.975	0.033	999
	DOY × Site	29	1040	35.861	1.9612	0.006	998
Nucleic acid	DOY	4	1555.7	388.93	11.901	0.001	998
	Site	8	283.46	35.432	1.0842	0.384	997
	DOY × Site	29	1453.8	50.129	1.534	0.026	998
Nitrogen	DOY	4	1522.9	380.72	14.754	0.001	999
	Site	8	89.631	11.204	0.43417	0.92	998
	DOY × Site	29	1586.7	54.712	2.1202	0.002	998
TCA cycle	DOY	4	681.04	170.26	7.3928	0.001	999
	Site	8	171.98	21.497	0.93341	0.528	999
	DOY × Site	29	1095.5	37.775	1.6402	0.03	997

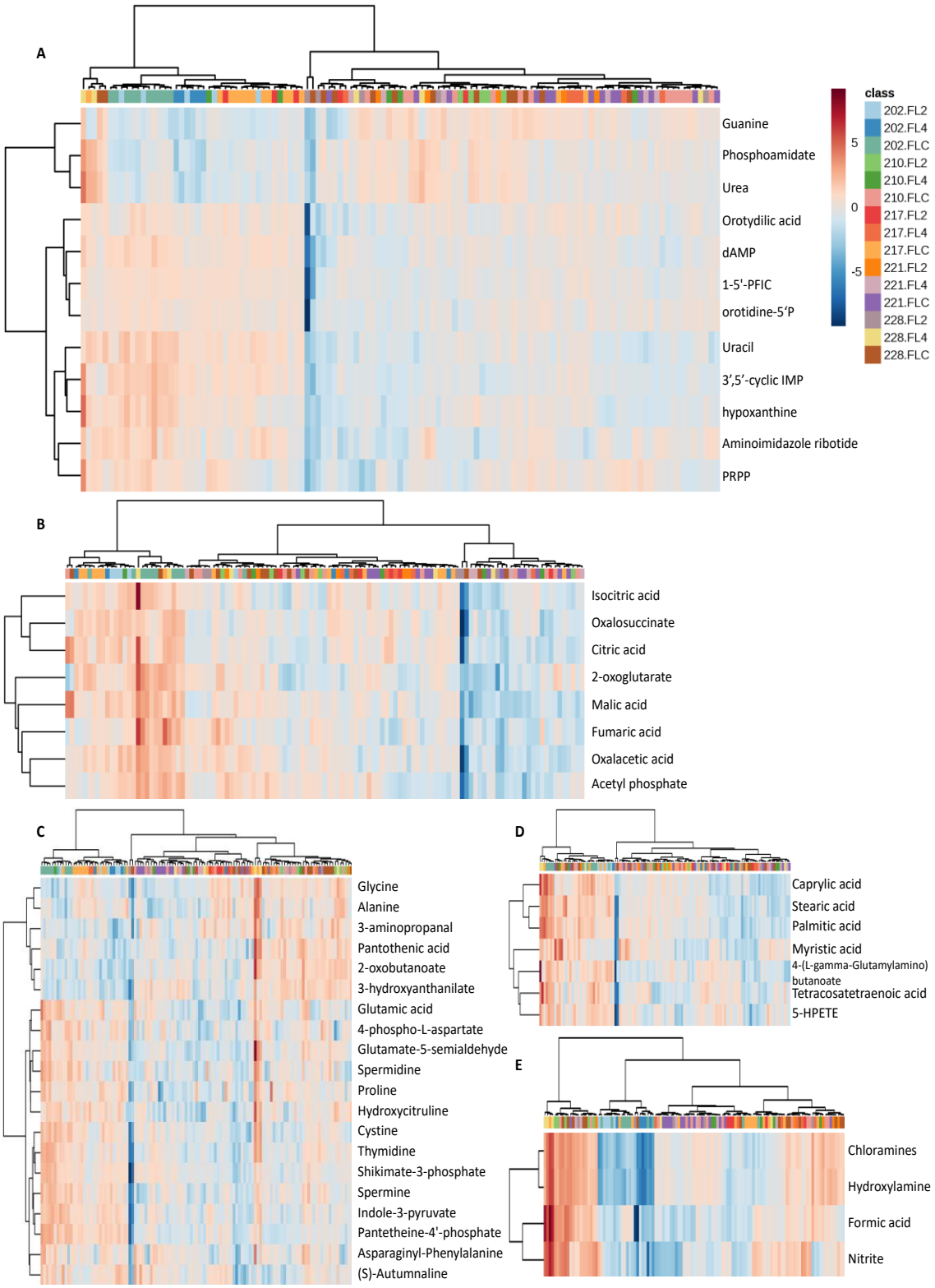

Figure 6. 12 Hierarchical cluster representation of the prominent pathways in Foxfonna valley cryoconite, showing DOY and site clustering and separation of metabolites aligned with (A) nucleic acid biosynthesis, (B) TCA cycle, (C) amino acid biosynthesis, (D) fatty acid biosynthesis and (E) nitrogen metabolism.

6.3.3.2. Integral metabolites influencing temporal and spatial dynamics

Separation and clustering patterns of major discriminatory variables using random forest classification revealed distinctive patterns for DOY 202, 217, 221 and 228. Further investigation into the metabolome on these days was necessary to unravel the main metabolites responsible for the observed effect.

The metabolite profile on DOY 202 consistently differentiated from other days during the sampling season. A very distinct profile was observed, separating the metabolites by site, however, there was no distinctive elevational effect, despite samples FLC4 and FLC8 being collected at similar elevations as FL2 and FL4, respectively. Samples from FLC exhibited high metabolite concentrations overall, FL2 intermediate concentrations and FL4 low concentrations. A metabolite with an exact mass of 94.9 units, silicic acid, was identified as the major variable of importance on DOY 202, using mean decrease accuracy when filtered by the random forest model.

Clustering patterns at DOY 217, 221 and 228 were less variable in the pathways, however, the mean decrease accuracy on each day identified the main discriminatory variables as metabolites with an exact mass of 561.54 units on DOY 217, 953.9 exact mass units on DOY 221 and 88.9 exact mass units on DOY 228. These correspond to the molecules rhodoxanthin, an unidentifiable molecule and oxalic acid respectively.

6.3.4. Co-occurrence network analysis

Network analysis of the valley glacier revealed a decline in the number of significant co-occurring members over time, using Spearman rank correlation (ρ >0.7, adjusted *P* <0.05). Positive correlations were abundant at DOY 202, revealing 37 nodes, with strong clustering of OTUs from the phylum *Firmicutes,* forming integral members of the community. Four independent clusters dominated by proteobacterial taxa also appear on DOY 202 (Figure 6. 13A). By DOY 210, the key community members formed a 19 node network with 3 distinguishable clusters of keystone taxa. *Cyanobacteria Phormidesmis*-33968 (D179) showed negative correlation to key member *Proteobacteria Rhizobiales*-19355 (D66), but was positively correlated to other associated key taxa *Saprospirales*-13192 (D13), *Pseudanabaenales*-17849 (D49) and *Sphingomonadales*-20155 (D72) (Figure 6. 13B). Key taxa were also present in the two independent clusters of *Firmicutes* and *Proteobacteria*, respectively. DOY 217 was made up of 17 nodes that showed associations between *Phormidesmis*-33968 (D179), *Nostocaceae*-32859 (D170) and *Saprospirales*-13192, but isolation of key member *Pseudanabaenales*-17849 and negative correlations between an *Actinobacteria* and *Proteobacteria* OTU (Figure 6. 13C). The correlations for DOY 221 (Figure 6. 13D) and 228 (Figure 6. 13E) revealed one prominent key member, *Saprospirales*-13192, present at low abundance in a network of 7 and 5 nodes, respectively. OTUs from the phyla *Firmicutes*, *Proteobacteria*, *Cyanobacteria* and *Bacteroidetes* were identified as integral components of valley glacier bacterial diversity, and despite low betweenness centrality values, may be key taxa in the cryoconite bacterial community (Table 6. 8).

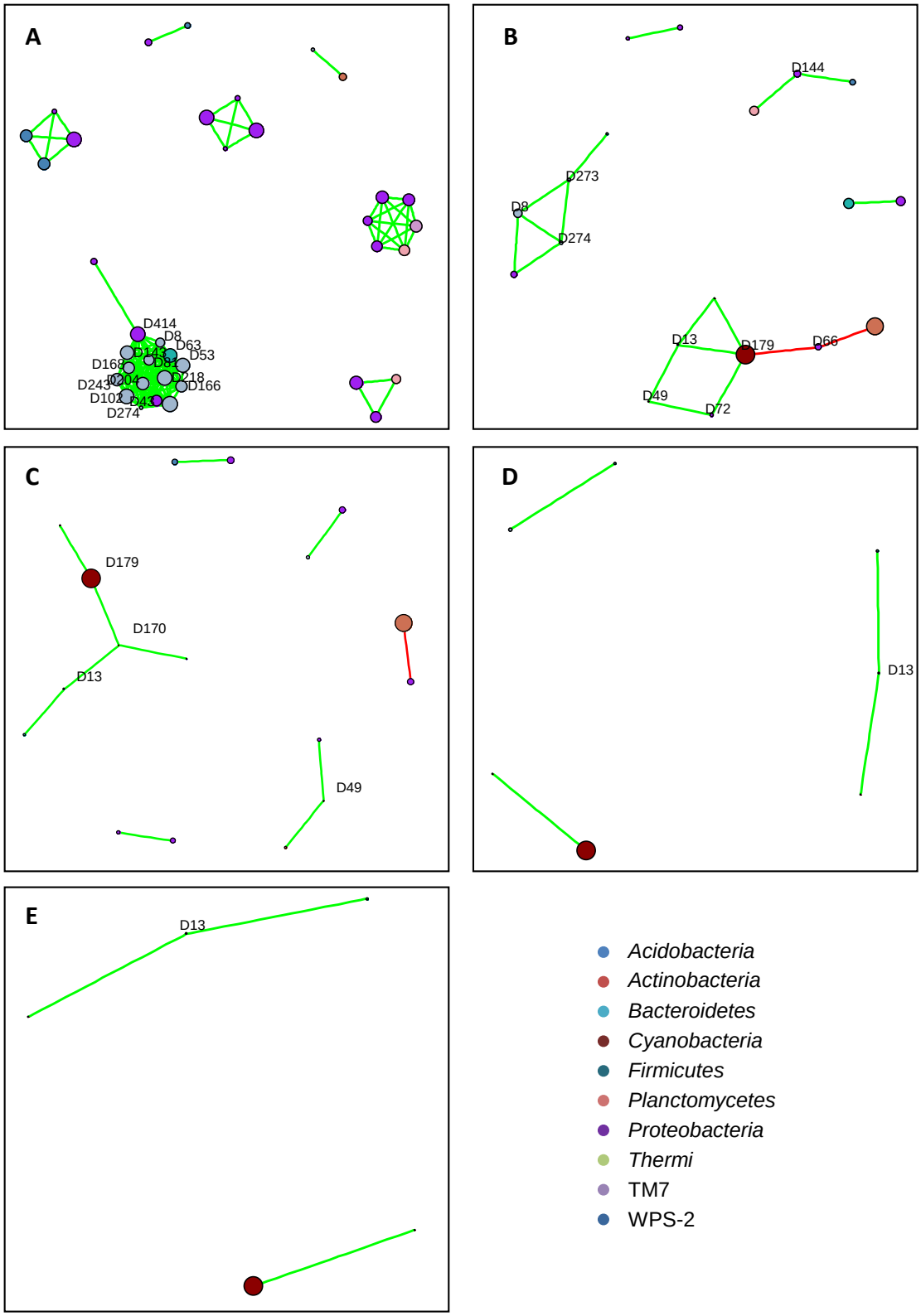

Figure 6. 13 Temporal co-occurrence network of valley glacier OTUs showing the change in community complexity on (A) DOY 202, (B) DOY 210, (C) DOY 217, (D) DOY 221, (E) DOY 228. Bottleneck taxa are labelled within each network plot. Green lines indicate positive correlation, red, negative correlation. Node size is relative to average relative abundance, while colour indicates OTU class.

Table 6. 8 Top-scoring keystone taxa from the Foxfonna valley glacier bacterial community identified per week, using the Greengenes database.

DOY	OTU	Node ID	BC	Phylum	Class	Order	Family	Genus
202	denovo-65782	D414	14	*Proteobacteria*	*Gammaproteobacteria*	*Pseudomonadales*	*Moraxellaceae*	*Acinetobacter*
210	denovo-33968	D179	9.5	*Cyanobacteria*	*Synechococcophycideae*	*Synechoccocales*	*Leptolyngbyaceae*	*Phormidesmis*
	denovo-19355	D66	5	*Proteobacteria*	*Alphaproteobacteria*	*Rhizobiales*	*Phyllobacteriaceae*	*Phyllobacterium*
	denovo-4660	D273	3	*Firmicutes*	*Bacilli*	*Bacillales*	*Planococcaceae*	-
	denovo-13192	D13	2.5	*Bacteroidetes*	*Saprospirae*	*Saprospirales*	*Chitinophagaceae*	-
	denovo-20155	D72	1.5	*Proteobacteria*	*Alphaproteobacteria*	*Sphingomonadales*	*Sphingomonadaceae*	-
	denovo-12072	D8	1	*Firmicutes*	*Clostridia*	*Clostridiales*	*Lachnospiraceae*	*Butyrivibrio*
	denovo-47295	D274	1	*Firmicutes*	*Clostridia*	*Clostridiales*	*Ruminococcaceae*	-
	denovo-29496	D144	1	*Proteobacteria*	*Alphaproteobacteria*	*Rhodospirillales*	*Rhodospirillaceae*	-
217	denovo-32859	D170	8	*Cyanobacteria*	*Nostocophycideae*	*Nostocales*	*Nostocaceae*	*Nostoc*
	denovo-33968	D179	4	*Cyanobacteria*	*Synechococcophycideae*	*Synechoccocales*	*Leptolyngbyaceae*	*Phormidesmis*
	denovo-13192	D13	4	*Bacteroidetes*	*Saprospirae*	*Saprospirales*	*Chitinophagaceae*	-
	denovo-17849	D49	1	*Cyanobacteria*	*Synechococcophycideae*	*Synechoccocales*	*Leptolyngbyaceae*	*Phormidesmis*
221	denovo-13192	D13	1	*Bacteroidetes*	*Saprospirae*	*Saprospirales*	*Chitinophagaceae*	-
228	denovo-13192	D13	1	*Bacteroidetes*	*Saprospirae*	*Saprospirales*	*Chitinophagaceae*	-

A similar network constituting bacterial taxa, metabolites and environmental parameters revealed an increasingly large network of metabolite nodes with positive and negative co-occurring members (Figure 6. 14). Environmental variables connected with physical geography displayed positive correlations between FAA and Eastings, FAA and aspect, slope and elevation, elevation and aspect, but were disconnected from biotic and metabolic variables in a tightly clustered group for DOY 202, 217, 221 and 228. Furthermore, incident radiation (weekly and seasonal) and Northings featured prominently and were well correlated with the main metabolite cluster for DOY 210 and 217. Network structure for each sampling day revealed limited clustering of metabolites at DOY 202 and strong, similar clustering at DOY 210 and 217. Good association of key metabolites that contributed to a potential bottleneck effect in the metabolome profile (Table 6. 9) with all significantly associated (but non-keystone) taxa was observed on DOY 210 and *Actinobacteria*-15849 (D33), *Cyanobacteria*-17869 (D50), *Actinobacteria*-27497 (D132) and *Proteobacteria*-20155 (D72) on DOY 217 in the main metabolite cluster. DOY 221 shows two large sub-clusters that connect via metabolite M360 (m/z 394.27) with negative correlation and the dissociation of all OTUs from the metabolites. At DOY 228, four sub-clusters are evident, with the largest consisting of key metabolites, and a smaller sub-cluster associating *Phormidesmis*-17869 (D50) with two unidentified metabolites of exact mass 1 597.63 (M2618) and 1 597.27 (M2617), the latter of which was connected to *Actinomycetales*-15849 (D33), that in turn connected to *Phyllobacterium*-19355 (D66).

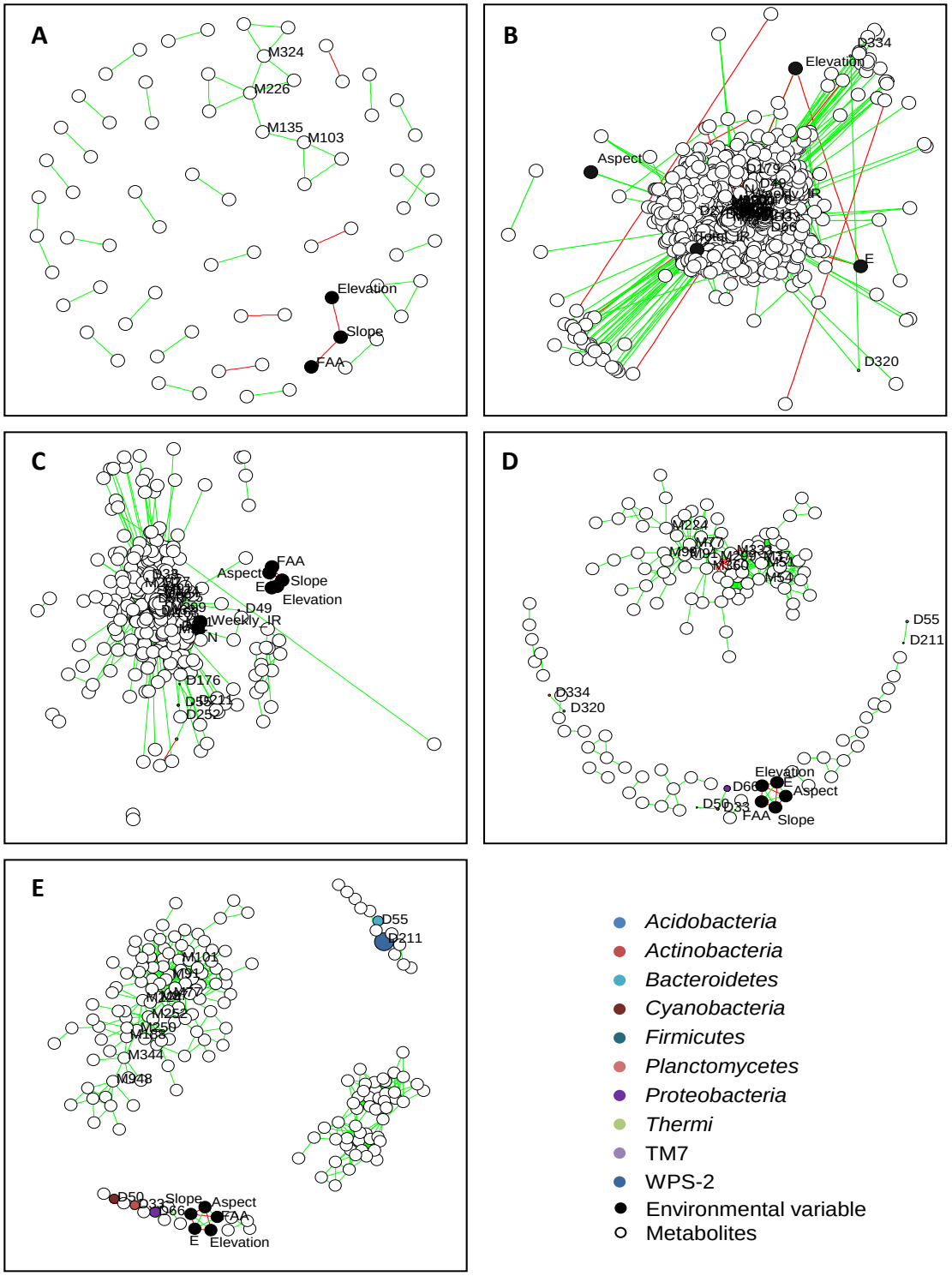

Figure 6. 14 Co-occurrence network of the significant pairwise Spearman correlations of OTUs (D), environmental variables and metabolites (M) in Foxfonna valley glacier cryoconite for DOY (A) 202, (B) 210, (C) 217, (D) 221 and (E) 228. (Green - positive correlation, red - negative correlation). Size of OTU node is relative to average relative abundance, while colour indicates OTU class. Size of metabolite (white) and environmental parameter (black) nodes are not indicative of abundance.

Table 6. 9 Top-scoring key metabolites identified by highest ten betweenness centrality (BC) from DOY 202 to DOY 228.

Node ID	Metabolite ID	Tentative ID	BC
M81	282.27	Oleic acid	1793.011
M52	107.9	2-hydroxyaniline	1740.596
M54	121.9	Nicotinic acid	1246.171
M123	378.27	Sphingosine-1-phosphate	1198.491
M80	254.27	Shikimate-3-phosphate	1018.238
M122	280.27	Linoleic acid	935.3301
M156	816.81	-	815.6667
M56	131.9	Oxalacetic acid	674.8579
M118	218	O-Succinyl-L-homoserine	480.5016
M74	117.9	L-Homoserine	448.0145

6.4. DISCUSSION

Valley glaciers have a physical geography that encourages numerous external factors to affect the microbial communities, a contrast to dome and ice sheet habitats. Gradient and elevation differences generate up-valley modifications in the form of changing light-dependant processes and hydrological flow, as well as autochthonous input from the surrounding sides and glacier terminus. Prior studies on the structure and diversity of the microbial community in Foxfonna valley glacier cryoconite have provided details on the diverse bacterial structure and high total carbon and nitrogen ratios in Svalbard cryoconite (Cameron *et al.*, 2012). However, investigations have been limited to once-off sampling of one or two communities as sites were not revisited. As such, temporal and spatial changes of the intrinsic communities, as well as indications of the potential function of the ecology in this niche, have been unestablished until now.

In this chapter, cryoconite communities extracted from 16S rRNA gene sequences were observed over different months within the same ablation season. Key members of the community were observed at each sampling day and demonstrated that cyanobacterial dominance in cryoconite is preceded by an abundance of *Proteobacteria* and *Firmicutes* and proceeded by the appearance of *Bacteroidetes* of the class *Chitinophagaceae*. However, these taxa were not identified as bottleneck taxa in metabolite co-occurrence networks, implying a minimal role in maintaining the metabolic profile of the cryoconite habitat. Positive association of metabolites and taxa were only observed later in the sampling season, however, these did not correlate with identifiable metabolites or previously high relative abundance taxa, apart from the core taxa *Sphingomonadaceae*-20155 (*Sphingopyxis*) at DOY 217. Core and pan genome analysis of the *Sphingopyxis* genus identified high representation of lipid transport and metabolism protein orthologues (Garcia-Romero *et al.*, 2016) consistent with their oligotrophic lifestyle. *Phyllobacterium*-19355 was similarly abundant at DOY 228; this microbe likely plays a role in nitrogen fixation, as these taxa have showed similar function in root nodules (Jiao *et al.*, 2015).

6.4.1. Foxfonna valley glacier cryoconite bacterial communities are sensitive to temporal changes

In this study of the structure, diversity and potential function of Foxfonna valley glacier cryoconite, it is evident that both time and space are integral to the restructuring of the bacterial community and metabolite profile during summer months. The changing relative abundance of the dominant *Alphaproteobacteria*

phyla and keystone *Gammaproteobacteria* taxon was indicative of seasonal variation from July to August. This is consistent with the effects of total and weekly incident radiation at each site, that significantly affects the concentration of photosynthetic products and microbes during late August. Consequently, it is not surprising that this environmental change selects for the bottleneck taxa *Cyanobacteria* during mid peak summer. However, this gradual increase in concentration is outweighed by the conspicuous representation of extracellular polymeric substances (EPS) and chlorophyll *a*, during the early period of sampling in July. This is indicative of a noteworthy surge in photosynthetic activity after the polar night, nourishing the oligotrophic community, that in turn exhausted cryoconite nutrients.

Similar effects have been reported in planktonic blooms in Kongsfjorden, Spitsbergen (van De Poll *et al.*, 2016). As a marine habitat, this is not directly comparable to a glacier, however, it provides a plausible explanation for the unexpectedly high concentrations of EPS and chlorophyll, and concomitant low photosynthetic cyanobacterial biomass on the valley glacier that is yet unobserved in Svalbard glaciers, soil and permafrost communities (Schostag *et al.*, 2015). It is worth mentioning that prolific algal blooms, biofilms and dirty ice were prevalent on the sampled transect from DOY 188 in the weeks prior to the indicated sampling season (Irvine-Fynn, 2017a), providing a potential explanation for the higher EPS and chlorophyll *a* concentrations, particularly as community turnover is rapid upon initiation of the melt season (Musilova *et al.*, 2015).

The combined action of EPS with the photosynthetic roles of the microphytes in cryoconite at DOY 202, created a physically stable, self-sufficient microenvironment of nutrients, capable of supporting microbiota in Foxfonna valley glacier cryoconite during the peak of summer. This is analogous to observations made by Langford *et al.* (2014) along the Midtre Lovenbreen glacier that identified increased EPS concentrations at high elevations, that is essential for cryoprotection and nutrient assimilation, and high chlorophyll *a* content at the glacier terminus and valley sides, suggesting allochthonous input, reduced physical disturbance and pigment accumulation (Langford *et al.*, 2014). Yoshimura *et al.* (1997) showed the contribution of ancient algal sources in stratified ice of Himalayan glaciers was typical of seasonal differences with altitudinal effects, leading to higher observance of red snow containing *Chlamydomonas nivalis* at lower gradients. This could also explain the higher observed concentrations of EPS and chlorophyll pigments. As communities had recently thawed from the increased summer temperatures, these pigment and polymeric compounds are potentially integral to maintaining microbial community viability, as their main function in extreme habitats is protection against salinity, freeze-thaw and shear stress, analogous to most marine bacteria (de Carvalho and Fernandes, 2010).

Environmental effects were determined to be insignificant contributors to community structure, early in the ablation season. Consequently, microbial taxa emerged as the main drivers of the bacterial community, identifying core taxa from the class *Alphaproteobacteria* as integral bottleneck taxa. It is interesting to note the

lack of *Cyanobacteria* in 16S rRNA gene sequences at this time point, particularly as Langford *et al.* (2014) has linked excesses in chlorophyll *a*:EPS production with filamentous cyanobacterial proliferation. However, these observations can potentially be explained by the legacy effect of snow algae and diatoms prevalent during early summer.

Foxfonna valley glacier is dependent upon the keystone *Gammaproteobacteria*, *Acinetobacter*-65782. *Acinetobacter* has been observed in saline water conditions, where it is a recognised contributor of polysaccharides (Tkavc *et al.*, 2011). As such, it may aid in the maintenance of the cryoconite granule as EPS concentrations decrease to create a more aerobic habitat for the cryoconite biosphere. During mid and late summer, a more consistent trend is observed, as the concentrations of both EPS and chlorophyll *a* associate well with *Cyanobacteria* relative abundances after DOY 202. Accordingly, a thinning effect of the adhesive properties of the granular matrix is observed, enhancing cryoconite phototaxis (Cook *et al.*, 2016a) and phototrophy during high incident radiation periods. This is supported by distance-based modelling at DOY 221 and 217 (APPENDIX IV, Table IV. 12 and Table IV. 14), as well as a significant indication of temporal influence on nucleic acid, nitrogen metabolism and tricarboxylic acid metabolites (Table 6. 7). Furthermore, lower concentrations of fatty acid and lipid content in the cryoconite metabolome, continues to support the hypothesis of EPS thinning. This is in addition to indicating chemical modifications in lipid content of the microbial community that is still inherently active, inferred from the high TCA and amino acid concentrations. At this

point in the sampling season, the cyanobacterial taxa, identified as *Phormidesmis* and *Nostoc,* have established as bottleneck taxa and are potentially responsible for engineering the summer community for optimal function, as well as playing a role in primary production, consistent with Foxfonna ice cap in the summer (Chapters 4 and 5).

It is interesting to note that the nucleic acid turnover, and thus cellular reproduction, is moderate at DOY 217, implying that the prevalent community is responsible for the heterotrophic lifestyle that characterises cryoconite communities (Mueller *et al.*, 2001; Hodson *et al.*, 2010b). However, the peaks in nucleic acid biosynthesis and metabolism, early and late in the sampling season, are indicative of points of rapid growth in the cryoconite community, potentially as a result of higher nutrient availability from allochthonous sources, microbial processing or washout from surrounding snow as a consequence of increased surface melt. While evidence of meltwater effects was observed on the valley glacier, the lack of stream channels at the elevations and sites investigated, indicate negligible hydrological influence, however, it may discretely deliver water and inorganic nutrients to the lower elevation communities.

6.4.2. Spatial effects on community structure are related to distance decay

The hypothesis that elevation can potentially influence the microbial communities is inferred from similar previous studies on elevational gradients. These reveal lower elevations have higher diversity as a consequence of higher nutrient introduction

from the surrounding environment, aeolian deposition, washout and consequent down-valley inoculation (Wilhelm *et al.*, 2013; Franzetti *et al.*, 2017). In contrast, studies of elevational gradients in High Arctic snow in the same region, have shown little variation with increased elevation (Hell *et al.*, 2013). Foxfonna distinguishes itself with a limited elevational influence by environmental parameters, a significant high influence by the bacterial taxa, indicative of species sorting over time, as revealed by Spearman Rho coefficient of all 13 observed phyla, amino acid metabolism and fatty acid biosynthesis pathways, as well as metabolome and bacterial co-occurrence networks (Figure 6. 13 and Figure 6. 14).

When compared to Foxfonna ice cap, that lies above the valley glacier, a stark contrast is evident in the bacterial community structure, as there is a greater overall biogeographical dispersal effect on the valley glacier. It was therefore expected that much of this distance decay effect was orchestrated by elevation, with the difference in species composition between sites confirmed by PERMANOVA (Table 6. 6). There is a strong temporal effect when observing the individual sampling days. Bacterial decay for elevation and distance were significant at two points (DOY 210 and 217) and above average for one (DOY 210), implying a combination of both elevation and distance were responsible for a decrease in bacterial diversity on the glacier over time. However, distance has a greater effect on community similarity than elevation (Figure 6. 6). Fatty acids and amino acid metabolites were the only pathways that appeared significantly affected by elevation and DOY, where transect samples had a stronger temporal influence than those at high and low elevation.

6.4.3. Metabolism indicates high microbial activity is driven by an alternate non-bacterial community

High rates of microbial abundance were observed on the valley glacier. Close association of the microbial community on valley glacier cryoconite facilitates diverse metabolic processes, biogeochemical cycling and niche differentiation, affording improved microbial growth and survival (Paerl *et al.*, 2000). Consequently, high concentrations of nucleic acid, fatty acid and amino acid biosynthesis intermediates and products are expected. However, co-occurrence network analysis confirms that the prokaryotic component of the cryoconite community does not directly influence the observed patterns.

Previous studies of bacterial production have revealed that less than 10% of the respiration in cryoconite holes are representative of the heterotrophic cryoconite bacteria, implying considerable top-down control on their abundance by an alternative source (Sawstrom *et al.*, 2002; Anesio *et al.*, 2010). The bacterial community is nonetheless actively contributing to oligotrophy in the cryoconite habitat of the valley glacier, with some association of activity between cyanobacterial taxa of the *Nostoc* and *Phormidesmis* genera (Figure 6. 9) during late July, when there is metabolic evidence of high microbial activity and cellular proliferation. The metabolites detected from nitrogen metabolism pathways (nitrite and chloramine, an ammonia derivative) highlight nitrification processes on the glacier during mid to late summer. The fluctuation of amino acids relates well with that of nitrogen

metabolism, inferring the community utilises labile amino acids to supplement organic N during periods of low nitrification (Fierer *et al.*, 2012).

Based on the dominant metabolites silicic acid and rhodoxanthin, and the elimination of bacteria and environmental roles in the valley glacier metabolome by distance-based redundancy analysis and PLS regression, it can be inferred that alternative microbiota such as photosynthesising microalgae and diatoms may play an integral role in driving the observed summer cryoconite metabolome. This excludes the cyanobacterial taxon *Phormidesmis priestleyi*-33968, that remains a prominent driver of the community during the mid summer, based on keystoneness, and *Microbacteriaceae*-62735, based on 16S rRNA gene region relative abundance. Observations of algae on the Foxfonna valley glacier transect and diatoms in *ex situ* microcosm investigations indicate that these organisms may be more reliable sources of organic carbon to bacterial communities than the underperforming cyanobacterial strains, under very low light conditions (Cook, 2017). This is supported by cyanobacterial absence in 16S rRNA gene sequences during the transition from winter to summer, corresponding well with low concurrent EPS concentration.

6.5. SUMMARY

Cryoconite originating from the Foxfonna valley glacier is comprised of a bacterial community dominated by *Alphaproteobacteria* taxon, *Phyllobacterium*, during mid summer and *Cyanobacteria* taxon, *Phormidesmis*, during later summer. This is evidence for a prominent species selection strategy, based on 16S rRNA gene

analysis. Temporal analysis reveals that the community is dependent upon the rate of melt experienced during the summer ablation period and incident radiation into the system. Elevation appears to influence the community structure, albeit to a lesser extent than the core community. Thus both local and regional effects sustain the cryoconite community in valley glacier habitats (Lindstrom and Langenheder, 2012). Metabolic analysis demonstrates the prominent role of pathways linked with heterotrophic and phototrophic microbiota, with evidence of non-bacterial taxa, potentially diatoms and algae that are widely recognised on the ice surface (Guedes *et al.*, 2011; Lutz *et al.*, 2016; Cook, 2017), playing a greater role in the metabolome when observed in co-occurrence networks. This implies strong control by these microbes on the bacterial diversity of Foxfonna valley cryoconite.

CHAPTER 7 – SEASONAL DYNAMICS AND ACTIVITY OF SUPRAGLACIAL BACTERIAL COMMUNITIES ON THE GREENLAND ICE SHEET

This chapter has been prepared for publication in the International Society for Microbial Ecology Journal by the author:

Gokul, J. K., Cameron, K. A., Hegarty, M., Irvine-Fynn, T. D. L., Cook, J. M., Mur, L. A. J. and Edwards, A. 2012. A twist in the tail: metabolically active rare taxa underpin bacterial dynamics in Greenland's Dark Region.

Study conceived by A.E., J.K.G. and J.M.C. Fieldwork conducted by A.E. and K.A.C. Laboratory work conducted by J.K.G. and M.H. Data analysis conducted by J.K.G., T.I.F. and A.E. Manuscript written by J.K.G, T.I.F., J.M.C., L.A.J.M. and A.E.

Section 7.3.3.1 was published in Environmental Microbiology by the author - APPENDIX VI:

Cook, J. M., Edwards, A., Bulling, M., Mur, L. A. J., Cook, S., Gokul, J. K., Cameron, K. A., Sweet, M. and Irvine-Fynn, T. D. L. 2016. Metabolome-mediated biocryomorphic evolution promotes carbon fixation in Greenlandic cryoconite holes. *Environmental Microbiology*.

7.1. INTRODUCTION

The surface of the Greenland Ice Sheet is a biologically active locale that supports a large variety of microbially diverse taxa in snow, meltwaters and sediment debris. Cryoconite and its hydrologically linked habitats are colonised by microbial communities with high diversity in the autochthonous bacteria, lending a stable community composition, even under melt conditions (Musilova *et al.*, 2015). Majority of the microbial activity and biogeochemical cycling on ice sheets is the responsibility of debris-living microbes, however, studies into the seasonal effects of ice surface

characteristics reveal an influence by melt rate and mass balance, in addition to cryoconite hole coverage, its relation to surface albedo and biological activity (Chandler *et al.*, 2015). This is supported by the work in previous chapters, highlighting the effect of melt season duration, area of ablation and incident radiation. Furthermore, these environmental parameters drive the taxon-taxon interactions that shape microbial communities in cryoconite habitats.

In contrast, stream and snow habitats created by seasonal melt, are more susceptible to immediate changes in their community structure and function because of the decreased mechanical stability offered by ice surfaces, due to seasonal glacial melt, runoff and wind perturbation. These communities are characterised by a diverse range of prokaryotic, eukaryotic and viral taxa, are spatially variable across the continent and are considerably influenced by biogeographical and biogeochemical conditions of dominant members on a local (Cameron *et al.*, 2016) and global scale (Edwards *et al.*, 2013c; Hell *et al.*, 2013; Chong *et al.*, 2015). However, investigations into the seasonal effects have not yet revealed the roles of key heterotrophic and photosynthetic bacteria that have been observed on the Greenland Ice Sheet and other High Arctic surface habitats.

Rare taxa (Sogin *et al.*, 2006), defined as those taxa that contribute to less than 1% relative abundance in a community, are predominant in a wide range of diverse ecosystems and contribute largely to the biomass and dynamics of the environment, despite their low abundances (Wilhelm *et al.*, 2014). Low rates of biological processes

in the supraglacial bacterial community may point towards a small component of the community contributing to the total biological activity. The rare biosphere, while sparse in nature, exhibits both temporal and spatial changes brought about by responses to environmental change and geographic location, resulting in the emergence of new dominant populations. These taxa are thought to play an integral role in complex and simple habitats, providing an extensive seed bank of genomic innovation (Sogin *et al.*, 2006). High throughput sequencing has enabled the detection and characterisation of those taxa that may contribute to as yet unexplained population dynamics, dispersion, predation and continued persistence (Lynch and Neufeld, 2015). Recent investigations into the metabolically active taxa revealed that rare taxa are disproportionately active relative to abundant taxa and may be involved in the cycling of organic compounds. Specifically, detection of rare taxa is directly proportional to the degree of random sampling including 'phantom taxa' that are present in cDNA but absent from rRNA genes (Klein *et al.*, 2016).

There are many studies focussing on comparative cDNA and rRNA research in maritime habitats on bacteria (Campbell *et al.*, 2011; Gaidos *et al.*, 2011; Aanderud *et al.*, 2015) and archaea (Wemheuer *et al.*, 2012), but fewer investigations on atmospheric (Klein *et al.*, 2016) and glacial habitats (Wilhelm *et al.*, 2014; Schostag *et al.*, 2015; Cameron *et al.*, 2016). This limits the true understanding of community dynamics as taxa can escape inclusion in small clone libraries (Sogin *et al.*, 2006) and rRNA gene data alone underestimates the functional role of rare microbiota in a community. The previous chapters have established an abundance of literature on

the structure and composition of ice sheet sediment, snow and ice communities. However, there is limited work linking the influence of adjacent microhabitats to determine the integrated temporal effect on microbial population activity and how these communities affect glacial melt. As the surface habitats of the Greenland Ice Sheet are characterised by a heterogenous combination of heterotrophic and autotrophic microbiota (Cook *et al.*, 2015b; Cook, 2016; Musilova *et al.*, 2017), they readily contribute to the active carbon accumulation on the glacial surface (Anesio *et al.*, 2009; Cook *et al.*, 2016a). This chapter aimed to determine the biotic drivers of the active summer bacterial community in cryoconite, snow and ephemeral stream environments on a localised area of the Greenland Ice Sheet. Understanding the precise role of the bacterial community is integral to untangling this contribution, particularly as current patterns of glacial melt and retreat create devastating global repercussions. By measuring the ratio of 16S rRNA gene and cDNA from 16S rRNA abundances, which are interpreted as markers of biomass and protein synthesis potential (Blazewicz *et al.*, 2013), at different time points in a single ablation season, the following hypotheses could be tested:

1. Supraglacial microhabitats have unique and distinct bacterial composition, as a consequence of differing hydrological and sediment habitats,
2. Temporal variations overshadow spatial effects, whereby potentially active bacteria exhibit responses to seasonal fluctuations,
3. The rare biosphere drives the observed dynamic bacterial community changes over time.

7.2. EXPERIMENTAL METHODS

7.2.1. Site description and sample collection

The automatic weather station (AWS) S6 on the Kangerlussuaq transect (K-transect) is located on Russell Glacier at 67° 05' N, 49° 23' W, 1 020 m a.s.l., in the south west of Greenland (Figure 7. 1). This region is characterised by high ablation and low accumulation during summer months (June - August). K-transect S6 is 1 of 18 AWS equipped to sample air temperature (°C), wind speed ($m.s^{-1}$), wind direction (°), humidity (%), pressure, surface radiation balance in visible (short wave radiation) and infrared (long wave radiation) wavelengths, sensible and latent heat fluxes. Environmental conditions that were observed at S6 in 2014 were recorded using the automated weather station. Hourly average data are transmitted via satellite link. This was sourced for the calculation of albedo, energy input and output, melt rate potential, turbulent heat fluxes driven by temperature and moisture gradients between the air and the ice surface, positive degree days and positive degree hours on the S6 weather station terrain surface, as the conditions extant in the 2015 season was analogous to that of 2014. Recorded data was represented graphically in Matlab R2012 and further edited in Adobe Illustrator CS3.

Samples were collected aseptically from the area around the S6 AWS by Dr. Arwyn Edwards and Dr Karen Cameron. Over the course of 7 weeks, three samples were collected once a week from cryoconite holes, adjacent snow and adjacent stream sites, providing a total of 21 samples of cryoconite sediment, 20 samples of snow and 21 samples of stream water. All samples were stored and transported for processing as described in Chapter 2, sections 2.2.1 and 2.2.2, respectively.

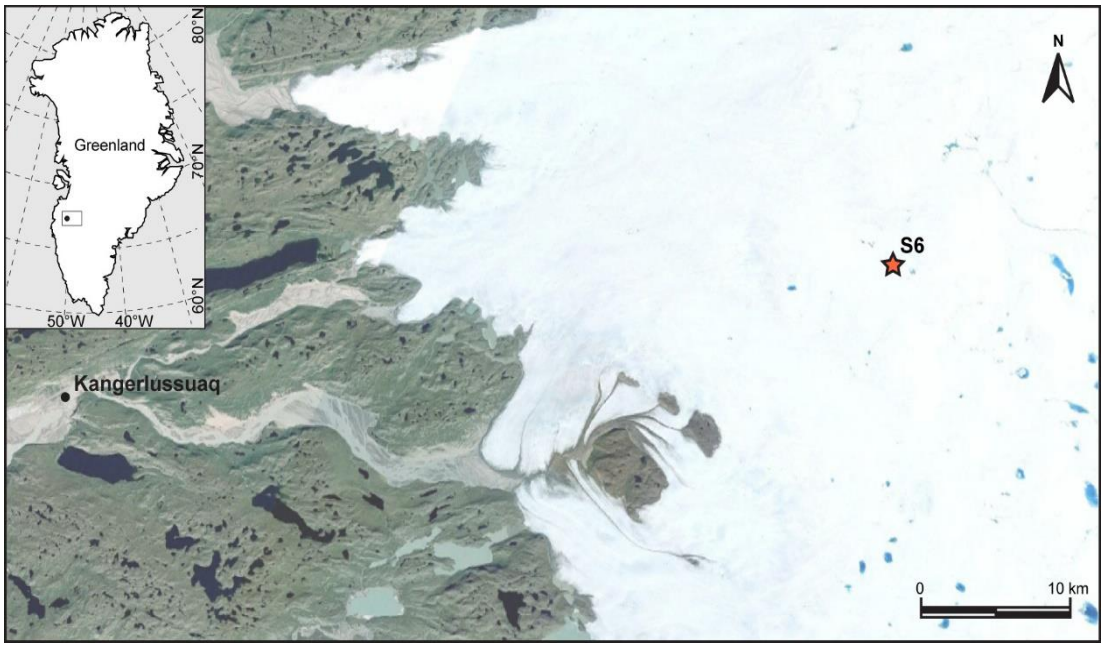

Figure 7. 1 Aerial view of the Kangerlussuaq transect, indicating the location of the sampling site, automatic weather station S6 on the western side of the Greenland Ice Sheet. Image credit: Dr. Tristram Irvine-Fynn.

7.2.2. Nucleic acid extraction and processing

Total nucleic acids were extracted from all cryoconite and glacial water samples using the PowerBiofilm™ RNA Isolation kit (MO BIO Laboratories Inc.) and PowerWater® Sterivex™ Isolation kit, as described in Chapter 2, section 2.4.2.1 and section 2.4.2.2. Aliquots of all samples were divided for DNA amplification and treatment with DNase for downstream synthesis of 16S rRNA gene region cDNA (Chapter 2, section 2.4.2.3).

PCR amplification of the 16S rRNA gene and 16S cDNA was performed as previously described in Chapter 2, section 2.5, before 16S region library generation (Chapter 2, section 2.6.3) for Illumina MiSeq 16S sequencing (Chapter 2, section 2.6.4) and bioinformatic and statistical analyses (Chapter 2, section 2.7). Sequences are available for viewing at EBI-SRA SRP073390: PRJNA318626. Potential keystone OTUs were identified using significant statistical correlations from community network structure using the R package, iGraph (Chapter 2, section 2.8).

7.2.3. Local and regional analysis of cryoconite community diversity

The genetic diversity of cryoconite holes and ice cores from 14 sites on the Greenland Ice Sheet (Figure 7. 2) from Cameron *et al.* (2016) (Accession ID PRJEB10526) was bioinformatically evaluated concurrently with S6 sequence data in QIIME 1.9.0 (Chapter 2, section 2.7). USEARCH6.1 chimera detection was used prior to OTU selection, as the magnitude of sequences processed as part of this dataset required the use of an alternate chimera detection platform in QIIME. Cryoconite sequences from Thule (THU), Qaqortoq (QAS), Kangerlussuaq (KAN-P), Tasiilaq (TAS) and Illulisat (DS) were extracted and compared to AWS S6 by distance-based modelling, to determine biogeographical effects on the cryoconite community at local and regional scales.

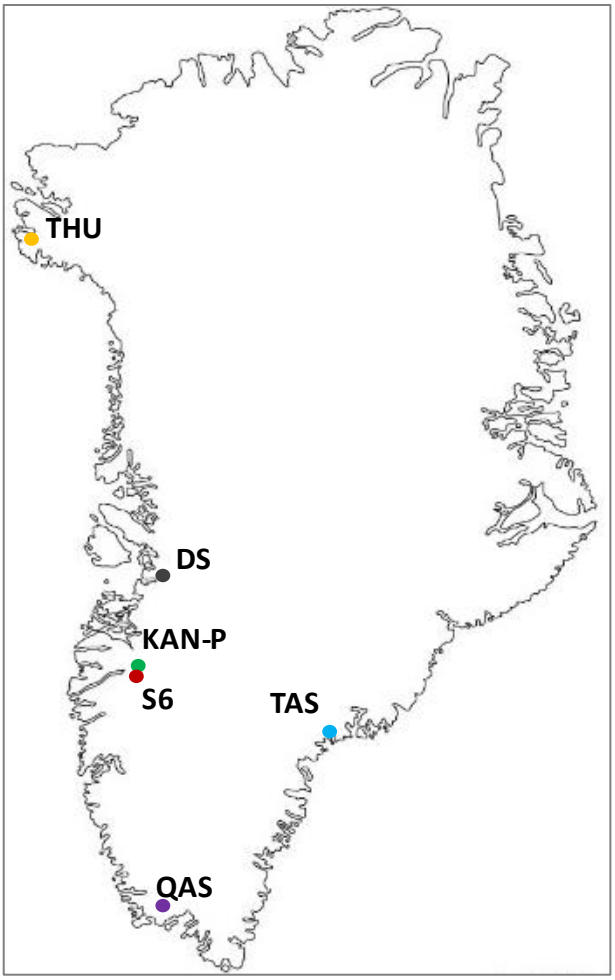

Figure 7. 2 Greenland map detailing sites Thule (THU), Illulisat (DS), Kangerlussuaq (KAN-P), AWS (S6), Tasiilaq (TAS) and Qaqortoq (QAS) adapted from Cameron *et al.* (2016).

7.3. RESULTS

Sequences were obtained for 124 samples for the combined 16S rRNA gene and 16S cDNA libraries from AWS S6. A total number of 2 673 556 reads were obtained after sequence processing, with a maximum of 130 001.0 reads (GrIScDNAcryo6.3), a minimum of 5 reads (GrISstream3.1) and a mean of 21 560.9 reads. The 126 16S rRNA gene and 16S cDNA cryoconite and ice core sequences from Cameron *et al.* (2016) concurrently analysed with the AWS S6 sequences, yielded 4 065 014 reads. Sequences were rarefied to 943 sequences per sample, resulting in the exclusion of

1 cryoconite 16S rRNA gene sample, 2 stream 16S rRNA gene samples, 3 cryoconite 16S cDNA samples, 3 snow 16S cDNA samples and 6 stream 16S cDNA samples from AWS S6 downstream analysis, in addition to 4 regional samples (DS.1.cDNA, DS.2.cDNA, TAS.U.A2b.cDNA, THU.L.1.cDNA).

The proceeding analysis details the AWS S6 bacterial community. Data clustered into 566 OTUs, allowing successful taxonomic assignment of 99.38% of OTUs cumulatively for S6 cryoconite, snow and stream water habitats at the phylum level, using the Greengenes 13_8 database. Approximately 13.59% of 16S rRNA gene OTUs and 14.40% 16S cDNA OTUs were shared between all three habitats. To remedy risk of potential reagent and laboratory contamination, controls of PCR amplified ultrapure water with no template were sequenced (Salter *et al.*, 2014). As these samples were automatically eliminated during rarefaction, independent analysis of unfiltered data was necessary, revealing 10 taxa from the phyla *Actinobacteria* (*Acidimicrobiales*), *Alphaproteobacteria* (*Sphingomonadaceae*¸ *Sphingomonas*, *Methylobacterium*), *Betaproteobacteria* (*Comamonadaceae*), *Bacteroidetes* (*Sphingobacteriaceae*, *Hymenobacter*, *Saprospiraceae*), *Chloroflexi* (*Thermogemmatisporaceae*) and WPS-2 that were absent from PCR controls but present at more than 0.01% relative abundance in the combined samples, suggesting they were introduced at the DNA extraction stage. Additionally, top-scoring taxa with >3 reads in negative controls were identified as *Salinibacterium, Microbacteriaceae*, *Streptophyta*, *Leptolyngbya*, *Kocuria* and *Sphingomonadaceae* (Table 7. 1).

Table 7. 1 Top-scoring potential contaminants identified from PCR control sequences.

OTU	Greengenes ID	No of reads in NTC	BLAST ID	Accession ID	%ID
denovo-87257	g_*Salinibacterium*	16	*Leifsonia* sp. URHE0078	LN876553.1	99
denovo-114112	f_*Microbacteriaceae*	12	*Salinibacterium amurskyense* IC A9	KU925169.1	98
denovo-125684	o_*Streptophyta*	11	*Roya obtusa*	KU646496.1	97
denovo-90892	g_*Leptolyngbya*	7	*Phormidesmis priestleyi* ANT.L66.1	AY493581.1	99
denovo-96273	g_*Kocuria*	4	*Kocuria subflava*	NR_144586.1	99
denovo-67624	f_*Sphingomonadaceae*	4	*Polymorphobacter* sp. Ap23E	KX990242.1	99
denovo-106624	f_*Microbacteriaceae*	3	*Salinibacterium amurskyense* IC A9	KU925169.1	98

7.3.1. Localised and regional distance decay effects

PRIMER 6 analysis of the transformed Bray-Curtis matrix of S6 sequence data revealed separation of 16S rRNA genes and 16S cDNA OTUs for each AWS S6 habitat, when viewed using principal co-ordinates analysis (Figure 7. 3). Cryoconite OTUs were spatially closer to each other, while snow and stream OTUs spanned a larger distance, with clear separation between 16S rRNA genes and 16S cDNA OTUs. Cryoconite 16S cDNA OTUs and stream 16S rRNA gene OTUs each formed separate tight clusters compared to snow 16S rRNA gene and 16S cDNA OTUs that sparsely clustered, while stream 16S cDNA OTUs displayed clear separation from other sites and a loose clustering pattern. This is supported by pairwise permutational analysis of variance (PERMANOVA) of nucleic acid and habitat, which revealed significant differences between cryoconite DNA and cDNA (t = 3.9087, P = 0.001), snow DNA and cDNA (t = 3.5971, P = 0.001) and stream DNA and cDNA (t = 4.4415, P = 0.001) communities.

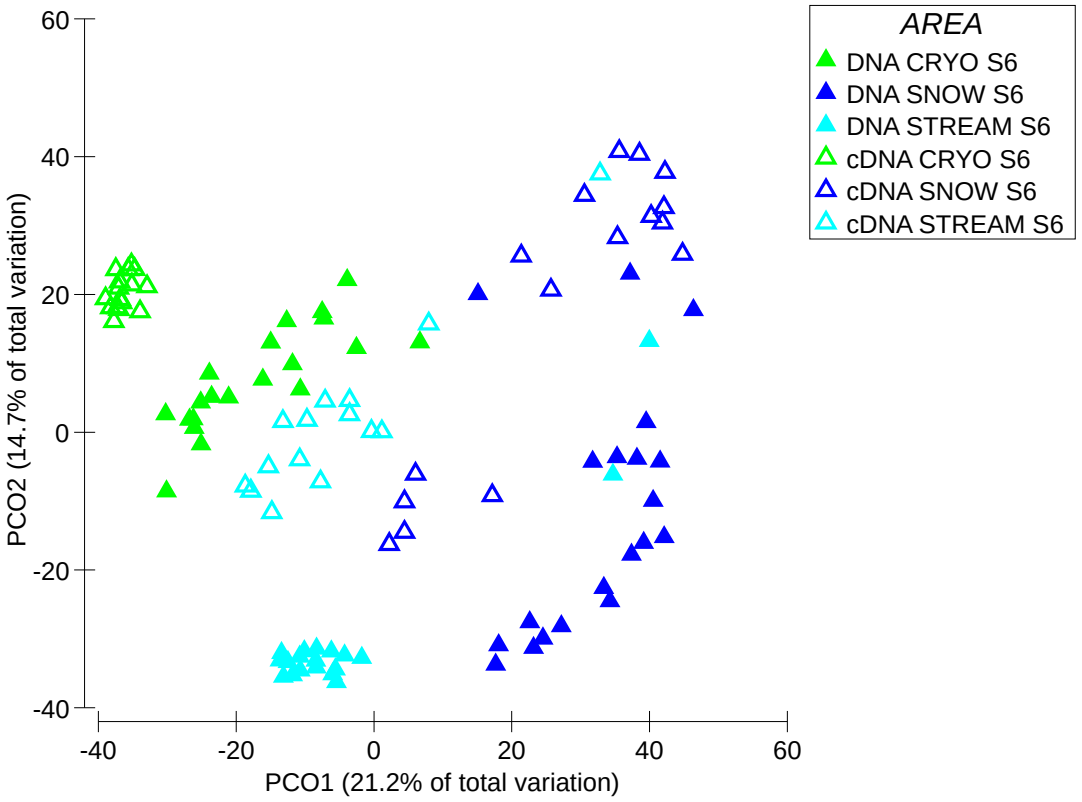

Figure 7. 3 Principal co-ordinates of Bray-Curtis distances for cryoconite, snow and stream OTUs observed on GrIS S6 weather station, showing the disparity between each habitat and nucleic acid type.

PERMANOVA established that the most significant contributors to community dynamics were habitat (pseudo-F = 29.366, *P* = 0.001), nucleic acid type (pseudo-F = 24.575, *P* = 0.001), interactions between habitat and nucleic acid (pseudo-F = 9.5699, *P* = 0.001), DOY (pseudo-F = 3.0737, *P* = 0.001), interactions between DOY and habitat (pseudo-F = 2.3714, *P* = 0.001) and interactions between DOY and nucleic acid (pseudo-F = 1.3907, *P* = 0.029). Two way analysis of similarity reveals a significant degree of dissimilarity for habitat between 16S rRNA gene and 16S cDNA (ANOSIM, Global R = 0.641, *P* = 0.001) and between habitats for 16S rRNA gene and 16S cDNA (ANOSIM, Global R = 0.713, *P* = 0.001).

Regional analyses by comparison of Bray-Curtis distance values against a pairwise distance matrix of S6 and 5 Greenland sites (Thule, Qaqortoq, Kangerlussuaq, Tasiilaq and Illulisat) by Spearman rank correlation revealed a significant but moderate effect of geographical orientation on the 16S rRNA gene and cDNA bacterial community ($\rho = 0.251$, $P = 0.01$). Similarity among locally observed taxa was evident, in addition to an increase in diversity over distance in cryoconite holes at THU and QAS, a decrease in cryoconite hole diversity over distance at KAN-P, DS and TAS and no biogeographical effect between S6 cryoconite holes (APPENDIX V, Figure V. 1). Furthermore, ice cores showed a significant distance decay ($\rho = 0.33$. $P = 0.01$), when compared to localised water habitats (snow: $\rho = 0.093$, $P = 0.065$; stream: $\rho = -0.023$, $P = 0.593$), with a combination of microbial interaction and environmental parameters driving the community.

7.3.2. Environmental correlations

Analysis of the recorded environmental variables highlighted diurnal changes for primary meteorological conditions (APPENDIX V, Figure V. 2). Short wave incident radiation (Panel 1) combined with incoming and outgoing long wave radiation (Panel 2) showed that the net influence of heat interacting with the ice surface was affected by albedo. Air temperature remained low but decreased for a short period after day 180, while relative humidity varied for the entire sampling season (Panel 3). Wind speed and direction (Panel 4) influenced the latent and sensible heat flux over melting surfaces, thereby affecting the turbulence-radiation interaction (Turb/Rad,

Panel 5), resulting in the higher melt rate observed early in the sampling season in the simulated melt model (Panel 6).

Incoming and outgoing short wave radiation (SWR), incoming and outgoing long wave radiation (LWR) and albedo were identified as the subset of variables best explaining the ecology of bacterial communities in snow and cryoconite. With the addition of melt rate, these variables were determined to best explain the ecology of stream environment communities. Additionally, analysis of environmental parameters showed a weak, yet significant relationship between bacterial community dissimilarity and environmental parameters (RELATE, R = 0.161, *P* = 0.001), as well as for the effect of geographic distance on the community at S6 and the rest of GrIS (RELATE, R = 0.228, *P* = 0.001). Stepwise selection of normalised variables predicting the bacterial communities in marginal tests were significant for Easting (pseudo-F = 5.7844, *P* = 0.001), Northing (pseudo-F = 4.4755, *P* = 0.001), total incoming SWR (pseudo-F = 4.4657, *P* = 0.001) and outgoing SWR (pseudo-F = 4.3073, *P* = 0.001), average incoming SWR (pseudo-F = 2.5682, *P* = 0.005) and outgoing SWR (pseudo-F = 4.0548, *P* = 0.001), total incoming LWR (pseudo-F = 4.2497, *P* = 0.001) and outgoing LWR (pseudo-F = 3.7428, *P* = 0.001) and average albedo (pseudo-F = 3.841, *P* = 0.002) (APPENDIX V, Table V. 2). Sequential tests similarly highlighted the impact of Northing (pseudo-F = 11.18, *P* = 0.001), total outgoing SWR (pseudo-F = 7.9405, *P* = 0.001) and cumulative melt (pseudo-F = 2.7077, *P* = 0.002) (APPENDIX V, Table V. 3).

A comparison of the environmental parameters against Spearman rank correlations of the supraglacial habitats showed significant correlations for OTUs from snow 16S rRNA genes (R = 0.684, *P* = 0.001), stream 16S rRNA genes (R = 0.546, *P* = 0.001), 16S snow cDNA (R = 0.385, *P* = 0.001) and 16S stream cDNA (R = 0.324, *P* = 0.001). Cryoconite habitats generated insignificant correlation to environmental variables, using this same method on 16S rRNA genes (R = 0.011, *P* = 0.44) and 16S cDNA (R = 0.017, *P* = 0.405) OTUs.

7.3.3. Taxonomic structure of bacterial communities

Observation of the data set in its entirety, revealed *Alphaproteobacteria* and *Cyanobacteria* as the most abundant in 16S cDNA sequences, while *Cyanobacteria*, *Alphaproteobacteria* and *Bacteroidetes* were most abundant in 16S rRNA gene sequences. These phyla contributed to the high relative abundance community of bacterial 16S rRNA genes and 16S cDNA, having a cumulative RA >1% across all three habitats. Significant differences were observed in the diversity indices for species richness for each habitat (ANOVA, F = 74.91, *P* <0.0001) and over time (ANOVA, F = 2.42, *P* = 0.0318), while evenness was only significant for habitat (ANOVA, F = 60.05, *P* <0.0001) (APPENDIX V, Table V. 1).

7.3.3.1. Cryoconite bacterial community structure

An examination of the cryoconite bacterial nucleic acid composition revealed greater OTU diversity in 16S rRNA genes (total DNA) (Figure 7. 4A) compared to 16S cDNA

(potentially active DNA) (Figure 7. 4B). *Cyanobacteria* active biomass dominated the cryoconite environment with 89.34% 16S RA in cDNA compared to 16.03% RA in 16S rRNA genes, where it was ranked third most abundant phylum. *Alphaproteobacteria* was second most abundant in active and total cryoconite communities (6.78% RA in 16S cDNA, 21.85% RA in 16S rRNA genes). *Actinobacteria* had a RA of 2.56% in cryoconite 16S cDNA, making it third most abundant (13.12% RA in 16S rRNA genes). *Bacteroidetes* appeared most abundant in cryoconite total DNA (23.89% RA in 16S rRNA genes, 0.15% RA in 16S cDNA). *Chloroflexi*, *Firmicutes* and *Gammaproteobacteria* contributed to 6.53%, 3.85% and 3.05% RA in 16S rRNA genes for cryoconite community diversity, but contributed to only 0.007%, 0.007% and 0.03% RA in 16S cDNA, respectively. Individual OTUs forming the main active cryoconite community (>1% RA) over 6 weeks belonged to the *Cyanobacteria* classes *Oscillatoriophycideae* (2 OTUs), *Synechococcophycideae* (10 OTUs), *Alphaproteobacteria* (1 OTU) and *Acidimicrobiia* (1 OTU).

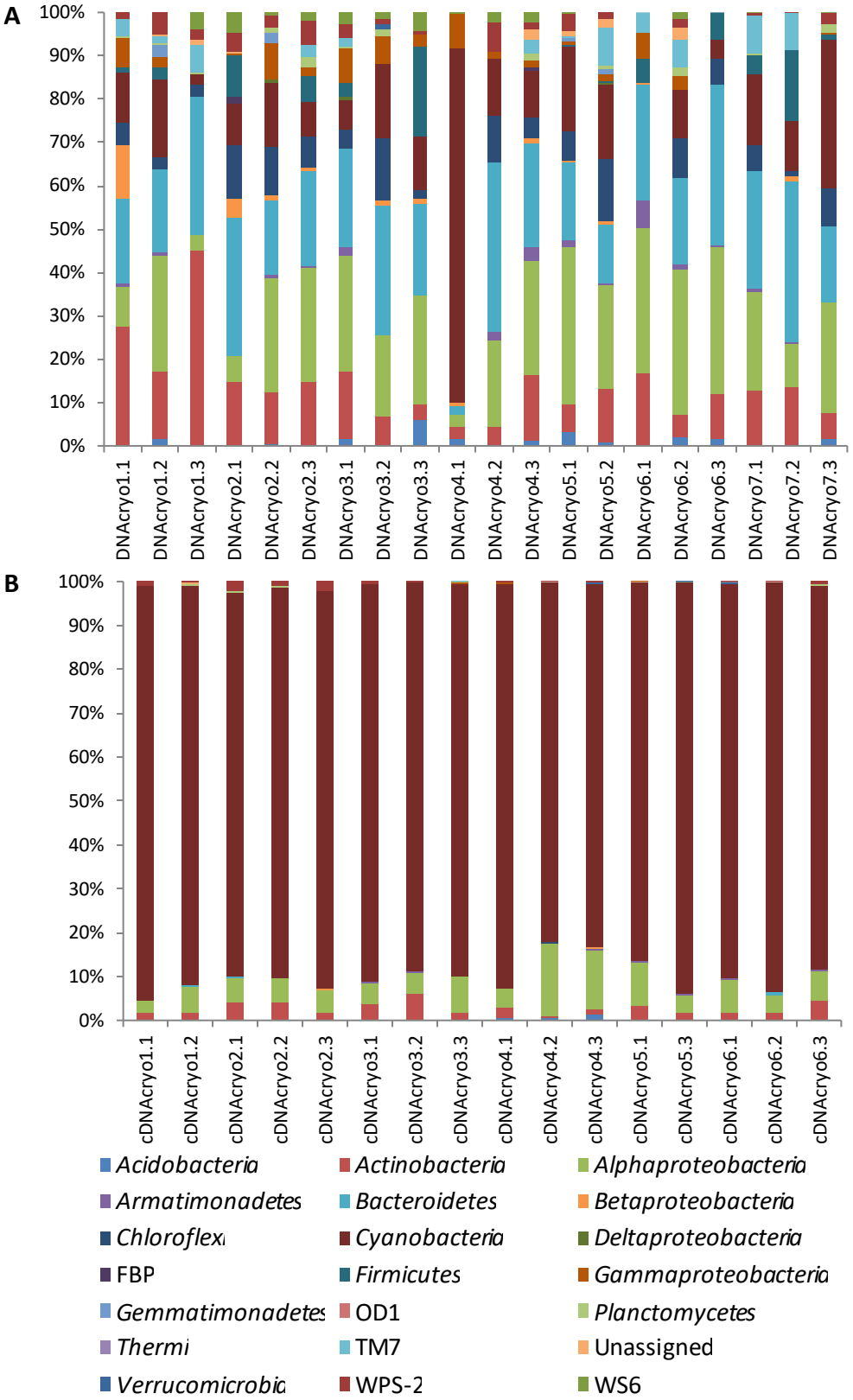

Figure 7. 4 Bacterial composition of the (A) 16S rRNA gene and (B) 16S cDNA in S6 cryoconite. Higher OTU diversity is observed in rRNA sequences than cDNA, however 16S cDNA results show cyanobacterial taxa dominate this environment.

A core community of 13 taxa was identified from high relative abundance 16S cDNA sequences, to determine the role of specific taxa in cryoconite (Table 7. 2). *Cyanobacteria* emerged as the highest contributing phylum, comprising 2 OTUs from the family *Xenococcaceae*, 2 OTUs from the family *Chamaesiphonaceae* and 8 OTUs from the genus *Phormidesmis*, in addition to single instances of *Alphaproteobacteria* (*Sphingomonadaceae*-16) and *Actinobacteria (Sphingomonadaceae*-12*)*. Of the core taxa, 4 OTUs were common to all Ice Sheet microhabitats, 7 OTUs displayed high 16S rRNA gene relative abundances and 6 OTUs constituted rare cryoconite taxa, as they were present at <1% RA. Multiple *Phormidesmis* OTUs appeared dominant in Greenland Ice Sheet cryoconite, having the closest named relatives identified as *Phormidesmis priestleyi* ANT.L66.1 (99% ID) and *Phormidesmis* sp. LD30 5700 TP (98% ID).

Table 7. 2 Rare and abundant bacterial community identified from Greenland S6 cryoconite sequences describing the closest environmental relative (CER) and closest named relative (CNR) to OTUs assigned with Greengenes taxonomy.

Greengenes ID	Overall DNA RA>1	Cryoconite DNA RA>1	Closest Environmental Relative (CER)	CER Accession	CER %ID	Habitat	Closest Named Relative (CNR)	CNR Accession	CNR %ID	Habitat
Leptolyngbya-3	+	+	Uncultured *cyanobacterium* clone LH16_269	KM112118.1	99	Antarctic benthic mats	*Phormidesmis priestleyi* ANT.L66.1	AY493581.1	99	Antarctic benthic mat
Xenococcaceae-6	+	+	Uncultured *cyanobacterium* clone FQSS103	EF522323.1	99	Colorado sandstone endolith	*Phormidium* sp. CCALA 726	GQ504036.1	92	Svalbard
Leptolyngbya-76		+	*Cyanobacterium* cWHL-1 16S	HQ230236.1	97	Canada snow	*Phormidesmis priestleyi* ANT.LG2.4	AY493580.1	98	Antarctic
Xenococcaceae-2773		+	Uncultured *cyanobacterium* clone FQSS103	EF522323.1	98	USA endolithic sandstone	*Chroococcus* sp. VP2-07	GQ504036.1	91	Italy and Spain - fountains
Leptolyngbya-106		+	Uncultured *bacterium* clone IT2-66	KX247359.1	98	China glacier forefield	*Phormidesmis priestleyi* ANT.LG2.4	AY493580.1	98	Antarctic
Leptolyngbya-1107			Uncultured *cyanobacterium* clone LH16_269	KM112118.1	99	Antarctic benthic mats	*Phormidesmis priestleyi* ANT.L66.1	AY493581.1	99	Antarctic benthic microbial mat
Leptolyngbya-290		+	Uncultured *cyanobacterium* clone H-D14	DQ181732.1	99	East Antarctic microbial mat	*Phormidesmis* sp. LD30 5700 TP	LN849930.1	98	Western Himalaya soil crust
Chamaesiphonaceae-41			Uncultured *bacterium* clone EpiUMB29	FJ849281.1	99	Arctic stream epilithon	*Chamaesiphon subglobosus* PCC 7430	AY170472.1	98	pure culture
Leptolyngbya-5202			Uncultured *cyanobacterium* clone LH16_269	KM112118.1	99	Antarctic benthic mats	*Phormidesmis priestleyi* ANT.L66.1	AY493581.1	99	Antarctic benthic microbial mat
Chamaesiphonaceae-107			Uncultured *cyanobacterium* clone p660_S12	JQ407506.1	99	Greenland glacier ice	*Chamaesiphon subglobosus PCC 7430*	AY170472.1	97	Culture collection
Leptolyngbya-11378			Uncultured cyanobacterium clone LH16_269	KM112118.1	99	Antarctic benthic mat	*Phormidesmis priestleyi* ANT.L66.1	AY493581.1	99	Antarctic
Leptolyngbya-60664			Uncultured cyanobacterium clone MIS88	FJ977129.1	99	High Arctic microbial mat	*Phormidesmis priestleyi* ANT.LG2.4	AY493580.1	98	Antarctic
Sphingomonadaceae-16		+	Uncultured bacterium clone Bysf-47-Sf10-014	JX967335.1	99	Norway granite	*Blastomonas natatoria*	Y13774.1	96	Fresh water
Acidimicrobiales-12	+		Uncultured bacterium clone AM 5.5m_4_43	HE616493.1	99	Finland Boreal Lake	*Aciditerrimonas ferrireducens* strain IC-18	NR_112972.1	94	Japan solfataric soil

Distance-based linear modelling demonstrated that 79.31% of the total variation observed within the S6 cryoconite dataset, can be explained by the community composition (Figure 7. 5). Redundancy analysis identified *Cyanobacteria* as the main driver in the 16S cDNA community of cryoconite over the entire summer season, while the remaining phyla could predict the ordination patterns observed in 16S rRNA genes. Evidence supporting the lack of correlation between rRNA and cDNA OTUs was gained via RELATE analysis (R = 0.213, *P* = 0.908). Similar analysis with normalised environmental parameters supported negligible impact on GrIS cryoconite, as all variables were non-contributing factors to the observed patterns for both marginal (pseudo-F range = 0.7 - 1.0369, *P* = 0.325 - 0.72) and sequential (pseudo-F = 0.40521 - 1.0369, *P* = 0.307 - 0.972) tests (APPENDIX V, Table V. 4 and Table V. 5).

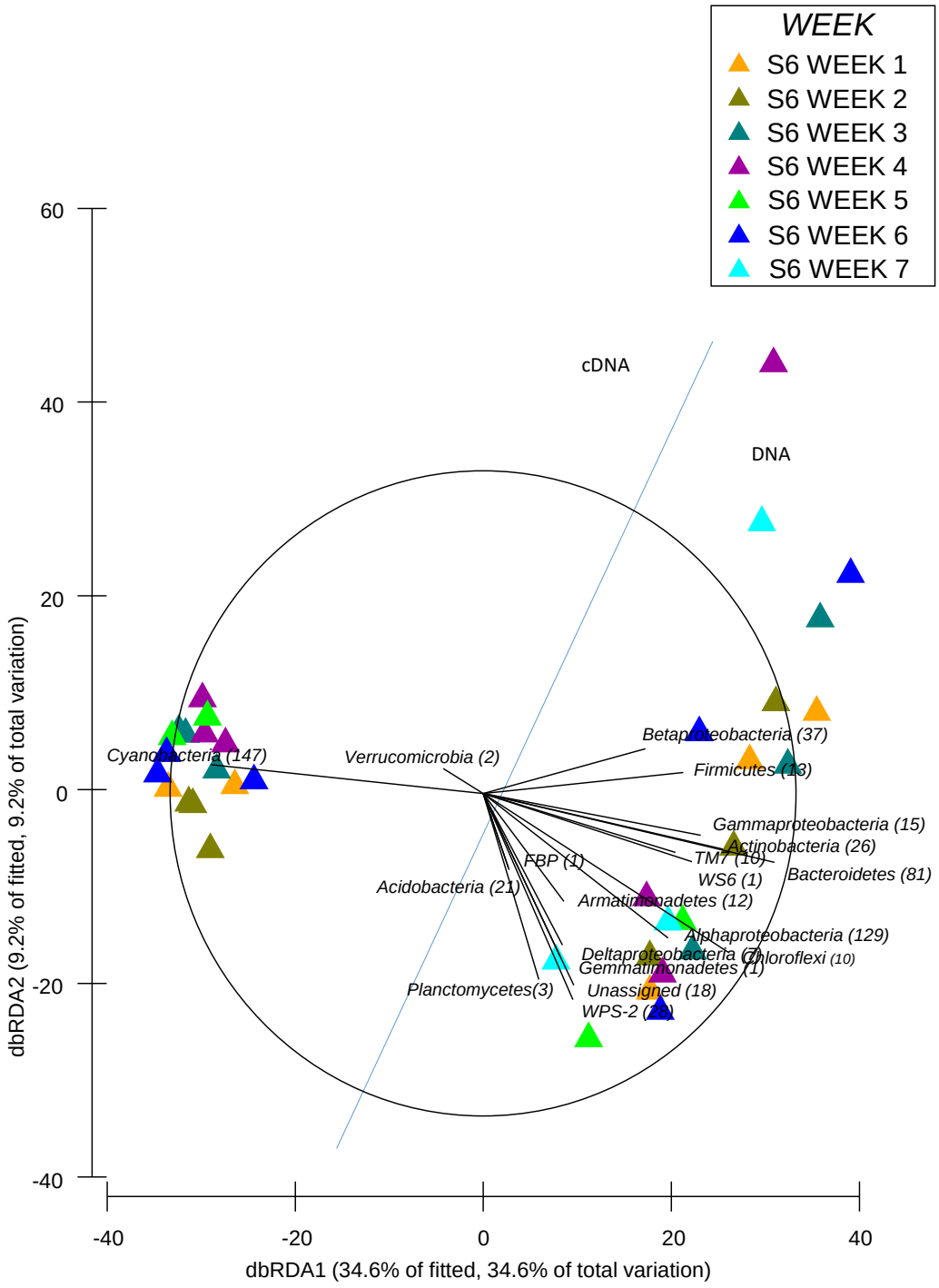

Figure 7. 5 Distance-based redundancy analysis showing the phyla that drive community diversity in 16S cDNA and 16S rRNA genes in cryoconite communities during the 7 week sampling season on GrIS, S6.

7.3.3.2. Snow bacterial community structure

Snow 16S rRNA gene communities (Figure 7. 6A) were more varied over time than 16S cDNA communities (Figure 7. 6B), with week 7 exhibiting fewer observed OTUs in both nucleic acid types. *Alphaproteobacteria* was identified as the most abundant phylum in both 16S cDNA (74.77% RA) and 16S rRNA gene sequences (12.56% RA) in snow bacterial communities. Distinct differences in the most abundant community members were observed between 16S cDNA and 16S rRNA genes. *Acidobacteria* was the second most active abundant phylum with a RA of 12.08% in 16S cDNA (2% RA in 16S rRNA genes). *Bacteroidetes* ranked as second most abundant in snow 16S rRNA (14.24% RA in 16S rRNA genes, 5.33% RA in 16S cDNA). *Gammaprotobacteria*, *Betaproteobacteria* and *Cyanobacteria* contributed to 4.1% RA in 16S cDNA (5.76% RA in 16S rRNA genes), 1.63% RA in 16S cDNA (5.66% RA in 16S rRNA genes) and 1.10% RA in 16S cDNA (58.35% RA in 16S rRNA genes), respectively, of the remaining core bacterial community.

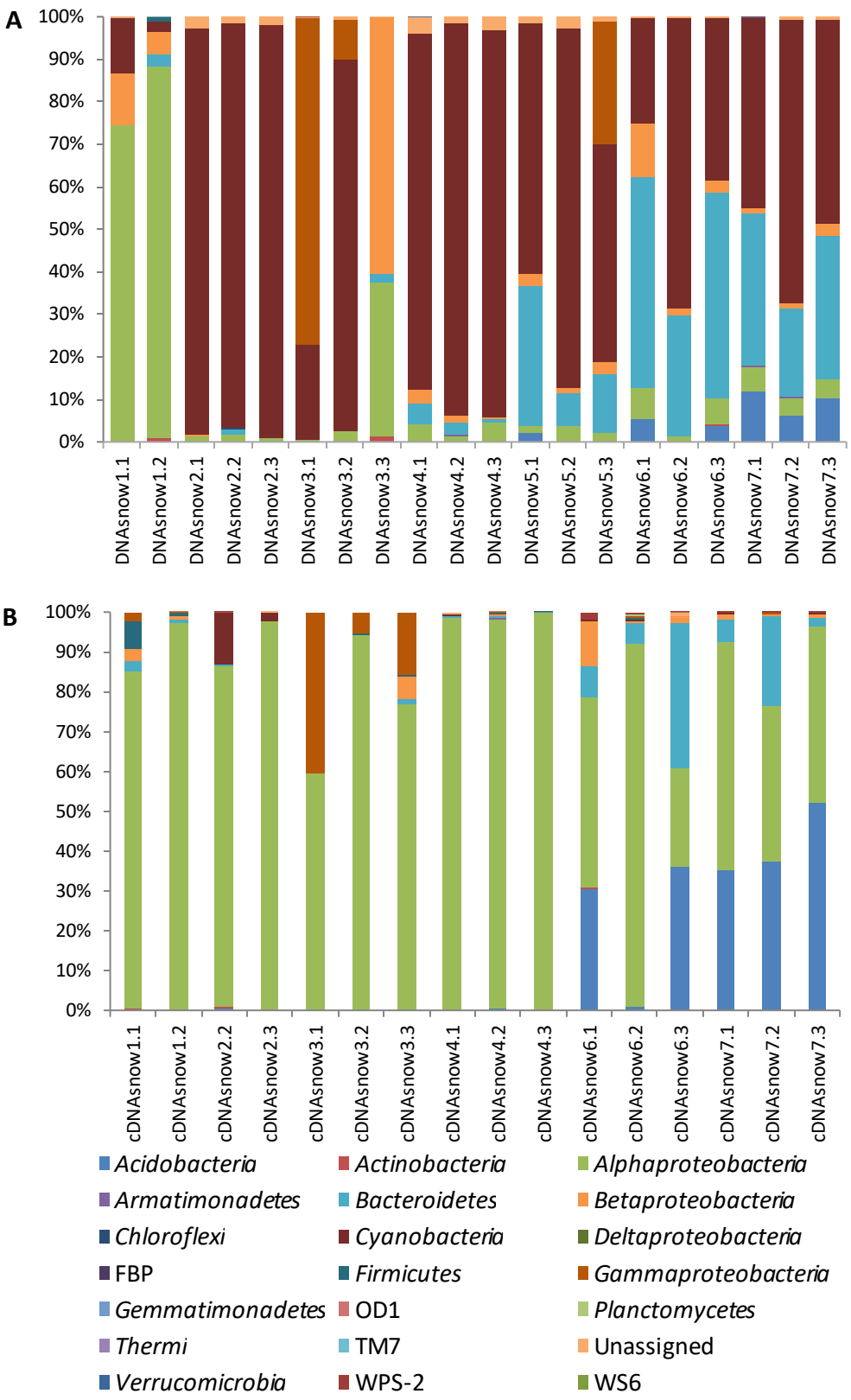

Figure 7. 6 Bacterial composition of the nucleic acids extracted from S6 snow samples show high diversity in (A) 16S rRNA genes and lower diversity but high abundance from *Alphaproteobacteria* taxa in (B) 16S cDNA.

Eighteen OTUs were identified as the main contributors of high relative abundance in snow 16S cDNA sequences and were dominated by *Alphaproteobacteria* (13 OTUs), *Acidobacteria* (2 OTUs), *Bacteroidetes* (2 OTUs) and *Gammaproteobacteria* (1 OTU). However, only 4 OTUs were confirmed as core taxa present in over 87% of the samples; these were *Methylobacterium*-1, *Methylobacterium*-6342, *Sphingomonas*-15 and *Methylobacterium*-1508 (Table 7. 3). These taxa, along with 2 other *Alphaproteobacteria* taxa, were specific to the snow habitat, while 3 OTUs were also present in cryoconite and stream microhabitats. The remaining 9 OTUs from *Alphaproteobacteria* (7 OTUs), *Bacteroidetes* (1 OTU) and *Acidobacteria* (1 OTU) were considered rare snow biota.

Table 7. 3 Rare and abundant bacterial community identified from Greenland S6 snow sequences describing the CER and CNR.

Greengenes ID	Overall DNA RA>1	Snow DNA RA>1	CER	CER Accession	CER %ID	Habitat	CNR	CNR Accession	CNR %ID	Habitat
Methylobacterium-1		+	Marine bacterium MSC10	EU753147.1	99	Massachusetts tidal flat sand	*Methylobacterium brachiatum* strain SH3102B93	KU173579.1	99	East China sea water
Acidobacteriaceae-17	+		Uncultured *Acidobacteria* bacterium clone IC3076	HQ595216.1	99	Svalbard ice	*Granulicella aggregans* TPB6028	NR_115070.1	99	Russian peat
Methylobacterium-6342		+	Uncultured *Alphaproteobacterium* clone CN-2_B05	EF219937.1	99	Antarctic soil Coal Nunatak	*Methylobacterium tardum* IHBB 11162	KR085941.1	99	Trans Himalaya lake water
Sphingomonas-15		+	Uncultured bacterium clone Bysf-47-Sf10-014	KP296188.1	99	Antarctic seawater	*Sphingomonas* sp. UYEF32	KU060875.1	99	Antarctic exfoliation rock
Rickettsiaceae-7571			Candidatus *Trichorickettsia mobilis*	HG315619.1	95	Wastewater	Candidatus *Trichorickettsia mobilis*	HG315619.1	95	Wastewater
Rickettsiaceae-39			Uncultured bacterium	AM945518.1	95	Arctic soil	Candidatus *Trichorickettsia mobilis*	AM945518.1	95	Wastewater
Methylobacterium-1508		+	Uncultured bacterium clone LIB079_B_C08	KM852235.1	99	Biofilm	*Methylobacterium brachiatum* ZJ0902B96	KU173699.1	98	East China seawater
Sphingomonadaceae-34		+	Uncultured bacterium clone QA4_1_042	LC076727.1	99	Greenland cryoconite	*Novosphingobium* sp. STM-24	LN890294.1	96	Freshwater
Sphingomonas-31			Uncultured bacterium clone LIB062_A_D01	KM851700.1	100	Biofilm	*Sphingomonas* sp. UV9	KR922276.1	99	Antarctic
Hymenobacter-7	+		Uncultured bacterium clone Bysf-33-Sf11-054	AB991133.1	99	Alaskan glacier	*Hymenobacter* sp. Ht11	JX949241.1	97	Chinese glacier
Methylobacterium-4640			Uncultured bacterium clone OTU582	KX957282.1	99	Denmark waterway sediment	*Methylobacterium radiotolerans* 6019	GU294328.1	99	Vietnam Leaf surface
Sphingomonadaceae-66			Uncultured bacterium clone: QA3_1_101	LC076722.1	99	Greenland cryoconite	*Polymorphobacter* sp. strain Ap23E	KX990242.1	98	Antarctic soil
Acetobacteraceae-33			Uncultured *Acidisphaera* sp.	AM940454.1	96	Arctic soil	*Acetobacteraceae* bacterium MP03	AM162403.1	95	Russia sphagnum Peat soil
Hymenobacter-693445			Uncultured bacterium clone Bysf-33-Sf11-054	AB991133.1	99	Alaskan glacier	*Hymenobacter* sp. Ht11	JX949241.1	97	China glacier
Acetobacteraceae-32		+	Uncultured *Acetobacteraceae* bacterium clone AhedenP18	FJ475456.1	99	Sweden soil	*Acidisphaera* sp. G45-3	KY777995.1	96	China acid mine drainage
Pseudomonas-46	+		Bacterium strain NBTE-P16	KY744370.1	99	Papua New Guinea seawater	*Pseudomonas azotoformans F77*	CP019856.1	99	soil
Acidobacteriaceae-5693			Uncultured *Acidobacteria* bacterium clone IC3076	HQ595216.1	99	Svalbard glacier ice	*Granulicella sapmiensis* S6CTX5A	NR_118023.1	97	Tundra soil
Caulobacteraceae-220			Uncultured bacterium clone YZF_97	KX119831.1	100	Tibet ice core	*Caulobacter vibrioides*	LN835442.1	100	Hungary lake water

There is a significant, but average correlation between 16S rRNA and cDNA OTUs in snow environments (RELATE, R = 0.529, *P* = 0.001). Redundancy analysis explained that 83.94% of the total variance in snow bacterial communities were due to the observed phyla (Figure 7. 7). Distance-based linear modelling identified *Gammaproteobacteria* as a predictor of the 16S cDNA community in weeks 1 - 4, *Firmicutes, Actinobacteria* and *Alphaproteobacteria* during weeks 4 - 6, and WPS-2 and *Acidobacteria* in week 7. Similar analysis of the normalised environmental parameters revealed significant influence from 17 out of 22 environmental variables, highlighting the role of DOY, outgoing solar incident radiation in marginal tests (APPENDIX V, Table V. 6) and melt, in addition to these factors, in sequential tests (APPENDIX V, Table V. 7).

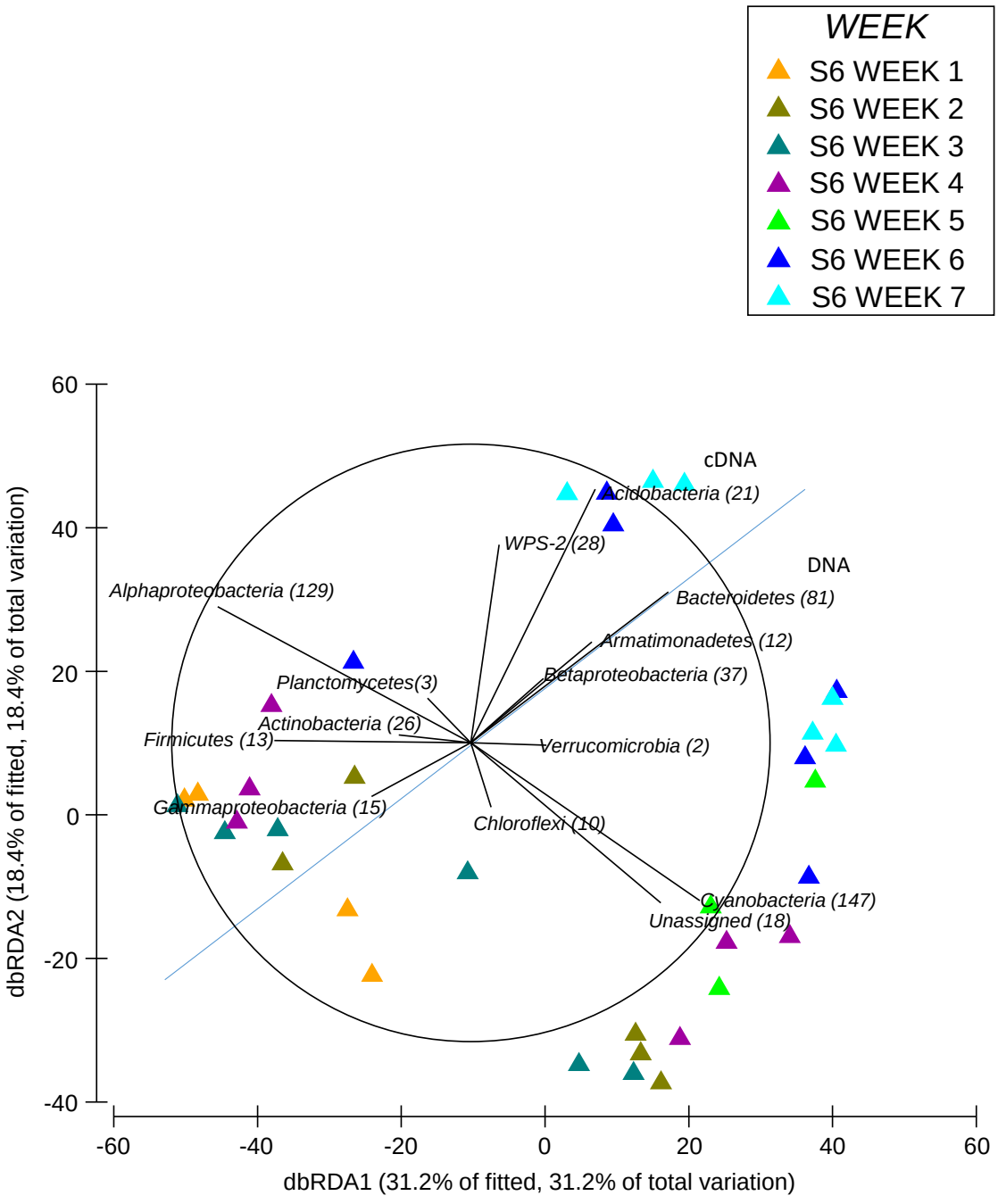

Figure 7. 7 Distance-based redundancy analysis of snow bacterial communities showing phyla that drive changes in 16S cDNA and 16S rRNA gene communities over time.

7.3.3.3. Stream bacterial community structure

Stream communities displayed the most bacterial diversity, when compared to cryoconite and snow communities, however, 16S cDNA stream bacterial composition (Figure 7. 8B) was still less diverse than 16S rRNA gene sequences (Figure 7.7A), displaying a clear oscillating pattern of dominant OTUs from week 1 to week 7. *Alphaproteobacteria* was the most dominant phylum in 16S cDNA stream bacterial communities (62.47% RA in 16S cDNA, 23.8% RA in 16S rRNA genes), followed by *Cyanobacteria* 14.08% RA in 16S cDNA (27.58% RA in 16S rRNA genes). *Verrucomicrobia* was third most abundant (6.71% RA in 16S cDNA, 3.18% RA in 16S rRNA genes), while *Betaproteobacteria* contributed to 6.3% RA in 16S cDNA and 14.53% RA in 16S rRNA genes. OTUs from the phylum *Acidobacteria* had a 3.08% RA in 16S cDNA (3.70% RA in rRNA genes) and were ranked similarly (5^{th} position) in both 16S cDNA and 16S rRNA gene communities. WPS-2, *Actinobacteria* and OD1 had 1.73% RA in 16S cDNA (1.95% RA in 16S rRNA genes), 0.47% RA in 16S cDNA (1.88% RA in 16S rRNA genes) and 1.59% RA in 16S cDNA (0.96% RA in 16S rRNA genes), respectively. *Bacteroidetes*, the third most abundant in stream water total DNA (16.73% RA in 16S rRNA genes) had a 16S cDNA abundance of 1.5%.

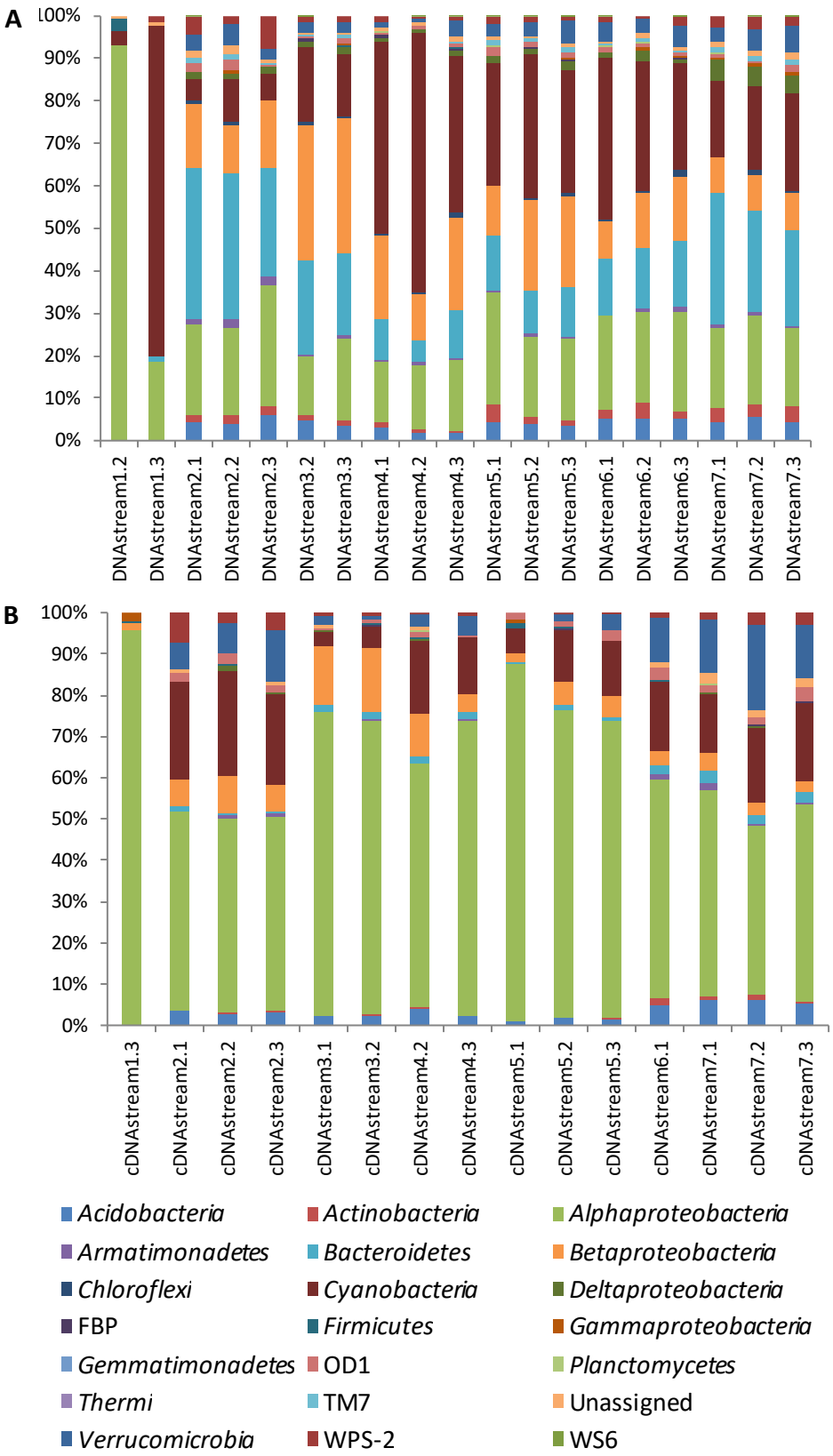

Figure 7. 8 Bacterial composition of the S6 stream communities shows higher diversity in (A) 16S rRNA genes, while (B) 16S cDNA shows temporal fluctuation of the potentially active bacterial community.

Fifteen high relative abundance taxa were observed in 16S cDNA stream OTUs, which showed strong presence of *Alphaproteobacteria* (8 OTUs) and *Cyanobacteria* (2 OTUs) (Table 7. 4). Lower, but still significantly present, were members of the *Verrucomicrobia* (1 OTU), *Betaproteobacteria* (2 OTUs), *Acidobacteria* (1 OTU) and WPS-2 (1 OTU). From the top-scoring taxa, 13 were identified as core taxa appearing in over 86% of the stream 16S cDNA sequences, 5 of which appeared as top-scoring taxa in cryoconite and snow 16S rRNA gene and 16S cDNA sequences, and 9 that were top-scoring taxa in stream 16S rRNA genes.

Table 7. 4 Rare and abundant bacterial community identified from Greenland S6 stream sequences describing the CER and CNR.

Greengenes ID	Overall DNA RA>1	Stream DNA RA>1	CER	CER Accession	CER %ID	Habitat	CNR	CNR Accession	CNR %ID	Habitat
Methylobacterium-1		+	Marine bacterium MSC10	EU753147.1	99	Massachusetts tidal flat sand	*Methylobacterium brachiatum* SH3102B93	KU173579.1	99	East China sea water
Leptolyngbya-3		+	Uncultured *cyanobacterium* clone LH16_269	KM112118.1	99	Antarctic benthic mat	*Phormidesmis priestleyi* ANT.L66.1	AY493581.1	99	Antarctic benthic mat
Candidatus *Xiphinematobacter*-26	+		Uncultured *Xiphinematobacteriaceae* bacterium clone AL5.23	GU047442.1	99	Arctic soil	*Spartobacteria* bacterium Gsoil 144	AB245342.1	92	Soil
Sphingomonadaceae-34		+	Uncultured bacterium clone QA4_1_042	LC076727.1	99	Greenland cryoconite	*Novosphingobium* sp. STM-24	LN890294.1	96	Freshwater
Methylobacterium-6342		+	Uncultured *alphaproteobacterium* clone CN-2_B05	EF219937.1	99	Antarctic soil	*Methylobacterium tardum* IHBB 11162	KR085941.1	99	Himalaya lake water
Sphingomonadaceae-16		+	Uncultured bacterium clone Bysf-47-Sf10-014	JX967335.1	99	Norway granite	*Blastomonas natatoria*	Y13774.1	96	Fresh water
Phyllobacterium-24			Uncultured bacterium clone PL3-9 16S	EU527093.1	99	China glacier snow	*Phyllobacterium* sp. MD10	KF358323.1	99	Tibet glacier snow
Sphingomonadaceae-14	+	+	Uncultured bacterium clone Bysf-47-Sf10-014	HQ622730.1	99	Svalbard ice	*Sphingopyxis* sp. JJ2203	JX304649.1	98	Korean lake
Acetobacteraceae-27		+	Uncultured bacterium gene clone Ms-10-Fx11-2-091	AB990033.1	99	USA:Alaska	*Roseomonas frigidaquae* ZSGR2	KC577560.1	95	-
Sphingomonas-15		+	Uncultured bacterium clone Bysf-47-Sf10-014	KP296188.1	99	Antarctic surface seawater	*Sphingomonas* sp. UYEF32	KU060875.1	99	Antarctic exfoliation rock
Comamonadaceae-5	+	+	*Polaromonas* sp. MDB2-14	JX949585.1	99	China glacier	*Polaromonas* sp. MDB2-14	JX949585.1	99	China glacier
Chamaesiphonaceae-41			Uncultured bacterium clone EpiUMB29	FJ849281.1	99	Arctic stream epilithon	*Chamaesiphon subglobosus* PCC 7430	AY170472.1	98	Pure culture
Acidobacteriaceae-17	+		Uncultured *Acidobacteria* bacterium clone IC3076	HQ595216.1	99	Svalbard ice	*Granulicella aggregans* TPB6028	NR_115070.1	99	Russia peat
WPS-2-20	+		Uncultured bacterium clone: QM_1_067	LC076745.1	100	Greenland cryoconite	*Heliorestis daurensis* BT-H1	NR_028721.1	84	Siberia soda lake
Oxalobacteraceae-47			Uncultured bacteria clone SL-Spring-E11	FR696925.1	99	Spain slush	*Actimicrobium antarcticum* KOPRI 25157	NR_118029.1	98	Antarctic seawater

Redundancy analysis shows that 85.5% of the total variation can be explained by stream community composition (Figure 7. 9). While no clear drivers of the 16S cDNA could be identified using this method, a transition of influence on communities was evident by *Firmicutes* in week 1, *Alphaproteobacteria* in week 2 and all remaining OTUs in week 7. Additionally, an average correlation between 16S rRNA and 16S cDNA OTUs was noted in S6 glacial streams (RELATE, R = 0.542, *P* = 0.001). Sequential tests revealed significant impact by cumulative melt, outgoing short and long wave incident radiation (APPENDIX V, Table V. 9), while marginal tests identified cumulative incoming short and long wave incident radiation and average albedo as predictors of community structure, in addition to the aforementioned variables (APPENDIX V, Table V. 8).

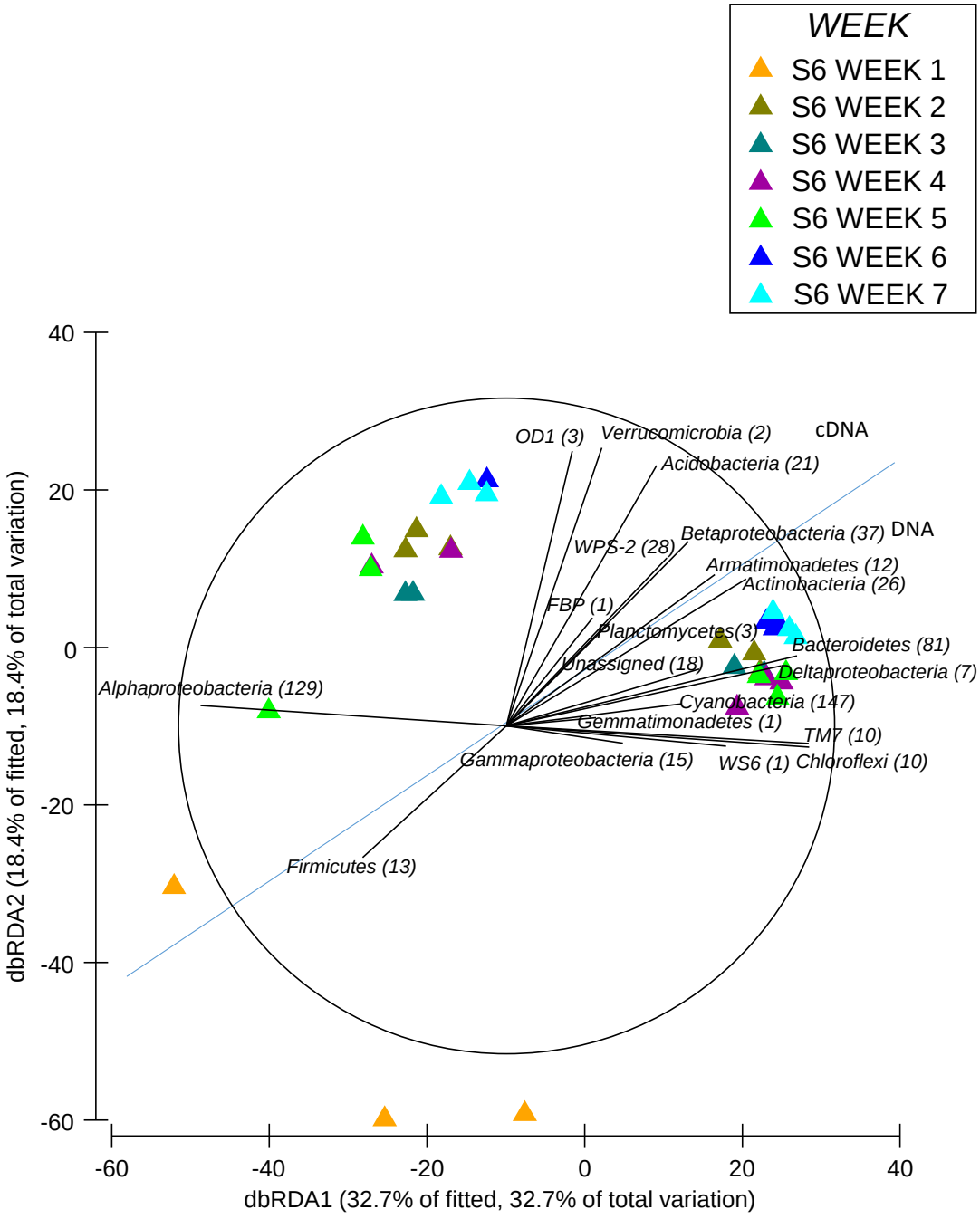

Figure 7. 9 Distance-based redundancy model of stream 16S cDNA and 16S rRNA gene OTUs with phyla as predictors of community diversity.

7.3.4. Associating bacterial relative abundance with potentially active taxa

OTUs were assigned as potentially active if the 16S cDNA relative abundance was greater than their 16S rRNA gene relative abundance. All other phyla were categorised as low RA and low activity phyla. *Cyanobacteria* was identified as the most active and abundant phylum of the cryoconite community on S6 (Figure 7. 10A), with the *Pseudanabaenaceae*, *Xenococcaceae*, *Chamaesiphonaceae*, *Nostocales* and an unassigned cyanobacterial class demonstrating the highest observed relative activity (Figure 7. 11A). *Alphaproteobacteria* families *Phyllobacteriaceae*, *Sphingomonadales* and *Rhizobiales* were active to a lesser extent. All other observed phyla were of high abundance but low activity potential. Cyanobacterial OTUs from the class *Synechococcophycideae* had the highest observed protein synthesis potential (PSP) (Figure 7. 12), with *Leptolyngbya*-76 contributing to 12.99% average PSP. OTUs from the classes *Acidimicrobiia* (4 OTUs), *Acidobacteriia* (1 OTU), *Actinobacteria* (4 OTUs), *Alphaproteobacteria* (39 OTUs), *Planctomycetia* (3 OTUs), *Ktedonobacteria* (1 OTU), *Saprospirae* (3 OTUs), *Sphingobacteriia* (2 OTUs), *Thermoleophilia* (1 OTU), TM7-1 (1 OTU) and WPS-2 (3 OTUs) displayed less than 1% PSP and had a distinct pattern for selective OTU recruitment over time, apart from *Actinobacterium*-12, *Sphingopyxis*-14 and WPS-2-20 that were abundant during all 5 weeks.

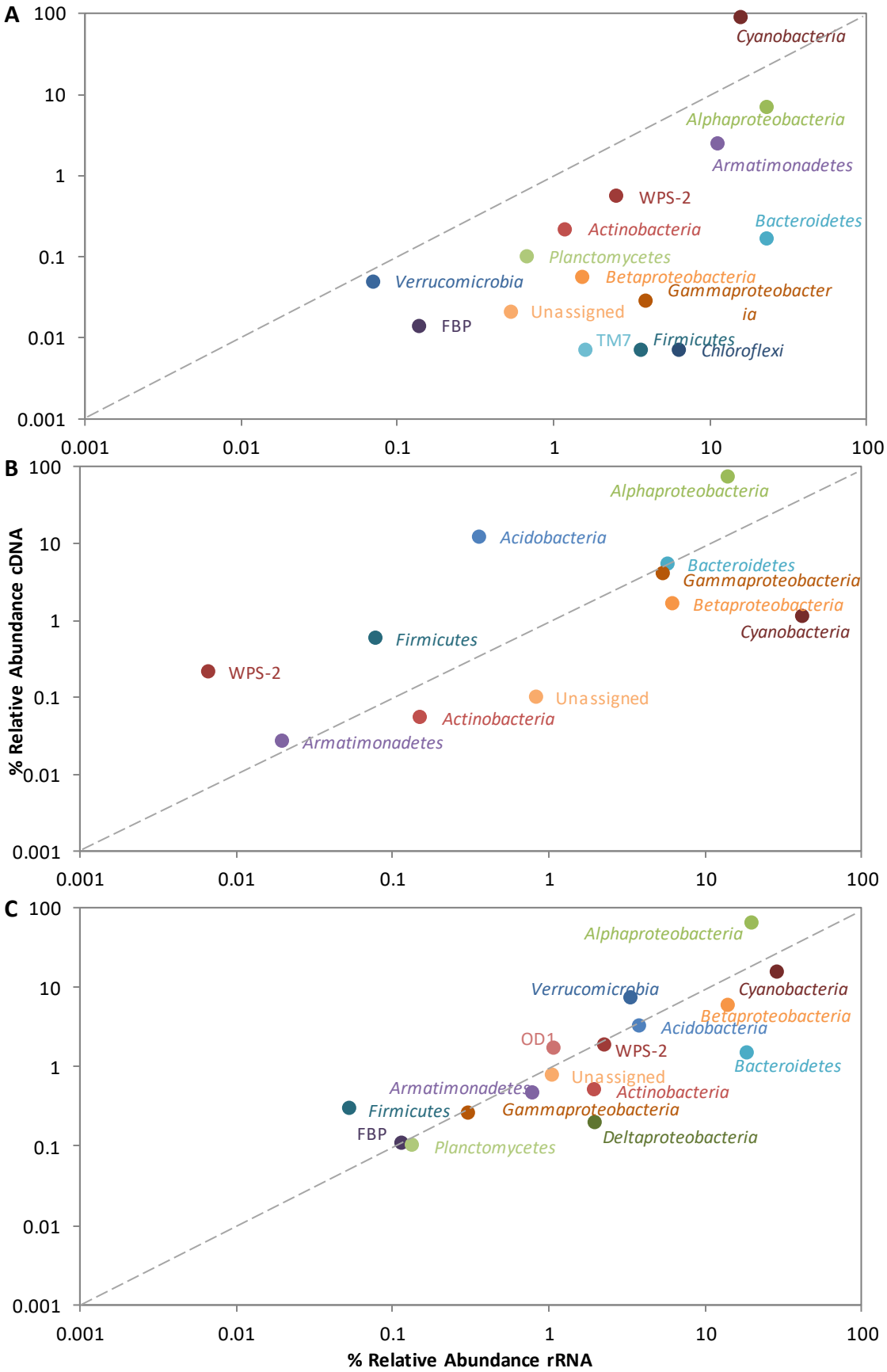

Figure 7. 10 Relative abundance of 16S cDNA and 16S rRNA gene phyla in (A) cryoconite, (B) snow and (C) stream communities. Points above the dotted line represent potentially active phyla.

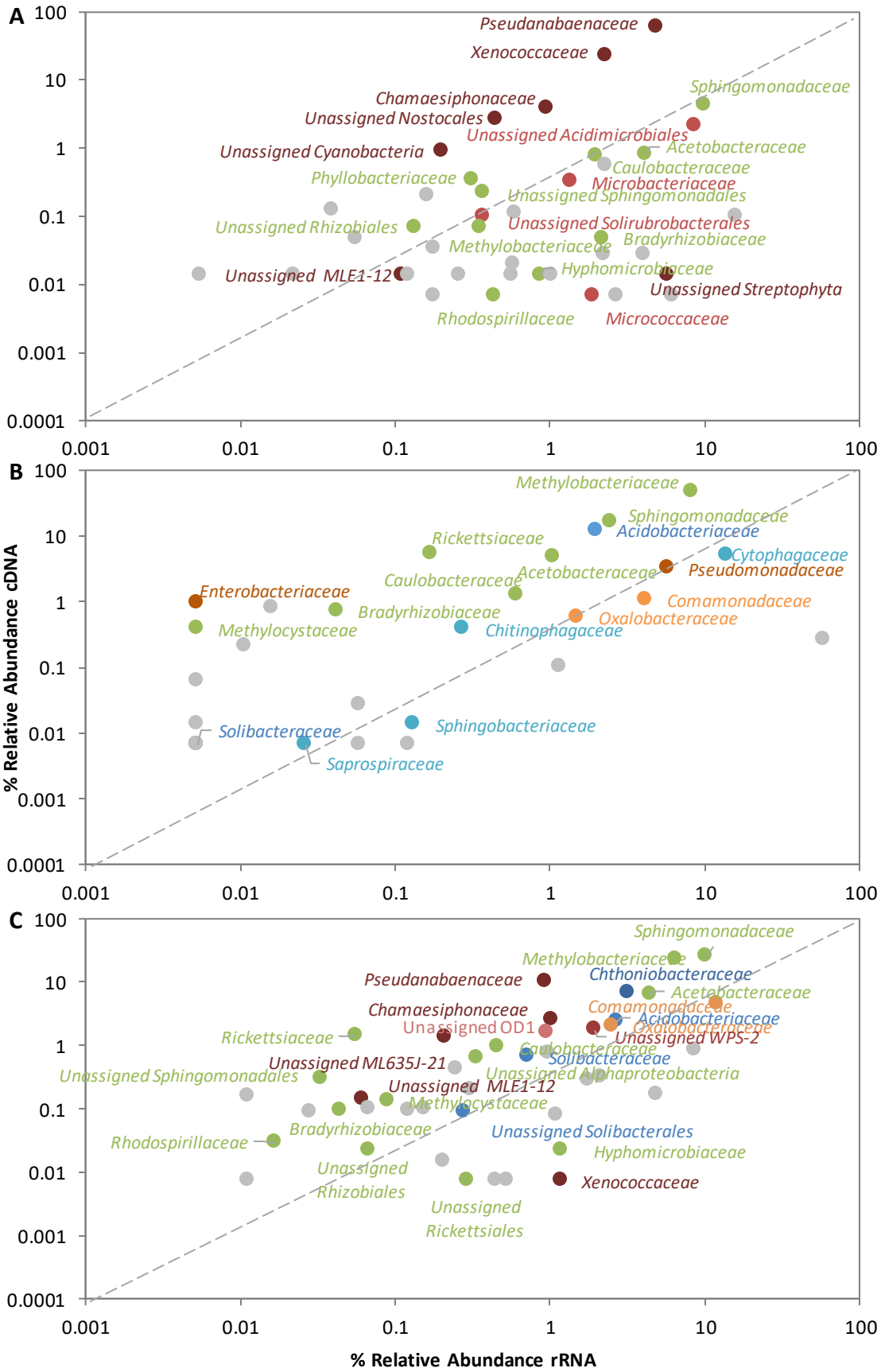

Figure 7. 11 Relative abundance of active 16S cDNA and 16S rRNA genes in (A) cryoconite, (B) snow and (C) stream, classified by family. Inactive and low abundance phyla are represented by gray points.

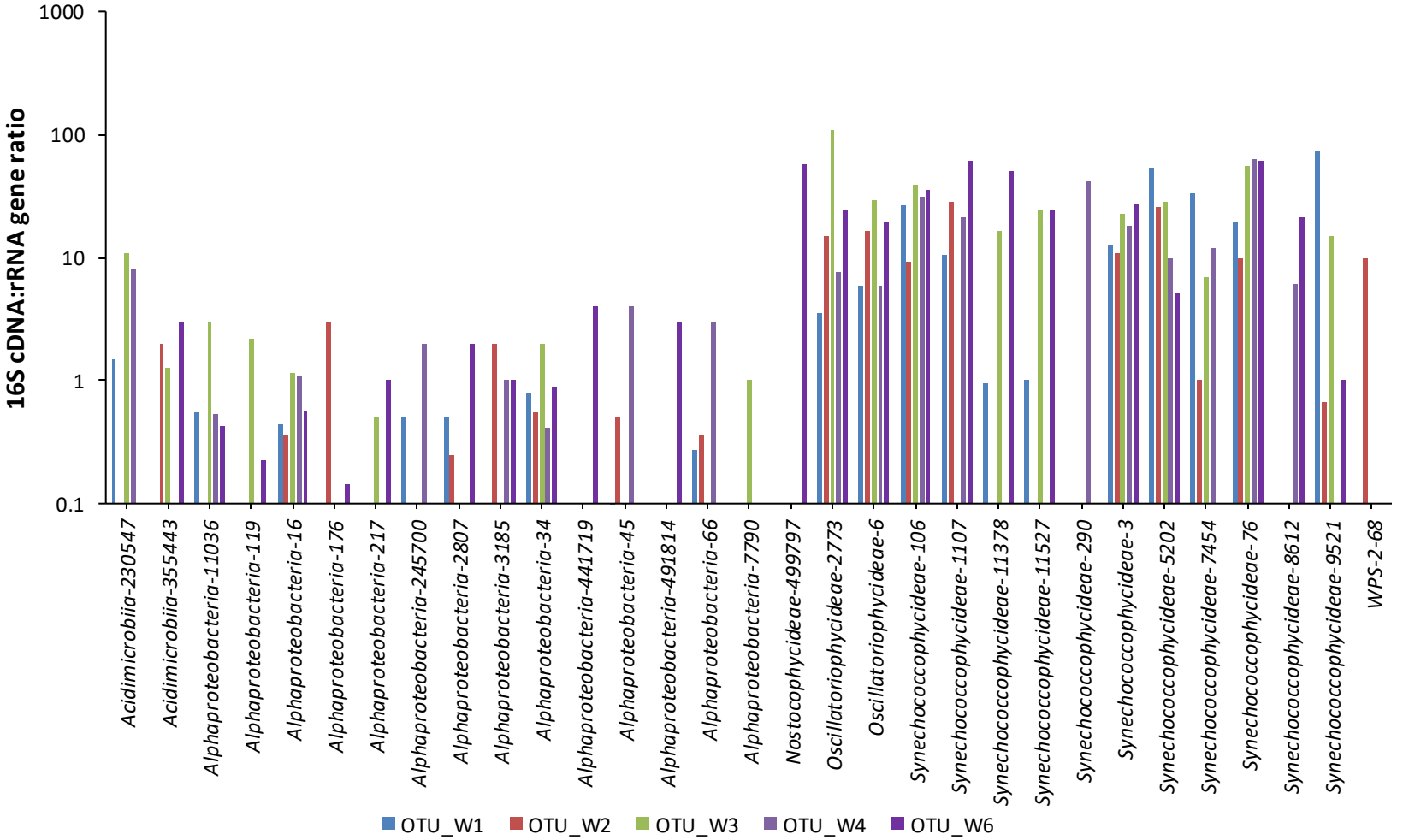

Figure 7. 12 Protein synthesis potential of specific taxa observed in cryoconite from week (W) 1 to 6, using 16S rRNA genes and 16S cDNA.

Relative abundance of snow bacterial phyla showed that *Alphaproteobacteria* (families *Methylobacterium, Sphingomonadaceae, Acetobacteraceae, Rickettsiaceae, Caulobacteraceae, Bradyrhizobiaceae* and *Methylocystaceae*), *Gammaproteobacteria* (families *Enterobacteriaceae* and *Pseudomonadaceae*), *Acidobacteria* (families *Acidobacteriaceae* and *Solibacteraceae*) and *Bacteroidetes* (family *Chitinophagaceae*) were the most abundant and active members of the snow community (Figure 7. 10B and Figure 7. 11B). *Firmicutes*, WPS-2 and *Armatimonadetes*, while active, were low in abundance. The remaining taxa from phyla *Bacteroidetes*, *Gammaproteobacteria*, *Betaproteobacteria* and *Cyanobacteria* displayed relatively high activity, apart from *Actinobacteria* and some unassigned phyla. Broad spectrum activity analysis of bacterial sequences from the snow environment showed that *Alphaproteobacteria* OTUs contributed to majority of the PSP (Figure 7. 13A). Most *Alphaproteobacteria* were preferentially abundant in each week, with *Methylobacterium*-6342 having the highest observed PSP (12.37%), however, *Methylobacterium*-1, a marine *Methylobacterium* species, *Sphingomonas*-15 and *Methylobacterium*-1508, *Methylobacterium brachiatum,* were active for nearly the entire season. *Acidobacteria* taxa were only present at high PSP towards the end of the season. Taxa that contributed to less than 1% PSP belonged to *Betaproteobacteria* (6 OTUs) during weeks 1, 3, 6 and 7, *Saprospirae* (2 OTUs) during weeks 3 and 7, *Sphingobacteriaceae* (1 OTU) at week 6, Chloroplast DNA (4 OTUs) at week 2, *Cytophagia* (6 OTUs) at week 6 - 7 and *Gammaproteobacteria* (4 OTUs) at week 3.

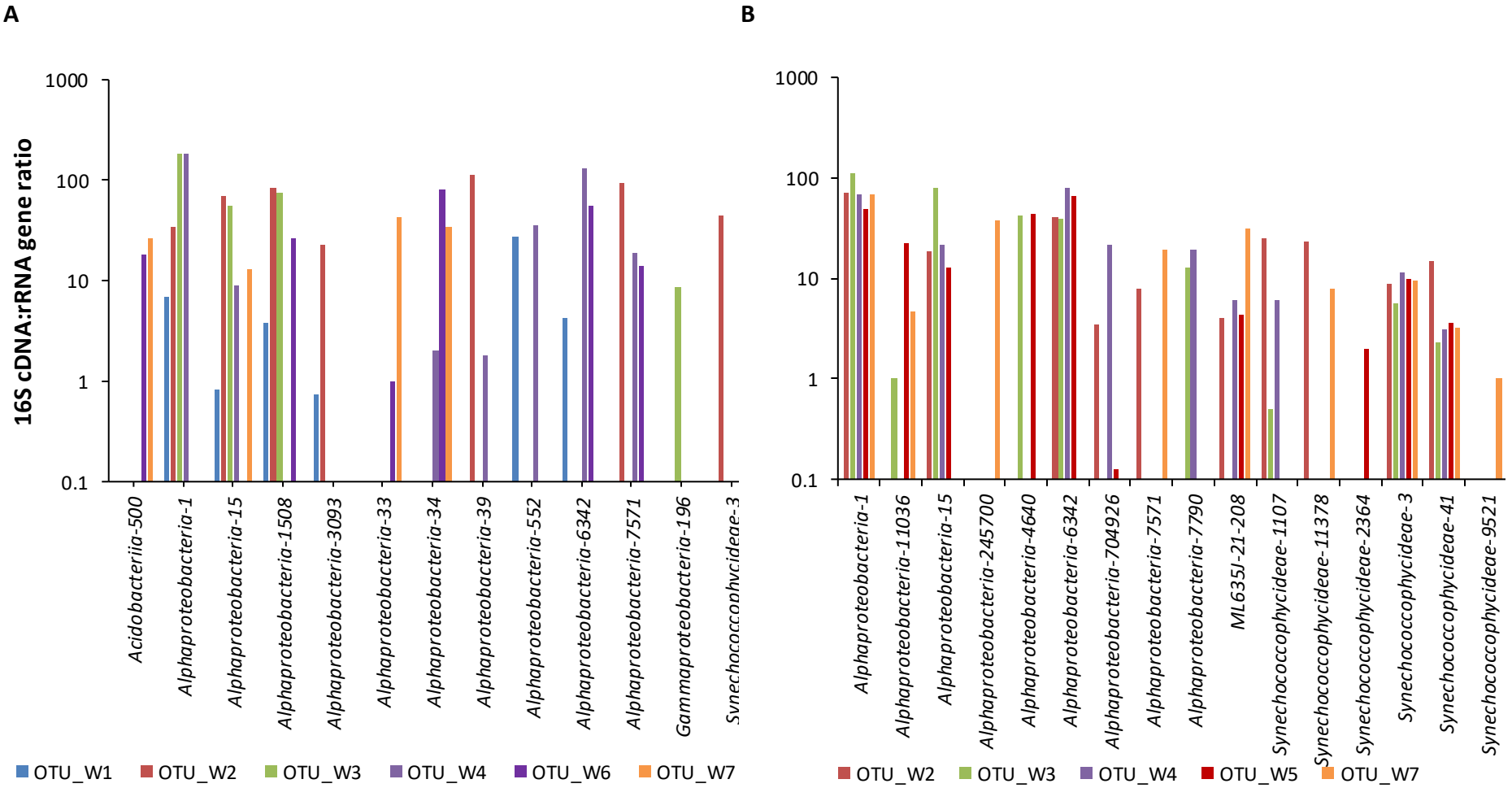

Figure 7. 13. Taxa specific protein synthesis potential observed in abundant (A) snow and (B) stream bacterial phyla, characterising the Greenland Ice Sheet using 16S rRNA gene region and 16S cDNA.

Stream bacterial communities had the most diverse range of potentially active taxa (Figure 7. 10C). *Alphaproteobacteria* (families *Sphingomonadaceae*, *Methylobacteriaceae*, *Acetobacteraceae*, *Rickettsiaceae*, *Caulobacteraceae*, *Sphingomonadales*, *Methylocystaceae*, *Bradyrhizobiaceae* and *Rhodospirillaceae*) are the most active and abundant member of the stream bacterial communities, followed by *Verrucomicrobia* (family *Chthoniobacteraceae*), OD1, *Firmicutes* and the cyanobacterial families *Pseudanabaenaceae*, *Chamaesiphonaceae*, ML635J-21 and MLE1-12 (Figure 7. 11C). In the stream community, high PSP was observed in denovo-17, *Granulicella aggregans*, denovo-22, candidatus *Planktophila limnetica*, *Alphaproteobacteria* taxa denovo-55, denovo-66, denovo-69, denovo-74, *Betaproteobacteria* denovo-5 (*Polaromonas* species), OD1 denovo-93 and *Saprospirae* taxa denovo-8 and denovo-80, over the entire sampling season (Figure 7. 13B). Additionally, *Methylobacterium*-1, *Blastomonas*-16, *Acetobacteraceae*-27, *Novosphingobium*-34 and the *Synechococcophycideae* taxa, *Chamaesiphon subglobosus*-41 and *Phormidesmis priestleyi*-3, displayed high PSP from week 2 - 7. Low PSP (>1% RA) was observed in *Actinobacteria* (1 OTU), *Alphaproteobacteria* (6 OTUs), *Betaproteobacteria* (1 OTU), OD1 (1 OTU), *Saprospirae* (2 OTUs) and WPS-2 (2 OTUs), also from week 2 - 7.

7.3.5. Rank abundance and relative recovery identifies the rare biosphere

Rare OTU status was ascribed to those taxa with a relative abundance of <1%. Taxa yielding percentages above this threshold were determined to be dominant, but constituted a small percentage of the total community in cryoconite (3.53%), snow

(1.94%) and streams (2.30%). The rank abundance curves explain that rare and exceptionally rare (<0.01%) OTUs in cryoconite contribute to 48% RA, 40.45% RA in snow and 42.36% RA in stream habitats, which additionally contribute to PSP at a threshold frequency of 1 (Denef *et al.*, 2016), during the 7 week sampling period.

A high relative recovery was observed in the cryoconite environment consisting of 291 OTUs. Cyanobacterial and alphaproteobacterial OTUs were the active dominant community members (Figure 7. 14A). Additionally, phantom OTUs were prominent with 48.41% abundance in cryoconite, but were limited to a few *Cyanobacteria*, *Alphaproteobacteria* and *Gammaproteobacteria* taxa. The relative recovery was low in the snow environment, with 271 ranked OTUs (Figure 7. 14B). Exceptionally rare OTUs were most active and were members of the phylum *Alphaproteobacteria,* which additionally contributed to the high phantom OTU percentage of the snow ecosystem (61.31%). Rare OTUs were abundant in the bacterial stream community (Figure 7. 14C) and phantom OTUs contributed to 42.93% of the composition. Relative recovery was the greatest in the stream environment, as 322 rankable OTUs could be distinguished. The phyla *Cyanobacteria*, *Alphaproteobacteria* and *Acidobacteria* demonstrated high activity in both rare and phantom OTUs, while *Deltaproteobacteria* showed activity solely in the rare OTU component.

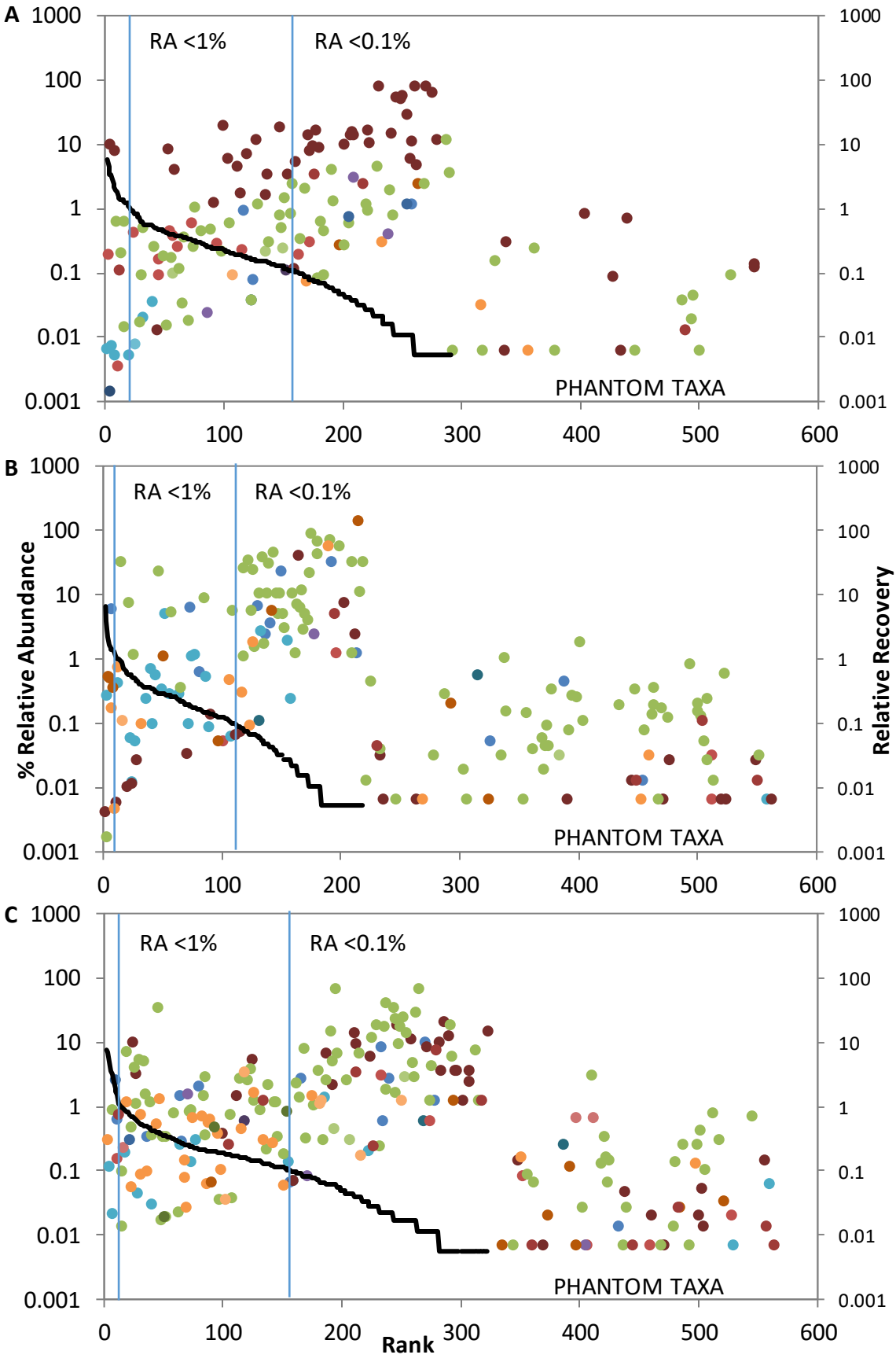

Figure 7. 14 Rank abundance of OTUs relative to their activity in (A) cryoconite, (B) snow and (C) stream communities, showing rare (RA <1%) and exceptionally rare (RA <0.01%) rare taxa.

7.3.6. Keystone taxa in the rare active supraglacial community of the Greenland Ice Sheet

Betweenness scores identified 16 keystone OTUs from 16S cDNA and 16 rRNA gene communities on the Greenland Ice Sheet. Nine *Alphaproteobacteria* OTUs (*Sphingomonadaceae*, *Acetobacteraceae* and *Methylobacterium*), 6 *Cyanobacteria* OTUs (*Leptolyngbya* and *Xenococcaceae*) and a single *Betaproteobacteria* OTU (*Comamonadaceae*) represent possible keystone members (Table 7. 5). Nine of these OTUs constitute the core S6 bacterial community that is representative of the rare and exceptionally rare biosphere, while 12 OTUs are taxa with high protein synthesis potential (Figure 7. 12).

Specific taxa-habitat-PSP connections can be observed for *Phormidesmis priestleyi*-3, whose presence overlaps in all 3 habitats, *Novosphingobium*-34, that overlaps in snow and cryoconite habitats, and *Methylobacterium*-1, *Sphingomonas*-15 and *Methylobacterium tardum*-6342, that overlap in snow and stream habitats. Keystone taxa, *Phormidium*-6, *Chroococcus*-2773, *Blastomonas*-16, *Phormidesmis*-290, *Leptolyngbya*-106 and *Leptolyngbya*-76 (*Phormidesmis* species), have high PSP in cryoconite, with the remaining denovo-1508 having high PSP in snow.

Table 7. 5 Keystone taxa identified from cryoconite, snow and stream habitats at weather station S6 and an indication of their rare OTU status (<1% RA) marked with a * and core OTUs within each habitat marked with a [x]. BC = betweenness centrality

OTU	Phylum	Class	Order	Family	Genus	BC	RA >1%	% RA Cryoconite	%RA Snow	% RA Stream
Denovo-14	*Proteobacteria*	*Alphaproteobacteria*	*Sphingomonadales*	*Sphingomonadaceae*	-	7.166667	+	1.39	0.10*	3.55 [x]
Denovo-5	*Proteobacteria*	*Betaproteobacteria*	*Burkholderiales*	*Comamonadaceae*	-	6.25	+	0.02*	1.02	7.55 [x]
Denovo-1	*Proteobacteria*	*Alphaproteobacteria*	*Rhizobiales*	*Methylobacteriaceae*	*Methylobacterium*	4.992857	+	0	0.93* [x]	0.40* [x]
Denovo-34	*Proteobacteria*	*Alphaproteobacteria*	*Sphingomonadales*	*Sphingomonadaceae*	-	4.75	+	1.27	0.04* [x]	0.86* [x]
Denovo-27	*Proteobacteria*	*Alphaproteobacteria*	*Rhodospirillales*	*Acetobacteraceae*	-	2.916667		0.32*	0.03	0.70* [x]
Denovo-6	*Cyanobacteria*	*Oscillatoriophycideae*	*Chroococcales*	*Xenococcaceae*	-	2.87619	+	2.12 [x]	0.01*	1.06
Denovo-2773	*Cyanobacteria*	*Oscillatoriophycideae*	*Chroococcales*	*Xenococcaceae*	-	2.542857		0.42* [x]	0	0.10*
Denovo-15	*Proteobacteria*	*Alphaproteobacteria*	*Sphingomonadales*	*Sphingomonadaceae*	*Sphingomonas*	2.15	+	0.01*	0.58*	0.53* [x]
Denovo-16	*Proteobacteria*	*Alphaproteobacteria*	*Sphingomonadales*	*Sphingomonadaceae*	-	1.833333	+	1.89 [x]	0.01*	0.59* [x]
Denovo-1508	*Proteobacteria*	*Alphaproteobacteria*	*Rhizobiales*	*Methylobacteriaceae*	*Methylobacterium*	1.37619		0	0.05 [x]	0.06*
Denovo-290	*Cyanobacteria*	*Synechococcophycideae*	*Pseudanabaenales*	*Pseudanabaenaceae*	*Leptolyngbya*	1.092857		0.02* [x]	0	0.01*
Denovo-32	*Proteobacteria*	*Alphaproteobacteria*	*Rhodospirillales*	*Acetobacteraceae*	-	1.083333		0.05*	0.15	0.50*
Denovo-3	*Cyanobacteria*	*Synechococcophycideae*	*Pseudanabaenales*	*Pseudanabaenaceae*	*Leptolyngbya*	0.75	+	3.47 [x]	0.02*	0.71* [x]
Denovo-106	*Cyanobacteria*	*Synechococcophycideae*	*Pseudanabaenales*	*Pseudanabaenaceae*	*Leptolyngbya*	0.509524		0.13* [x]	0	0.03*
Denovo-76	*Cyanobacteria*	*Synechococcophycideae*	*Pseudanabaenales*	*Pseudanabaenaceae*	*Leptolyngbya*	0.509524		0.23* [x]	0	0.05*
Denovo-6342	*Proteobacteria*	*Alphaproteobacteria*	*Rhizobiales*	*Methylobacteriaceae*	*Methylobacterium*	0.2	+	0	0.30* [x]	0.06* [x]

7.4. DISCUSSION

Greenland Ice Sheet bacterial communities reveal a vastly diverse taxonomic profile that is highly specific in snow and cryoconite communities, while ephemeral streams exhibit a bacterial profile that is an amalgamation of the two previously mentioned microhabitats. The potential activity of the observed microbes demonstrates that majority of the activity in cryoconite and stream environments is attributed to *Cyanobacteria* of the *Phormidesmis*-like genus and to *Methylobacterium* taxa in the snowpack. Top-scoring members in each habitat contributed to both core OTU and keystone taxa that potentially drive each community. It is interesting to note the presence of *Methylobacterium* as dominant in glacial water habitats, particularly as the observed taxa closely resemble those observed in Chinese sea water (*Methylobacterium brachiatum*, Accession ID KU173579.1) and Trans-Himalayan lake ecosystems (*Methylobacterium tardum*, Accession ID KR085941.1). Additionally, they are among known contaminants of bacterial samples, as described by Salter *et al.* (2014), however, the role of lab and kit contaminants in this investigation was shown to be negligible by eliminating the biased influence of contaminant genera with negative control sequences. From the large proportion of observed taxa present at lower abundance than in previous chapters, and the high 16S cDNA:16S rRNA gene ratio, it is logical to deduce that the Ice Sheet community is highly influenced by the readily fluctuating rare, but metabolically active, bacterial taxa that reside therein (Campbell *et al.*, 2011; Aanderud *et al.*, 2015).

7.4.1. Greenland Ice Sheet bacterial communities display spatial and temporal variability

The bacteria uncovered in weather station S6 supraglacial communities were revealed to be highly diverse within the Kangerlussuaq region, with a weak, yet unquestionable relationship to Greenlandic cryoconite and ice communities previously described from Tasiilaq in the north east, Qaqortoq in the south west and Thule in the north west. This is supported by taxonomic affiliations that have shown preference to *Phormidesmis* (KAN P and THU) and candidate phylum WPS-2 (QAS, TAS*)* (Stibal *et al.*, 2015b; Cameron *et al.*, 2016). The RNA pool provides a more reliable determination of the recent cellular activity, due to the short half-life of extracellular RNA, when compared with DNA, in addition to being governed by rapid rates of intracellular turnover (Novitsky, 1986). Within the S6 locale, the community of heterotrophic bacteria in cryoconite, snow and stream water, show inherent differences in total biomass (16S rRNA gene) and potential activity (16S cDNA), within and between habitats. The significant differences observed between total and active communities are congruent with previous work by Stibal *et al.* (2015b) in mirror studies at inland and marginal areas on the Greenland Ice Sheet. Similarities persisted in both ephemeral stream and snow habitats, indicating a trend of the activity on the supraglacial surface to be attributed to a small group of taxa from *Cyanobacteria* and *Proteobacteria* subclasses that are recruited from the rare biosphere.

Commonly recognised cryoconite taxa from the family *Pseudanabaenaceae,* now known to belong to the clade *Phormidesmis*, dominate S6 cryoconite for the duration

of the season, with individual OTUs displaying preferential high activity during specific weeks. This differs from the rest of GrIS that exhibits high 16S rRNA gene abundance of *Phormidesmis*-35 and high potential activity, based on 16S cDNA presence for a taxon in the candidate phylum WPS-2 (Cameron *et al.*, 2016). These results are, however, in agreement with recent data from Greenland that demonstrated co-dominance of *Proteobacteria* and *Cyanobacteria* in active communities (Edwards *et al.*, 2014b; Stibal *et al.*, 2015b). Snow and stream habitats, while distinct in genomic variation and high potential activity, revealed an environment sensitive to the lack of mechanical stability and changing environmental conditions, particularly to the effect of melt, incident radiation and albedo, the latter of which minimally affected S6 cryoconite bacterial communities. The aquatic glacier environments varied greatly over the duration of the summer months, with marine *Methylobacterium*-1 (*Alphaproteobacteria*) dominant and active during early summer, in both snow and stream habitats, giving way to *Granulicella aggregans*-17 (*Acidobacteriaceae*) in snow communities and *Spartobacterium*-26 (*Verrucomicrobia*) in stream communities, later in the season. The observed high activity is consistent with epifluorescence microscopy-based cell counts of Greenland ice surface samples (Stibal *et al.*, 2015a), inferring a baseline supply of cellular material from localised atmospheric sources, when observing alpha diversity indices.

Functional redundancy may be the primary factor influencing the temporal fluctuation in bacterial community composition in each habitat (Allison and Martiny, 2008; Shade *et al.*, 2014) and may be more robust in habitats such as ephemeral

streams, as evidenced by the increasing species richness. The higher intensity of the transient changes in taxa abundance and potential activity, steers the niche habitat, be it cryoconite, snow or stream, favouring selection of more resilient nutrient providers or decomposers. This creates a seasonal shift in the bacterial community, enhancing the capacity of microbial community survival under more nutrient starved conditions, following the period of intense growth, microbial turnover and environmental stability, similar to that observed in 16S analyses of the active layer of permafrost (Schostag *et al.*, 2015). This pattern is frequently detected in macroorganisms, where the importance of local natural cues, such as resource limitation, oxygen or temperature stress and stochastic perturbations (Keeley, 1987; Lewis, 2007), and regional cues, like air temperature and incident radiation (Hairston *et al.*, 1990; Vazquez-Yanes and Orozco-Segovia, 1990), drive an organisms entry and exit into high or low metabolic activity periods.

7.4.2. Active and rare taxa dominate surface habitats at weather station S6

Community sustainability in consistently nutrient poor and low temperature conditions requires periodic changes in abundance of the organisms that dominate, to survive starvation conditions in a narrow niche. It can be postulated that the high levels of activity in permanently rarer species and potential keystone taxa prevalent in cryoconite, snow and stream habitats on the Greenland Ice Sheet facilitate this, as the environment has specifically selected for transiently rare taxa (Lynch and Neufeld, 2015). The rare biosphere contains both dormant and active slow-growing taxa, emphasising the disparity between the rare biosphere and a seed bank. Jones

and Lennon (2010) confirm that many studies have hypothesised the connection between abundant and rare taxa and active and inactive metabolic rates, however, relatively few studies have linked bacterial dynamics with environmental and potential metabolic activity over time (Edwards *et al.*, 2014b; Stibal *et al.*, 2015b; Cameron *et al.*, 2016). Here, algorithmically identified keystone bacteria that are recognised as rare taxa, associate well with high relative abundance and high protein synthesis potential taxa in each of the S6 habitats, allowing a model of community initiation and growth in summer months on ice sheets to be predicted.

Bacterial taxa present at a relative abundance of less than 1% exhibited disproportionately high potential activity and were the most abundant members of the cryoconite, snow and stream communities (Figure 7. 12 and Figure 7. 13). These taxa form the rare biosphere on the surface of S6, demonstrating continued high stability in cryoconite and substantial variation over the duration of the Arctic summer in snow and stream habitats. This observation is consistent with recent temporal and structural observations in the nearby Leverett glacier (Musilova *et al.*, 2015). Highly preserved winter habitats on ice surfaces are exposed to stochastic sampling, air-ice surface interaction and an abundance of legacy DNA in the cryosphere during summer, however, minimal influence of aeolian origin has been established in cryoconite compared to snow communities, when considering cell counts and air and supraglacial surface bacterial diversity (Musilova *et al.*, 2015). It can be inferred from this knowledge that the presence of phantom OTUs (Klein *et al.*, 2016) are a consequence of these seeding events, accounting for the high 16S rRNA

gene:16S cDNA ratios observed in glacial habitats. These taxa additionally form part of the exceptionally rare biosphere, displaying 16S rRNA gene abundances of <0.01%.

Insights into the protein synthesis potential of each supraglacial habitat, highlights the preference of specific low abundance keystone species, namely *Chroococcus*, *Phormidesmis*, *Sphingomonas, Acetobacteraceae*, *Polaromonas* and *Methylobacterium,* in cryoconite, snow melt and glacial streams, further supporting the role of these taxa as cryosphere ecosystem engineers. The typical long 'tail' effect in the relative abundance in each habitat (Figure 7. 14) provides evidence of transiently active dominant OTUs, as well as recruitment from rare OTUs later in the summer. This is consistent with the Shade *et al.* (2014) study of conditionally rare taxa, that explains the recruitment of bacteria into dominant roles as they exit dormancy, as a consequence of environmental fluctuations in dry soil ecosystems introduced to water. In cryoconite, these dominant taxa are often *Phormidesmis* and *Phormidium* species, that provide the primary essential structural integrity and nutrient source (via EPS) to the rest of the cryoconite community in a transient fashion. They consequently recruit previously dormant freeze-thaw tolerant cyanobacterial taxa (*Xenococcaceae* and *Nostocales*) for their photosynthetic and nitrogen fixation abilities in mid and late summer, because of the more favourable weather conditions. Additionally, the potentially active cyanobacterial community coincides with peaks in *Alphaproteobacteria* potential activity, as in Stibal *et al.* (2015b), alongside taxa that are frequently recruited from the rare biosphere for their multitude of chemoorganotrophic functions in maintaining biogeochemical balance

in the cryoconite habitat, including sugar assimilation (*Sphingomonadales*) and carbon acquisition (*Acidimicrobiales*) from simple carbon compounds (*Methylobacterium*).

Majority of the changes in community dynamics of these disproportionally rare taxa can be explained by the effects of time (PERMANOVA, pseudo-F = 2.9236, $P = 0.001$) and space (PERMANOVA, pseudo-F = 29.599, $P = 0.001$) and the interaction between the two (PERMANOVA, pseudo-F = 1.9161, $P = 0.004$), supporting observations in one out of two papers based on recent similar Greenland Ice Sheet cryoconite studies (Stibal *et al.*, 2015b; Cameron *et al.*, 2016). The large percentage of variation that exists in the 16S rRNA gene region across all environments limits the degree to which changing environmental conditions predict the overall abundance of DNA. Redundancy analysis of the 16S cDNA sequences show that each habitat has a unique bacterial driver from the rare biosphere (Figure 7. 13A), sequentially identifying *Methylobacterium*-1 and *Blastomonas*-16 as the major contributors to the rare biosphere diversity in ice sheet snow and stream habitats.

Similarly, environmental factors that can predict the snow and cryoconite rare biospheres were identified as incident radiation and the degree of melt (Figure 7. 15B), which is further supported by RELATE analysis of the environmental factors prevalent on the Greenland Ice Sheet (R = 0.125, $P = 0.014$), with a visible time effect. Without active melt, there is no liquid water available to penetrate the porous weathering crust of the Greenland Ice Sheet. Majority of the meltwater generated is

at the surface of the ice sheet, as described in studies by Bartholomew *et al.* (2010), Sole *et al.* (2011), Cowton *et al.* (2013), Chandler *et al.* (2013) and Chu (2014). Recent work suggests that there are depth limited aquifers in the Kangerlussuaq weathering crust, indicative of the critical role of ice sheet hydrology on GrIS (Cooper *et al.*, 2017). However, within the S6 area, the prevalence of low gradient slow moving ice stabilises the cryoconite hole hydrology (Cook *et al.*, 2016a; Cook *et al.*, 2016b). Furthermore, similar to the Foxfonna dome and valley glacier studies, the absence of stream channels at the sites investigated, demonstrates a lack of hydrological influence. Instead, *biotic* effects significantly outweigh any external environmental actions observed.

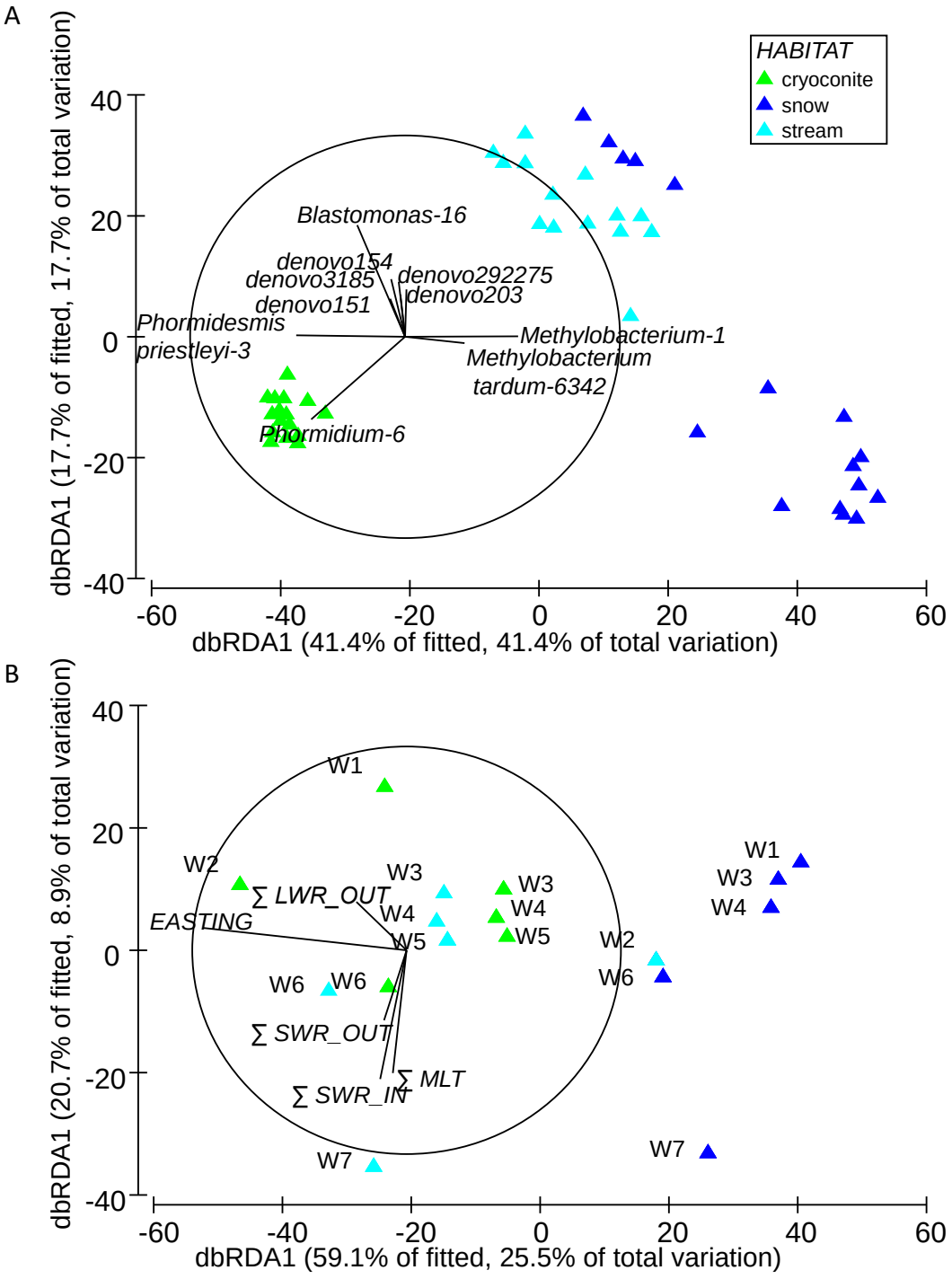

Figure 7. 15 Distance-based redundancy ordination highlighting the GrIS (A) bacterial community predictors and (B) environmental predictors with correlation >0.2.

It is worth mentioning that these rare active taxa display a minutely higher distance decay in supraglacial habitats ($\rho = 0.236$, $P = 0.02$) compared to the abundant active community ($\rho = 0.229$, $P = 0.01$), congruent with other studies that demonstrate rare taxa exhibit distinct spatial distributions akin to the abundant community (Liu *et al.*, 2015). Evidently, this is no surprise as the rare localised community is constrained by the same variables as the abundant community, with little statistical variation (APPENDIX V, Table V. 10, Table V. 11, Table V. 12 and Table V. 13). In contrast, the higher significance of distance decay at the regional scale confirms the hypothesis that the dynamics of rare taxa assembly follow the prediction of the Hubbell model, that organisms with the same fitness can occupy a given environment depending on migration, compositional drift and extinction (Hubbell, 2001), with simultaneous environmental filtering.

When observed individually, only the snow rare biosphere was directly affected by the constraints imposed by the environment ($R = 0.489$, $P = 0.001$), particularly incoming and outgoing short wave radiation and the melt rate during late summer. The main influence is derived from the dominant taxa *Methylobacterium*-1 and *Methylobacterium*-6342. *Methylobacterium* is widely recognised as a contaminant of filter units in extraction kits (Salter *et al.*, 2014; Glassing *et al.*, 2016), however, by employing negative controls from PCR amplicon preparation through to library generation and sequencing, false positive identification of this bacteria was negated. Independent bioinformatic analysis of the 16S rRNA gene region and 16S cDNA sequences with the negative controls revealed *Methylobacterium* taxa were present

at 10.83% RA, in the filtered unrarefied dataset, outweighing the observed 0.00012% RA, in both 16S rRNA gene and 16S cDNA negative control sequences.

A stand-out feature of the snow environment bacterial community is the lack of potentially active *Cyanobacteria* as the main photoautotrophic organism, despite favourable conditions of light and melt. Considering that snow communities of the Greenland Ice Sheet actively support early and late season microalgae species (Yallop *et al.*, 2012; Lutz *et al.*, 2015b), it is possible that these highly phototrophic taxa provide the necessary primary nutrients, while the heterotrophic bacterial community allows maintenance of most essential nutrients via decomposition and natural apoptosis. They may further contribute to protein and lipid-like dissolved organic matter (DOM) during early melt season and lignin-like DOM in late melt season (Bhatia *et al.*, 2010). The sequestering of the necessary nitrogen is obtained via the surrounding stream and cryoconite habitat, supporting the appearance of N_2-fixing *Acetobacteraceae* later in the summer. The overall rare snow community is also abundant in biosurfactant-producing *Pseudomonas* species and possible endocytobionts (*Rickettsiaceae*) involved in bacterial biocontrol, in addition to the *Alphaproteobacteria* that are highly prevalent in all habitats and for the entire duration of the Greenlandic summer.

Glacier-fed stream communities are described as highly dynamic ecosystems for microbial growth, permitted by the relatively constant conditions that are predominant (Wilhelm *et al.*, 2014). As majority of the identified taxa are in active

states, stream ecosystems are not prone to maintaining pro-dormancy taxa when compared to the sedentary and stabilised cryoconite niche. Furthermore, dormancy may not reliably be inferred from active and bulk 16S communities, according to recent simulations of rRNA:cDNA ratios by Steven *et al.* (2017). Musilova *et al.* (2017) found that microbial production significantly correlated with the concentration of labile dissolved organic species in glacier surface meltwater. *Phormidesmis* taxa, alongside the cohort of transiently recruited *Alphaproteobacteria*, form the main bacterial community of the stream ecosystem. As adjacent habitats are characterised by similar high abundance taxa with high potential activity, it can be inferred that the increased hydrological activity in summer months permits the dispersal of these taxa in linked habitats.

Comparative studies with recent work on Greenland Ice Sheet demonstrate many similarities and contrasts with the bacterial communities prevalent in cryoconite and snow habitats. Stibal *et al.* (2015b) found that the differences in community activity between margin and interior cryoconite were more distinct and significant for site than the bacterial community. This is no surprise as biogeography has now been shown to moderately impact the structure and diversity of bacterial communities on the Greenland Ice Sheet (APPENDIX V, Figure V. 1) (Cameron *et al.*, 2016). At the localised scale, the marginal habitat is analogous to weather station S6, resulting in the similar bacterial community composition, as well as the co-dominance of cyanobacterial and proteobacterial taxa. Despite the similarity in bacterial community composition with that study, richness estimates and OTU counts of

cryoconite on AWS S6 shows negligible differences between total biomass and potentially active taxa, however, 16S rRNA gene region and 16S cDNA sequences are distinct in community composition. Activity of cyanobacterial taxa in S6 are highlighted as stable throughout the ablation season, congruent with Musilova *et al.* (2015). Radiolabelled carbon signals indicated that primary productivity in cryoconite increase during the ablation season, coinciding with the increasing relative abundances of photoautotrophic *Cyanobacteria*, and the subsequent heterotrophic uptake of organic carbon from the co-dominant proteobacterial taxa (Musilova *et al.*, 2015).

While the primary colonisation of both snow and cryoconite surfaces were demonstrated in these previous studies, neither were able to demonstrate the effect of the succession of rare active taxa from primary colonisers that exhibit fast turnover after the initial melt, and the role of specific taxa in this process. Evidence for this is provided by the temporal changes in protein synthesis potential of cryoconite (Figure 7. 12) and ephemeral streams (Figure 7. 13B). This indicates robust control by numerous co-dominant *Synechococcophycideae* and *Alphaproteobacteria*, in cryoconite, snow and stream habitats (Figure 7. 13A), being constrained by alphaproteobacterial activity. Some of these represent key taxa involved in ecosystem engineering, primary productivity (*Phormidesmis priestleyi*-3), and degradation of organic compounds (*Sphingomonas*-15, *Methylobacterium*-6342 and *Methylobacterium*-1) (White *et al.*, 1996; Haruta and Kanno, 2015).

7.5. SUMMARY

High community turnover (Wilhelm *et al.*, 2013) is essential to maintain bacterial diversity in all glacial surface habitats. Abiotic conditions, specifically incident radiation and surface melt, drives some of the variation in the snow and ephemeral stream bacterial communities, while the cryoconite habitat maintains a stable assemblage during the ablation season. The heterotrophic bacteria and phototrophic *Cyanobacteria* observed, display strong seasonal fluctuations on the Greenland Ice Sheet, that is possibly co-ordinated by the rare taxa that dominate over the course of the summer. Metabolically diverse and multi stress tolerant generalist taxa *Methylobacterium* and *Sphingomonas* (Haruta and Kanno, 2015), form the basis of ice and snow communities, while cryoconite and glacial stream habitats are governed by selected C*yanobacteria* and *Proteobacteria* taxa. Thus, the dynamic nature of the ice sheet environment can be explained by interactions that exist between the cryosphere, the active community of primary producers and the rare heterotrophic consortium.

CHAPTER 8 – GENERAL DISCUSSION

The supraglacial surface represents an interface between ice and the atmosphere which is conducive to microbial life, supporting the phototrophic and heterotrophic microbial communities that dominate snow, ice and cryoconite habitats. Invaluable insights into the assembly, biogeography and function of microbial communities across multiple scales can be gained from understanding the distributions of microbiota (Bell *et al.*, 2005; Bell, 2010). As such, understanding the organization of community composition can provide insights into the microbial colonization of an extreme environment and the consequential interactions with melt responses of glacial ice surfaces.

The principal aim of this thesis was to untangle the complex spatial and temporal interactions prevalent in supraglacial surface communities in Svalbard and Greenland. This was achieved by successfully establishing the metabolome of synthetic newly seeded and natural cryoconite communities and the 16S rRNA gene complement and 16S rRNA-derived ribosomal profile of ice surface habitats on Foxfonna, Svalbard and the South-western margin of the Greenland Ice Sheet, during the Arctic summer melt season that is favourable to microbial growth. Synthetic cryoconite revealed the stages in early cryoconite development by microscopy, as well as provided an indication of the metabolites integral to these communities under idealized summer conditions, in terms of temperature and photosynthetically active radiation receipt. Authentic cryoconite was then investigated on Foxfonna ice cap, to

establish the abundant bacterial community prevalent, the cryoconite metabolic profile and their respective responses to topology and microclimate. Cryoconite from the Foxfonna ice cap outlet valley glacier was investigated to establish elevation and temporal controls on these communities and their metabolomes. Finally, the bacterial community of Greenland Ice Sheet surfaces were investigated to observe changes in the active bacterial community over time within different habitats.

8.1. Technical considerations

Culture independent analytical techniques have revolutionised investigations of microbial communities, specifically for gene sequencing of PCR amplified marker genes and whole genome shotgun metagenomics. While these deep sequencing techniques provide extensive information revealing exquisite microbial interactions, taxonomic distribution can be affected as a result of technical caveats and methodological limitation. Each chapter in this compilation focused upon extensive coverage of a single site and solely targeted the bacterial community for sequence-based analyses. This informed on the strategic development of aims and hypotheses for the consecutive chapters. The presence of notable eukaryotic and viral supraglacial communities (Sawstrom *et al.*, 2002) has previously been established beyond the scope of this research, as well as reliable reports of Archaea associated with cryoconite, albeit from Alpine and Antarctic cryoconite (Cameron *et al.*, 2012; Hamilton *et al.*, 2013). 16S rRNA gene sequences derived from both Ion Torrent semiconductor sequencing and Illumina® sequencing platforms did not yield Archaea-specific amplicons during the taxonomic affiliation process in QIIME, in line

with other work, suggesting that Archaea are not detected in Arctic cryoconite (Edwards *et al.*, 2011; Cameron *et al.*, 2012); as such, research was focused upon the bacterial community.

Differing DNA extraction processes generate discernible inconsistencies in genomic DNA yield and quality. Here, bulk DNA extraction coupled with amplicon semiconductor sequencing of the 16S rRNA gene was initially employed, in line with many other contemporary studies in microbial ecology (Prosser, 2012). This was then modified to DNA extraction using commercial kits for high throughput 16S rRNA gene and 16S cDNA Illumina sequencing. These studies all entail systematic biases in extraction, amplification and sequencing (Lee *et al.*, 2012), in addition to potential contamination risk from reagents and laboratory (Salter *et al.*, 2014). As such, rigorous attention was paid to eliminate potential sources of error or contamination, including a randomized processing order and the inclusion and analysis of procedural and sequencing control specimens. For Foxfonna ice cap, bulk DNA extracts included templates from both active and inactive taxa (Blazewicz *et al.*, 2013; Klein, 2015), thus the detection of temporal variation in activity levels is precluded (Stibal *et al.*, 2015b). This is not the case in other chapters that use the ice cap study as preliminary evidence to further detect temporal variation in activity, as determined by metabolomic activity on the ice cap in Chapter 5, metabolomic spatio-temporal variation in valley glacier cryoconite in Chapter 6 and 16S rRNA gene:16S cDNA ratios in ice sheet habitats in Chapter 7.

All field sites identified the integral role of *Cyanobacteria*, specifically the dominant taxon identified in the Greengenes database as *Leptolyngbya*, a commonly observed species in the Arctic. It should be noted that the highly dominant OTUs on Foxfonna ice cap (*Leptolyngbya*-40205), Foxfonna valley glacier (*Leptolyngybya*-33968, *Leptolyngbya*-57985) and Greenland Ice Sheet (*Leptolyngbya*-3, *Leptolyngbya*-76, *Leptolyngbya*-106, *Leptolyngbya*-1107, *Leptolyngbya*-290, *Leptolyngbya*-5202¸ *Leptolyngbya*-11378, *Leptolyngbya*-60664) assigned to this genus within the Greengenes taxonomy database, possess closest named relatives within three Antarctic strains (Accession ID AY493580.1, AY493581, AY493581.1) and a Svalbard strain of *Phormidesmis priestleyi* (Accession ID KU219729.1), which is also the closest relative of Sanger-sequenced clone library *Oscillatorean* cyanobacterial OTUs from cryoconite elsewhere on Svalbard (Edwards *et al.*, 2011), and dominates the active bacterial community of cryoconite on the southwestern margin of the Greenland Ice Sheet (Cook *et al.*, 2016a). As the phylogenetic placement of *Cyanobacteria* from the cold biosphere improves (Chrismas *et al.*, 2015; Chrismas *et al.*, 2016), so will the taxonomic affiliation of this cryoconite ecosystem engineer, which currently resides within the *Phormidesmis*-like clade of cold adapted *Cyanobacteria*.

8.2. The mechanism of cryoconite conglomeration

Inputs of microbes and mineral dusts are essential for the initiation of the agglomeration process that promotes entrainment of minerals by the growth of filamentous microbes and microbial EPS driven by primary production. Microbial accumulation on ice surfaces mediates the formation of cryoconite to support the

microbial activity of a heterotrophic microniche. This was demonstrated by the observation of newly seeded microcosms that exhibited strong signals of microbial colonisation on individual granules prior to agglomeration. Examination of the pioneering communities has revealed an evolution of seed communities from a matrix of granular sediment and minerals to filamentous aggregates, with evidence of high extracellular polymeric substances and primary production from the heterogenous microbial biomass. This is consistent with the first hypothesis on the process of establishment of cryoconite communities, that

> *There is an increase in visually detectable biomass, extracellular polymeric substances and chlorophyll a attributed to debris accumulation, pioneer microbes and filamentous Cyanobacteria*.

Alpha diversity analyses of cryoconite from natural Arctic cryoconite have indicated that both local and regional particulates are responsible for the observed diversity (Musilova *et al.*, 2015; Stibal *et al.*, 2015b), which is further supported by diversity index observations across the three different glacier surfaces investigated (APPENDIX II, Table II. 2, APPENDIX IV, Table IV. 6 and APPENDIX V, Table V. 1). Furthermore, natural cryoconite ecosystems demonstrate that

> *There is increased physical and chemical stability afforded by cryoconite granules over time, as a result of the combined action of carbohydrate agglomeration and primary production by photosynthesis.*

This is driven by allochthonous input and primary production by early blooms of unicellular algae and diatoms that predominate in Foxfonna during the summer, and

have been witnessed on glacier surfaces in polar and Alpine locations, as recorded in a recent review of the microbiome of glaciers and ice sheets (Anesio *et al.*, 2017). It is important, however, to also consider the impact of hydrology in natural versus synthetic microcosms, as hydrologic mixing of biotic, abiotic and mineralogical contributions (Langford *et al.*, 2010) adds an important hydrological element to biocryomorphlogy (Cook *et al.*, 2015a), due to the ability of hydraulic disturbances to induce erosion or disassembly in natural ecosystems.

Cryoconite environments have generally been described as stable habitats, however, 16S rRNA gene profiles have established notable fluctuations in the bacterial community (Chapter 6), similar to those in Italian Alpine glacier cryoconite (Franzetti *et al.*, 2016a). However, this is not a representation of the *active* community, and since the active and total communities can show significant differences in community composition and structure, based on Spearman rank values (APPENDIX V, Table V. 10, Table V. 11, Table V. 12, Table V. 13), it is uncertain that the metabolically active bacteria present mirror the observed 16S rRNA fluctuations. It can be confirmed, however, that there is a fluctuation in the metabolism in cryoconite over time, specifically for carbon degradation, nuclear material biosynthesis and amino acid production and metabolism (indicative of the transition from the utilisation of allochthonous and autochthonous input to the reserve fuels in the form of fatty acids), high ATP concentration and $NADH/NAD^+$ ratio created by heterotrophic metabolism. When considering the incorporation of bio-limiting nutrients in these habitats, it is observed that the Greenland Ice Sheet exports phosphorus to the Arctic

oceans via freshwater discharge (Hawkings *et al.*, 2016), providing sufficient phosphorus for biological utilisation, nitrogen, that is usually inert in the atmosphere, is fixed by cyanobacterial taxa (Hodson *et al.*, 2005), in addition to the presence of silica (silicic acid) (Hawkings *et al.*, 2017) and iron from continental crusts, biological turnover and aeolian deposition. As a consequence of these limitations and abundances, multiple species can compete in Arctic habitats, given their intrinsic abilities for light utilisation, temperature adaptation and growth rate modification on the supraglacial surface.

It is evident from confocal microscopy that pioneering cryoconite communities are heavily dependent upon the action of phototrophic filamentous *Cyanobacteria*, such as *Leptolyngbya*, *Phormidium* and *Phormidesmis,* for the formation of granules by aggregation of adjacent minerals and soil particulates. Within established microcosms, this process was absent; these granules are known to persist for 3 - 7 years before degradation (Takeuchi *et al.*, 2010). Furthermore, metabolic activity determined by the major contributors to the cryoconite metabolome, strongly indicates a heterotrophic lifestyle in newly seeded communities during the initial seeding phase, despite the abundance of primary producers on the surface of the newly forming cryoconite granule. Conversely, established communities demonstrate negligible changes in their physical attributes over time. However, the surface of the granule is characterised by large clusters of microbial biomass intermingled with photosynthetic cyanobacterial filaments. Examination of the metabolome of this microcosm community reveals consistent levels of heterotrophic

microbial activity for the duration of the simulated summer, as well as metabolic indications of primary production from the phototrophs present, consistent with recent work on lidded Antarctic cryoconite by Bagshaw *et al.* (2016). The contrasts evident in the metabolome of pioneer and established communities address the second hypothesis in the evolution of the pioneering cryoconite community,

> *The pioneer cryoconite metabolome is profoundly different from the established metabolome, as a consequence of enhanced early microbial growth,*

providing metabolic insights on the previously unclear transition from seed community to established cryoconite.

8.3. The supraglacial bacterial community

Microbial glacial communities are recognised as homes for a myriad of bacterial species that persist across different habitats worldwide. Analysis of the bacterial diversity across the three field sites revealed notable taxonomic similarity at the phylum level, demonstrating 14 bacterial lineages common to all supraglacial surfaces studied (*Acidobacteria*, *Actinobacteria*, *Alphaproteobacteria*, *Armatimonadetes*, *Bacteroidetes*, *Betaproteobacteria*, *Chloroflexi*, *Cyanobacteria*, *Deltaproteobacteria*, *Gammaproteobacteria*, *Gemmatimonadetes*, *Thermi*, TM7, WPS-2 and unassigned taxa) and only 4 phyla specific to the larger glacial bodies, the valley glacier and ice sheet (*Firmicutes*, *Planctomycetes*, *Verrucomicrobia*, WS6). This is consistent with clone library studies of cryoconite across three Svalbard glaciers (Edwards *et al.*, 2011), indicating that the Arctic cryoconite biosphere may be a

contiguous ecological zone. In contrast, Arctic snowpack bacterial communities and Alpine cryoconite and ice margin environments predominantly support high relative abundances of *Betaproteobacteria and Bacteroidetes* (Edwards *et al.*, 2013b; Edwards *et al.*, 2013c; Hell *et al.*, 2013; Franzetti *et al.*, 2016a). This demonstrates that cryoconite assemblages in Alpine and Arctic habitats are structurally different, confirming continental scale biogeographic influences on the cryoconite microbiome, as both localised and long range aeolian transport of propagules contribute to initiation of cryoconite development (Musilova *et al.*, 2015). This is congruent with reports of aeolian deposits in the same study, reflecting consistent air and snow bacterial community and cell numbers in Arctic habitats, but a different cryoconite bacterial diversity.

In this study, *Cyanobacteria* of the *Phormidesmis* clade can be recognised as a key engineer in the formation of granular cryoconite (Hodson *et al.*, 2010b; Langford *et al.*, 2010; Takeuchi *et al.*, 2010) in the Arctic environments sampled. The magnitude of physical adhesion from mechanical filament binding and secreted extracellular polymeric substances are a key factor in maintaining the stable habitat of the cryoconite hole (Chapter 3). Based on the experimental evidence provided in the preceding chapters and the predominance of this taxa in other Arctic (Hodson *et al.*, 2010a; Jungblut *et al.*, 2010; Zeng *et al.*, 2013), Alpine (An *et al.*, 2010; Bartrons *et al.*, 2012) and Antarctic (Komárek *et al.*, 2009) cryoconite holes, it can be confirmed that these cyanobacterial taxa are ecosystem engineers (Edwards *et al.*, 2014b) on Arctic ice surfaces and have an integral role in shaping the community in topographically

constrained habitats. Furthermore, sediment, stream and snow habitats demonstrate an overlap of *Phormidesmis priestleyi* as a keystone taxon, revealing the prominent role of this *Cyanobacteria* in ensuring physical stability of microbial assemblages and primary production in all supraglacial habitats during peak ablation periods in the Arctic. The remaining commonly observed taxa that form the core bacterial community are involved in regulating the function of the ecosystem, primarily by species selection and recruiting from a seed community of rare taxa present within the long tail of a taxon abundance curve (Fuhrman, 2009) observed in less physically stable habitats, such as snow and ephemeral streams in Chapter 7 (Edwards *et al.*, 2013c; Musilova *et al.*, 2015). This supports the hypothesis on Greenland ice sheet that

> *Supraglacial microhabitats have unique and distinct bacterial composition, as a consequence of differing hydrological and sediment habitats*.

8.3.1. Topographical and environmental effects on bacterial community structure and activity

Three topographically different ice masses were investigated in two different regions of the Arctic. Clear evidence of topographic and environmental influences has been demonstrated in each of these habitats, highlighting the climatic variables that impact ice cap, valley glacier and ice sheet communities. Climate influences, based on regional differences such as positive degree days, positive degree hours, incident radiation, albedo and temperature, are found to affect the bacterial assemblage, along with more indirect mechanisms, such as melt rate, particularly on locations

such as the valley glacier and the ice cap. This is exemplified by the first part of the Chapter 4 hypothesis,

> *The effect of environmental … filters can be evaluated by examining physical parameters … of ice cap cryoconite microbiota...*

In Greenland however, environmental variables displayed a strong diurnal effect rather than the expected seasonal effect, which is in stark contrast to valley glacier and ice cap ecosystems in Svalbard, that revealed strong seasonal and regional controls on the microbial community (Lindstrom and Langenheder, 2012; Schostag *et al.*, 2015). Previous studies have shown evidence of inter-regional and inter-glacier differences in cryoconite bacterial communities, supporting the results observed on Foxfonna cryoconite and Greenland Ice Sheet surface habitats. In fact, bacterial community composition can differ between snow, ice and cryoconite habitats, depending on spatial variability, from sites on the same glacier, between adjacent glaciers and between polar regions (Edwards *et al.*, 2011; Cameron *et al.*, 2012; Lutz *et al.*, 2017). Furthermore, the extent of spatial variation within the scale of individual glaciers has been clarified, establishing moderate contribution of localised environmental factors, strong contribution of intrinsic properties of cryoconite granules and linked snow and stream habitats on glacial surfaces in the Arctic, contrary to observations in Langford *et al.* (2014) and Edwards *et al.* (2011). These habitats have additional significant influence by topographical factors such as elevation, slope and aspect, based on statistical predictions from redundancy analysis and distance-based linear modelling (APPENDIX II, APPENDIX IV and APPENDIX V) of core, tail, rare and active taxa across Foxfonna ice cap (Chapter 4, section 4.4.3),

Foxfonna valley glacier (Chapter 6, section 6.3.2.1) and Greenland Ice Sheet weather station S6 (Chapter 7, section 7.3.2).

Both the synthetic and natural cryoconite metabolome reveal the importance of major metabolic intermediates from the tricarboxylic acid cycle, amino acid metabolism and nucleic acid biosynthesis. These processes are direct indicators of microbial activity and carbon utilisation by the heterotrophic microbiota colonising cryoconite granules, driving cellular activity and reproduction. Majority of the observed variation in the metabolome in both ideal and natural cryoconite are accounted for by these pathways, as evidenced by their prominence in the cryoconite metabolome for synthetic cryoconite (Chapter 3), Foxfonna ice cap (Chapter 5) and Foxfonna valley glacier (Chapter 6). The biosynthetic and metabolic potential of natural cryoconite is inexplicably influenced by the localised abiotic factors, namely incident radiation, melt season duration, temperature and elevation, with distinct Cartesian influence, supporting the claim that

> *Differences in metabolic pathways are related to shifts in solar input on the ice cap due to topography.*

In fact, recent work has highlighted that phototaxis is a key process in cryoconite (Cook *et al.*, 2016a) that potentially promotes access to less aerobic regions of the habitat in Greenlandic cryoconite holes. Evidence of this in the cryoconite assemblage is established by fluctuating EPS conditions (Chapter 6, section 6.3.1), however, this is both a temporally and biotically controlled process, as early summer algal blooms and diatoms skew the metabolomic profile, consistent with a similar

investigation of Longyearbreen cryoconite (Langford *et al.*, 2014). Furthermore the thermal regime of the Foxfonna glacier demonstrated a diurnal melt effect, whereby the melt season starts at least 10 - 12 days before the sampling period in this investigation, implying that the microbes are sustained by allochthonous dissolved organic matter during the early season (Irvine-Fynn, 2017b) before transitioning to utilising autochthonous nutrient resources.

8.4. Temporal and spatial variability of supraglacial microbial communities

8.4.1. Impact of biogeography on community dynamics

Investigations of the distribution of biodiversity over space and time offers insights into taxon dispersal and interactions on glacial surfaces (Martiny *et al.*, 2006). Biogeographical influence is evident in the supraglacial microbial communities of ice caps, thus the hypothesis

> *The relative influence of dispersal on an ice cap can be predicted by distance decay relationships,*

can be confirmed in this habitat, as well as the other two Arctic field sites investigated, revealing moderate local and regional biogeographic patterns in the microbial communities in Arctic habitats. Previous work had indicated that distance decay effects were negligible in the shaping of neighbouring valley glacier communities (Edwards *et al.*, 2011). Overall, it is evident that the bacterial communities are sensitive to distance-based dispersal at a local and regional scale, surpassing the effects of gradient on communities, for both core and tail communities in ice cap and valley glacier systems, contradicting the hypothesis that

Elevation-related effects will outweigh other spatial influences in bacterial richness, diversity and microbial metabolism,

in valley glaciers. The prevalent bacterial taxa are both cosmopolitan and endemic to the Arctic region, challenging traditional theories (van der Gast, 2015), and their composition and structure are potentially related to the rates of microbial activities and the composition of organic matter inoculant. Evidence of this has been described by Finlay and Esteban (2001) and is supported in this investigation by the prevalence of metabolic markers for ubiquitous microbial activity in different habitats and high protein synthesis potential of rare taxa, indicative of the activity of the microbial population (Steven *et al.*, 2017). Furthermore, the distance decay of abundant and rare taxa suggests spatial and temporal specificity personified by the pronounced effects of specific taxa, more precisely *Chloroflexi*, *Gemmatimonadetes* and *Acidobacteria* in ice caps, and *Betaproteobacteria* (DOY 202 - 210, *Gammaproteobacteria* (DOY 210), *Cyanobacteria* (DOY 217 - 221), *Planctomycetes* (DOY 217), *Firmicutes* (DOY 221), TM7 (DOY 217 - 221), WPS-2 (DOY 217 - 228) and *Armatimonadetes* (DOY 228) in valley glaciers. It is possible that specific traits in the life history of these taxa drive their dispersal (Chu *et al.*, 2010; DeBruyn *et al.*, 2011).

It is clear that the rare biosphere is governed by local factors, while the abundant communities are controlled by regional factors. Therefore, the ubiquity of core taxa within each habitat and the high resemblance (>97%) of 16S rRNA V1 - V2 regions to genes present in a range of global ice and water habitats suggests a broad distribution of these taxa in the cryosphere, increasing the likelihood of propagation. Similar

trends have been observed in a survey of the communities of bacterioplankton in lakes and reservoirs in China (Liu *et al.*, 2015). However, there is evidence of the genetic distance of bacterial phylotypes increasing with geographic distance in the glacial genus *Polaromonas* (Franzetti *et al.*, 2013), implying that the habitat-species specificity is only as good as the depth of taxonomic classification.

8.4.2. Spatial influences on community dynamics

In the topographically constrained Foxfonna ice cap it was hypothesised that

> *Microbial influence on Foxfonna ice cap drives the observed metabolite profile in cryoconite.*

Of the two natural systems investigated by mass spectrometry, this habitat was solely able to predict the metabolic profile from the variables investigated, demonstrating remarkable influence from the core taxon *Phormidesmis priestleyi*. Its role as an integral shaper of the activity in the microbial community in a constrained habitat can therefore not be doubted. The prominence of a few strains of *Phormidesmis priestleyi* that is ubiquitous across all cryoconite environments in the sites studied, their abundance in 16S rRNA sequences and the overlap of *Phormidesmis priestleyi* as a key ecosystem engineer in sediment, stream and snow habitats, reveal the prominent role of this *Cyanobacteria* in ensuring physical stability of microbial assemblages and primary production in all supraglacial habitats during peak ablation periods in the Arctic (Komárek *et al.*, 2009; Langford *et al.*, 2010; Chrismas *et al.*, 2016; Uetake *et al.*, 2016).

This does not discount the role of other taxa identified as key habitat engineers. The phylum level community represented by sequence analysis of 16S rRNA genes and 16S cDNA remains consistent between all sites during the summer period and notable taxa-specific dominance is prevalent at each site. In fact, rare taxa from the *Alphaproteobacteria* (family *Sphingomonadales*) and *Betaproteobacteria* (family *Comamonadaceae*) classes have been identified as key taxa in the aquatic areas of the Greenland Ice Sheet. While the environmental conditions were only minimally able to predict community structure for ice sheet cryoconite, an entirely different outcome was observed in these water-based habitats, as the strong influence of diurnal melt were linked to the changes in protein synthesis potential and thus the activity of the community.

8.4.3. Temporal influences on community dynamics

Strong temporal changes dominate the metabolomes of synthetic established cryoconite, synthetic newly seeded cryoconite and natural cryoconite. In the case of the microcosm study, all differences observed between established cryoconite and pioneer cryoconite metabolomes are a consequence of the microbial community, as strict measures were taken to avoid external parameter influence. As no sequence-based analysis was performed, clear associations could not be made to bacteria responsible for the observed profile. However, based on the expression patterns of statistically significant metabolites, amino acid metabolism and biosynthesis is the process integral to the early development of cryoconite granules, supporting the role of actively growing microbiota in establishing the cryoconite habitats. Furthermore,

observations of humic acid related compounds (benzoic acids, nicotinic acid and cinnamic acid) and sulfate metabolites (APPENDIX I, Table I. 3) may provide an indication of the metabolic mechanism for cryoconite darkening and mineral weathering in pioneer cryoconite habitats, that is essential for cryoconite hole formation (Takeuchi, 2002). In natural and established cryoconite, however, metabolic intermediates of biological processes dominated the cryoconite metabolome, congruent with those observed in pioneer microcosms. Additional contribution from lipid and carotenoid production were prominent in Foxfonna valley glacier and displayed fluctuating concentrations and changes in the variables of note, further demonstrating that

> *Key metabolic compounds will be more sensitive to temporal differences as a consequence of nutrient stability afforded by microbial activity*.

It is striking that the early sampling season recognised the presence of silicic acid, a chemical compound that is abundant in the Earth's crust and surface layers of the ocean. Silica on glacier surfaces is likely an artefact of weathering and consequent deposition of minerals, as the oxygenated form combines with quartzes, feldspars and other minerals in the Earth's crust, creating a CO_2 sink. The biogeochemical cycle of silica is regulated by diatoms that convert it to biogenic silica that is incorporated into their cell walls or 'frustules' (Struyf *et al.*, 2009). Unpublished investigations of microbial growth in glacial sediment under low light in laboratory conditions, demonstrate the emergence and succession of diatoms from *Cyanobacterial* taxa, potentially accounting for its presence (Cook, 2017). This could imply an important role for glacial diatom flora that are prevalent in both Arctic and Antarctic cryoconite

(Mueller *et al.*, 2001; Yallop and Anesio, 2010; Cameron *et al.*, 2012). Further evidence of the unique community activity at this point in the summer season on Foxfonna valley glacier is demonstrated by the exceedingly high EPS and chlorophyll *a* concentration. This can be accounted for by the thermal melt regime that promotes the consumption of allochthonous dissolved organic matter by the prominent algal taxa visible on the ice surface. The key taxon identified as a bottleneck species during this time is *Acinetobacter*, a *Gammaproteobacteria* observed in lake ice that is resistant and tolerant to radiation (Sattler and Storrie-Lombardi, 2010). 16S rRNA gene sequences showed that *P. priestleyi* established itself as the keystone taxon after the early colonisation of the *Gammaproteobacteria* and continued to dominate as a core species and ecosystem engineer for the duration of the Arctic summer. However, observation of the 16S rRNA gene:16S cDNA ratios of cryoconite bacteria on the Greenland Ice Sheet demonstrates that high relative abundances of 16S rRNA gene sequences do not imply activity of these taxa.

In Greenland, ice sheet surfaces with little topological forces and remarkable elevation differences from Svalbard demonstrate a stable prominent active cyanobacterial community of *Nostoc* and *Phormidesmis*, despite their low observed relative abundance. In contrast, ephemeral streams and snow communities appear idiosyncratic, exhibiting a bacterial community that is in constant flux, however, functionality can remain steady as long as it is maintained by populations within the community, demonstrating that

Supraglacial microhabitats have unique and distinct bacterial composition, as a consequence of differing hydrological and sediment habitats.

The temporal dynamics of Greenland Ice Sheet cryoconite bacterial communities are stable throughout the ablation season, confirming reports by Musilova *et al.* (2015). While another study of the ice and interior was unable to draw conclusions on the temporal variations of the community, a rudimentary ecosystem of primary production by *Cyanobacteria* and heterotrophy by *Proteobacteria*, *Bacteroidetes* and *Actinobacteria* was described, in addition to the as yet unidentified role of candidate phyla (WPS-2 and TM7) that predominate on Greenland Ice Sheet surfaces (Stibal *et al.*, 2015b; Cameron *et al.*, 2016). The study of the activity and rare taxa prevalent on the ice sheet verifies the hypothesis that

Temporal variations overshadow spatial effects whereby potentially active bacteria exhibit responses to seasonal fluctuations,

just as in Foxfonna valley glacier. However, evidence of this is strongest in snow habitats, as the cryoconite active bacterial community demonstrates robust stability for the duration of the sampling period. Distinct weekly changes were nonetheless noticeable in all the habitats investigated. Similar cyclical occurrences have been observed in marine habitats (Campbell *et al.*, 2011).

It is imperative to mention that significant differences were demonstrated between 16S rRNA gene and 16S cDNA sequences in both aquatic and sediment habitats.

Broad shifts in community diversity has been captured by 16S rRNA genes over time. Combined with the minimal interference on the community structure, a distinct species selection mechanism emerges at the scale of 16S rRNA (Van der Gucht *et al.*, 2007; Langenheder and Székely, 2011). Records of insights addressing *in situ* community diversity by species sorting has been recorded in benthic invertebrates (Josefson, 2016), microbiota of glacier-fed streams (Wilhelm *et al.*, 2013) and most recently in Alpine glaciers (Franzetti *et al.*, 2017).

Specific OTUs showed marked shifts in abundance and protein synthesis potential, allowing identification of the rare active taxa that are integral to cryoconite, snow and stream habitats. The prevalence of common taxa such as *Phormidesmis priestleyi*-3 (cryoconite, snow and stream), *Methylobacterium*-1, *Methylobacterium*-6342 and *Sphingomonadaceae*-15 (snow and stream) in these habitats could imply that ubiquitous generalist taxa in the surface glacial environment may be responsible for a bottom-up (resources), top-down (grazers) regulation mechanism, a transport of 'seed bank' taxa mechanism, or a combination of these parameters over time, driving the diversity in cryoconite, snow and stream habitats (Pedrós-Alió, 2012; Hugoni *et al.*, 2013).

8.4.4. Impact of biotic filtering on community dynamics

Within natural systems, temporal changes and spatial changes may be a consequence of the combined action of the microbial community and abiotic influence, as described in ice sheet surface analysis of bulk and active communities (Cameron *et*

al., 2016). Recently, biotic filtering by competition, cooperation and ecosystem engineering (Goberna *et al.*, 2014) has been recognised as a driver of community composition on glacial surfaces focusing on algal colonisation (Lutz *et al.*, 2015a) and cyanobacterial ecosystem engineers (Edwards *et al.*, 2014b). Microscopy and sequence analysis of cryoconite from Greenland, Svalbard and Norway has revealed an abundance of microfauna such as Cercozoans, Alveolates and Metazoa (*Tardigrada* and *Rotifera*), the latter of which contributes to a significant proportion of diversity (45%) (Cameron *et al.*, 2012; Kaczmarek *et al.*, 2015; Zawierucha *et al.*, 2015; Zawierucha *et al.*, 2016; Zawierucha *et al.*, 2017). As such, their grazing process could be responsible for contributions to both the metabolic potential in these Arctic habitats, as well as directly influencing top-down population control within cryoconite holes. They have exhibited a positive correlation with eukaryotic microalgae in cryoconite holes with high sediment loads, high N:P ratios and high allochthonous guano input, revealing a successful mechanism for the recycling of limiting nutrients (Vonnahme *et al.*, 2016). Furthermore, viral shunt process releases lower concentrations of DOM into the cryoconite microbial loop via microbial lysis (Rassner *et al.*, 2016), potentially limiting the action of grazers, but still contributing to nutrient fluctuations.

Investigations of the bacterial communities colonising the ice cap revealed that

> *The effect of ... biotic filters can be evaluated by examining … taxon interactions of ice cap cryoconite microbiota ...,*

but is not limited to this topographically constrained habitat. In all Arctic habitats, bacterial taxa prove to predict the overall community structure better than any physical parameter. In Foxfonna ice cap and valley glacier communities, it is the core bacterial community of specific taxa that predicts the community dynamics of total and tail bacterial populations, while in Greenland,

> *The rare biosphere drives the observed dynamic bacterial community changes over time*.

The placement of filamentous *Cyanobacteria*, *Proteobacteria*, *Bacteroidetes* and *Actinobacteria* as prominent centralised bottleneck OTUs argues that these taxa are key to habitat and microniche sustainability. Consistent with prior work, *Cyanobacteria* observed on most glacier surfaces form the primary producers, additionally affording mechanical stability as a consequence of EPS secretion and filamentous growth by *Lyngbya*, *Nostoc* and *Phormidesmis* species (Hodson *et al.*, 2010b; Langford *et al.*, 2010). The proteobacterial taxa *Comamonadaceae* (Darcy *et al.*, 2011; Franzetti *et al.*, 2013) and *Sphingomonadaceae* (Edwards *et al*., 2011), the *Actinobacteria* and *Bacteroidetes* class *Saprospirae* have been identified in soil habitats, so act as decomposers contributing to the necromass and humic acid content required to create a nutrient rich habitat for the heterotrophic consortium.

8.5. Broader implications of microbial effects on glaciers and ice sheets

Recent ice age cycles are estimated to be 90 000 to 115 000 years in length. The primary cycle controlling paleoclimate in this time is linked with inter-glacial warming, a finding that is endorsed by the Intergovernmental Panel on Climate

Change (I.P.C.C., 2013; I.P.C.C., 2014). Research on the modulation of ice ages has suggested that the glacial - inter-glacial cycle is primarily controlled by albedo. However, ice core data revealed that approximately every 70 000 years, high albedo causes a decrease in global temperatures and CO_2 concentrations, to the extent that carbon sinks develop, resulting in desertification of high altitude forests and grasslands. Consequently, the settling of aeolian transported eroded sediment and dust on ice sheet surfaces lowers the albedo, in turn enhancing surface melt (Ellis and Palmer, 2016). As microbial colonisation and activity in Arctic cryoconite, snow and stream contributes to the fluctuating CO_2 levels (Musilova *et al.*, 2015), rapid glacial melt and retreat is further promoted, in addition to establishing a shorter inter-glacial period. Glacial melt in the Arctic has rapidly accelerated in a short period during recent years. The modelling of long term ecological change predicts that future climate change in the Arctic may enhance microbial growth and respiration rates, increasing CO_2 emissions from soils over the next two centuries (Bradley *et al.*, 2017). As many Arctic ecosystems are interdependent ecosystems, driving changes in the physical, geochemical and biologically linked processes (Harding *et al.*, 2011), the microbiology of Arctic glaciers and ice sheets will require ongoing surveillance to monitor the feedbacks on atmospheric warming.

CHAPTER 9 – CONCLUSION

In extreme habitats with high influence from external factors, it is essential for microbial communities to maintain consistent performance, despite the often-fluctuating environmental conditions. However, this can be challenging as the mechanisms driving the response of microbial communities are idiosyncratic. This study shows a distinct transient behaviour in the allochthonous bacteria on the different supraglacial surfaces, indicative of species sorting, as taxa appear selective to their community, physical environment and biogeochemical state in the cryosphere.

Investigations into the structure and diversity of the different Arctic habitats have revealed core and keystone bacteria as strong drivers of cryoconite communities. Filamentous *Cyanobacteria* are fundamental to the formation of cryoconite granules from weathered minerals and sediments accumulated on the ice surface, as they offer mechanical support from adhesion through extracellular polymers and physical binding, addressing the first of the overarching hypotheses in Chapter 1,

> *Cryoconite formation is a result of biotic interactions from initial allochthonous input, whereby filamentous and extracellular polymeric substance producing microbiota adhere microbially colonised particulates to sustain a metabolically active niche.*

Furthermore, metabolic markers for humification and weathering have been uncovered, demonstrating the contribution of cryoconite microbiota in these processes.

As Arctic habitats are interdependent, it is expected that localised and regional factors drive the community structure. To this end, topographically constrained habitats display greater impacts from environmental factors, particularly those related to Cartesian position, incident radiation, temperature and hydrology. Valley glaciers and ice sheets, in contrast, demonstrate the instrumental effects of albedo and melt in both cryoconite and aquatic habitats. This addresses hypothesis b,

> *The glacial surface bacterial community is sensitive to climatic changes, whereby escalating temperatures, solar incident radiation and linked habitats impact species selection.*

Furthermore, there are clear localised effects of bacterial distance decay prevalent in Svalbard cryoconite and Greenland Ice Sheet snow and ephemeral streams, indicating surface melt as the driving force in Arctic bacterial biogeography, with the exception of cryoconite holes on ice sheets that are governed by regional factors.

The bacterial community in Svalbard and Greenland surface snow and ice is extremely active during the peak summer periods, mediating previously unrecorded levels of activity. Majority of the activity can be attributed to both abundant and rare communities as a consequence of species selection, highlighting the hypothesis that

Supraglacial bacterial assemblages are governed by interspecies competition, whereby taxon-taxon interactions in any specific habitat fluctuates over a transitory period.

The drastic changes observed in surface albedo for the duration of the Arctic ablation season are likely a result of the combined effect of photoautotrophy and heterotrophy, leading to increased melting upon glaciers (Hodson *et al.*, 2010b). Bacterial and algal photosynthetic pigments and biomass decomposition darken the ice in their decomposition process (Takeuchi *et al.*, 2001b). Concurrently, *Cyanobacteria*-mediated cryoconite formation promotes granule aggregation (Langford *et al.*, 2010) and widening in cryoconite holes (Cook *et al.*, 2016a) that significantly accelerates glacier melting (Fountain *et al.*, 2004; Irvine-Fynn *et al.*, 2010), which has the potential to liberate substantial volumes of melt water to the oceans (I.P.C.C., 2013). Competition and predation are often the primary reason for such transitions in microbial communities over time, particularly in low nutrient environments such as the supraglacial ecosystem. Recruitment of taxa from the rare biosphere is evident in cryoconite, snow and stream habitats and may be responsible for supporting the seasonal shifts to activity in favourable conditions, while possibly generating the essential nutrient reserves required during the high dormancy periods.

Overall, it can be confirmed that microbiota colonising High Arctic and Greenlandic glaciers contribute significantly to initiating and maintaining the complex interactions of the cosmopolitan organisms that inhabit one of the harshest physical conditions

on Earth. Broader outlooks on how understanding the microbial consortia that inhabit the cryosphere and their geochemical constituents contributes greatly to climate change models predicting the effects of global melt and glacial retreat, as well as astrobiological research and may additionally provide a foundation for a molecular evolutionary understanding of the snowball earth hypothesis (several intervals of intense, global glaciation during the Precambrian era) (Kirschvink et al. 2000). Remarkable technological advances have recently minimised the effects of long term storage and artefacts by use of in-field whole genome sequencing units such as the Nanopore MinION system (Edwards *et al.*, 2016; Jain *et al.*, 2016) for targeted next-generation DNA sequencing reactions and mobile phone microscopy (Kuhnemund *et al.*, 2017), recording timely, yet accurate, responses in microbial community composition previously unobserved in extreme habitats. These investigations are key to understanding both immediate and long term effects of microbial colonisation in an area sensitive to small scale environmental changes, that informs on large scale ice sheet consequences, which may prove imperative to predicting and mitigating future global events.

REFERENCES

Aanderud, Z. T., Jones, S. E., Fierer, N. & Lennon, J. T. 2015. Resuscitation of the rare biosphere contributes to pulses of ecosystem activity. *Frontiers in Microbiology,* 6**,** 24.

Abram, F. 2015. Systems-based approaches to unravel multi-species microbial community functioning. *Computational and Structural Biotechnology Journal,* 13**,** 24-32.

Acinas, S. G., Haverkamp, T. H., Huisman, J. & Stal, L. J. 2009. Phenotypic and genetic diversification of *Pseudanabaena* spp. (cyanobacteria). *International Society for Microbial Ecology Journal,* 3**,** 31-46.

Allison, S. D. & Martiny, J. B. H. 2008. Resistance, resilience, and redundancy in microbial communities. *Proceedings of the National Academy of Sciences,* 105**,** 11512-11519.

An, L. Z., Chen, Y., Xiang, S. R., Shang, T. C. & Tian, L. D. 2010. Differences in community composition of bacteria in four glaciers in western China. *Biogeosciences,* 7**,** 1937-52.

Anesio, A. M., Hodson, A. J., Fritz, A., Psenner, R. & Sattler, B. 2009. High microbial activity on glaciers: importance to the global carbon cycle. *Global Change Biology,* 15**,** 955-960.

Anesio, A. M. & Laybourn-Parry, J. 2011. Glaciers and ice sheets as a biome. *Trends in Ecology & Evolution,* 27**,** 219-25.

Anesio, A. M., Lutz, S., Chrismas, N. A. M. & Benning, L. G. 2017. The microbiome of glaciers and ice sheets. *Biofilms and Microbiomes,* 3.

Anesio, A. M., Sattler, B., Foreman, C., Telling, J., Hodson, A., Tranter, M. & Psenner, R. 2010. Carbon fluxes through bacterial communities on glacier surfaces. *Annals of Glaciology,* 51**,** 32-40.

Ayala, J. A., Cava, F. & de Pedro, M. A. 2012. CWSR (Cell Wall Stress-sensing Regulatory) systems in gram negative bacteria. *In:* REQUENA, J. M. (ed.) *Stress Response in Microbiology.* Madrid, Spain: Caister Academic Press.

Bachy, C., Lopez-Garcia, P., Vereshchaka, A. & Moreira, D. 2011. Diversity and vertical distribution of microbial eukaryotes in the snow, sea ice and seawater near the north pole at the end of the polar night. *Frontiers in Microbiology,* 2**,** 106.

Bagshaw, E. A., Wadham, J. L., Tranter, M., Perkins, R., Morgan, A., Williamson, C. J., Fountain, A. G., Fitzsimons, S. & Dubnick, A. 2016. Response of Antarctic cryoconite microbial communities to light. *FEMS Microbiology Ecology,* 92**,** fiw076.

Baran, R., Brodie, E. L., Mayberry-Lewis, J., Hummel, E., Da Rocha, U. N., Chakraborty, R., Bowen, B. P., Karaoz, U., Cadillo-Quiroz, H., Garcia-Pichel, F. & Northen, T. R. 2015. Exometabolite niche partitioning among sympatric soil bacteria. *Nature Communications,* 6**,** 8289.

Barberán, A., Bates, S. T., Casamayor, E. O. & Fierer, N. 2012. Using network analysis to explore co-occurrence patterns in soil microbial communities. *International Society for Microbiol Ecology Journal,* 6**,** 343-51.

Barria, C., Malecki, M. & Arraiano, C. M. 2013. Bacterial adaptation to cold. *Microbiology,* 159**,** 2437-2443.

Bartholomew, I., Nienow, P., Mair, D., Hubbard, A., King, M. A. & Sole, A. 2010. Seasonal evolution of subglacial drainage and acceleration in a Greenland outlet glacier. *Nature Geoscience,* 3**,** 408-411.

Bartrons, M., Catalan, J. & Casamayor, E. O. 2012. High bacterial diversity in epilithic biofilms of oligotrophic Mountain Lakes. *Microbial Ecology,* 64**,** 860-9.

Battin, T. J., Wille, A., Sattler, B. & Psenner, R. 2001. Phylogenetic and functional heterogeneity of sediment biofilms along environmental gradients in a glacial stream. *Appled and Environmental Microbiology,* 67**,** 799-807.

Beales, N. 2004. Adaptation of microorganisms to cold temperatures, weak acid preservatives, low pH, and osmotic stress: A review. *Comprehensive Reviews in Food Science and Food Safety,* 3.

Beckmann, M., Parker, D., Enot, D. P., Duval, E. & Draper, J. 2008. High-throughput, nontargeted metabolite fingerprinting using nominal mass flow injection electrospray mass spectrometry. *Nature Protocols,* 3**,** 486-504.

Bell, T. 2010. Experimental tests of the bacterial distance-decay relationship. *International Society for Microbial Ecology Journal,* 4**,** 1357-65.

Bell, T., Ager, D., Song, J. I., Newman, J. A., Thompson, I. P., Lilley, A. K. & van der Gast, C. J. 2005. Larger islands house more bacterial taxa. *Science,* 308**,** 1884.

Bellas, C. M., Anesio, A. M., Telling, J., Stibal, M., Tranter, M. & Davis, S. 2013. Viral impacts on bacterial communities in Arctic cryoconite. *Environmental Research Letters,* 8**,** 045021.

Benn, D. I. & Evans, D. J. A. 2010. *Glaciers & Glaciation,* New York, USA, Routledge.

Berry, D. & Widder, S. 2014. Deciphering microbial interactions and detecting keystone species with co-occurrence networks. *Frontiers in Microbiology,* 5**,** 219.

Bevan, S., Luckman, A., Murray, T., Sykes, H. & Kohler, J. 2007. Positive mass balance during the late 20th century on Austfonna, Svalbard, revealed using satellite radar interferometry. *Annals of Glaciology,* 46**,** 117-122.

Bhatia, M. P., Das, S. B., Longnecker, K., Charette, M. A. & Kujawinski, E. B. 2010. Molecular characterization of dissolved organic matter associated with the Greenland ice sheet. *Geochimica et Cosmochimica Acta,* 74**,** 3768-3784.

Blazewicz, S. J., Barnard, R. L., Daly, R. A. & Firestone, M. K. 2013. Evaluating rRNA as an indicator of microbial activity in environmental communities: limitations and uses. *International Society for Microbiol Ecology Journal,* 7**,** 2061-8.

Bøggild, C. 1997. *Different melt regimes indicated by surface albedo measurements at the Greenland ice sheet margin - Application of TM image,* Paris, European Association of Remote Sensing Laboratories.

Bøggild, C. E., Brandt, R. E., Brown, K. J. & Warren, S. G. 2010. The ablation zone in northeast Greenland: Ice types, albedos and impurities. *Journal of Glaciology,* 56.

Bradley, J. A., Anesio, A. M. & Arndt, S. 2017. Microbial and biogeochemical dynamics in glacier forefields are sensitive to century-scale climate and anthropogenic change. *Frontiers in Earth Science,* 5.

Bradley, J. A., Arndt, S., Šabacká, M., Benning, L. G., Barker, G. L., Blacker, J. J., Yallop, M. L., Wright, K. E., Bellas, C. M., Telling, J., Tranter, M. & Anesio, A. M. 2016.

Microbial dynamics in a High Arctic glacier forefield: a combined field, laboratory, and modelling approach. *Biogeosciences,* 13**,** 5677-5696.

Brauer, M. J., Yuan, J., Bennett, B. D., Lu, W., Kimball, E., Botstein, D. & Rabinowitz, J. D. 2006. Conservation of the metabolomic response to starvation across two divergent microbes. *Proceedings of the National Academy of Sciences,* 103**,** 19302-7.

Brooks, A. N., Turkarslan, S., Beer, K. D., Lo, F. Y. & Baliga, N. S. 2011. Adaptation of cells to new environments. *Wiley Interdisciplinary Reviews: Systems Biology and Medicine,* 3**,** 544-61.

Burrows, S. M., Elbert, W., Lawrence, M. G. & Poschl, U. 2009. Bacteria in the global atmosphere - Part 1: Review and synthesis of literature data for different ecosystems. *Atmospheric Chemistry and Physics,* 9**,** 9263-9280.

Buzzini, P., Branda, E., Goretti, M. & Turchetti, B. 2012. Psychrophilic yeasts from worldwide glacial habitats: diversity, adaptation strategies and biotechnological potential. *FEMS Microbiology Ecology,* 82**,** 217-241.

Cameron, K. A., Hodson, A. J. & Osborn, A. M. 2012. Structure and diversity of bacterial, eukaryotic and archaeal communities in glacial cryoconite holes from the Arctic and the Antarctic. *FEMS Microbiology Ecology,* 82**,** 254-67.

Cameron, K. A., Stibal, M., Chrismas, N., Box, J. & Jacobsen, C. S. 2017. Nitrate addition has minimal short-term impacts on Greenland Ice Sheet supraglacial prokaryotes. *Environmental Microbiology Reports,* 9**,** 144-150.

Cameron, K. A., Stibal, M., Zarsky, J., Gozdereliler, E., Schostag, M. & Jacobsen, C. S. 2016. Supraglacial bacterial community structures vary across the Greenland Ice Sheet. *FEMS Microbiology Ecology,* 92.

Campbell, B. J., Yu, L., Heidelberg, J. F. & Kirchman, D. L. 2011. Activity of abundant and rare bacteria in a coastal ocean. *Proceedings of the National Academy of Sciences,* 108 12776–12781.

Caporaso, J. G., Kuczynski, J., Stombaugh, J., Bittinger, K., Bushman, F. D., Costello, E. K., Fierer, N., Gonzalez Pena, A., Goodrich, J. K., Gordon, J. I., Huttley, G. A., Kelley, S. T., Knights, D., Koenig, J. E., Ley, R. E., Lozupone, C. A., McDonald, D., Muegge, B. D., Pirrung, M., Reeder, J., Sevinsky, J. R., Turnbaugh, P. J., Walters, W. A., Widmann, J., Yatsunenko, T., Zaneveld, J. & Knight, R. 2010. QIIME allows analysis of high-throughput community sequencing data. *Nature Methods,* 7**,** 335 - 336.

Castello, J. D. & Rogers, S. O. 2004. Life in ancient ice. *In:* CASTELLO, J. D. & ROGERS, S. O. (eds.). Princeton: Princeton University Press.

Chandler, D. M., Alcock, J. D., Wadham, J. L., Mackie, S. L. & Telling, J. 2015. Seasonal changes of ice surface characteristics and productivity in the ablation zone of the Greenland Ice Sheet. *The Cryosphere,* 9**,** 487-504.

Chandler, D. M., Wadham, J. L., Lis, G. P., Cowton, T., Sole, A., Bartholomew, I., Telling, J., Nienow, P., Bagshaw, E. B., Mair, D., Vinen , S. & Hubbard, A. 2013. Evolution of the subglacial drainage system beneath the Greenland Ice Sheet revealed by tracers. *Nature Geoscience,* 6**,** 195-198.

Chen, M. Y., Lee, D. J., Tay, J. H. & Show, K. Y. 2007. Staining of extracellular polymeric substances and cells in bioaggregates. *Applied Microbiology and Biotechnology,* 75**,** 467-74.

Chen, P. S., Tsai, F. T., Lin, C. K., Yang, C. Y., Chan, C. C., Young, C. Y. & Lee, C. H. 2010. Ambient influenza and avian influenza virus during dust storm days and background days. *Environmental Health Perspectives,* 118**,** 1211-1216.

Chong, C. W., Pearce, D. A. & Convey, P. 2015. Emerging spatial patterns in Antarctic prokaryotes. *Frontiers in Microbiology,* 6**,** 1058.

Chrismas, N. A., Anesio, A. M. & Sanchez-Baracaldo, P. 2015. Multiple adaptations to polar and alpine environments within *cyanobacteria*: a phylogenomic and Bayesian approach. *Frontiers in Microbiology,* 6**,** 1070.

Chrismas, N. A., Barker, G., Anesio, A. M. & Sanchez-Baracaldo, P. 2016. Genomic mechanisms for cold tolerance and production of exopolysaccharides in the Arctic cyanobacterium *Phormidesmis priestleyi* BC1401. *BMC Genomics,* 17**,** 533.

Christner, B. C., Hvitko II, B. H. & Reeve, J. N. 2003a. Molecular identification of bacteria and eukarya inhabiting an Antarctic cryoconite hole. *Extremophiles,* 2003**,** 177-183.

Christner, B. C., Mosley-Thompson, E., Thompson, L. G. & Reeve, J. N. 2003b. Bacterial recovery from ancient glacial ice. *Environmental Microbiology,* 5**,** 433-436.

Chu, H., Fierer, N., Lauber, C. L., Caporaso, J. G., Knight, R. & Grogan, P. 2010. Soil bacterial diversity in the Arctic is not fundamentally different from that found in other biomes. *Environmental Microbiology,* 12**,** 2998-3006.

Chu, V. W. 2014. Greenland ice sheet hydrology: A review. *Progress in Physical Geography,* 38**,** 19-54.

Clarke, K. R. & Warwick, R. M. 2001. *Change in Marine Communities: An Approach to Statistical Analysis and Interpretation*, Plymouth Marine Laboratory, UK.

Cook, J. 2016. Supraglacial Biogeochemistry. *Geomorphological Techniques.* British Society for Geomorphology.

Cook, J., Edwards, A. & Hubbard, A. 2015a. Biocryomorphology: Integrating microbial processes with ice surface hydrology, topography, and roughness. *Frontiers in Earth Science,* 3.

Cook, J., Edwards, A., Takeuchi, N. & Irvine-Fynn, T. 2015b. Cryoconite: The dark biological secret of the cryosphere. *Progress in Physical Geography,* 40**,** 66-111.

Cook, J., Hodson, A., Telling, J., Anesio, A., Irvine-Fynn, T. & Bellas, C. 2010. The mass–area relationship within cryoconite holes and its implications for primary production. *Annals of Glaciology,* 51**,** 106-110.

Cook, J. M. 28 March 2017. *RE: Algae and diatoms as reliable sources of organic carbon to bacterial communities* Type to GOKUL, J. K.

Cook, J. M., Edwards, A., Bulling, M., Mur, L. A., Cook, S., Gokul, J. K., Cameron, K. A., Sweet, M. & Irvine-Fynn, T. D. L. 2016a. Metabolome-mediated biocryomorphic evolution promotes carbon fixation in Greenlandic cryoconite holes. *Environmental Microbiology*.

Cook, J. M., Hodson, A. J. & Irvine-Fynn, T. D. L. 2016b. Supraglacial weathering crust dynamics inferred from cryoconite hole hydrology. *Hydrological Processes,* 30**,** 433-446.

Cooper, M. G., Smith, L. C., Rennermalm, A. K., Miège, C., Pitcher, L. H., Ryan, J. C., Yang, K. & Cooley, S. 2017. Near surface meltwater storage in low-density

bare ice of the Greenland ice sheet ablation zone. *The Cryosphere Discussions*, 1-25.

Costerton, J. W., Irvin, R. T. & Cheng, K. J. 1981. The bacterial glycocalyx in nature and disease. *Annual Review of Microbiology,* 35**,** 299-324.

Cowan, D. A. & Ah Tow, L. 2004. Endangered Antarctic environments. *Annual Review of Microbiology,* 58**,** 649-90.

Cowan, D. A., Chown, S. L., Convey, P., Tuffin, M., Hughes, K., Pointing, S. & Vincent, W. F. 2011. Non-indigenous microorganisms in the Antarctic: Assessing the risks. *Trends in Microbiology,* 19**,** 540-548.

Cowton, T., Nienow, P., Sole, A., Wadham, J., Lis, G., Bartholomew, I., Mair, D. & Chandler, D. 2013. Evolution of drainage system morphology at a land-terminating Greenlandic outlet glacier. *Journal of Geophysical Research: Earth Surface,* 118**,** 29-41.

Csardi, G. & Nepusz, T. 2006. *The igraph software package for complex network research,* Budapest, Hungary.

Dallmann, W. K., Kjaernet, T. & Nottvedt, A. 2001. *Geological map of Svalbard 1:100,000 Sheet C9G Adventdalen*. Norwegian Polar Institute.

Darcy, J. L., Lynch, R. C., King, A. J., Robeson, M. S. & Schmidt, S. K. 2011. Global distribution of *Polaromonas* phylotypes - evidence for a highly successful dispersal capacity. *PLoS One,* 6**,** e23742.

Daws, C. & Rewcastle, K. E. 2015. Microbes in the middle: Elevation gradients reveal drivers of belowground ecosystem processes with climate change. *Pursuit - The Journal of Undergraduate Research at the University of Tennessee,* 6.

de Carvalho, C. C. & Fernandes, P. 2010. Production of metabolites as bacterial responses to the marine environment. *Marine Drugs,* 8**,** 705-27.

DeBruyn, J. M., Nixon, L. T., Fawaz, M. N., Johnson, A. M. & Radosevich, M. 2011. Global biogeography and quantitative seasonal dynamics of *Gemmatimonadetes* in soil. *Applied and Environmental Microbiology,* 77**,** 6295-300.

DeForce, E. October 2014. *RE: Co-extraction of DNA and RNA using the PowerWater® Sterivex™ DNA Isolation kit.* Type to EDWARDS, A.

Deming, J. W. 2002. Psychrophiles and polar regions. *Current Opinion in Microbiology,* 5**,** 301-309.

Demmig-Adams, B., Gilmore, A. M. & Adams, W. W. 1996. Carotenoids 3: in vivo function of carotenoids in higher plants. *Federation of American Societies for Experimental Biology Journal,* 10**,** 403-12.

Denef, V. J., Fujimoto, M., Berry, M. A. & Schmidt, M. L. 2016. Seasonal succession leads to habitat-dependent differentiation in ribosomal RNA:DNA ratios among freshwater lake bacteria. *Frontiers in Microbiology*.

DeSantis, T. Z., Hugenholtz, P., Larsen, N., Rojas, M., Brodie, E. L., Keller, K., Huber, T., Dalevi, D., Hu, P. & Andersen, G. L. 2006. Greengenes, a chimera-checked 16S rRNA gene database and workbench compatible with ARB. *Applied and Environmental Microbiology,* 72**,** 5069-72.

Detheridge, A. P., Brand, G., Fychan, R., Crotty, F. V., Sanderson, R., Griffith, G. W. & Marley, C. L. 2016. The legacy effect of cover crops on soil fungal populations in a cereal rotation. *Agriculture, Ecosystems and Environment,* 228**,** 49-61.

Dupont, F., Royer, A., Langlois, A., Gressent, A., Picard, G., Fily, M., Cliche, P. & Chum, M. 2012. Monitoring the melt season length of the Barnes Ice Cap over the 1979-2010 period using active and passive microwave remote sensing data. *Hydrological Processes,* 26**,** 2643-2652.

E.E.A. 2016. Indicator assessment: Glaciers. *Glaciers CLIM 007.* Copenhagen, Denmark: European Environmental Agency.

Edgar, R. C. 2010. Search and clustering orders of magnitude faster than BLAST. *Bioinformatics,* 26**,** 2460-2461.

Edgar, R. C., Haas, B. J., Clemente, J. C., Quince, C. & Knight, R. 2011. UCHIME improves sensitivity and speed of chimera detection. *Bioinformatics,* 27**,** 2194-2200.

Edwards, A., Anesio, A. M., Rassner, S. M., Sattler, B., Hubbard, B., Perkins, W. T., Young, M. & Griffith, G. W. 2011. Possible interactions between bacterial diversity, microbial activity and supraglacial hydrology of cryoconite holes in Svalbard. *International Society for Microbial Ecology Journal,* 5**,** 150-60.

Edwards, A. & Cook, S. 2015. Microbial dynamics in glacier forefield soils show succession is not just skin deep. *Molecular Ecology***,** 963-966.

Edwards, A., Debbonaire, A. R., Sattler, B., Mur, L. A. J. & Hodson, A. J. 2016. Extreme metagenomics using nanopore DNA sequencing: a field report from Svalbard, 78° N. *bioRxiv*.

Edwards, A., Douglas, B., Anesio, A. M., Rassner, S. M., Irvine-Fynn, T. D. L., Sattler, B. & Griffith, G. W. 2013a. A distinctive fungal community inhabiting cryoconite holes on glaciers in Svalbard. *Fungal Ecology,* 6**,** 168-176.

Edwards, A., Irvine-Fynn, T., Mitchell, A. C. & Rassner, S. M. E. 2014a. A germ theory for glacial systems? *Wiley Interdisciplinary Reviews: Water*.

Edwards, A., Mur, L. A., Girdwood, S. E., Anesio, A. M., Stibal, M., Rassner, S. M., Hell, K., Pachebat, J. A., Post, B., Bussell, J. S., Cameron, S. J., Griffith, G. W., Hodson, A. J. & Sattler, B. 2014b. Coupled cryoconite ecosystem structure-function relationships are revealed by comparing bacterial communities in alpine and Arctic glaciers. *FEMS Microbiology Ecology,* 89**,** 222-37.

Edwards, A., Pachebat, J. A., Swain, M., Hegarty, M., Hodson, A. J., Irvine-Fynn, T. D. L., Rassner, S. M. E. & Sattler, B. 2013b. A metagenomic snapshot of taxonomic and functional diversity in an alpine glacier cryoconite ecosystem. *Environmental Research Letters,* 8**,** 035003.

Edwards, A., Rassner, S. M. E., Anesio, A. M., Worgan, H. J., Irvine-Fynn, T. D. L., Wyn Williams, H., Sattler, B. & Griffith, G. W. 2013c. Contrasts between the cryoconite and ice-marginal bacterial communities of Svalbard glaciers. *Polar Research,* 32.

Ellis, R. & Palmer, M. 2016. Modulation of ice ages via precession and dust-albedo feedbacks. *Geoscience Frontiers*.

Engelhardt, M., Schuler, T. & Andreassen, L. M. 2013. Glacier mass balance of Norway 1961–2010 calculated by a temperature-index model. *Annals of Glaciology,* 54**,** 32-40.

Ewert, M. & Deming, J. W. 2013. Sea ice microorganisms: Environmental constraints and extracellular responses. *Biology (Basel),* 2**,** 603-628.

Felip, M., Sattler, B., Psenner, R. & Catalan, J. 1995. Highly active microbial communities in the ice and snow cover of high mountain lakes. *Applied and Environmental Microbiology,* 61**,** 2394-2401.

Fierer, N., Jackson, J. A., Vilgalys, R. & Jackson, R. B. 2005. Assessment of soil microbial community structure by use of taxon-specific quantitative PCR assays. *Applied and Environmental Microbiology,* 71**,** 4117-4120.

Fierer, N., Lauber, C. L., Ramirez, K. S., Zaneveld, J., Bradford, M. A. & Knight, R. 2012. Comparative metagenomic, phylogenetic and physiological analyses of soil microbial communities across nitrogen gradients. *International Society for Microbiol Ecology Journal,* 6**,** 1007-17.

Finlay, B. J. & Esteban, G. F. 2001. Ubiquitous microbes and ecosystem function. *Limnetica,* 20**,** 31-43.

Fountain, A. G., Nylen, T. H., Monaghan, A., Basagic, H. J. & Bromwich, D. 2009. Snow in the McMurdo Dry Valleys, Antarctica. *International Journal of Climatology*.

Fountain, A. G., Tranter, M., Nylen, T. H., Lewis, K. J. & Mueller, D. R. 2004. Evolution of cryoconite holes and their contribution to meltwater runoff from glaciers in the McMurdo Dry Valleys, Antarctica. *Journal of Glaciology,* 50**,** 35-45.

Franzetti, A., Navarra, F., Tagliaferri, I., Gandolfi, I., Bestetti, G., Minora, U., Azzoni, R. S., Diolaiuti, G., Smiraglia, C. & Ambrosini, R. 2016a. Temporal variability of bacterial communities in cryoconite on an alpine glacier. *Environmental Microbiology Reports*.

Franzetti, A., Navarra, F., Tagliaferri, I., Gandolfi, I., Bestetti, G., Minora, U., Azzoni, R. S., Diolaiuti, G., Smiraglia, C. & Ambrosini, R. 2017. Potential sources of bacteria colonizing the cryoconite of an Alpine glacier. *PLoS One,* 12**,** e0174786.

Franzetti, A., Tagliaferri, I., Gandolfi, I., Bestetti, G., Minora, U., Mayer, C., Azzoni, R. S., Diolaiuti, G., Smiraglia, C. & Ambrosini, R. 2016b. Light-dependent microbial metabolisms drive carbon fluxes on glacier surfaces. *International Society for Microbiol Ecology Journal,* 16.

Franzetti, A., Tatangelo, V., Gandolfi, I., Bertolini, V., Bestetti, G., Diolaiuti, G., D'Agata, C., Mihalcea, C., Smiraglia, C. & Ambrosini, R. 2013. Bacterial community structure on two alpine debris-covered glaciers and biogeography of *Polaromonas* phylotypes. *International Society for Microbial Ecology Journal,* 7**,** 1483-92.

Frolund, B., Palmgren, R., Keiding, K. & Nielsen, P. H. 1996. Extraction of extracellular polymers from activated sludge using a cation exchange resin. *Water Research,* 30**,** 1749-1758.

Fuhrman, J. A. 2009. Microbial community structure and its functional implications. *Nature,* 459**,** 193-9.

Gabet, E. J., Reichman, O. J. & Seabloom, E. W. 2003. The effects of bioturbation on soil processes and sediment transport. *Annual Review of Earth and Planetary Sciences,* 31**,** 249-273.

Gaidos, E., Rusch, A. & Ilardo, M. 2011. Ribosomal tag pyrosequencing of DNA and RNA from benthic coral reef microbiota: community spatial structure, rare members and nitrogen-cycling guilds. *Environmental Microbiology,* 13**,** 1138-52.

Garcia-Romero, I., Perez-Pulido, A. J., Gonzalez-Flores, Y. E., Reyes-Ramirez, F., Santero, E. & Floriano, B. 2016. Genomic analysis of the nitrate-respiring *Sphingopyxis granuli* (formerly *Sphingomonas macrogoltabida*) strain TFA. *BMC Genomics,* 17**,** 93.

Gerphagnon, M., Latour, D., Colombet, J. & Sime-Ngando, T. 2013. A double staining method using SYTOX Green and calcofluor white for studying fungal parasites of phytoplankton. *Applied and Environmental Microbiology,* 79.

Ghobakhlou, A., Laberge, S., Antoun, H., Wishart, D. S., Xia, J., Krishnamurthy, R. & Mandal, R. 2013. Metabolomic analysis of cold acclimation of Arctic *Mesorhizobium* sp. strain N33. *PLoS One,* 8**,** e84801.

Glassing, A., Dowd, S. E., Galandiuk, S., Davis, B. & Chiodini, R. J. 2016. Inherent bacterial DNA contamination of extraction and sequencing reagents may affect interpretation of microbiota in low bacterial biomass samples. *Gut Pathogens,* 8**,** 24.

Goberna, M., García, C. & Verdú, M. 2014. A role for biotic filtering in driving phylogenetic clustering in soil bacterial communities. *Global Ecology and Biogeography,* 23**,** 1346-1355.

Gokul, J. K., Hodson, A. J., Saetnan, E. R., Irvine-Fynn, T. D. L., Westall, P. J., Detheridge, A. P., Takeuchi, N., Bussell, J. S., Mur, L. A. & Edwards, A. 2016. Taxon interactions control the distributions of cryoconite bacteria colonizing a High Arctic ice cap. *Molecular Ecology,* 25**,** 3752–3767.

Griffin, D. W., Kellogg, C. A. & Shinn, E. A. 2001. Dust in the wind: Long range transport of dust in the atmosphere and its implication for global public and ecosystem health. *Global Change and Human Health,* 2**,** 20-33.

Griffiths, R. I., Whiteley, A. S., O'Donnell, A. G. & Bailey, M. J. 2000. Rapid method for coextraction of DNA and RNA from natural environments for analysis of ribosomal DNA- and rRNA-based microbial community composition. *Applied and Environmental Microbiology,* 66**,** 5488-5491.

Grzesiak, J., Gorniak, D., Swiatecki, A., Aleksandrzak-Piekarczyk, T., Szatraj, K. & Zdanowski, M. K. 2015. Microbial community development on the surface of Hans and Werenskiold Glaciers (Svalbard, Arctic): a comparison. *Extremophiles,* 19**,** 885-97.

Guedes, A. C., Amaro, H. M. & Malcata, F. X. 2011. Microalgae as sources of carotenoids. *Marine Drugs,* 9**,** 625-44.

Haas, B. J., Gevers, D., Earl, A. M., Feldgarden, M., Ward, D. V., Giannoukos, G., Ciulla, D., Tabbaa, D., Highlander, S. K., Sodergren, E., Methe, B., DeSantis, T. Z., Consortium, T. H. M., Petrosino, J. F., Knight, R. & Birren, B. W. 2010. Chimeric 16S rRNA sequence formation and detection in Sanger and 454-pyrosequenced PCR amplicons. *Genome Research*.

Haga, D. I., Iannone, R., Wheeler, M. J., Mason, R., Polishchuk, E. A., Fetch, T., van der Kamp, B. J., McKendry, I. G. & Bertram, A. K. 2013. Ice nucleation properties of rust and bunt fungal spores and their transport to high altitudes, where they can cause heterogeneous freezing. *Journal of Geophysical Research: Atmospheres,* 118**,** 7260-7272.

Haggin, P. 2012. Giant Iceberg Breaks Off Greenland Glacier. *TIME*.

Hairston, N. G., Jr., Dillon, T. A. & De Stasio, B. T., Jr. 1990. A field test for the cues of diapause in a freshwater copepod. *Ecology* 71**,** 2218-2223.

Hallbeck, L. 2009. Microbial processes in glaciers and permafrost. *Svensk Kärnbränslehantering AB Report.* Stockholm, Sweden: Svensk Kärnbränslehantering AB.

Hamilton, T. L., Peters, J. W., Skidmore, M. L. & Boyd, E. S. 2013. Molecular evidence for an active endogenous microbiome beneath glacial ice. *International Society for Microbiol Ecology Journal,* 7**,** 1402-12.

Hanssen-Bauer, I., Førland, E. J., Haddeland, I., Hisdal, H., Mayer, S., Nesje, A., Nilson, J. E. Ø., Sandven, S., Sandø, A. B., Sorteberg, A. & Ådlandsvik, B. 2015. Climate in Norway 2100. Knowledge basis for climate change adaptation. *National Climate Change Secretariat Report.*

Harding, T., Jungblut, A. D., Lovejoy, C. & Vincent, W. F. 2011. Microbes in High Arctic snow and implications for the cold biosphere. *Applied and Environmental Microbiology,* 77**,** 3234-43.

Haruta, S. & Kanno, N. 2015. Survivability of microbes in natural environments and their ecological impacts. *Microbes and Environments,* 30**,** 123-5.

Hawkings, J., Wadham, J., Tranter, M., Telling, J., Bagshaw, E., Beaton, A., Simmons, S.-L., Chandler, D., Tedstone, A. & Nienow, P. 2016. The Greenland Ice Sheet as a hot spot of phosphorus weathering and export in the Arctic. *Global Biogeochemical Cycles,* 30**,** 191-210.

Hawkings, J. R., Wadham, J. L., Benning, L. G., Hendry, K. R., Tranter, M., Tedstone, A., Nienow, P. & Raiswell, R. 2017. Ice sheets as a missing source of silica to the polar oceans. *Nature Communications,* 8**,** 14198.

Hegarty, M. 16 June 2015. *RE: Illumina sequence processing in BaseSpace.* Type to GOKUL, J. K. & HILL, R.

Hell, K., Edwards, A., Zarsky, J., Podmirseg, S. M., Girdwood, S., Pachebat, J. A., Insam, H. & Sattler, B. 2013. The dynamic bacterial communities of a melting High Arctic glacier snowpack. *International Society for Microbial Ecology Journal,* 7**,** 1814-1826.

Hill, R., Saetnan, E. R., Scullion, J., Gwynn-Jones, D., Ostle, N. & Edwards, A. 2016. Temporal and spatial influences incur reconfiguration of Arctic heathland soil bacterial community structure. *Environmental Microbiology,* 18**,** 1942-1953.

Hjelle, A. 1993. *Geology of Svalbard (English language edition),* Oslo, Norsk Polarinstitutt.

Hock, R. 2005. Glacier melt: a review of processes and their modelling. *Progress in Physical Geography,* 29**,** 362-391.

Hodkinson, I. D., Coulson, S. J. & Webb, N. R. 2003. Community assembly along proglacial chronosequences in the high Arctic: vegetation and soil development in north-west Svalbard. *Journal of Ecology,* 91**,** 651-663.

Hodson, A., Anesio, A. M., Ng, F., Watson, R., Quirk, J., Irvine-Fynn, T., Dye, A., Clark, C., McCloy, P., Kohler, J. & Sattler, B. 2007. A glacier respires: Quantifying the distribution and respiration CO_2 flux of cryoconite across an entire Arctic supraglacial ecosystem. *Journal of Geophysical Research: Biogeosciences,* 112**,** 1-9.

Hodson, A., Anesio, A. M., Tranter, M., Fountain, A., Osborn, M., Priscu, J., Laybourn-Parry, J. & Sattler, B. 2008. Glacial ecosystems. *Ecological Monographs,* 78**,** 41-67.

Hodson, A., Bøggild, C., Hanna, E., Huybrechts, P., Langford, H., Cameron, K. & Houldsworth, A. 2010a. The cryoconite ecosystem on the Greenland ice sheet. *Annals of Glaciology,* 51**,** 123-9.

Hodson, A., Brock, B., Pearce, D., Laybourn-Parry, J. & Tranter, M. 2015. Cryospheric ecosystems: a synthesis of snowpack and glacial research. *Environmental Research Letters,* 10**,** 110201.

Hodson, A., Cameron, K., Bøggild, C., Irvine-Fynn, T., Langford, H., Pearce, D. & Banwart, S. 2010b. The structure, biological activity and biogeochemistry of cryoconite aggregates upon an Arctic valley glacier: Longyearbreen, Svalbard. *Journal of Glaciology,* 56**,** 349-362.

Hodson, A. J., Mumford, P. N., Kohler, J. & Wynn, P. M. 2005. The High Arctic glacial ecosystem: new insights from nutrient budgets. *Biogeochemistry,* 72**,** 233-256.

Hood, E., Battin, T. J., Fellman, J., O'Neel, S. & Spencer, R. G. M. 2015. Storage and release of organic carbon from glaciers and ice sheets. *Nature Geosciences,* 8**,** 91-96.

Hubbell, S. P. 2001. *The unified neutral theory of biodiversity and biogeography,* Princeton, NJ, USA, Princeton University Press.

Hughes, K. A. & Lawley, B. 2003. A novel Antarctic microbial endolithic community within gypsum crusts. *Environmental Microbiology,* 5**,** 555-565.

Hugoni, M., Taib, N., Debroas, D., Domaizon, I., Dufournel, I. J., Bronner, G., Salter, I., Agogué, H., Mary, I. & Galand, P. E. 2013. Structure of the rare archaeal biosphere and seasonal dynamics of active ecotypes in surface coastal waters. *Proceedings of the National Academy of Sciences,* 110**,** 6004-6009.

I.P.C.C. 2013. Climate change synthesis report 2013. *Contribution of Working Groups I, II and III to the Fourth Assessment Report of the Intergovernmental Panel on Climate Change*. Geneva, Switzerland.

I.P.C.C. 2014. Climate change synthesis report 2014. *In:* TEAM, T. C. W., PACHAURI, R. K. & MEYER, L. (eds.) *Contribution of Working Groups I, II and III to the Fifth Assessment Report of the Intergovernmental Panel on Climate Change.* Geneva, Switzerland.

Irvine-Fynn, T. D. 2017a. *RE: Foxfonna transect algal blooms.* Type to GOKUL, J. K.

Irvine-Fynn, T. D. & Edwards, A. 2014. A frozen asset: the potential of flow cytometry in constraining the glacial biome. *Cytometry A,* 85**,** 3-7.

Irvine-Fynn, T. D., Edwards, A., Newton, S., Langford, H., Rassner, S. M., Telling, J., Anesio, A. M. & Hodson, A. J. 2012. Microbial cell budgets of an Arctic glacier surface quantified using flow cytometry. *Environmental Microbiology,* 14**,** 2998-3012.

Irvine-Fynn, T. D. L. 19 May 2017b. *RE: Foxfonna thermal regime 2011.* Type to EDWARDS, A. & GOKUL, J. K.

Irvine-Fynn, T. D. L., Bridge, J. W. & Hodson, A. J. 2010. Rapid quantification of cryoconite: Granule geometry and in situ supraglacial extents, using examples from Svalbard and Greenland. *Journal of Glaciology,* 56**,** 297-308.

Irvine-Fynn, T. D. L., Hanna, E., Barrand, N. E., Porter, P. R., Kohler, J. & Hodson, A. J. 2014. Examination of a physically based, high-resolution, distributed Arctic temperature-index melt model, on Midtre Lovénbreen, Svalbard. *Hydrological Processes,* 28**,** 134-149.

Irvine-Fynn, T. D. L., Hodson, A. J., Moorman, B. J., Vatne, G. & Hubbard, A. L. 2011. Polythermal glacier hydrology: A review. *Reviews of Geophysics,* 49.

Jain, M., Olsen, H. E., Paten, B. & Akeson, M. 2016. The Oxford Nanopore MinION: delivery of nanopore sequencing to the genomics community. *Genome Biology,* 17**,** 239.

Jarvis, R. M., Broadhurst, D., Johnson, H., O'Boyle, N. M. & Goodacre, R. 2006. PYCHEM: a multivariate analysis package for python. *Bioinformatics,* 22**,** 2565-6.

Jiao, Y. S., Yan, H., Ji, Z. J., Liu, Y. H., Sui, X. H., Zhang, X. X., Wang, E. T., Chen, W. X. & Chen, W. F. 2015. *Phyllobacterium sophorae* sp. nov., a symbiotic bacterium isolated from root nodules of *Sophora flavescens*. *International Journal of Systematic and Evolutionary Microbiology,* 65**,** 399-406.

Jones, S. E. & Lennon, J. T. 2010. Dormancy contributes to the maintenance of microbial diversity. *Proceedings of the National Academy of Sciences,* 107**,** 5881-5886.

Josefson, A. B. 2016. Species sorting of benthic invertebrates in a salinity gradient - Importance of dispersal limitation. *PLoS One,* 11**,** e0168908.

Jungblut, A. D., Lovejoy, C. & Vincent, W. F. 2010. Global distribution of cyanobacterial ecotypes in the cold biosphere. *International Society for Microbial Ecology Journal,* 4**,** 191-202.

Kaczmarek, Ł., Jakubowska, N., Celewicz-Gołdyn, S. & Zawierucha, K. 2015. The microorganisms of cryoconite holes (algae, Archaea, bacteria, cyanobacteria, fungi, and Protista): a review. *Polar Record,* 52**,** 176-203.

Kanehisa, M., Goto, S., Hattori, M., Aoki-Kinoshita, K. F., Itoh, M., Kawashima, S., Katayama, T., Araki, M. & Hirakawa, M. 2006. From genomics to chemical genomics: new developments in KEGG. *Nucleic Acids Research,* 34**,** D354-D357.

Keeley, J. E. 1987. Role of fire in seed germination of woody taxa in California chaparral. *Ecology* 68**,** 434-443.

Klein, A. M., Bohannan, B. J., Jaffe, D. A., Levin, D. A. & Green, J. L. 2016. Molecular evidence for metabolically active bacteria in the atmosphere. *Frontiers in Microbiology,* 7**,** 772.

Klein, D. A. 2015. Partial formalization: An approach for critical analysis of definitions and methods used in bulk extraction-based molecular microbial ecology. *Open Journal of Ecology,* 05**,** 400-407.

Klindworth, A., Pruesse, E., Schweer, T., Peplies, J., Quast, C., Horn, M. & Glockner, F. O. 2013. Evaluation of general 16S ribosomal RNA gene PCR primers for classical and next-generation sequencing-based diversity studies. *Nucleic Acids Research,* 41**,** e1.

Knief, C. 2014. Analysis of plant microbe interactions in the era of next generation sequencing technologies. *Frontiers in Plant Science,* 5**,** 216.

Knight, P. G. 1999. Glacier Hydrology. *Glaciers.* Cheltenham, United Kingdom: Stanley Thorned Ltd.

Kohshima, S. 1987. Glacial biology and biotic communities. *Evolution and coadaptation in biotic communities. Kyoto, Kyoto University. Faculty of Science***,** 77-92.

Komárek, J., Kaštovský, J., Ventura, S., Turicchia, S. & Šmarda, J. 2009. The *Cyanobacterial* genus *Phormidesmis*. *Algological Studies,* 129**,** 41-59.

Krieger, C. J., Zhang, P., Mueller, L. A., Wang, A., Paley, S., Arnaud, M., Pick, J., Rhee, S. Y. & Karp, P. D. 2004. MetaCyc: a multiorganism database of metabolic pathways and enzymes. *Nucleic Acids Research,* 32**,** D438-D442.

Kuhnemund, M., Wei, Q., Darai, E., Wang, Y., Hernandez-Neuta, I., Yang, Z., Tseng, D., Ahlford, A., Mathot, L., Sjoblom, T., Ozcan, A. & Nilsson, M. 2017. Targeted DNA sequencing and *in situ* mutation analysis using mobile phone microscopy. *Nature Communications,* 8**,** 13913.

Kupfer, H., Herber, A. & König-Langlo, G. 2006. Radiation measurements and synoptic observations at Ny-Ålesund. *In:* KUPFER, H. (ed.) *Variation of the Radiation and Meteorological Parameters of the BSRN-Station Ny-Ålesund/ Spitsbergen 1993 – 2002.* Jena: Friedrich-Schiller-University.

Kupper, F. C., Gaquerel, E., Cosse, A., Adas, F., Peters, A. F., Muller, D. G., Kloareg, B., Salaun, J. P. & Potin, P. 2009. Free fatty acids and methyl jasmonate trigger defense reactions in *Laminaria digitata*. *Plant and Cell Physiology,* 50**,** 789-800.

Lang, X. F. & Erpicum, M. 2015. Stable climate and surface mass balance in Svalbard over 1979-2013 despite the Arctic warming. *The Cryosphere,* 9**,** 83-101.

Langenheder, S. & Székely, A. J. 2011. Species sorting and neutral processes are both important during the initial assembly of bacterial communities. *The International Society for Microbial Ecology Journal,* 5**,** 1086-1094.

Langford, H., Hodson, A., Banwart, S. & Bøggild, C. 2010. The microstructure and biogeochemistry of Arctic cryoconite granules. *Annals of Glaciology,* 51**,** 87-94.

Langford, H. J., Irvine-Fynn, T. D. L., Edwards, A., Banwart, S. A. & Hodson, A. J. 2014. A spatial investigation of the environmental controls over cryoconite aggregation on Longyearbreen glacier, Svalbard. *Biogeosciences,* 11**,** 5365-5380.

Lankadurai, B. P., Nagato, E. G. & Simpson, M. J. 2013. Environmental metabolomics: An emerging approach to study organism responses to environmental stressors. *Environmental Reviews,* 21**,** 180-205.

Le Page, M. 2017. Global sea ice is at lowest level ever recorded. *New Scientist*.

Lee, C. K., Herbold, C. W., Polson, S. W., Wommack, K. E., Williamson, S. J., McDonald, I. R. & Cary, S. C. 2012. Groundtruthing next-gen sequencing for microbial ecology-biases and errors in community structure estimates from PCR amplicon pyrosequencing. *PLoS One,* 7**,** e44224.

Lewis, K. 2007. Persister cells, dormancy and infectious disease. *Nature Reviews Microbiology,* 5**,** 48-56.

Lindstrom, E. S. & Langenheder, S. 2012. Local and regional factors influencing bacterial community assembly. *Environmental Microbiology Reports,* 4**,** 1-9.

Link, H., Fuhrer, T., Gerosa, L., Zamboni, N. & Sauer, U. 2015. Real-time metabolome profiling of the metabolic switch between starvation and growth. *Nature Methods,* 12**,** 1091-7.

Liu, L., Yang, J., Yu, Z. & Wilkinson, D. M. 2015. The biogeography of abundant and rare bacterioplankton in the lakes and reservoirs of China. *International Society for Microbiol Ecology Journal,* 9**,** 2068-77.

Lutz, S., Anesio, A. M., Edwards, A. & Benning, L. G. 2015a. Microbial diversity on Icelandic glaciers and ice caps. *Frontiers in Microbiology,* 6**,** 307.

Lutz, S., Anesio, A. M., Edwards, A. & Benning, L. G. 2017. Linking microbial diversity and functionality of Arctic glacial surface habitats. *Environmental Microbiology,* 19**,** 551-565.

Lutz, S., Anesio, A. M., Field, K. & Benning, L. G. 2015b. Integrated 'omics', targeted metabolite and single-cell analyses of Arctic snow algae functionality and adaptability. *Frontiers in Microbiology,* 6**,** 1323.

Lutz, S., Anesio, A. M., Raiswell, R., Edwards, A., Newton, R. J., Gill, F. & Benning, L. G. 2016. The biogeography of red snow microbiomes and their role in melting arctic glaciers. *Nature Communications,* 7**,** 11968.

Lynch, M. D. & Neufeld, J. D. 2015. Ecology and exploration of the rare biosphere. *Nature Reviews Microbiology,* 13**,** 217-29.

MacDonell, S. & Fitzsimons, S. 2008. The formation and hydrological significance of cryoconite holes. *Progress in Physical Geography,* 32**,** 595-610.

MacLeod 2002. Geometric morphometrics and geological form-classification systems. *Earth Science Reviews***,** 1-15.

Margesin, R., Sproer, C., Zhang, D. C. & Busse, H. J. 2013. *Polaromonas* glacialis sp. nov. and *Polaromonas cryoconiti* sp. nov., isolated from alpine glacier cryoconite. *International Journal of Systematic and Evolutionary Microbiology,* 63**,** 2313–2314.

Martiny, J. B., Bohannan, B. J., Brown, J. H., Colwell, R. K., Fuhrman, J. A., Green, J. L., Horner-Devine, M. C., Kane, M., Krumins, J. A., Kuske, C. R., Morin, P. J., Naeem, S., Ovreas, L., Reysenbach, A. L., Smith, V. H. & Staley, J. T. 2006. Microbial biogeography: Putting microorganisms on the map. *Nature Reviews Microbiology,* 4**,** 102-12.

Masuko, T., Minami, A., Iwasaki, N., Majima, T., Nishimura, S. & Lee, Y. C. 2005. Carbohydrate analysis by a phenol-sulfuric acid method in microplate format. *Analytical Biochemistry,* 339**,** 69-72.

McEntyre, J. & Ostell, J. 2012. The NCBI Handbook (Internet). Bethesda (MD): National Center for Biotechnology Information (US).

McLean, A. L. 1918. Bacteria of ice and snow in Antarctica. *Nature,* 102**,** 35-39.

Mikucki, J. A. & Priscu, J. C. 2007. Bacterial diversity associated with Blood Falls, a subglacial outflow from the Taylor Glacier, Antarctica. *Applied and Environmental Microbiology,* 73**,** 4029-39.

Mitchell, A. C., Lafreniere, M. J., Skidmore, M. L. & Boyd, E. S. 2013. Influence of bedrock mineral composition on microbial diversity in a subglacial environment. *Geology,* 41**,** 855-858.

Miteva, V. 2008. Bacteria in snow and glacier ice. *Psychrophiles: from Biodiversity to Biotechnology*.

Møller, A. K., Søborg, D. A., Abu Al-Soud, W., Sørensen, S. J. & Kroer, N. 2013. Bacterial community structure in High-Arctic snow and freshwater as revealed by pyrosequencing of 16S rRNA genes and cultivation. *Polar Research,* 32.

Mooney, C. 2017. Scientists just found a strange and worrying crack in one of Greenland's biggest glaciers *The Washington Post*.

Morgan-Kiss, R. M., Priscu, J. C., Pocock, T., Gudynaite-Savitch, L. & Huner, N. P. 2006. Adaptation and acclimation of photosynthetic microorganisms to

permanently cold environments. *Microbiology and Molecular Biology Reviews,* 70**,** 222-52.

Mortazavi, R., Attiya, S. & Ariya, P. A. 2015. Arctic microbial and next-generation sequencing approach for bacteria in snow and frost flowers: Selected identification, abundance and freezing nucleation. *Atmospheric Chemistry and Physics,* 15**,** 6183-6204.

Mueller, D. R., Vincent, W. F., Pollard, W. H. & Fritsen, C. H. 2001. Glacial cryoconite ecosystems: A bipolar comparison of algal communities and habitats. *Nova Hedwigia***,** 173-197.

Musilova, M., Tranter, M., Bamber, J. L., Takeuchi, N. & Anesio, A. 2016. Experimental evidence that microbial activity lowers the albedo of glaciers. *Geochemical Perspectives Letters***,** 106-116.

Musilova, M., Tranter, M., Bennett, S. A., Wadham, J. & Anesio, A. M. 2015. Stable microbial community composition on the Greenland Ice Sheet. *Frontiers in Microbiology,* 6.

Musilova, M., Tranter, M., Wadham, J., Telling, J., Tedstone, A. & Anesio, A. M. 2017. Microbially driven export of labile organic carbon from the Greenland ice sheet. *Nature Geosciences,* advance online publication.

N.S.I.D.C., Fettweis, X., Box, J., Mote, D., van As, D. & Shuman, C. 2016. 2016 Melt season in review. *Greenland Ice Sheet Today* [Online].

Nekola, J. C. & White, P. S. 1999. The distance decay of similarity in biogeography and ecology. *Journal of Biogeography,* 26**,** 867-878.

Nesje, A., Bakke, J., Dahl, S. O., Lie, Ø. & Matthews, J. A. 2008. Norwegian mountain glaciers in the past, present and future. *Global and Planetary Change,* 60.

Neu, T. R. 1996. Significance of bacterial surface-active compounds in interaction of bacteria with interfaces. *Microbiological Reviews,* 60**,** 151–166.

Nielsen, P. H., Jahn, A. & Palmgren, R. 1997. Conceptual model for production and composition of exopolymers in biofilms. *Water Science and Technology,* 36**,** 11-19.

Novitsky, J. A. 1986. Degradation of dead microbial biomass in a marine sediment. *Applied Environmental Microbiology,* 52**,** 504-509.

Paerl, H. W., Pickney, J. L. & Steppe, T. F. 2000. Cyanobacterial-bacterial mat-consortia: Examining the functional unit of microbial survival and growth in extreme environments. *Environmental Microbiology,* 2**,** 11-26.

Pearce, D. A., Bridge, P. D., Hughes, K. A., Sattler, B., Psenner, R. & Russell, N. J. 2009. Microorganisms in the atmosphere over Antarctica. *FEMS Microbiology Ecology,* 69**,** 143-57.

Pedrós-Alió, C. 2012. The rare bacterial biosphere. *Annual Review of Marine Science,* 4**,** 449-66.

Peura, S., Bertilsson, S., Jones, R. I. & Eiler, A. 2015. Resistant microbial cooccurrence patterns inferred by network topology. *Applied and Environmental Microbiology,* 81**,** 2090-7.

Pons, P. & Latapy, M. 2006. Computing Communities in Large Networks Using Random Walks. *Journal of Graph Algorithms and Applications,* 10**,** 191-218.

Power, M. E. & Mills, L. S. 1995. The keystone cops meet in Hilo. *Trends in Ecology and Evolution,* 10.

Prescott, L. M., Harley, J. P. & Klein, D. A. 2002. *Microbiology* Boston McGraw-Hill.

Price, P. B. 2000. A habitat for psychrophiles in deep Antarctic ice. *Proceedings of the National Academy of Sciences,* 97**,** 1247-1251.

Priscu, J. C. & Christner, B. C. 2004. Earth's icy biosphere. *Microbial Diversity and Prospecting*.

Prosser, J. I. 2012. Ecosystem processes and interactions in a morass of diversity. *FEMS Microbiology Ecology,* 81**,** 507-19.

Rassner, S. M. E., Anesio, A. M., Girdwood, S. E., Hell, K., Gokul, J. K., Whitworth, D. E. & Edwards, A. 2016. Can the bacterial community of a High Arctic glacier surface escape viral control? *Frontiers in Microbiology*.

Řeháková, K., Stibal, M., Šabacká, M. & Řehák, J. 2009. Survival and colonisation potential of photoautotrophic microorganisms within a glacierised catchment on Svalbard, High Arctic. *Polar Biology,* 33**,** 737-745.

Remias, D., Lütz-Meindl, U. & Lütz, C. 2005. Photosynthesis, pigments and ultrastructure of the alpine snow alga *Chlamydomonas nivalis*. *European Journal of Phycology,* 40**,** 259-268.

Rice, D. 2017. The massive crack in the Antarctic ice shelf is hanging on by a 12-mile 'thread'. *USA Today*.

Rime, T., Hartmann, M. & Frey, B. 2016. Potential sources of microbial colonizers in an initial soil ecosystem after retreat of an alpine glacier. *International Society for Microbial Ecology Journal*.

Rippka, R., Deruelles, J., Waterbury, J. B., Herdman, M. & Stanier, R. Y. 1979. Generic assignments, strain histories and properties of pure cultures of *Cyanobacteria*. *Journal of General Microbiology,* 111**,** 1-61.

Ruiz-Sola, M. Á. & Rodríguez-Concepción, M. 2012. Carotenoid biosynthesis in *Arabidopsis*: A colorful pathway. *The Arabidopsis Book / American Society of Plant Biologists,* 10**,** e0158.

Rutter, N., Hodson, A., Irvine-Fynn, T. & Solås, M. K. 2011. Hydrology and hydrochemistry of a deglaciating high-Arctic catchment, Svalbard. *Journal of Hydrology,* 410**,** 39-50.

Sadykov, M. R., Zhang, B., Halouska, S., Nelson, J. L., Kreimer, L. W., Zhu, Y., Powers, R. & Somerville, G. A. 2010. Using NMR metabolomics to investigate tricarboxylic acid cycle-dependent signal transduction in *Staphylococcus epidermidis*. *Journal of Biological Chemistry,* 285**,** 36616-24.

Salipante, S. J., Kawashima, T., Rosenthal, C., Hoogestraat, D. R., Cummings, L. A., Sengupta, D. J., Harkins, T. T., Cookson, B. T. & Hoffman, N. G. 2014. Performance Comparison of Illumina and Ion Torrent Next-Generation Sequencing Platforms for 16S rRNA-Based Bacterial Community Profiling. *Appled and Environmental Microbiology,* 80**,** 7583-7591.

Salter, S. J., Cox, M. J., Turek, E. M., Calus, S. T., Cookson, W. O., Moffatt, M. F., Turner, P., Parkhill, J., Loman, N. J. & Walker, A. W. 2014. Reagent and laboratory contamination can critically impact sequence-based microbiome analyses. *BMC Biology,* 12.

Sattler, B. & Storrie-Lombardi, M. C. 2010. L.I.F.E in Antarctic lakes. *In:* BEJ, A. K., AISLABIE, J. & ATLAS, R. M. (eds.) *Polar Microbiology: The Ecology, Biodiversity and Bioremediation Potential of Microorganisms in Extremely Cold Environments.* Boca Raton: CRC Press

Sawstrom, C., Mumford, P., Marshall, W., Hodson, A. J. & Laybourn-Parry, J. 2002. The microbial communities and primary productivity of cryoconite holes in an Arctic glacier (Svalbard 79 °N). *Polar Biology,* 25**,** 591–596.

Schloss, P. D., Westcott, S. L., Ryabin, T., Hall, J. R., Hartmann, M., Hollister, E. B., Lesniewski, R. A., Oakley, B. B., Parks, D. H., Robinson, C. J., Sahl, J. W., Stres, B., Thallinger, G. G., Van Horn, D. J. & Weber, C. F. 2009. Introducing mothur: open-source, platform-independent, community-supported software for describing and comparing microbial communities. *Applied and Environmental Microbiology,* 75**,** 7537-41.

Schostag, M., Stibal, M., Jacobsen, C. S., Baelum, J., Tas, N., Elberling, B., Jansson, J. K., Semenchuk, P. & Prieme, A. 2015. Distinct summer and winter bacterial communities in the active layer of Svalbard permafrost revealed by DNA- and RNA-based analyses. *Frontiers in Microbiology,* 6**,** 399.

Scott, E. M. 1985. *Secondary metabolism and differentiation in fungi*, Blackwell Publishing Ltd.

Segawa, T., Ishii, S., Ohte, N., Akiyoshi, A., Yamada, A., Maruyama, F., Li, Z., Hongoh, Y. & Takeuchi, N. 2014. The nitrogen cycle in cryoconites: naturally occurring nitrification-denitrification granules on a glacier. *Environmental Microbiology,* 16**,** 3250-62.

Sengupta, D. & Chattopadhyay, M. K. 2013. Metabolismin bacteria at low temperature: A recent report. *Journal of Biosciences,* 38**,** 409-412.

Shade, A., Caporaso, J. G., Handelsman, J., Knight, R. & Fierer, N. 2013. A meta-analysis of changes in bacterial and archaeal communities with time. *International Society for Microbial Ecology Journal,* 7**,** 1493-506.

Shade, A., Jones, S. E., Caporaso, J. G., Handelsman, J., Knight, R., Fierer, N. & Gilbert, J. A. 2014. Conditionally rare taxa disproportionately contribute to temporal changes in microbial diversity. *MBio,* 5**,** e01371-14.

Shade, A., Peter, H., Allison, S. D., Baho, D. L., Berga, M., Burgmann, H., Huber, D. H., Langenheder, S., Lennon, J. T., Martiny, J. B., Matulich, K. L., Schmidt, T. M. & Handelsman, J. 2012. Fundamentals of microbial community resistance and resilience. *Frontiers in Microbiology,* 3**,** 417.

Sharp, M., Parkes, J., Cragg, B., Fairchild, I. J., Lamb, H. & Tranter, M. 1999. Widespread bacterial populations at glacier beds and their relationship to rock weathering and carbon cycling. *Geology,* 27**,** 107.

Shibata, A., Goto, Y., Saito, H., Kikuchi, T., Toda, T. & Taguchi, S. 2006. Comparison of SYBR Green I and SYBR Gold stains for enumerating bacteria and viruses by epifluorescence microscopy. *Aquatic Microbial Ecology,* 43**,** 223-231.

Singh, P., Singh, S. M., Tsuji, M., Prasad, G. S. & Hoshino, T. 2014. *Rhodotorula svalbardensis* sp. nov., a novel yeast species isolated from cryoconite holes of Ny-Alesund, Arctic. *Cryobiology,* 68**,** 122-8.

Skidmore, M. L., Foght, J. M. & Sharp, M. J. 2000. Microbial life beneath a High Arctic glacier. *Applied and Environmental Microbiology,* 66**,** 3214-3220.

Smith, D. J. 2011. The high life: Transport of microbes in the atmosphere. *EOS, Transactions, American Geophysical Union* [Online], 92.

Smith, L. C., Chu, V. W., Yang, K., Gleason, C. J., Pitcher, L. H., Rennermalm, A. K., Legleiter, C. J., Behar, A. E., Overstreet, B. T., Moustafa, S. E., Tedesco, M., Forster, R. R., LeWinter, A. L., Finnegan, D. C., Sheng, Y. & Balog, J. 2015.

Efficient meltwater drainage through supraglacial streams and rivers on the southwest Greenland ice sheet. *Proceedings of the National Academy of Sciences,* 112**,** 1001-6.

Sogin, M. L., Morrison, H. G., Huber, J. A., Mark Welch, D., Huse, S. M., Neal, P. R., Arrieta, J. M. & Herndl, G. J. 2006. Microbial diversity in the deep sea and the underexplored "rare biosphere". *Proceedings of the National Academy of Sciences,* 103**,** 12115-20.

Sole, A. J., Mair, D. W. F., Nienow, P. W., Bartholomew, I. D., King, M. A., Burke, M. J. & Joughin, I. 2011. Seasonal speedup of a Greenland marine-terminating outlet glacier forced by surface melt-induced changes in subglacial hydrology. *Journal of Geophysical Research,* 116.

Soule, M. C. K., Longnecker, K., Johnson, W. M. & Kujawinski, E. B. 2015. Environmental metabolomics: Analytical strategies. *Marine Chemistry,* 177**,** 374-387.

Steven, B., Hesse, C., Soghigian, J., Gallegos-Graves, L. V. & Dunbar, J. 2017. Simulated rRNA/DNA ratios show potential to misclassify active populations as dormant. *Applied Environmental Microbiology,* 83:**,** e00696-17.

Stibal, M., Gozdereliler, E., Cameron, K. A., Box, J. E., Stevens, I. T., Gokul, J. K., Schostag, M., Zarsky, J. D., Edwards, A., Irvine-Fynn, T. D. & Jacobsen, C. S. 2015a. Microbial abundance in surface ice on the Greenland Ice Sheet. *Frontiers in Microbiology,* 6**,** 225.

Stibal, M., Hasan, F., Wadham, J. L., Sharp, M. J. & Anesio, A. M. 2012. Prokaryotic diversity in sediments beneath two polar glaciers with contrasting organic carbon substrates. *Extremophiles,* 16**,** 255-65.

Stibal, M., Lawson, E. C., Lis, G. P., Mak, K. M., Wadham, J. L. & Anesio, A. M. 2010. Organic matter content and quality in supraglacial debris across the ablation zone of the Greenland ice sheet. *Annals of Glaciology,* 51**,** 1-8.

Stibal, M., Sabacka, M. & Kastovska, K. 2006. Microbial communities on glacier surfaces in Svalbard: Impact of physical and chemical properties on abundance and structure of cyanobacteria and algae. *Microbial Ecology,* 52**,** 644-54.

Stibal, M., Schostag, M., Cameron, K. A., Hansen, L. H., Chandler, D. M., Wadham, J. L. & Jacobsen, C. S. 2015b. Different bulk and active bacterial communities in cryoconite from the margin and interior of the Greenland ice sheet. *Environmental Microbiology Reports,* 7**,** 293-300.

Stibal, M. & Tranter, M. 2007. Laboratory investigation of inorganic carbon uptake by cryoconite debris from Werenskioldbreen, Svalbard. *Journal of Geophysical Research: Biogeosciences,* 112**,** 1-9.

Stibal, M., Tranter, M., Benning, L. G. & Rehak, J. 2008. Microbial primary production on an Arctic glacier is insignificant in comparison with allochthonous organic carbon input. *Environmental Microbiology,* 10**,** 2172-8.

Stoeck, T., Kasper, J., Bunge, J., Leslin, C., Ilyin, V. & Epstein, S. 2007. Protistan diversity in the Arctic: A case of paleoclimate shaping modern biodiversity? *PLoS ONE,* 2.

Struyf, E., Smis, A., Van Damme, S., Meire, P. & Conley, D. J. 2009. The global biogeochemical silicon cycle. *Silicon,* 1**,** 207-213.

Stuart, R. K., Mayali, X., Lee, J. Z., Craig Everroad, R., Hwang, M., Bebout, B. M., Weber, P. K., Pett-Ridge, J. & Thelen, M. P. 2015. Cyanobacterial reuse of extracellular organic carbon in microbial mats. *International Society for Microbial Ecology Journal*.

Suzuki, T., Fujikura, K., Higashiyama, T. & Takata, K. 1997. DNA staining for fluorescence and laser confocal microscopy. *The Journal of Histochemistry & Cytochemistry,* 45**,** 49-53.

Swenson, N. G., Mi, X., Kress, W. J., Thompson, J., Uriarte, M. & Zimmerman, J. K. 2013. Species-time-area and phylogenetic-time-area relationships in tropical tree communities. *Ecology and Evolution,* 3**,** 1173-83.

Takeda, M., Nakano, F., Nagase, T., Iohara, K. & Koizumi, J. I. 1998. Isolation and chemical composition of the sheath of *Sphaerotilus natans*. *Bioscience, Biotechnology, and Biochemistry,* 62**,** 1138– 1143.

Takeuchi, N. 2002. Optical characteristics of cryoconite (surface dust) on glaciers: the relationship between light absorbency and the property of organicmatter contained in the cryoconite. *Annals of Glaciology***,** 409-414.

Takeuchi, N. & Kohshima, S. 2004. A Snow Algal Community on Tyndall Glacier in the Southern Patagonia Icefield, Chile. *Arctic, Antarctic and Alpine Research,* 36**,** 92-99.

Takeuchi, N., Kohshima, S. & Segawa, T. 2003. Effect of cryoconite and snow algal communities on surface albedo on maritime glaciers in South Alaska. *Bulletin of Glaciological Research,* 20**,** 21-27.

Takeuchi, N., Kohshima, S. & Seko, K. 2001a. Structure, Formation, and Darkening Process of Albedo-Reducing Material (Cryoconite) on a Himalayan Glacier: A Granular Algal Mat Growing on the Glacier. *Arctic, Antarctic, and Alpine Research,* 33**,** 115.

Takeuchi, N., Kohshima, S. & Seko, K. 2001b. Structure, formation, and darkening process of albedo-reducing material (cryoconite) on a Himalayan glacier: A granular algal mat growing on the glacier. *Arctic, Antarctic and Alpine Research,* 33**,** 115-122.

Takeuchi, N., Kohshima, S., Yoshimura, Y., Seko, K. & Fujita, K. 2000. Characteristics of cryoconite holes on a Himalayan glacier, Yala Glacier Central Nepal. *Bulletin of Glaciological Research,* 17**,** 51-59.

Takeuchi, N., Nishiyama, H. & Zhongqin, L. 2010. Structure and formation process of cryoconite granules on Urumqi glacier No. 1, Tien Shan, China. *Annals of Glaciology,* 51**,** 9-14.

Tang, J. 2011. Microbial Metabolomics. *Current Genomics,* 12**,** 391-403.

Telling, J., Anesio, A. M., Tranter, M., Stibal, M., Hawkings, J., Irvine-Fynn, T., Hodson, A., Butler, C., Yallop, M. & Wadham, J. 2012. Controls on the autochthonous production and respiration of organic matter in cryoconite holes on high Arctic glaciers. *Journal of Geophysical Research: Biogeosciences,* 117**,** 1-10.

ThermoFisherScientific 2014a. Ion PGM™ Sequencing 400 Kit - Technology Access User Guide. *In:* TORRENT, L. T. I. (ed.). Life Technologies.

ThermoFisherScientific 2014b. Ion PGM™ Template OT2 400 Kit User Guide. *In:* TORRENT, L. T. I. (ed.). Life Technologies.

Tkavc, R., Gostincar, C., Turk, M., Visscher, P. T., Oren, A. & Gunde-Cimerman, N. 2011. Bacterial communities in the 'petola' microbial mat from the Secovlje salterns (Slovenia). *FEMS Microbiology Ecology,* 75**,** 48-62.

Tsuji, M. 2016. Cold-stress responses in the Antarctic basidiomycetous yeast *Mrakia blollopis*. *Royal Society Open Science,* 3**,** 160106.

Uetake, J., Naganuma, T., Hebsgaard, M. B., Kanda, H. & Kohshima, S. 2010. Communities of algae and cyanobacteria on glaciers in west Greenland. *Polar Science,* 4**,** 71-80.

Uetake, J., Tanaka, S., Segawa, T., Takeuchi, N., Nagatsuka, N., Motoyama, H. & Aoki, T. 2016. Microbial community variation in cryoconite granules on Qaanaaq Glacier, NW Greenland. *FEMS Microbiology Ecology,* 92.

van De Poll, W. H., Maat, D. S., Fischer, P., Rozema, P. D., Daly, O. B., Koppelle, S., Visser, R. J. W. & Buma, A. G. J. 2016. Atlantic Advection Driven Changes in Glacial Meltwater: Effects on Phytoplankton Chlorophyll-a and Taxonomic Composition in Kongsfjorden, Spitsbergen. *Frontiers in Marine Science,* 3.

van der Gast, C. J. 2015. Microbial biogeography: the end of the ubiquitous dispersal hypothesis? *Environmental Microbiology,* 17**,** 544-6.

Van der Gucht, K., Cottenie, K., Muylaert, K., Vloemans, N., Cousin, S., Declerck, S., Jeppesen, E., Conde-Porcuna, J. M., Schwenk, K., Zwart, G., Degans, H., Vyverman, W. & De Meester, L. 2007. The power of species sorting: local factors drive bacterial community composition over a wide range of spatial scales. *Proceedings of the National Academy of Sciences,* 104**,** 20404-9.

Vazquez-Yanes, C. & Orozco-Segovia, A. 1990. Ecological significance of light controlled seed germination in two contrasting tropical habitats. *Oecologia* 83**,** 171-175.

Viant, M. R. 2007. Metabolomics of aquatic organisms: the new 'omics' on the block. *Marine Ecology Progress Series,* 332**,** 301-306.

Vick-Majors, T. J., Priscu, J. C. & Amaral-Zettler, L. A. 2014. Modular community structure suggests metabolic plasticity during the transition to polar night in ice-covered Antarctic lakes. *International Society for Microbial Ecology Journal,* 8**,** 778-89.

Vincent, W. F. 2000. Evolutionary origins of Antarctic microbiota: invasion, selection and endemism. *Antarctic Science,* 12**,** 374-385.

Vonnahme, T. R., Devetter, M., Žárský, J. D., Šabacká, M. & Elster, J. 2016. Controls on microalgal community structures in cryoconite holes upon high-Arctic glaciers, Svalbard. *Biogeosciences,* 13**,** 659-674.

Wadham, J., Kohler, J., Hubbard, A., Nuttall, A. M. & Rippin, D. 2006. Superimposed ice regime of a high Arctic glacier inferred using ground-penetrating radar, flow modeling, and ice cores. *Journal of Geophysical Research,* 111.

Waldner, P. A. & Burch, H. 1996. Chemistry of snow melt runoff. Birmensdorf, Switzerland: WSL, Swiss Federal Institute for Forest, Snow and Landscape Research.

Wang, Q., Garrity, G. M., Tiedje, J. M. & Cole, J. R. 2007. Naive Bayesian classifier for rapid assignment of rRNA sequences into the new bacterial taxonomy. *Applied and Environmental Microbiology,* 73**,** 5261-7.

Warren, C. R. 2008. Rapid measurement of chlorophylls with a microplate reader. *Journal of Plant Nutrition,* 31**,** 1321-1332.

Wemheuer, B., Wemheuer, F. & Daniel, R. 2012. RNA-based assessment of diversity and composition of active archaeal communities in the German Bight. *Archaea,* 2012**,** 695826.

West, N. E. 1990. Structure and function of microphytic soil crusts in wildland ecosystems of arid to semi-arid regions. *In:* M. BEGON, A. H. F. & MACFADYEN, A. (eds.) *Advances in Ecological Research.* Academic Press.

White, D. C., Sutton, S. D. & Ringelberg, D. B. 1996. The genus *Sphingomonas*: physiology and ecology. *Current Opinion in Biotechnology,* 7**,** 301-306.

Wilhelm, L., Besemer, K., Fasching, C., Urich, T., Singer, G. A., Quince, C. & Battin, T. J. 2014. Rare but active taxa contribute to community dynamics of benthic biofilms in glacier-fed streams. *Environmental Microbiology,* 16**,** 2514-24.

Wilhelm, L., Singer, G. A., Fasching, C., Battin, T. J. & Besemer, K. 2013. Microbial biodiversity in glacier-fed streams. *International Society for Microbiol Ecology Journal,* 7**,** 1651-60.

Womack, A. M., Bohannan, B. J. M. & Green, J. L. 2010. Biodiversity and biogeography of the atmosphere. *Philosophical Transactions of the Royal Society B: Biological Sciences,* 365**,** 3645-3653.

Xia, J., Sinelnikov, I. V., Han, B. & Wishart, D. S. 2015. MetaboAnalyst 3.0—making metabolomics more meaningful. *Nucleic Acids Research,* 43**,** W251–W257.

Yallop, M. L. & Anesio, A. M. 2010. Benthic diatom flora in supraglacial habitats: a generic-level comparison. *Annals of Glaciology,* 51.

Yallop, M. L., Anesio, A. M., Perkins, R. G., Cook, J., Telling, J., Fagan, D., MacFarlane, J., Stibal, M., Barker, G., Bellas, C., Hodson, A., Tranter, M., Wadham, J. & Roberts, N. W. 2012. Photophysiology and albedo-changing potential of the ice algal community on the surface of the Greenland ice sheet. *International Society for Microbiol Ecology Journal,* 6**,** 2302-13.

Yoshimura, Y., Kohshima, S. & Ohtani, S. 1997. A community of snow algae on a Himalayan glacier: Change of algal biomass and community structure with altitude. *Arctic and Alpine Research,* 29**,** 126-137.

Zak, D. R. & Kling, G. W. 2006. Microbial community composition and function across an Arctic Tundra landscape. *Ecology,* 87**,** 1659-1670.

Zalar, P. & Gunde-Cimerman, N. 2014. Cold-adapted yeasts in Arctic habitats. *In:* BUZZINI, P. & MARGESIN, R. (eds.) *Biodiversity, Adaptation Strategies and Biotechnological Significance.*

Zarsky, J. D., Stibal, M., Hodson, A., Sattler, B., Schostag, M., Hansen, L. H., Jacobsen, C. S. & Psenner, R. 2013. Large cryoconite aggregates on a Svalbard glacier support a diverse microbial community including ammonia-oxidizing archaea. *Environmental Research Letters,* 8**,** 035044.

Zawierucha, K., Buda, J., Pietryka, M., Richter, D., Łokas, E., Lehmann-Konera, S., Makowska, N. & Bogdziewicz, M. 2017. Snapshot of micro-animals and associated biotic and abiotic environmental variables on the edge of the south-west Greenland ice sheet. *Limnology*.

Zawierucha, K., Kolicka, M., Takeuchi, N. & Kaczmarek, Ł. 2015. What animals can live in cryoconite holes? A faunal review. *Journal of Zoology,* 295**,** 159-169.

Zawierucha, K., Ostrowska, M., Vonnahme, T. R., Devetter, M., Nawrot, A. P., Lehmann, S. & Kolicka, M. 2016. Diversity and distribution of Tardigrada in Arctic cryoconite holes. *Journal of Limnology,* 75**,** 545-559.

Zeng, Y. X., Li, H. R., Zhang, F., Yan, M., Yu, Y., He, J. F. & Sun, K. 2013. Diversity of bacteria in surface ice of Austre Lovenbreen glacier, Svalbard. *Archives of Microbiology,* 195**,** 313-322.

Zhang, S. W., Wei, Z. G., Zhou, C., Zhang, Y. C. & Zhang, T. H. Exploring the interaction patterns in seasonal marine microbial communities with network analysis. 7th International Conference on Systems Biology (ISB), 2013. 63-68.

Zhang, Y., Cong, J., Lu, H., Deng, Y., Liu, X., Zhou, J. & Li, D. 2016. Soil bacterial endemism and potential functional redundancy in natural broadleaf forest along a latitudinal gradient. *Nature Scientific Reports,* 6**,** 28819.

Zhu, Y., Graham, J. E., Ludwig, M., Xiong, W., Alvey, R. M., Shen, G. & Bryant, D. A. 2010. Roles of xanthophyll carotenoids in protection against photoinhibition and oxidative stress in the cyanobacterium *Synechococcus* sp. strain PCC 7002. *Archives of Biochemistry and Biophysics,* 504**,** 86-99.